Host-pathogen interactions of natural killer cells and *Aspergillus fumigatus*: Relevance of immune cell cross-talk and fungal recognition receptors

Wirt-Pathogen Interaktionen von natürlichen Killerzellen und *Aspergillus fumigatus*: Relevanz von Immunzellinteraktionen und fungalen Erkennungsrezeptoren

Doctoral thesis for a doctoral degree

at the Graduate School of Life Sciences,

Julius-Maximilians-Universität Würzburg,

Section Infection and Immunity

submitted by

Esther Weiß

from

Miltenberg

Würzburg **2019**

Submitted on: …….

Members of the *Promotionskomitee*:

Chairperson:	Prof. Dr. med. Georg Gasteiger
Primary Supervisor:	Prof. Dr. rer. nat. Jürgen Löffler
Supervisor (Second):	Priv.-Doz. Dr. med. Niklas Beyersdorf
Supervisor (Third):	Prof. Dr. med. Thomas Dandekar

Date of Public Defence: ……

Date of Receipt of Certificates: ……

Die hier vorliegende Arbeit wurde in der Zeit von Januar 2016 bis Dezember 2019 in der Medizinischen Klinik und Poliklinik II des Universitätsklinikums Würzburg angefertigt.

Contents

Summary

The human pathogen *Aspergillus (A.) fumigatus* is a fungal mold that can cause severe infections in immunocompromised hosts. Pathogen recognition and immune cell cross-talk are essential for clearing fungal infections efficiently. Immune cell interactions in particular may enhance individual cell activation and cytotoxicity towards invading pathogens.

This study analyzed the reciprocal cell activation of natural killer (NK) cells and monocyte-derived dendritic cells (moDCs) after stimulation with *A. fumigatus* cell wall fractions and whole-cell lysates. Furthermore, the impact of the on moDCs expressed fungal receptors Dectin-1 and TLR-2 on NK cell activation was analyzed. Stimulation of moDCs with ligands for Dectin-1 and TLR-2 and transfer of soluble factors on autologous NK cells showed that moDCs could induce NK cell activation solely by secreting factors. In summary, both cell types could induce reciprocal cell activation if the stimulated cell type recognized fungal morphologies and ligands. However, moDCs displayed a broader set of *A. fumigatus* receptors and, therefore, could induce NK cell activation when those were not activated by the stimulus directly.

Consequently, new fungal receptors should be identified on NK cells. The NK cell characterization marker CD56 was reduced detected in flow cytometry after fungal co-culture. Notably, this decreased detection was not associated with NK cell apoptosis, protein degradation, internalization, or secretion of CD56 molecules. CD56 was shown to tightly attach to hyphal structures, followed by its concentration at the NK-*A. fumigatus* interaction site. Actin polymerization was necessary for CD56 relocalization, as pre-treatment of NK cells with actin-inhibitory reagents abolished CD56 binding to the fungus. Blocking of CD56 suppressed fungal mediated NK cell activation and secretion of the immune-recruiting chemokines MIP-1α, MIP-1β, and RANTES, concluding that CD56 is functionally involved in fungal recognition by NK cells.

CD56 binding to fungal hyphae was inhibited in NK cells obtained from patients during immune-suppressing therapy after allogeneic stem cell transplantation (alloSCT). Additionally, reduced binding of CD56 correlated with decreased actin polymerization of reconstituting NK cells challenged with the fungus. The immune-suppressing therapy with corticosteroids negatively influenced the secretion of MIP-1α, MIP-1β, and RANTES in NK cells after fungal stimulation *ex vivo*. Similar results were obtained when NK cells from healthy donors were treated with corticosteroids prior to fungal co-culture. Thus, corticosteroids were identified to have detrimental effects on NK cell function during infection with *A. fumigatus*.

Zusammenfassung

Der humanpathogene Pilz *Aspergillus (A.) fumigatus* kann lebensbedrohliche Infektionen in immunsupprimierten Patienten verursachen. Die Immunerkennung von Pathogenen sowie die Wechselwirkungen zwischen Immunzellen sind essentiell für die erfolgreiche Bekämpfung von Pilzinfektionen. Zell-Zell-Interaktionen tragen zur gegenseitigen Aktivierung bei und können somit die Zytotoxizität gegenüber eindringenden Pathogenen steigern.

In dieser Arbeit wurde die gegenseitige Zellaktivierung von natürlichen Killerzellen (NK-Zellen) und die aus Monozyten generierten, dendritischen Zellen (DZ) nach Stimulation mit Zellwandfraktionen und Zelllysaten des Pilzes *A. fumigatus* analysiert. Des Weiteren wurde der Einfluss dendritischer Rezeptoren auf die NK-Zellaktivierung untersucht. Die Stimulation mit Liganden für Dectin-1 und TLR-2 induzierte die Freisetzung löslicher Faktoren, welche ausreichend waren, um autologe NK-Zellen zu stimulieren. Zusammenfassend ist zu sagen, dass DZ mehr Rezeptoren zur Pilzerkennung exprimieren und somit NK-Zellen auch dann aktivieren konnten, wenn diese, aufgrund fehlender Rezeptoren, nicht stimuliert wurden.

Basierend auf diesen Ergebnissen sollten neue Pathogen-Erkennungsrezeptoren auf NK-Zellen identifiziert werden. Der Charakterisierungsmarker CD56 zeigte nach fungaler Kokultur eine reduzierte Detektion in durchflusszytometrischen Analysen. Die verminderte Proteindetektion von CD56 war nicht assoziiert mit Apoptose, Internalisation, Sekretion oder Proteindegradierung. Weitere Analysen bestätigten eine starke CD56-Bindung zu Pilzhyphen, gefolgt von einer Konzentration des Proteins an der NK-*A. fumigatus* Interaktionsstelle. Diese Relokalisation zeigte eine Abhängigkeit zu Aktin, da Zytoskelett-Inhibitoren die CD56-Bindung am Pilz verhinderten. Eine spezifische Blockade von CD56 Rezeptoren reduzierte die Freisetzung der immun-rekrutierenden Chemokine MIP-1α, MIP-1β und RANTES, was folgern ließ, dass CD56 eine funktionelle Rolle in der Pilzerkennung der NK-Zellen hat.

NK-Zellen, die während einer Immunsuppressionstherapie aus Empfängern einer allogenen Stammzelltransplantation (alloSZT) gewonnen wurden, zeigten eine inhibierte Bindung von CD56 an Pilzhyphen. Diese korrelierte mit einer reduzierten Aktinpolymerisation nach fungaler Stimulation. Weiterhin hemmte eine Immunsuppressionstherapie mit Corticosteroiden die Sekretion von MIP-1α, MIP-1β und RANTES in NK-Zellen, die mit Pilz *ex vivo* stimuliert wurden. Ähnliches war zu beobachten, wenn NK-Zellen von gesunden Spendern vor Pilzstimulation mit Corticosteroiden vorbehandelt wurden. Daraus folgend wurde den Corticosteroiden ein negativer Einfluss auf die NK-Zellfunktion bei Pilzinfektionen zugesprochen.

1 Introduction

1.1 *Aspergillus fumigatus* morphologies, pathology, and diagnostics

1.1.1 The conidia

A. fumigatus is a saprophytic, opportunistic fungal mold primarily found on degrading biomass, e.g., rotten organic material. Depending on the environmental nutrient supply, the morphology of *Aspergillus spp.* ranges from dormant conidia to germlings, growing hyphae, and conidiophores [1-4]. *A. fumigatus* can perform asexual and sexual reproduction; however, sexual reproduction occurs very rarely and only under certain conditions [5]. Thus, the asexual life cycle is the more general form of reproduction.

The first stage of the fungal morphology is the conidia – a 2-3 µm small roundish structure surrounded by the so-called 'rodlet layer' (Figure 1). This surface rodlet coat is immunologically inert and inhibits immune cell activation until the conidial germination and cracking of the rodlet layer occur [6]. The hydrophobin RodA mediates the unique, patterned structure of the rodlet layer, and ΔrodA conidia have different binding characteristics to host proteins, e.g., albumin, collagen, fibrinogen, or laminin [7-10]. However, the deletion of RodA does not impact virulence in a murine pulmonary-infection model [11].

Under the rodlet layer lies the conidial cell wall, consisting of α-glucans, β-glucans, chitin, galactomannan, and melanin (Figure 1) [12-14]. DHN (1,8-dihydroxynaphtalene) melanin, which is responsible for the green/bluish color of the fungus, protects the conidia from phagolysosomal acidification (pH < 5) and thus favors fungal survival and growth [15, 16]. Furthermore, DHN melanin shields the fungus against UV radiation and masks pathogen-associated molecular patterns (PAMPs), thereby inhibiting immune responses [6, 17]. Conidia are thought to display low metabolic activity since they are majorly important to overcome starvation conditions and for fungal dissemination [18]. However, they produce toxins that trigger necrotic cell death of pneumocytes or alter neutrophil function by inhibiting the communication with other immune cells [19, 20].

The first host-pathogen contact occurs in the lung, where inhaled conidia interact with alveolar epithelial cells, lung macrophages, neutrophils, and the complement system [21-25]. In that way, hundreds of conidia are inhaled and cleared daily without any damage to

the host [26, 27]. However, *A. fumigatus* infections might become life-threatening in immunosuppressed conditions, in which first-line barriers are ineffective, and conidia outgrow and invade deeper tissues.

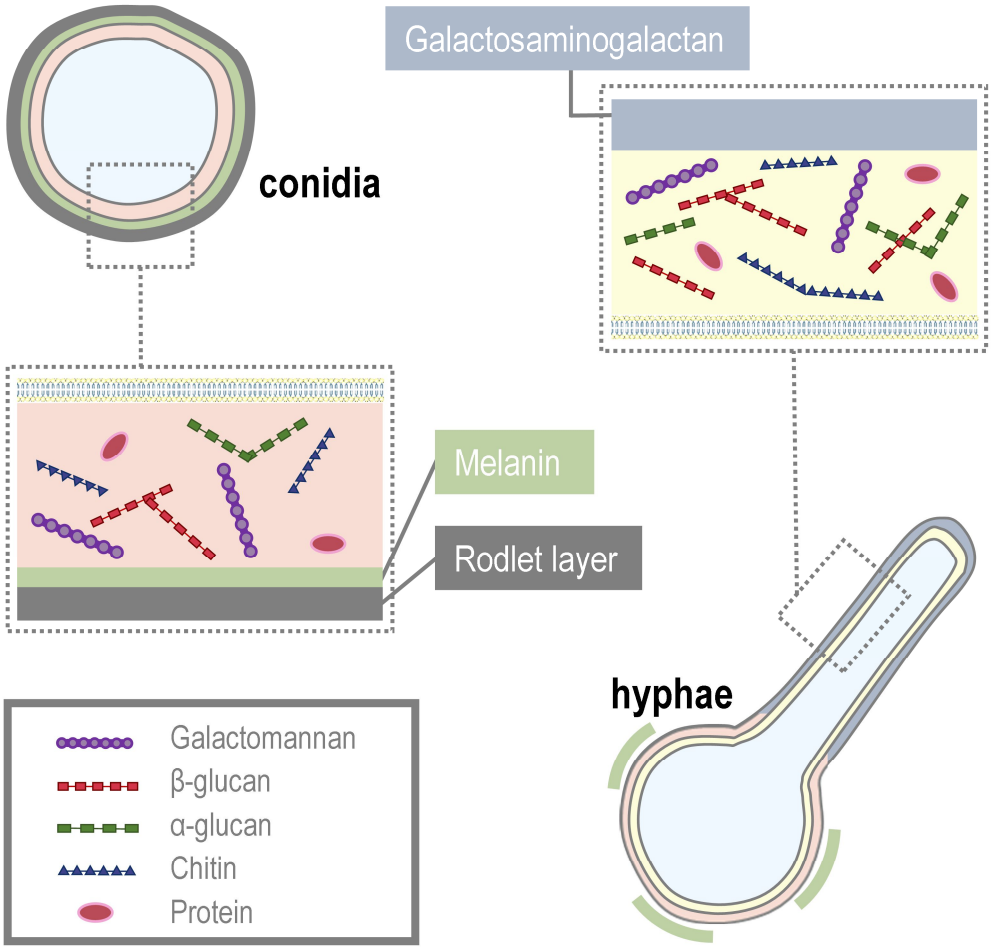

Figure 1: The cell wall composition of *A. fumigatus* conidia and hyphae. The rodlet layer shields the conidia from immunological detection. Melanin, mainly DHN melanin, is responsible for the green/bluish color of the conidia. After settling on an optimal nutrient medium, conidia germinate and develop into hyphae, which are covered with the exopolysaccharide galactosaminogalactan.The cell wall consists of 90 % polysaccharides, including galactomannan, β-glucans, α-glucans, and chitin. The figure was designed after the model from [28, 29].

1.1.2 Germ tubes and hyphae

Once settled on an optimal nutrient medium, conidia switch to the second morphological stage of the fungus – the germlings/germ tubes. Those structures are unique since they display the remainings of the conidial cell wall and new polysaccharides at the outgrown parts (Figure 1) [29, 30]. Interestingly, the cell wall biosynthesis is a highly dynamic process

since different external stimuli, e.g., medium composition, low O_2/high CO_2 ratios, and antifungals can change the cell wall composition [31].

The cell wall consists of up to 90 % of polysaccharides, such as β-(1,3)-glucan, α-(1,3)-glucan, chitin, galactosaminogalactan, and galactomannan (Figure 1) [13, 28, 29, 32]. These sugars have different functions, e.g., the stability of the cell wall, adhesion, protection against extracellular stress, blocking of immune responses, and induction of host cell apoptosis [33-36]. Some of these sugars are recognized by the immune system and therefore play an essential role in fungal recognition, such as chitin [37]. Furthermore, some sugars, e.g., galactomannan, can modulate and inhibit immune responses [37-39].

In general, germ tubes are more efficiently recognized by the immune system compared to conidia and thus lead to stronger immunological reactions. Therefore, germ tubes are often used to study host-pathogen interactions [40, 41]. *A. fumigatus* germ tubes can grow and invade deeper lung tissues, thereby mediating epithelial cell destruction and release of lactate dehydrogenase (LDH) which can be used as a molecular marker for cell damage [42, 43]. Germ tubes eventually grow larger and reach the morphological stage of fungal hyphae, which are long, filamentous, septate structures. Hyphae can reach and invade blood vessels, thereby disseminating into other body parts by the bloodstream and induce hematogenously disseminated aspergillosis [44].

1.1.3 Immune status

As mentioned above, the immune system can rapidly clear inhaled *A. fumigatus* conidia in healthy individuals. However, different immunological conditions, ranging from hypersensitivity to absent immunological responses, affect the fungal clearance and favor the growth and distribution in the human body (Figure 2) [45]. Hypersensitivity to *Aspergillus spp*. is characterized by overshooting immune responses including allergic reactions, and over 20 allergens have been described for *A. fumigatus* so far (www.allergen.org).

Allergic bronchopulmonary aspergillosis (ABPA) is a disease mostly affecting asthmatic or cystic fibrosis patients, in which Th2 hypersensitivity in response to *A. fumigatus* leads to elevated IgE serum levels and eosinophilia [46-48]. Since Th2 responses were shown to be non-protective against *A. fumigatus* infections, ABPA patients are susceptible to develop pulmonary infiltrates or bronchiectasis [49, 50]. A saprophytic aspergillosis infection (aspergilloma) occurs by the colonization of a pre-existing pulmonary cavity or ectatic bronchus. Aspergillomas are non-invasive, mass-like fungal balls combined with inflammatory cells, mucus, and cellular debris that mainly affect patients with chronic obstructive pulmonary disease (COPD), bronchiectasis, cystic fibrosis or chronic lung cavities [51].

Invasive aspergillosis (IA) is the most severe form of an *Aspergillus* infection, affecting mainly immunocompromised patients after solid organ transplantation, chronic granulomatous disease, hematological malignancies, HIV patients, or patients undergoing alloSCT (Figure 2) [52]. In alloSCT patients, the incidence of developing IA ranges between 5 % to 10 %, and the overall mortality rate is devastating with 50-100 % [52, 53].

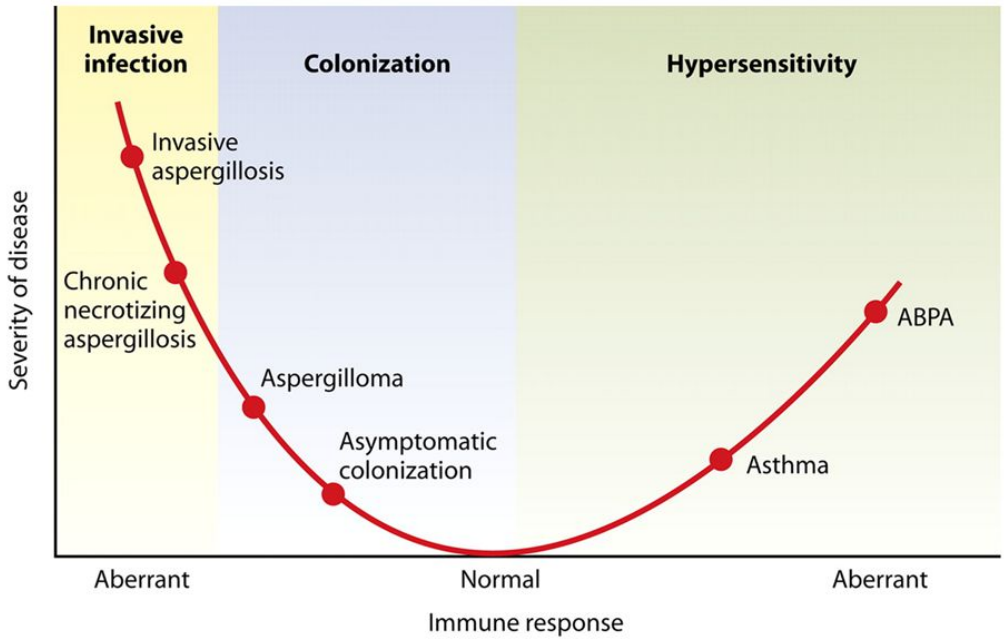

Figure 2: *Aspergillus* mediated diseases. Depending on the immunological status, *A. fumigatus* infections may lead to various severe complications, including allergic bronchopulmonary aspergillosis (ABPA), asthma, asymptomatic colonization, aspergilloma, chronic, necrotizing aspergillosis and invasive aspergillosis (IA). Figure adapted from [45].

1.1.4 Risk factors after alloSCT

Circulating *A. fumigatus* conidia in the environment display a potential infection risk for immunosuppressed patients after alloSCT [54-56]. Schmitt and colleagues showed that despite the relatively low abundance of *A. fumigatus* (0.3 %) among the airborne fungi, 44 % of the molds isolated from patients were derived from *A. fumigatus* [57]. High-efficiency particulate air (HEPA) filters were invented to clean the hospital air from pathogens, e.g. circulating *A. fumigatus* conidia [58]. However, IA manifests in 5 % to 10 % after receiving an allograft, and several factors have been identified that increase the risk of developing IA:

(a) Immune cell reconstitution/ neutropenia

Early phases after alloSCT are characterized by the reconstitution of innate immune cells, e.g., neutrophils, eosinophils, basophils, monocytes, and NK cells. Patients experience a neutropenic state in which neutrophils are absent or represented by a very low

amount of cells (< 0.5 x 10^9 cells/L) (Figure 3). Neutrophil reconstitution takes 14-30 days after alloSCT and may be further delayed by the use of specific drugs and therapies [59, 60]. In this pre-engraftment phase, life-threatening infections with various pathogens, including bacteria, viruses, and fungi become more likely, and neutropenia was described as a risk factor for developing IA (Figure 3) [61].

(b) Graft-versus-host disease (GvHD)

The post-alloSCT period is further characterized by T and B cell deficiency for up to 2 years, and lymphopenia was associated with the development of IA [62-65]. Donor T cells may induce overreacting immune responses due to human leukocyte antigen (HLA)-mismatch, leading to graft-versus-host disease (GvHD) [66]. GvHD is defined by epithelial tissue destruction and mainly affects the skin, the gastrointestinal tract, the liver, and the eyes [67-69]. Despite treatment, acute GvHD remains the second leading cause of death after alloSCT and acute GvHD grades III to IV, acute GvHD grades II to IV, and chronic extensive GvHD are further risk factors for developing IA [63, 70].

(c) Glucocorticoid therapy

Glucocorticosteroids belong to the first-line treatment after the occurrence of GvHD [71, 72]. These cell-permeable steroids bind to glucocorticoid receptors in the cytoplasm. Glucocorticoid-receptor-complexes translocate into the nucleus, bind to glucocorticoid response elements (GREs), and function as transcriptional inducers or repressors, or interact with other transcription factors and influence target gene expression [73-76]. In particular, glucocorticoids inhibit pro-inflammatory signaling, e.g., NF-κB, ERK-1/2, JNK-1, and AP-1 activity [76, 77]. Glucocorticoids mediate a higher susceptibility to invasive fungal infections by inhibiting several cell functions, e.g. the cytotoxicity of polymorphonuclear neutrophils (PMNs), lymphocyte proliferation, and the cytokine production, cell migration, and phagocytotic ability of macrophages, and monocytes [78-83].

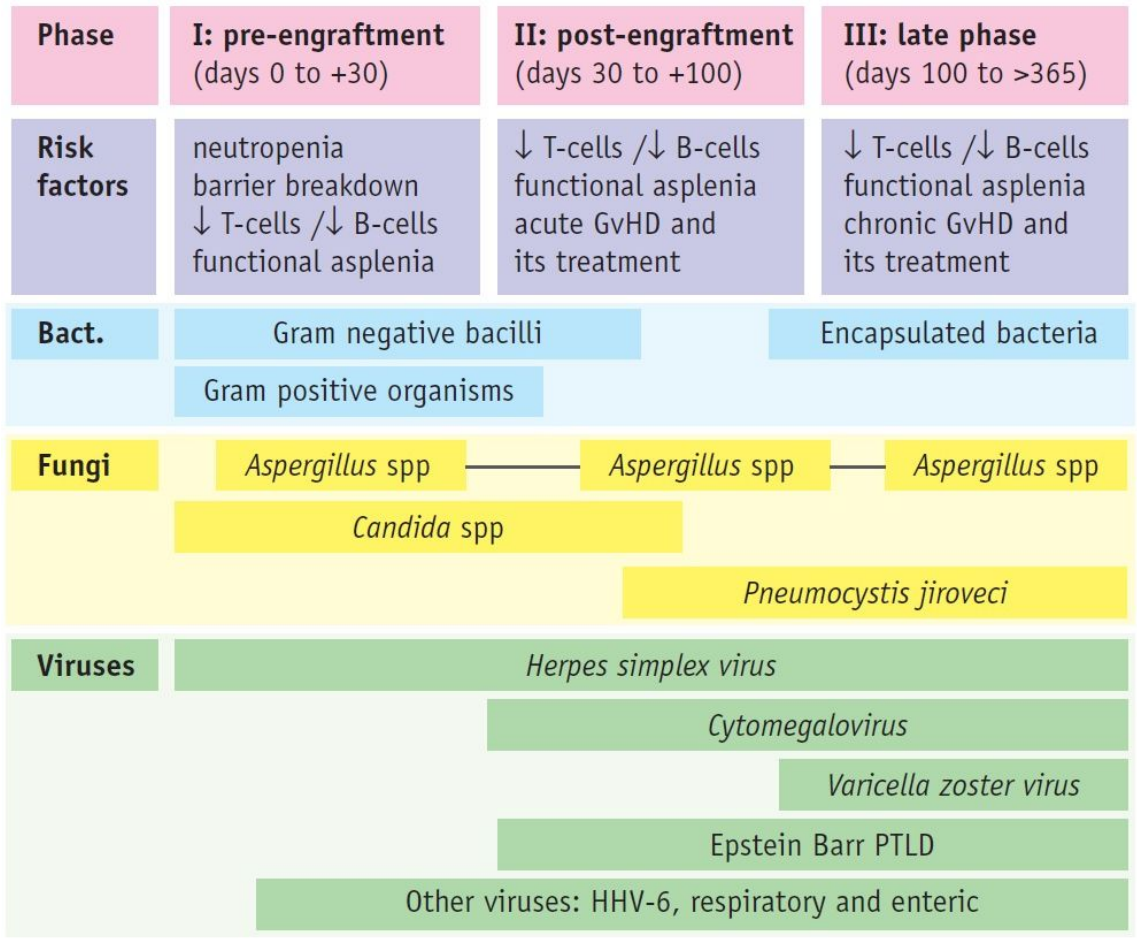

Figure 3: Phases after alloSCT. In the pre-engraftment phase, neutropenia is a risk factor for different kinds of infections, including viruses, bacteria, and fungi. In the post-engraftment phase, patients might suffer from acute graft-versus-host disease (GvHD), whereas chronic GvHD emerges in later phases. *Aspergillus* infections might occur in all three phases after alloSCT. Figure adapted from the EBM handbook 2012 [64].

1.1.5 Diagnosis of IA

Different assays were established that enhance the detection and diagnosis of fungal byproducts and infections in different human samples, e.g., bronchoalveolar lavage (BAL), whole blood, serum, and plasma [84-86]. These assays detect fungal species with different sensitivity and specificity, depending on the use of the biological sample and the time after infection [87, 88].

The β-D-glucan enzyme-linked immunosorbent assay (ELISA) detects β-(1,3)-glucan, which is present in the cell wall of various fungi and thus is not *Aspergillus* specific [89, 90]. In contrast, *Aspergillus* specific galactomannan, present in serum and other body fluids, can be detected by the PLATELIA™ *Aspergillus Ag* test [89]. However, the sensitivity is decreased by over 30 % under antifungal therapy [91].

The lateral flow device (LFD) assay offers a fast and specific discovery of live *A. fumigatus* hyphae in BAL or serum [92]. The detection is based on the monoclonal antibody binding to a structure only released from growing *A. fumigatus* hyphae [92]. However, this assay harbors several disadvantages and is, therefore, critically discussed in the literature [93].

Detection of specific fungal DNA is a valuable tool to pinpoint the species and strain and thus enabling specific therapy [94]. Therefore, *Aspergillus* PCR was recently included in the updated EORTC (European Organization for Research and Treatment of Cancer) guidelines for the diagnosis and management of aspergillosis [95]. These guidelines define possible, probable, and proven aspergillosis based on the appearance of host factors, clinical criteria, and microbiological findings [96]. A possible IA requires the presence of a host factor and clinical criteria, whereas a probable IA is given when cases further meet the criteria for a mycological finding (Figure 4).

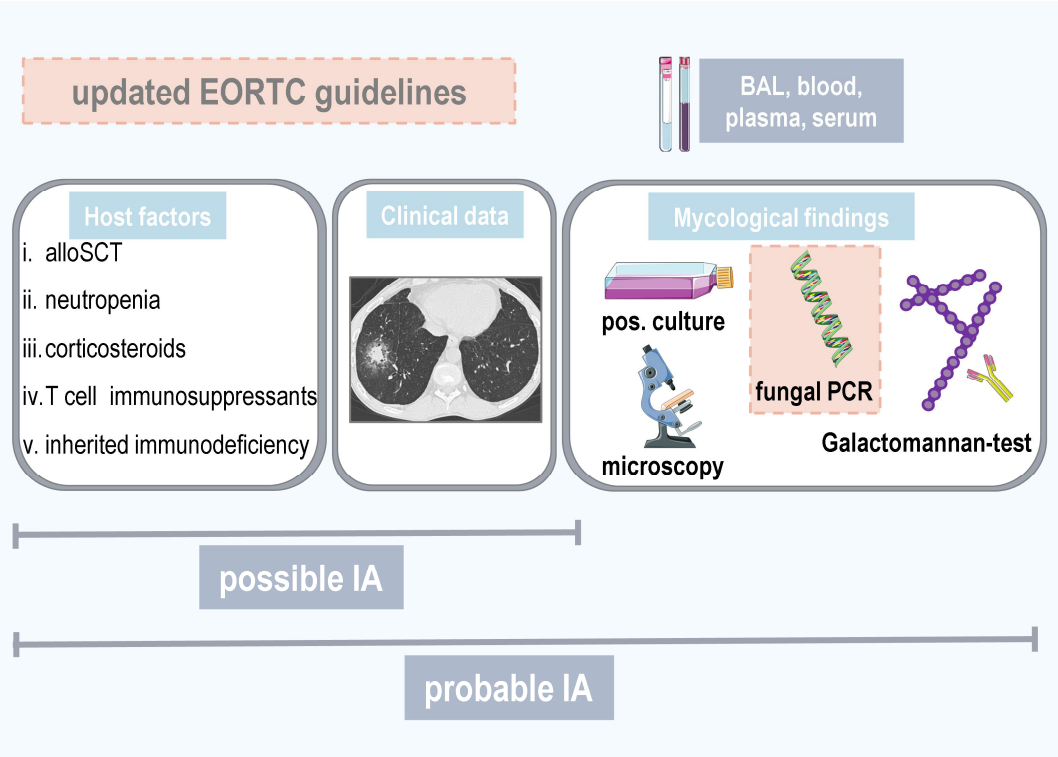

Figure 4: Updated EORTC guidelines. Critical host factors and the fulfillment of clinical factors define a possible IA, whereas the presence of a further mycological finding corresponds to a probable IA. Since December 2019, EORTC guidelines include the fungal PCR test within the group of mycological findings. CT scan acquired from [51].

A proven IA is characterized by either the recovery of mold from sterile body material or the detection of characteristic fungal morphologies by needle aspiration or biopsy accompanied by associated tissue damage [96]. Host factors include the recipience of an allograft, a recent history of neutropenia (< 0.5 x 10^9 cells/L for > 10 days), corticosteroid

treatment (minimum dose of 0.3 mg/kg/day for > 3 weeks), T cell immunosuppressant treatment, or an inherited severe immunodeficiency (Figure 4) [96]. A computed tomography (CT) scan with characteristic signs of an *Aspergillus* infection and the occurrence of a tracheobronchitis meet the criteria of a clinical factor. Mycological criteria include either direct tests (positive fungal culture or microscopy from BAL, sputum, bronchial brush, or sinus aspirate) or indirect tests. Indirect tests may be the detection of fungal galactomannan by the PLATELIA™ assay, or two consecutive, positive fungal PCRs (Figure 4).

1.1.6 Antifungal treatment

Antifungal therapy is applied under suspicion of a fungal infection. Voriconazole and isavuconazole are the preferred antifungals for first-line treatment of pulmonary IA [89]. Triazoles inhibit the ergosterol synthesis from lanosterol in the fungal cell membrane [97, 98]. These antifungals specifically target the cytochrome P450-dependent lanosterol 14α-demethylase (Erg11p), which catalyzes the reaction from lanosterol to ergosterol. In consequence, toxic methylsterol is accumulated and leads to fungal growth inhibition and cell death [99, 100].

Mutations in Erg11p mostly cause resistance to azole treatment, which is also documented for clinical isolates of *A. fumigatus* [101, 102]. A study performed in the Netherlands reports the occurrence of azole-resistant *Aspergillus* strains to be up to 9.4 % and claimed the high azole usage for crop protection as a possible source. Devastatingly, azole-resistant fungal infections were associated with high mortality rates within 12 weeks of diagnosis [103]. These studies highlight the importance of the responsible usage of antifungals and the need for future research in the development of alternative antifungal agents.

1.2 Interaction of *A. fumigatus* with the host

1.2.1 First-line barriers

After inhalation, conidia travel into the lungs and may reach the lower respiratory tract due to their small size (Figure 5) [8]. As the first physical barrier, respiratory epithelial cells express fungal pathogen recognition receptors (PRRs), which regulate the gene expression of pro-inflammatory cytokines, production of reactive oxygen species (ROS), and secretion of antimicrobial peptides upon fungal contact [104].

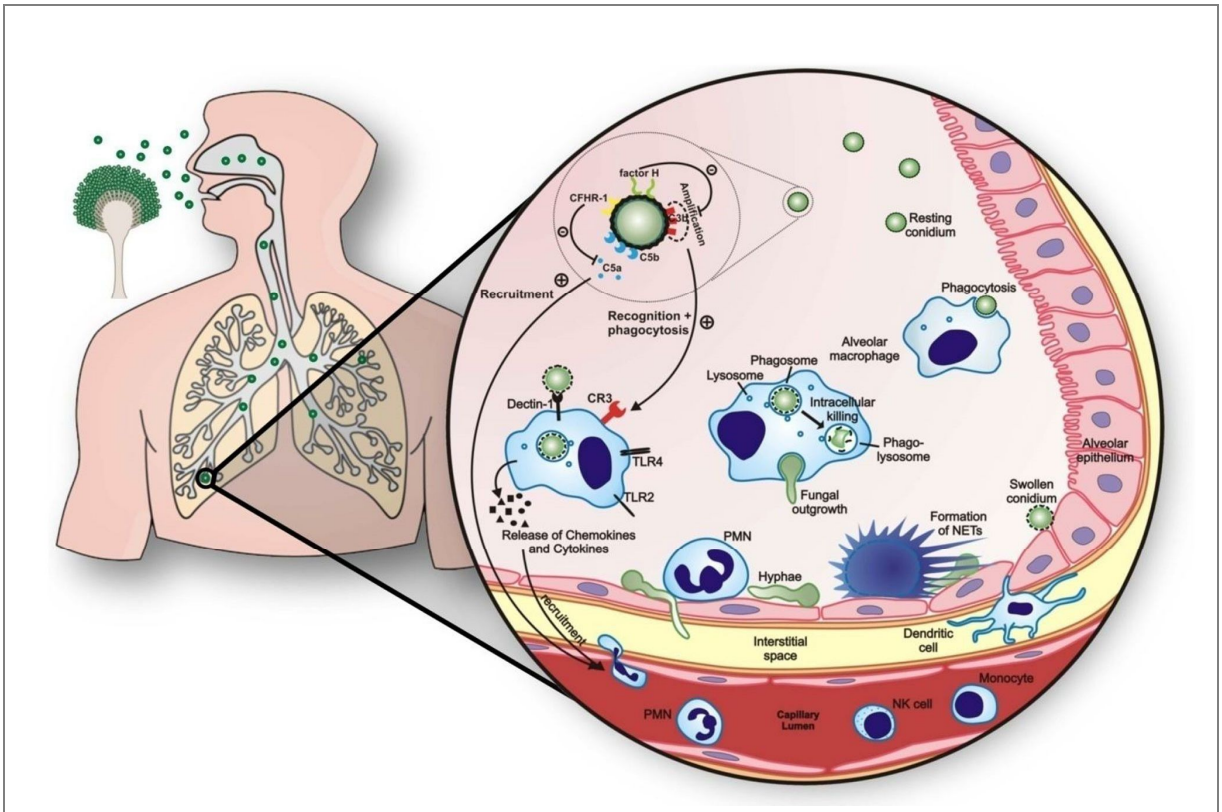

Figure 5: Conidial and hyphal morphologies interact with the human host. Inhaled *A. fumigatus* conidia reach the alveolar epithelium, which secretes defensins and antimicrobial peptides after fungal recognition. Alveolar macrophages and PMNs are proficient in killing fungal conidia by phagocytosis and neutrophil extracellular traps (NET) formation. Marking of *A. fumigatus* by the complement system further enables the phagocytosis by macrophages and PMNs. If not successfully cleared, conidia may outgrow and infiltrate deeper tissues. After endothelial infiltration, *A. fumigatus* hyphae can enter the bloodstream, where they interact with further immune cells, e.g. monocytes and NK cells. Figure adapted from [105].

PRRs are expressed on a variety of immune cells and bind to PAMPs on different fungal morphologies [23, 106]. DHN melanin, which covers *A. fumigatus* conidia, is recognized by the recently described PRR MelLec [23], while Dectin-2 binds to hyphal structures through the recognition of galactomannan [106].

Toll-like receptors (TLRs) are well-conserved fungal PRRs. TLR-2 was recently shown to directly bind to the cell wall polysaccharide chitin, while TLR-9 was actively recruited to *A. fumigatus* containing phagosomes [107, 108]. However, one of the best-studied fungal PRRs remains the β-1,3-glucan receptor Dectin-1 that is expressed on PMNs, macrophages, monocytes, and bronchial and alveolar epithelial cells [21, 109-112].

Soluble PRRs may opsonize PAMPs on the fungal surface. Opsonization leads to the activation of the complement system and marks conidia and germ tubes for phagocytosis by PMNs and other phagocytes that express the respective receptors, e.g., CR3 and CR1, on their surface [25, 113]. CR3 can further bind to unopsonized fungi by the interaction of β-1,3-glucan to the carbohydrate-binding site located in CD11b [114]. Once recognized either via PRRs or opsonization, *A. fumigatus* conidia are phagocytosed and killed via ROS in cytotoxic granules [115]. The severity of ineffective ROS production is documented in patients with chronic granulomatous disease that are susceptible to a variety of fungal diseases [116]. PMNs may further inhibit fungal growth by the formation of neutrophil extracellular traps (NETs) [117]. NETs mainly consist of DNA, histones, and granular proteins. High local concentrations of antimicrobial peptides lead to the degradation of virulence factors and the killing of the trapped pathogen [118].

1.2.2 Dendritic cells

Dendritic cells (DCs) develop from hematopoietic progenitor cells in the bone marrow and were firstly identified by their T cell-stimulating function [119, 120]. Those classical DCs (cDCs) can be divided into cDC1 and cDC2 [121]. Besides cDcs, plasmacytoid DCs (pDCs) were discovered that produce type 1 interferon in response to pathogens [122].

In blood, there are different DC subsets, namely pDCs and myeloid DCs (mDCs, cDC1, and cDC2). While pDCs display low fungicidal activity against conidia, *A. fumigatus* hyphae were shown to induce the secretion of TNF-α and INF-α by the interaction of Dectin-2 and galactomannan [106, 123, 124]. Stimulation with *A. fumigatus* morphologies induces the secretion of pro-inflammatory cytokines in mDCs, e.g., IL-6, TNF-α, IFN-γ, and IL-8 [124]. PDCs and mDCs are poorly represented in the human peripheral blood (pDC: 0.16-0.45 %; mDCs: 0.05-0.18 %); thus, alternative ways to perform *in vitro* studies with high cell numbers were developed [125].

Monocyte-derived DCs (moDCs) can be generated *in vitro* after $CD14^+$ isolation from peripheral blood mononuclear cells (PBMCs) and stimulation with GM-CSF and IL-4 for several days [126]. Compared to the DC subsets in the human blood, moDCs rather share similarities with mDCs than pDCs [124]. Following stimulation with *A. fumigatus* morphologies, moDCs secrete pro-inflammatory cytokines, e.g., IFN-γ, IL-12p70, IL-6, IL-8, IL-23,

and IL-17 [41, 124]. An inflammatory milieu can induce the differentiation from monocytes to inflammatory DCs (infDCs) *in vivo*, which were shown to share transcriptional similarities with *in vitro* generated moDCs [127, 128]. Immature moDCs are $CD1a^{+}CD14^{-}$ and express fungal PRRs, e.g. DC-SIGN (Dendritic Cell-Specific Intercellular adhesion molecule-3-Grabbing Non-integrin), Dectin-1, Dectin-2, Mannose receptor (MR), TLR-2, and TLR-4 (Figure 6) [123, 126, 129-133].

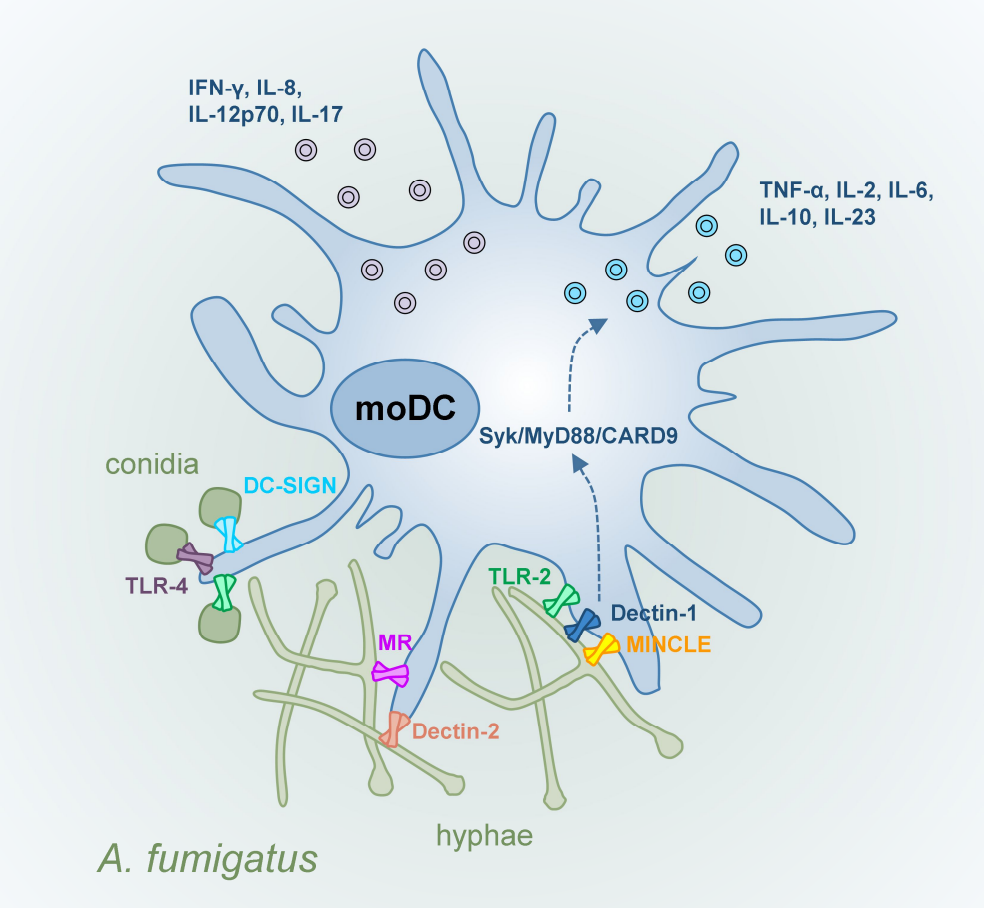

Figure 6: Fungal recognition and cytokine secretion by moDCs. MoDCs bind to *A. fumigatus* conidia and germ tubes with classical TLRs and C-type lectin receptors. Subsequently, effector mechanisms and cytokine secretion are initiated. Dectin-1 signaling induces the secretion of TNF-α, IL-2, IL-6, IL-10, and IL-23.

The C-type lectin receptor Dectin-1 recognizes β-(1,3)-glucans and induces signaling by synergizing with other receptors, e.g., TLR-2 and TLR-4 [109, 134]. Dectin-1 has an intracellular immunoreceptor tyrosine-based activation motif (ITAM)-like motif, and after ligand binding, Dectin-1 is tyrosine-phosphorylated by Src kinases. Canonical and non-canonical NF-κB signaling is initiated by Syk/Card9 signaling or Raf-1 [135-138]. Additionally, Syk was shown to induce MAPK activation independent of Card9, and Dectin-1 signaling can further lead to NFAT activation [138-140]. Finally, Dectin-1 mediated activation initiates the differentiation of T-helper 17 (Th17) and T-helper 1 (Th1) $CD4^{+}$ T cells *in vitro* [141].

1.2.3 NK-DC cross-talk

Cross-talk of immune cells is important to recruit further leukocytes to sites of inflammation, enhance immune cell function, and activate the adaptive immunity [142-145]. The interaction of NK cells and DCs with other cell types during infection with *A. fumigatus* was reported before [146, 147]. DC-neutrophil interactions were shown to be essential for DC maturation and migration to lymph nodes in an intrapulmonary infection model of *A. fumigatus*, as immature DCs accumulated in the lungs of neutropenic mice [146]. In another study, NK cell-derived IFN-γ was responsible for stimulating the anti-fungal activity of alveolar macrophages in *A. fumigatus* infected mice [147].

NK-DC cross-talk takes place in lymphoid organs and inflamed tissue and is defined by cell contact-dependent and independent mechanisms (Figure 7) [148-150]. NK cell activation can be triggered by MHC class I-related chain A and B (MICA/B)-NKG2D or CXC3CL1-CXC3CR1 interactions (Figure 7) [151, 152]. A study by Borg *et al.* showed that IL-12, present at the immunological synapse between NK cells and DCs, mediates NK cell activation and IFN-ɣ secretion [153]. NK cells can induce lysis of immature DCs by the interaction of DNAM-1 with its ligands poliovirus receptor (PVR) and Nectin-2 [154] (Figure 7). Interestingly, the activating NK cell receptor NKp30 can have a dual function and either initiates DC lysis or DC maturation by the secretion of IFN-α [149, 154].

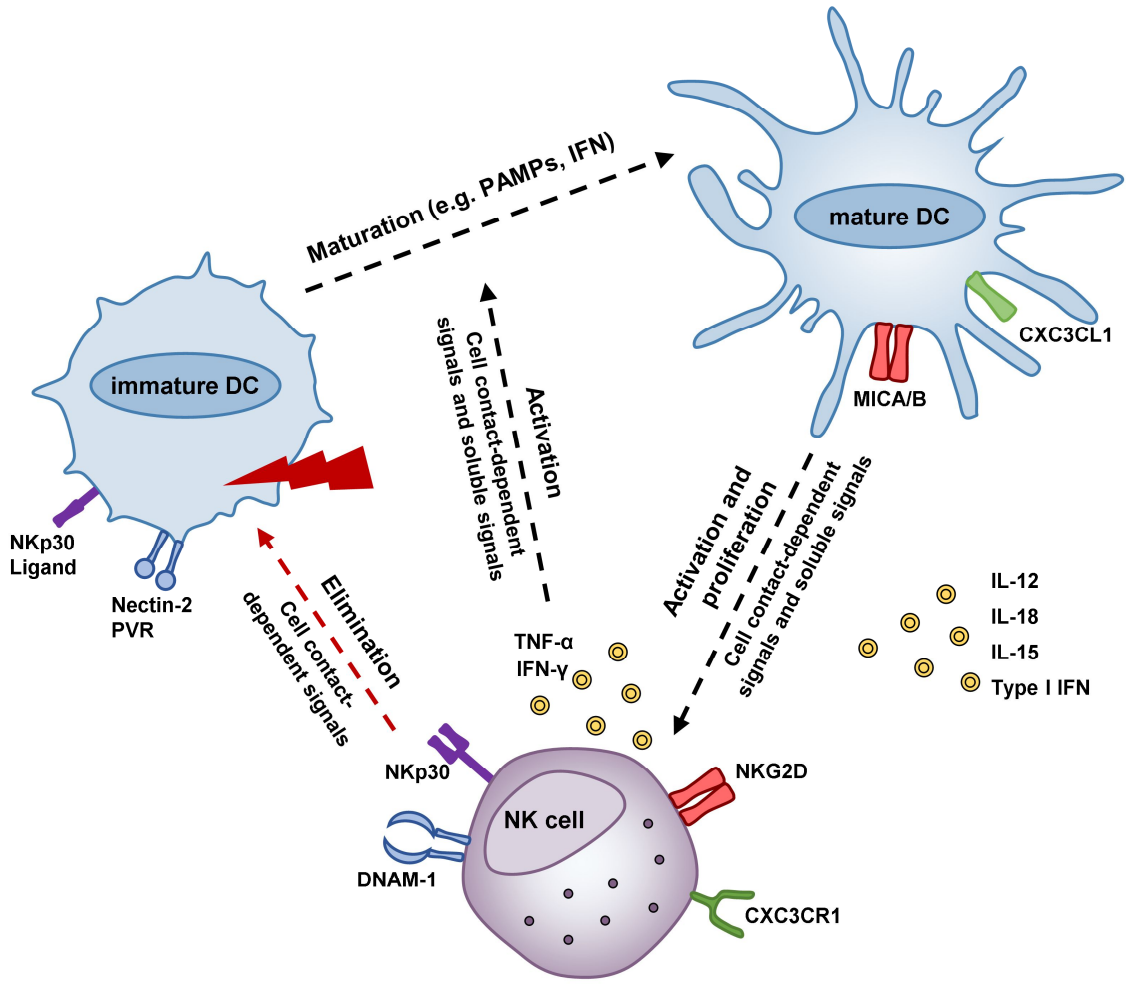

Figure 7: Soluble and cell contact-dependent NK-DC cross-talk. Reciprocal NK-DC interactions lead to the activation of both cell types. NK cells can lyse immature DCs or induce DC maturation by cell contact and independent mechanisms. Furthermore, mature DCs induce NK cell effector function by soluble and contact-dependent cross-talk. Figure adapted and modified from [155].

1.3 Natural killer cells

1.3.1 NK cell development

NK cells are innate lymphocyte cells derived from CD34+ progenitors. The NK cell development was long thought to occur in the bone marrow; however, recent studies show that CD34+ progenitor cells derived from the bone marrow can circulate and further develop in secondary lymphoid organs [156]. NK cells display a highly diverse subset with variable surface marker expression within the innate lymphoid cells (ILCs), as reviewed by Freud *et al.* [157].

NK cell maturation is directly linked to enhanced cell motility. By measuring the mean square displacement (MSD) during the development from CD34+ hematopoietic cells to NK cells over 21 days, Lee and Mace could demonstrate the progressive increase in the MSD throughout cell differentiation. To later stages in NK cell development, heterogeneity of cell migration was observed and correlated with the phenotypic heterogeneity of the NK cell subsets defined by flow cytometry [158].

In the blood, NK cells constitute to 5-20 % of the lymphocytes. Based on their surface expression of CD56 and CD16, NK cells are grouped into two major NK cell subsets, namely $CD56^{bright}CD16^{lo/-}$ and $CD56^{dim}CD16^{+}$ (Figure 8) [159-161]. In humans, around 90 % of the blood NK cells are $CD56^{dim}CD16^{pos}$, whereas the rest remain $CD56^{bright}CD16^{neg}$ [161]. While $CD56^{bright}$ NK cells are potent cytokine producers, $CD56^{dim}$ NK cells are proficient in lysing target cells, such as tumors or virally infected cells [162, 163]. There is multiple evidence that $CD56^{bright}$ cells are direct precursors of the $CD56^{dim}$ subset [164-166].

1.3.2 NK cell cytotoxicity

NK cell effector function is controlled by signals from inhibitory and activating receptors (Figure 8) [167-170]. According to the ‘missing-self hypothesis’, lysis of targets is mediated by the absence or reduced expression of major histocompatibility complex (MHC) class I molecules on ‘non-self’ cells [171]. Killer cell immunoglobulin-like receptors (KIR) recognize and bind autologous MHC molecules, thereby activate the immunoreceptor tyrosine-based inhibitory motif (ITIM) domain leading to an inhibition of NK cell effector function [172]. Since tumors and virally infected cells hardly express MHC molecules on their surface, the missing signals from inhibitory receptors lead to a shift of NK cell function towards activation and target cell lysis [173-175].

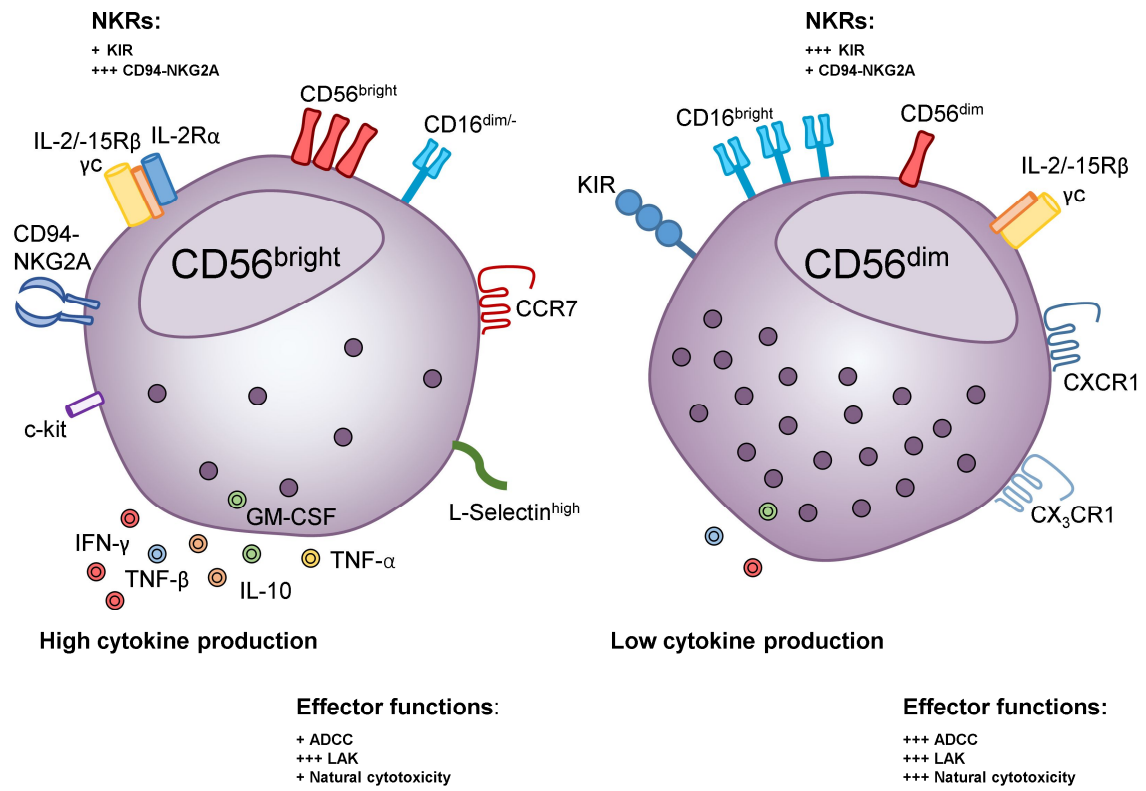

Figure 8: NK cell subsets in the peripheral blood. The major NK cell subsets in the human blood are $CD56^{bright}$ and $CD56^{dim}$ NK cells. $CD56^{bright}$ NK cells express the homing receptor CCR7, are highly stimulated by IL-2, secrete cytokines, and show a high surface expression of CD56. In contrast, $CD56^{dim}$ NK cells display a lower abundance of CD56 molecules on their surface, express chemotactic receptors, KIRs, and the antibody-dependent cellular cytotoxicity (ADCC) receptor CD16. Both subsets display high lymphokine-activated killer (LAK) activity. Figure adapted and modified from [176].

The immunological synapse (IS) between NK cells and target cells is formed after target cell recognition by activating NK cell receptors, actin-dependent reorganization of those receptors, and microtubule-dependent relocalization of cytolytic granules to the IS [177]. Released at the IS, the pore-forming protein perforin enables the entry of the pro-apoptotic granzyme B into the target cell, while proteins that are present on the NK cell after exocytosis prevent killer mediated self-destruction [178-180]. Granzymes induce target cell apoptosis by the cleavage of several proteins, e.g., caspase-3, DNA-PK, and Bid [181-183].

The granzyme/perforin pathway is a fast process (~20 min after target cell recognition), which can occur in serial killing events [184]. Besides serial killing, NK cells can eliminate targets by the interaction of Fas-ligand (FasL) and TNF-related apoptosis-inducing ligand (TRAIL) with the respective receptors on the target cell [185, 186]. This interaction leads to the activation of the Caspase 8/10 signaling pathway in target cells and subsequently to cell

apoptosis [187-190]. While serial killing is a fast and periodic event, death receptor-mediated target cell apoptosis occurs later after recognition (~2 h) and is seen as the 'final killing event' [184].

1.3.3 NK cells and pathogens

NK cells play essential roles in pathogenic infections with, e.g., viruses, bacteria, protozoa, and fungi [191-195]. Among the fungal pathogens, human NK cell receptors were identified as PRRs for *Cryptococcus (C.) neoformans*, *Candida (C.) glabrata,* and *Candida (C.) albicans* [191, 192]. The C-type lectin receptor NKp30 recognizes β-(1,3)-glucan at the surface of *C. albicans* and *C. neoformans* and induces granule repolarization and fungal killing [191, 196]. The activating human NK cell receptor NKp46 and the mouse ortholog NCR1 were shown to bind the fungal adhesins Epa1, Epa6, and Epa7 and mediate fungal killing of *C. glabrata* (Figure 9) [192].

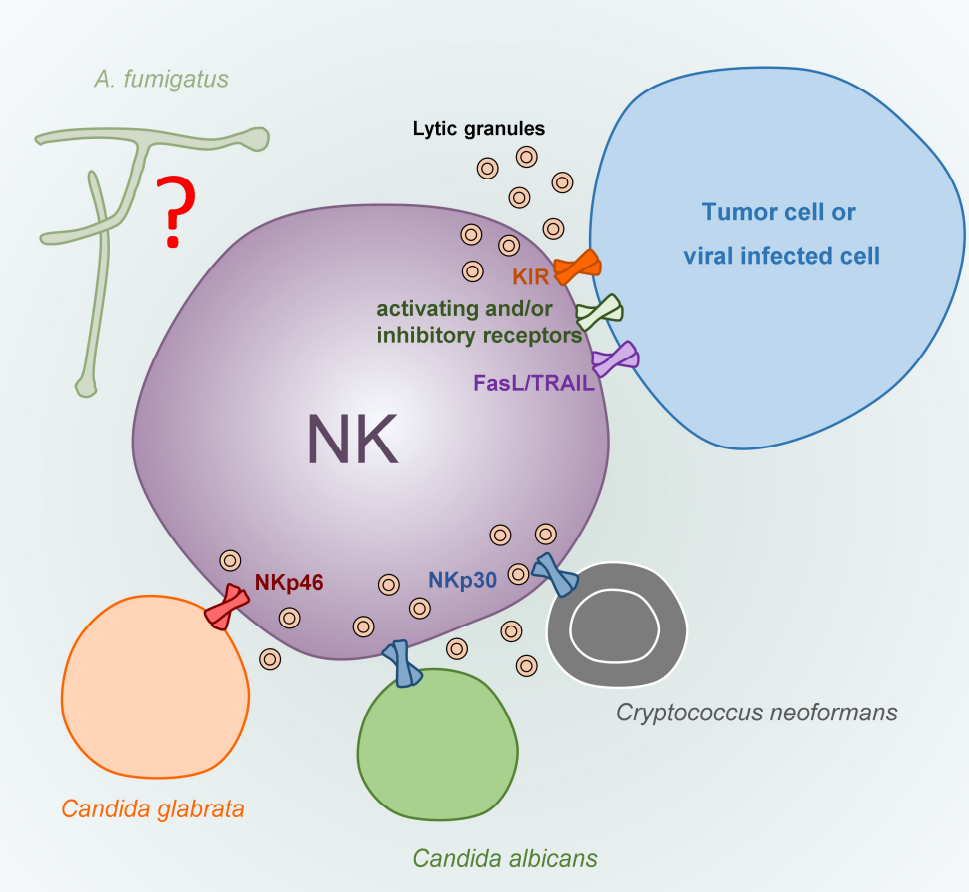

Figure 9: NK cell interaction with target cells. Killer cell Ig-like receptor (KIR) signaling following interaction with major histocompatibility complex (MHC) class I molecules inhibits NK cell killing. NK cells can recognize target cells by activating and inhibitory receptors, and cytotoxicity is mediated by granzyme/perforin or death receptor signaling (FasL/TRAIL). Pathogenic fungi are recognized by NKp30 (*Candida albicans* and *Cryptococcus neoformans*) or NKp46 (*Candida glabrata*), leading to the release of cytotoxic granules. The PRR for *A. fumigatus* remains unknown so far.

The PRR for *A. fumigatus* remains unknown so far but would be of great interest, as several studies implicate the importance of NK cells during *A. fumigatus* infections. Morrison *et al.* demonstrated that CCL2-mediated NK cell migration into lungs of neutropenic mice was critical for early host defense mechanisms during IA [197]. A later study performed by Park *et al.* showed that NK cells are the early source of IFN-γ in the lungs of mice developing IA and that IFN-γ is essential to stimulate further innate immune cells, e.g. alveolar macrophages [147, 198]. The relevance of NK cells in a clinical setting was shown by Stuehler *et al.,* showing that patients after alloSCT had a worsened outcome of IA in cases of delayed NK cell reconstitution or lowered NK cell counts in the peripheral blood [199]. Hence, NK cells support the innate immune system during IA infections and especially may have a protective function during neutropenia.

1.3.4 CD56

The neural cell adhesion molecule (NCAM1, CD56) is mainly studied in the nervous system, where it plays a crucial role in neuronal development, synaptic plasticity, and regeneration, as reviewed by Ditlevsen *et al.* [200]. CD56 consists of three major isoforms that are generated by alternative splicing from a single gene on chromosome 11[201-204]. These isoforms differ in size and can contain extracellular, transmembrane and/or intracellular domains. CD56 may include all three domains (180 kD isoform), a shorter intracellular domain (140 kD isoform), or only an extracellular domain with a transmembrane GPI anchor (120 kD isoform) [201, 205, 206].

The extracellular domain contains five immunoglobulin-like (Ig) domains followed by two fibronectin type III (FNIII) domains [207, 208]. The Ig domains are involved in homophilic binding to other CD56 molecules on the same (*cis*) or on other cells (*trans*) [209]. Additionally, CD56 can interact with extracellular matrix components, e.g., heparin or collagen [210, 211]. CD56 is expressed on different leukocyte subsets, e.g., T cells, monocytes, and dendritic cells, but the highest expression is observed on NK cells that express all three isoforms [176, 212-214].

In particular, CD56 was shown to play a crucial role during NK cell maturation. A study from Mace *et al.* showed that CD56, Src family kinases, and CD62L are required for $CD56^{bright}$ NK cell motility on stromal cells. By the addition of CD56 blocking antibodies to the *in vitro* differentiation, the frequency of stage 4 $CD56^{bright}$ NK cells was decreased, and CD34+ precursor cells accumulated, concluding that CD56 is involved in NK cell development [215].

There is multiple evidence that CD56 might be involved in cytotoxicity as CD56+ tumor cells are more sensitive to NK cell-mediated cytotoxicity and ectopic CD56 expression on CD56- tumor cells increases target cell lysis [216, 217]. Interestingly, CD56 down-regulation after incubation of healthy NK cells in sera from chronic lymphocytic leukemia (CLL) patients reduced target cell lysis, further indicating a role for CD56 in cytotoxicity [218]. CD56 can be post-translational modified with, e.g., polysialic acid (PSA) on the Ig5 domain [219]. This post-translational modification is unique since the chain length of loaded PSA can reach up to 370 residues [220]. Sialyltransferases catalyze this reaction and thereby mediate the highly negative charge of CD56 [221]. PSA was shown to be involved in NK cell activation and cytotoxicity [220, 222].

1.4 Aims of the thesis

Immune cell interactions may enhance individual cell responses to pathogens. NK cells and DCs are cells of the innate immune system that were shown to interact directly and indirectly with the fungal mold *A. fumigatus*. Therefore, this study aimed to investigate immune cell interactions in the context of NK-DC cross-talk during *A. fumigatus* infections. The recognition of fungal morphologies is mediated by PRRs, which interact with PAMPs on the pathogen's surface. In contrast to moDCs, *Aspergillus* specific PRRs are rarely studied on NK cells. Therefore, the aim was to stimulate NK cells and moDCs with *A. fumigatus* morphologies and ligands for PRRs, and analyze the reciprocal cell activation by co-culturing stimulated cells with the autologous, unstimulated counter cell type.

Additionally, cytokines and chemokines that correspond to NK-DC cross-talk should be analyzed. In particular, this study aimed to investigate the impact of secreted factors after stimulation of the moDC receptors Dectin-1 and TLR-2 on NK cell activation. Therefore, signaling of Dectin-1 and TLR-2 should be silenced or blocked on post-transcriptional and protein levels, followed by stimulation with specific PRR ligands and transfer of soluble factors on autologous NK cells (Figure 10).

Since there is no PRR on NK cells known that recognizes *A. fumigatus*, the aim of the thesis was to identify the fungal interaction partner on NK cells (Figure 10). Therefore, live-cell co-cultures and screening of possible receptor candidates with flow cytometric and microscopic approaches should be performed.

NK cells were shown to counteract fungal infections, as patients after alloSCT display a higher risk to develop IA when NK cell reconstitution is delayed, or cell counts are diminished in the peripheral blood. Therefore, the goal was to characterize functional differences between NK cells derived from recipients of an allograft and healthy individuals (Figure 10). This should be performed by isolating NK cells from the peripheral blood of patients on defined time points after alloSCT (60, 90, 120, and 180 days). NK cells would be challenged with live *A. fumigatus* germ tubes before analyzing NK cells regarding the expression of surface receptors and secretion of soluble factors.

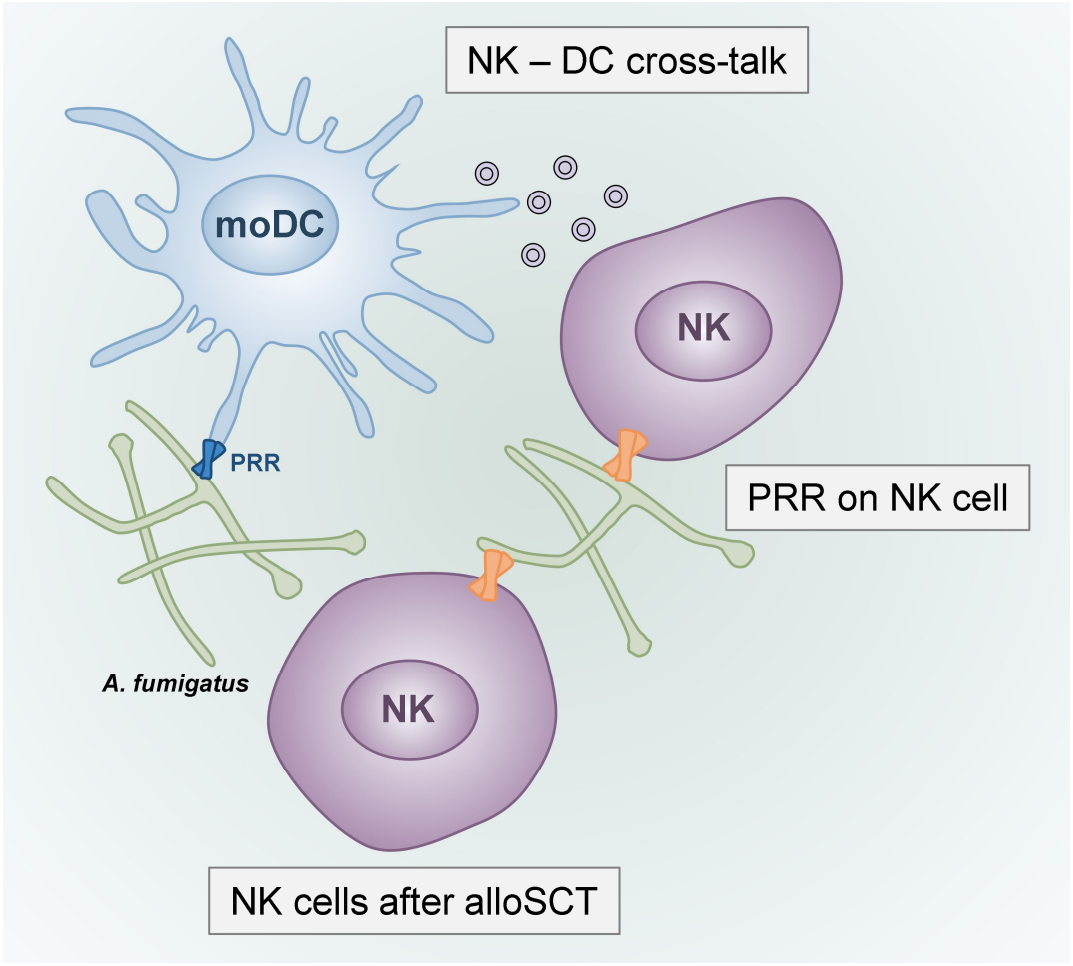

Figure 10: Aim of the thesis. The aim of the thesis was to investigate NK-DC cross-talk during infection with *A. fumigatus*. In particular, the impact of the on moDCs expressed PRRs Dectin-1 and TLR-2 on NK cell activation should be analyzed. Due to the lack of known fungal PRRs on NK cells, screening for possible fungal recognition receptors on NK cells should be performed. Additionally, the function of NK cells after allogeneic stem cell transplantation (alloSCT) should be investigated and compared with NK cells derived from healthy donors.

2 Material and Methods

2.1 Material

2.1.1 Equipment and consumables

Tables 1 and 2 list the used equipment and the consumables in the study.

Table 1: Equipment used in the study.

Designation	Brand name/specification	Manufacturer
2D *d*STORM (microscopy)	IX-71	Olympus
3D *d*STORM (microscopy)	Axio Observer.Z1 equipped with a water-immersion objective (LD C-Apochromat 63x/1.15W Corr M27)	Carl Zeiss Microscopy
Cell counter	VICELL XR	Beckman Coulter
Cell culture incubator	CO_2 Incubator C60	Labotect
Cell culture incubator	CO2-Inkubator HERAcell 240	Thermo Scientific
Centrifuge	Centrifuge 5415 R	Eppendorf
Centrifuge	Galaxy Mini Centrifuge	VWR
Centrifuge	Heraeus® Multifuge® 3SR and 3S	Thermo Scientific
Centrifuge	MC-6400 Centrifuge	Hartenstein
Centrifuge	Rotanta 46 RC	Hettich
Confocal Laser Scanning Microscopy	LSM700 System with a Plan-Apochromat 63x/1.40 oil immersion objective	Carl Zeiss Microscopy
Cryostorage system and liquid nitrogen tank	K Series Cryostorage System with XL-240 tank	Tec-lab GmbH
DNA gel documentation system	AlphaImager™ Light Cabinet	Biozym
DNA gel electrophoresis system	BluePower 500	Serva
ELISA reader	GENios Microplate Reader and Infinite® 200 PRO	Tecan
ELISA washer	hydroFLEX microplate washer	Tecan
Flow cytometer	BD FACSCalibur	BD Bioscience
Fridge and freezer	CUP 3021 and HERAfreeze	Liebherr
Hemocytometer	Neubauer Improved	HBG Henneber-Sander
Laboratory Seesaw	Duomax 1030	Heidolph
Laboratory Seesaw	Mini Rocker Shaker	Hartenstein
MACS separator	Quadro MACS Separator	Miltenyi Biotec
Magnetic stirrer	Variomag Electronicrührer	Monotherm
Microscope	Microscopes Eclipse 50i and TS 100	Nikon
Microwave	MM41568	Micromaxx®
Mister Frostie	Cryogenic storage system K series	Taylor-Wharton
Multiplex Reader	Bio-Plex 200 System	Bio-Rad
PCR pipetting box	DNA/RNA UV-Cleaner box UVC/T-AR	BioSan

Table 1 (continued): Equipment used in the study.

Designation	Brand name/specification	Manufacturer
pH meter	pH 211 Microprocessor pH Meter	Hanna instruments
Pipettes	Pipettes Eppendorf Reference and Xplorer	Eppendorf
Pipettus	Accu-jet pro	Brand
Protein gel casting system	Mini-PROTEAN 3 system	Bio-Rad
Real-time PCR machine	StepOnePlus™	Applied Biosystems
Scales	AED	Kern
Scales	GF-2000	AND Instruments
SEM (Scanning Electron Microscopy)	JSM-7500F with a detector for secondary electrons (SEI detector)	JEOL
Semi-dry blotting chamber	BlueFlash-M	Serva
Shaker	HT	Infors AG
SIM (Structured Illumination Microscopy)	Elyra S.1 with a Plan-Apochromat 63x/1.4 oil objective in combination with 642nm, 561nm, and 405nm laser lines	Carl Zeiss Microscopy
Sonificator	UP50H	Hielscher Ultrasonics
Spectrophotometer	NanoDrop 1000	Peqlab
Thermal cycler	Eppendorf 5341	Eppendorf
Thermal cycler	9800 Fast Thermal Cycler	Applied Biosystems
Vortexer	Vortex Genie 2	Scientific Industries
Waterbath	Waterbath Memmert	Memmert
Workbench	MSC-Advantage™	Thermo Scientific

Table 2: Consumables used in the study.

Designation	Brand name/ specification	Manufacturer
12-well plate	Multiwell™ 12 well	BD Bioscience
200 µl tubes	Multiply®- µStrip Pro 8-strip low profile	Sarstedt
24-well plate	Multiwell™ 12 well	BD Bioscience
48-well plate	Multiwell™ 12 well	BD Bioscience
6-well plate	Multiwell™ 12 well	BD Bioscience
75-flasks	CellSTAR®	Greiner Bio-One
8 well chambers (microscopy)	8-well Tissue Culture Chambers	Sarstedt
96-well half area (ELISA)	Costar® Assay Plate, Clear, Flat Bottom, Half Area, High Binding, Polystyrene	Corning
96-well plate	Multiwell™ 12 well	BD Bioscience
96-well plate (ELISA)	Microplate, 96 well, PS, F- Bottom	Greiner bio-one
96-well plate (PCR)	MicroAmp™ 96 well Tray for VeriFlex™ Blocks	Applied Biosystems
Blotting paper	Mini Trans-Blot® Filter Paper	Bio-Rad
Cell scraper	Cell Scraper 16 cm	Sarstedt
Cell strainer	BD Falcon™ Cell Strainer, 40 µm	BD Bioscience

Table 2 (continued): Consumables used in the study.

Designation	Brand name/ specification	Manufacturer
Coverslips (microscopy)	18 mm round coverslips	Hartenstein
Cryopreservation tubes	CryoTube Vials	Nunc
EDTA whole blood collection columns	S-Monovette® 9 ml K3E 1.6 mg EDTA/ml	Sarstedt
Electroporation cuvettes	Gene Pulse Cuvette 0.4 cm	Bio-Rad
Falcons (15 and 50 ml)	CellStar Tubes	Greiner Bio-One
Filter tips (1000 µl)	TipOne 1000 µl XL Graduated Filter Tip	StarLab
Filter tips (20 and 100 µl)	Biosphere Filter Tips	Sarstedt
Flow cytometry tube	Polystyrene round-bottom tube, 5 ml	BD Bioscience
MACS separation column	LS Column	Miltenyi Biotec
Medical X-ray film	Fuji SuperRX	Hartenstein
Microplates for ELISA (96 well)	Flat bottom, binding, crystal-clear	Greiner Bio-One
Needle (20G)	BD Microlance 3 20G needles	BD
Nitrocellulose membrane	Protan, Nitrocellulose-Transfer membrane, 0.45 µm	Schleicher-Schell
Object slides (microscopy)	object glass slides	Hartenstein
Optical adhesive cover/ sealing strip (ELISA)	ELISA Plate Sealers	R&D Systems®
Optical adhesive cover/ sealing strip (PCR)	Sealing tape, optically clear	Sarstedt
Pasteur pipette	Transfer Pipette 3.5 ml	Sarstedt
Protein gel electrophoresis gels	Mini-PROTEAN® TGX™ Precast Gels	Bio-Rad
Reaction tube	Micro Tubes (1.5 and 2 ml)	Sarstedt
Serological pipettes (5, 10, and 25 ml)	Cellstar Serological Pipettes	Greiner Bio-One
Syringes (2, 5, and 10)	BD Discardit II	BD

2.1.2 Kits

The used kits are listed in Table 3. All the kits were stored accordingly to the manufacturer's instructions.

Table 3: Kits used in the study.

Designation	Brand Name	Contents	Cat. No.	Manufacturer
cDNA synthesis kit	First Strand cDNA Synthesis	M-MuLV Reverse Transcriptase (20 U/µl), RiboLock RNase Inhibitor (20 U/µl), 5X Reaction Buffer, 10mM dNTP Mix, Random Hexamer Primer (100 µM, 0.2 µg/ml), Water, nuclease-free	K1612	Thermo Scientific
DNA digestion kit	RNAse-Free DNase Set	DNase I, RNase-Free (lyophilized), 1500 Kunitz units Buffer RDD, RNase-free water	79254	Qiagen

Table 3 (continued): Kits used in the study.

Designation	Brand Name	Contents	Cat. No.	Manufacturer
ELISA (CCL3/MIP-1α)	DuoSet® Detection System	Capture Antibody, Detection Antibody, Standard, and Streptavidin-HRP	DY270-05	R&D
ELISA (CCL4/MIP-1β)	DuoSet® Detection System	Capture Antibody, Detection Antibody, Standard, and Streptavidin-HRP	DY271-05	R&D
ELISA (CCL5/RANTES)	ELISA MAX™ Deluxe Set	Coating Buffer (5X), Capture Antibody (200X), Assay Diluent (5X), Detection Antibody (200X), Avidin-HRP (1000X)	440804	BioLegend
ELISA (perforin)	Human Perforin ELISA Set	Capture antibody, Detection biotinylated anti-Perforin antibody, PRF1 Standard, Ready-to-use TMB, Streptavidin-HRP	Ab83709	Abcam
Intrastaining kit	Cytofix/ Cytoperm™	Cytofix/Cytoperm™ (1X) Perm/Wash Buffer (10X)	554714	BD Bioscience
Monocyte isolation beads	CD14 MicroBeads	2 ml CD14 MicroBeads, human	130-050-201	Miltenyi Biotec
Multiplex immunoassay for DCs	ProcartaPlex® Multiplex Immunoassay	IL-1α, IL-1β, IL-2, IL-6, IL-8, IL-10, IL-12p70, IL-15, IL-18, TNF-α, MIP-3α, IP-10, and IFN-γ	-	eBioscience
Multiplex immunoassay for NK cells	ProcartaPlex® Multiplex Immunoassay	MIP-1α, MIP-1β, RANTES, Perforin, Granzyme B, IL-8, IL-6, TNF-α, IL-1α, GM-CSF, IFN-γ	-	eBioscience
NK cell isolation beads	NK cell Isolation Kit	1 ml NK Cell Biotin-Antibody Cocktail, 2 ml NK Cell MicroBead Cocktail	130-092-657	Miltenyi Biotec
RNA isolation kit	RNeasy MiniKit	RNeasy Mini Spin Columns, Buffer RLT, Buffer RW1, Buffer RPE, RNase-Free Water	74106	Qiagen
Whole blood NK cell isolation kit	MACSxpress® Whole Blood NK Cell Isolation Kit	Buffer A, Buffer B, lyophilized beads conjugated to monoclonal antibodies (3 vials)	130-098-185	Miltenyi Biotec

2.1.3 Reagents, cytokines, and buffers

Table 4 lists the reagents used in the study. If not stated otherwise, all reagents were stored accordingly to the manufacturer's recommendations.

Table 4: Reagents used in the study

Designation	Brand Name	Contents	Cat. No.	Manufacturer
Agarose	Agarose Standard	500 g Agarose Standard	3810.3	Roth
Antibiotic	Refobacin®	Gentamycinsulfat 80 mg	PZN-7829173	Merck

Table 4 (continued): Reagents used in the study.

Designation	Brand Name	Contents	Cat. No.	Manufacturer
Coenzyme Q_0 (XTT)	2,3-Dimethoxy-5-methyl-*p*-benzoquinone	1 g of Coenzyme	D9150-1G	Sigma-Aldrich
Culture medium	RPMI 1640 with and without phenol red	Rosewell Park Memorial Institute 1640 medium, GlutaMAX™-I (glutamine) supplement, HEPES	72400-054	LifeTechnologies (Invitrogen)
Development solution (western blot)	Development solution for medical x-ray processing	Reagents A (1000 ml) and B (250 ml)	HT536	AGFA
DMSO	DMSO	Dimethylsulfoxide	HN47.1	Roth
DNA ladder	100bp ladder	0.5 ml DNA ladder 500 µg/ml	N3231L	New England Biolabs
DNA loading buffer	Gel Loading Dye, Blue (6X)	4 ml of gel loading dye	B7021S	New England Biolabs
ECL western blot solution	Clarity Western ECL Substrate	100 ml Clarity western luminol/enhancer solution 100 ml peroxide solution	170-5060	Bio-Rad
EDTA	EDTA	Ethylenediaminetetraacetic acid disodium salt solution, 0.5 M	E7889	Sigma-Aldrich
Ethanol 100 %	Ethanol 100 %	-	32205-1l	Sigma-Aldrich
Ethanol 70 %	Ethanol 70 %	-	-	UKW Pharmacy
Ethidium bromide solution	Ethidium bromide solution	10 ml solution	E1510	Sigma-Aldrich
FACS Clean	BD FACS Clean Solution	Clean Solution (5 l)	340345	BD Bioscience
FACS Flow	BD FACS Flow Sheath Fluid	Flow Solution (20 l)	342003	BD Bioscience
FACS Rinse	BD FACS Rinse Solution	Rinse Solution (5 l)	340346	BD Bioscience
FCS	FBS	Fetal Bovine Serum	F7524	Sigma-Aldrich
Ficoll	Biocoll Separating Solution	Density 1.077 g/ml, isotonic	L6115	Biochrom
Fixation solution (western blot)	Rapid Fixer for medical x-ray processing	1000 ml of fixation solution	2828Q	AGFA
Formaldehyde	Formaldehyde solution 37 %	37 % formalin stabilized with methanol (1000 ml)	7398.1	Roth
H_2SO_4	H_2SO_4	1 mol/l $H2_SO_4$ (1000 ml)	X873.1	Roth
HBSS	Hank's Balanced Salt Solution (HBSS)	with $NaHCO_3$, calcium chloride and magnesium sulfate	H6648	Sigma-Aldrich
Mounting medium	ProLong™ Gold Antifade Mountant	5 x 2 ml mounting reagent	P36934	Thermo Scientific
NaOH	NaOH	1 mol/l NaOH (1000 ml)	1.09137.1000	Merck
Poly-D-lysine	Poly-D-lysine hydrobromide	10 mg of lyophilized poly-D-lysine	P7886-10mg	Sigma-Aldrich

Table 4 (continued): Reagents used in the study.

Designation	Brand Name	Contents	Cat. No.	Manufacturer
Protease inhibitor tablets	cOmplete	Protease Inhibitor Cocktail tablets in a glass vial	1169498001	Roche Life Science
Protein gel electrophoresis buffer	10X TGS	25 mM Tris, 192 mM Glycine, 0.1 % SDS, pH 8.3 (1X dilution)	1610732	Bio-Rad
Protein ladder	PageRuler Prestained Ladder	170 – 10 kDa ladder	26616	Thermo Scientific
Protein loading buffer	4X SDS	4X SDS	70607-3	Merck
Red blood lysis solution	Red Blood Cell Lysis Solution	Red Blood Cell Lysis Solution, 10X	130-094-183	Miltenyi Biotec
RNA stabilizing reagent	RNAprotect	250 ml RNAprotect Cell Reagent	76526	Qiagen
SimplyBlue™ staining solution	SimplyBlue™ SafeStain	staining solution (1 l)	LC6060	Thermo Scientific
Sterile water	Aqua B. Braun	-	0123	B. Braun
SYBR green mastermix	iTaq™ Universal SYBR® Green Supermix	2x concentrated, ready-to-use reaction qPCR master mix	172-5124	Bio-Rad
TAE 10X buffer	UltraPure™ TAE Buffer	400 mM Tris-acetate 10 mM EDTA	15558-042	Invitrogen
TMB substrate	TMB Substrate Solution	2x 110 ml Substrate A and B	421101	BioLegend®
Trypan blue	Trypan Blue	Trypan Blue solution (0.4 %)	93595	Sigma-Aldrich
Tween® 20	Tween® 20	1000 ml of reagent	P1379-1L	Sigma-Aldrich
Water	Ampuwa®	-	PZN-1214482	FreseniusKabi
XTT sodium salt	XTT sodium salt	500 mg XTT reagent	X4626-500mg	Sigma-Aldrich

Table 5 lists the cytokines and stimulants used for NK cell and moDC cell cultures. All cytokines were stored in aliquots at -20°C if not stated otherwise.

Table 5: Cytokines and stimulants used in cell culture.

Designation	Stock solution and storage	Final concentration	Cat. No.	Manufacturer
***A. fumigatus* whole cell lysate**	Diluted in 1X PBS and stored in aliquots at -20 °C	1 µg/ml (NK cells), 5 µg/ml (moDCs)	BA132VS	Manufactured by Serion® Immunologics and sold by Lophius Bioscience
AI (alkali-insoluble) cell wall lysate	Stored at 4 °C	5 µg/ml	-	[223, 224]

Table 5 (continued): Cytokines and stimulants used in cell culture.

Designation	Stock solution and storage	Final concentration	Cat. No.	Manufacturer
LPS (TLR-2/TLR-4 ligand)	0.1 µg/ml in HBSS	1 µg/ml	Tlrl-eklps	InvivoGen
Negative control siRNA	20 µM AllStars Negative Control siRNA in ET-free water, stored in aliquots at -20 °C	1.25 µM	1027280	Qiagen
Proleukin® S (IL-2)	50,000 U/ml in HBSS, stored in aliquots at -20 °C	1000 U/ml	Ordered by UKW pharmacy	Novartis
TLR-2 blocking antibody	0.1 mg/ml in ET-free water, stored in aliquots at -20 °C	10 µg/ml	mab2-mtlr2	Invivogen
Zymosan (TLR-2/Dectin-1 ligand)	1 mg/ml in HBSS, stored in aliquots at 4 °C	10 µg/ml	Tlrl-zyn	InvivoGen
Zymosan depleted (Dectin-1 ligand)	5 mg/ml in HBSS, stored in aliquots at -20 °C	100 µg/ml	Tlrl-zdzn	InvivoGen

Table 6 lists the self-made solutions. If not stated otherwise, buffers were stored at room temperature.

Table 6: Self-made solutions.

Designation	Contents and preparation
1st antibody diluent (Western blotting)	Dilute the 1st antibody as desired in 5 % milk in TBST or 5 % BSA in 12 ml TBST, add 0.05 % Sodium azide, store at 4 °C
2nd antibody diluent (Western blotting)	Dilute the 2nd antibody 1:10,000 in 5 % milk in TBST in a total volume of 10 ml, store at 4 °C
Blocking solution and antibody staining solution (microscopy)	Dissolve 5 % BSA in HBSS, store at 4 °C
Cell culture medium	RPMI 1640 supplemented with 10 % FCS and 120 µg/ml Refobacin, store at 4 °C
Fixation solution (microscopy)	Dissolve 3 % formaldehyde in RPMI, store at 4 °C
HBSS buffer (cell isolation)	HBSS supplemented with 1 % FCS and 2mM EDTA, store at 4 °C
PBS, 10X	Dissolve 80 g NaCl, 11.6 g Na_2HPO_4, 2 g KH_2PO_4, and 2 g KCl in1 l H_2O and adjust pH to 7.4
PBS, 10X	Dissolve 80 g NaCl, 11.6 g Na_2HPO_4, 2 g KH_2PO_4, and 2 g KCl to 1l with H_2O, adjust pH to 7.4
PE-buffer (Western blotting)	Dissolve 40 g Urea, 10 ml Glycerin, 1 g SDS, and 1.21 g Tris in 1 l H_2O and adjust pH to 6.8, dissolve one tablet of protease inhibitor in 10 ml buffer supplemented with 5 µl 1 M DTT, store in aliquots at -20 °C
Ponceau staining solution (Western blotting)	Dissolve 0.5 g Ponceau S in 100 ml acetic acid
Semi-dry blotting buffer	Dissolve 3.03 g Tris, 14.41 g Glycine in 895 ml H_2O, add 100 ml methanol and 5 ml 10 % SDS diluted in water, adjust pH to 8.3 and store at 4 °C

Table 6 (continued): Self-made solutions.

Designation	Contents and preparation
TBS, 10X	Dissolve 12.18 g Tris and 87.66 g NaCl to 1 l with H_2O, adjust pH to 7.5
TBST (Western blotting)	Dilute 50 ml TBS stock solution to 1X TBS with H_2O
Wash buffer (ELISA)	Dissolve 100 ml PBS stock solution (10X) to 1X PBS, add 0.05 % Tween® 20 and fill up to 1l with H_2O

Table 7 lists the used primers in the study. Primers were diluted with nuclease-free water and stored at -20 °C.

Table 7 Primers used in the study.

Gene	Accession Number	Forward primer	Reverse primer
ALAS	NM_000688.5	GGCAGCACAGATGAAT-CAGA	CCTCCATCGGTTTTCA-CACT
CD56	NM_000615.7	GAACGACGAGGCTGAG-TACA	ACGAAGCCTTTTCTT-CGCTG
Dectin-1	NM_197947.2	CTGGT-GATAGCTGTGGTCCTG	AAGAACCCCTGTGGTTTT-GACA

2.1.4 Antibodies and fluorescent dyes

The used antibodies and fluorescent dyes are listed in Tables 8-10. The antibodies used for microscopy and flow cytometry were stored at 4 °C, while western blot antibodies were stored at -20 °C. The used fluorescent dyes were kept at -20 °C.

Table 8: Anti-human Antibodies and dyes used for flow cytometry.

Target	Host	Isotype	Conjugation	Staining conc.	Clone	Manufacturer
2B4	Mouse	IgG1	FITC	1:40	C1.7	Biolegend
CD14	Mouse	IgG2a	FITC	1:50	M5E2	BD Bioscience
CD16	Human	IgG1	FITC	1:50	REA423	Miltenyi Biotec
CD16	Mouse	IgG1	PerCP	1:20	3G8	Biolegend
CD1a	Mouse	IgG1	APC	1:50	HI149	BD Bioscience
CD3	Mouse	IgG2a	PerCP	1:50	BW264/56	Miltenyi Biotec
CD56	Mouse	IgG1	FITC	1:40	B159	BD
CD56	Mouse	IgG1	APC	1:20	2331	BD
CD69	Human	IgG1	APC	1:50	REA824	Miltenyi Biotec
CD69	Mouse	IgG1	FITC	1:40	FN50	Biolegend
CD80	Mouse	IgG1	APC	1:25	2D10	Miltenyi Biotec
CD83	Mouse	IgG1	FITC	1:20	HB15e	BD Bioscience
CD86	Mouse	IgG2b	PE	1:50	IT2.2	Biolegend
Dectin-1	Mouse	IgG2b	PE	1:20	259931	R&D

Table 8 (continued): Anti-human Antibodies and dyes used for flow cytometry.

Target	Host	Isotype	Conjugation	Staining conc.	Clone	Manufacturer
DNAM-1	Mouse	IgG1	APC	1:40	11A8	Biolegend
F-actin	-	-	Jasplakinolides labelled with Alexa Fluor 647	1:10	-	Spirochrome
HLA-ABC	Human	IgG1	PE	1:20	REA	Miltenyi Biotec
HLA-DR	Mouse	IgG2a	PE	1:50	G46-6	BD Bioscience
Iso. ctrl.	Mouse	IgG1	FITC	*	RMG-1	Biolegend
Iso. ctrl.	Mouse	IgG1	PerCP	*	MOPC-21	Biolegend
Iso. ctrl.	Mouse	IgG1	APC	*	MOPC-21	BD Bioscience
Iso. ctrl.	Mouse	IgG1	FITC	*	X40	BD Bioscience
Iso. ctrl.	Mouse	IgG1	APC	*	X-56	Miltenyi Biotec
Iso. ctrl.	Mouse	IgG1	APC	*	RMG1-1	Biolegend
Iso. ctrl.	Mouse	IgG1	PE	*	X-56	Miltenyi Biotec
Iso. ctrl.	Mouse	IgG1	PE	*	RMG-1	Biolegend
Iso. ctrl.	Mouse	IgG1	PE	*	X40	BD Bioscience
Iso. ctrl.	Mouse	IgG2a	FITC	*	MOPC-173	Biolegend
Iso. ctrl.	Mouse	IgG2a	PerCP	*	S43.10	Miltenyi Biotec
Iso. ctrl.	Mouse	IgG2a	PE	*	G155178	BD Bioscience
Iso. ctrl.	Mouse	IgG2a	PE	*	S43.10	Biolegend
Iso. ctrl.	Mouse	IgG2a	APC	*	RMG2a-62	Biolegend
Iso. ctrl.	Mouse	IgG2b	PE	*	RMG2b-1	Biolegend
Iso. ctrl.	Mouse	IgG2b	PE	*	27-35	BD Bioscience
Iso. ctrl.	Human	-	FITC	-	REA293	Miltenyi Biotec
Iso. ctrl.	Human	-	PE	-	REA293	Mitenyi Biotec
NKG2D	Mouse	IgG1	PE	1:50	1D11	Miltenyi Biotec
NKp30	Mouse	IgG1	PE	1:40	P30-15	Biolegend
NKp44	Mouse	IgG1	PE	1:40	P44-8.1	BD Bioscience
NKp46	Mouse	IgG1	PE	1:40	9E-2	BD Bioscience
NTB-A	Mouse	IgG1	PE	1:40	NT-7	Biolegend
TLR-2	Mouse	IgG2a	PE	1:20	TL2.1	Biolegend
TLR-4	Mouse	IgG2a	APC	1:20	HTA125	Biolegend
α-mouse	Goat	Ig	APC	1:20	polyclonal	BD Bioscience

*corresponding to the concentration of the staining antibody

Table 9: Antibodies and dyes used for microscopy.

Target	Antibody / Dye	Staining conc.	Manufacturer
CD56	Mouse anti-human CD56 Alexa Fluor™ 647 (HCD56)	1:50	Biolegend
Cell wall (*A. fumigatus*)	Calcofluor White Stain	Ready-to-use solution	Thermo Scientific
F-actin	Phalloidin Alexa Fluor™ 555	1:100	Thermo Scientific

Table 10: Antibodies used for western blotting.

Target	Host	Conjugation	Working conc.	Clonality	Molecular weight	Manufacturer
α-mouse	Horse	HRP-linked	1:10,000	Polyclonal	-	Cell Signaling
α-rabbit	Goat	HRP-linked	1:10,000	Polyclonal	-	Cell Signaling
CD56	Mouse	-	1:500	123C3	120 to 220 kDa	Cell Signaling
SDHA	Rabbit	-	1:1000	Polyclonal	70 kDa	Cell Signaling

2.1.5 Software

The used software for data analyses is listed in Table 11.

Table 11: Software used in the study.

Designation	Version	Application	Manufacturer
BD CellQuest™ Pro	3.3.1	Analysis of flow cytometric data	BD Bioscience
EndNote	X7	Citation program	Thomson Reuters
Fiji	-	Analysis of microscopic images and western blots	Fiji
FlowJo	X10	Analysis of flow cytometric data	Tree Star Inc.
GraphPad Prism	7	Statistical analysis and graphical design	GraphPad Software
Microsoft Excel	15-16	Calculations	Microsoft
Microsoft PowerPoint	15-16	Presentations	Microsoft
Microsoft Word	15-16	Thesis writing	Microsoft
NanoDrop Software	3.1.0	Measurement of protein and RNA concentrations	PeqLab
NCBI Pick Primers	-	Primer design	NCBI
rapid*d*STORM	3.3.1	Reconstruction of *d*STORM images from recorded 2D and 3D image stacks	[225]
StepOne Software	2.3	Real-time PCR data analysis	Applied Biosystems

2.2 Methods

2.2.1 Cultivation of Fungal strains

2.2.1.1 Generation of conidial suspensions

The human *A. fumigatus* isolate ATCC46645 (American Type Culture Collection) was used in most of the experiments. To analyze NK cell binding to different fungal strains, *A. niger* (CBS 553.65), *A. clavatus* (CBS 114.48), *A. flavus* (CBS 625.66), and *C. albicans* (SC5314) were tested in direct co-cultivation. *Aspergillus* strains were plated on malt extract agar plates (kindly provided by the Institute for Hygiene and Microbiology, University of Würzburg) at 35 °C until conidiophores (green/bluish color) were visible. Conidia were harvested by adding 10 ml of sterile water and removing the conidia smoothly with a cotton swab. The conidial suspension was filtered two times over a 40 µm cell strainer and was counted with a hemocytometer. Conidial solutions were stored in water at 4 °C. *C albicans* was cultured as recently described [226].

2.2.1.2 Generation of germ tubes

For germ tube generation, 2 x 10^7 conidia were transferred in a 50 ml tube supplemented with 20 ml RPMI 1640 (or RPMI + 10 % FCS for *A. niger*) under constant shaking for 9-15 h at 25 °C. *C. albicans* colonies were cultured to stationary phase [226] and transferred to RPMI 1640 at 37 °C for 6 h to induce germination. Fungal growth was monitored by microscopy, and germ tubes were centrifuged at 5,000 x g for 10 min. The supernatant was discarded, and 5 ml RPMI + 10 % FCS were added to reach a final concentration of 4 x 10^6 germ tubes/ml. Germ tubes were passed three times through a 20G needle to obtain a single-germ tube solution. For stimulation with live *A. fumigatus* germ tubes, an MOI of 0.5 and a co-cultivation time of 6 h was used.

2.2.1.3 Inactivation of *A. fumigatus* and *C. albicans*

For stimulations with inactivated fungus, 1 x 10^8 conidia were transferred in a 50 ml tube to generate germ tubes as described above. After centrifugation, germ tubes were resuspended in 1 ml of 100 % ethanol and were incubated for 30 min at RT. The solution was transferred into a 2 ml reaction tube, and three washing steps (full speed, 5 min) with 2 ml of distilled water were performed. Germ tubes were resuspended in RPMI and counted using a hemocytometer. The successful inactivation was monitored by plating 1 x 10^6 of

inactivated germ tubes in RPMI at 37 °C. If no growth was detected, germ tubes were used for cell stimulation using an MOI of 1.

2.2.1.4 Generation of cell wall fractions and lysate

The mycelial cell wall fractions were prepared and kindly provided by the group of Jean-Paul Latgé (Institut Pasteur, Paris). Therefore, the *A. fumigatus* strain CEA17 (AkuB^{ku80} *pyrG*Δ) was used [227]. This strain was used in previous studies to increase the frequency of homologous recombination, and the group of Latgé used it as a control for the analysis of the cell wall constitution [227, 228]. The preparation of cell wall fractions was performed by hot-alkali treatment as described in previous studies [223, 224]. The alkali-insoluble (AI) cell wall fraction (working concentration 5 µg/ml) is rich in β-1,3 glucans, chitin, galactomannans, and galactosaminogalactans, whereas the alkali-soluble (AS) fraction (working concentration 10 µg/ml) mainly consists of α-1,3 glucans and galactomannans [228]. The mycelial cell wall fractions were stored at 4 °C and used for stimulation of moDCs or NK cells for 9-24 h. The commercially available *A. fumigatus* lysate was generated from the whole mycelium. Therefore, the cell wall was cracked by liquid nitrogen, followed by ultrasonic treatment. The plasma membrane was disrupted by filtering the lysate over a French press under high pressure [229]. The fungal lysate was inactivated by filtration, and internal quality checks were performed.

2.2.1.5 Metabolic analysis

The tetrazolium salt XTT (2,3-bis-[2-methoxy-4-nitro-5-sulfophenyl]-2H-tetrazolium-5-carboxanilide) was used for measuring the fungal metabolism. XTT is a yellow dye that is reduced to an orange formazan dye by viable cells only. This reaction is related to NADH production through glycolysis, and the amount of formazan dye formed correlates to the number of metabolically active cells [230, 231]. The XTT assay was also shown to be applicable for fungi [232]. *A. fumigatus* conidia (0.5 x 10^5) were plated in a volume of 50 µl of RPMI in 96-well plats at 37 °C for 16 h. The supernatant of the formed mycelium was smoothly removed and exchanged by 100 µl of NK cell supernatants cultured alone or with *A. fumigatus* germ tubes that were meanwhile stored at -20 °C. Medium was plated as a control, and XTT reagent was used as the blank control. 96-well plates were incubated for 6 h at 37 °C before supernatants were removed, and empty wells were measured at an absorbance of 600 nm with an ELISA reader (Tecan). The XTT reagent was prepared 30 min before the stimulation time ended by mixing 0.0122 g of the tetrazolium salt with 24.5 ml of HBSS and heating the solution to 55 °C for 30 min (water bath). Co-enzyme (0.00122 g) was added, and the XTT-ready-to-use solution was vortexed rigorously before

100 µl XTT ready-to-use solution was applied to the mycelium. After an incubation time of 30 min at 37 °C, absorbance was measured at a wavelength of 450 nm. The OD (optical density) values measured for the wells with hyphae incubated in supernatants of former co-cultures (NKAF) were divided by the ones obtained from hyphae incubated in supernatants from NK cell cultures (NK). The OD values measured at 600 nm and 450 nm were inserted in the following equation, and the fungal damage was calculated:

$$\text{Fungal damage (\%)} = 100 - \frac{([OD_{450} - OD_{600}]_{NKAF} - [OD_{450} - OD_{600}]_{blank})}{([OD_{450} - OD_{600}]_{NK} - [OD_{450} - OD_{600}]_{blank})} \times 100 \quad (1)$$

2.2.2 Human immune cell isolation and culture

2.2.2.1 PBMC isolation

Peripheral blood mononuclear cells (PBMCs) were isolated from leukoreduction system (LRS) chambers, which are a byproduct of platelet donations and mainly contain white blood cells from healthy individuals. LRS chambers were obtained from the Institute of Transfusion Medicine and Haemotherapy from the University Hospital Würzburg. PBMCs were isolated by ficoll-hypaque density gradient centrifugation. For that, peripheral blood from LRS chambers was transferred into a 50 ml tube and mixed with HBSS buffer supplemented with EDTA and FCS (RT) to a volume of 50 ml. The blood solution was divided and smoothly layered onto two 50 ml tubes containing 15 ml ficoll each. Density gradient centrifugation was performed at 800 x g for 20 min (RT) at the lowest acceleration and brake settings. The PBMC layer was collected with a Pasteur pipette and transferred in a fresh 50 ml tube. The tube was filled to 50 ml with HBSS buffer and was centrifuged at 120 x g for 15 min (RT) at the lowest acceleration and brake settings. This washing step was performed two times before PBMCs were counted with a cell viability analyzer. All following centrifugation steps were performed at 300 x g and 4 °C at the highest acceleration and brake settings if not stated otherwise.

2.2.2.2 MoDC generation

Monocytes were isolated from PBMCs by magnetic separation of $CD14^+$ cells following the manufacturer's instructions. Monocyte-derived dendritic cells (moDCs) were generated by culturing 2.5 x 10^6 cells in a volume of 3 ml per well (6-well plate) in the presence of 250 µg/ml GM-CSF and 10 µg/ml IL-4 for five days. One-third of the volume was exchanged on the second and fourth day after monocyte isolation. Therefore, 1 ml per well was removed, centrifuged, and supplemented with the three-fold concentration originally used for IL-4 and GM-CSF. After moDC generation, cells were harvested with a cell scraper using

pre-warmed HBSS buffer. Cells were centrifuged and resuspended in fresh cell medium. For RNAi experiments, moDCs were electroporated on the fourth day after monocyte isolation and cultured at a cell concentration of 1 x 10^6 cells/well in 12-well plates in the presence of IL-4 and GM-CSF for 24 h. For stimulation, moDCs were cultured at a concentration of 1 x 10^6 cells/ml in the presence of the stimulus for 16 or 24 h.

2.2.2.3 NK cell isolation

NK cell isolation from PBMCs or whole blood (30 ml whole blood collected in 3x 9 ml EDTA blood collection tubes) was performed by depletion of all other cell types with magnetically labeled antibodies following the manufacturer's instructions. In the case of NK cell isolation from whole blood, red blood cell lysis was performed for 2 min (RT) after collecting the target cell fraction from the separated blood sample. NK cell isolation from patients was performed on defined time points after alloSCT and patient characteristics are displayed in Table 12.

Table 12: Patient characteristics.

ID	Gender	Age (yrs)	Day 60	Day 90	Day 120	Day 180	GvHD with systemic CS treatment	CS treatment duration	CS dosage
2	female	36	CSA	CSA	CSA, pred	CSA, pred	no	>18 weeks	low-dose
4	male	59	CSA, MMF	CSA, MMF	CSA	noT	no	-	-
5	male	62	MMF	pred	pred	noT	skin	~4 weeks	initial high doses
6	female	60	CSA, MMF	CSA, MMF	CSA, hydrocort	CSA, hydrocort	no	>20 weeks	low-dose
7	male	57	MMF	noT	noT	noT	no	-	-
8	female	49	CSA, MMF	CSA	CSA, Rituximab	CSA, pred, rapa	skin, IT	~3 weeks	initial high doses
9	male	55	rapa, MMF, hydrocort, CSA	MMF, CSA	CSA	CSA, pred, rapa	skin, IT	~4 weeks	initial high doses
10	male	63	pred, rapa	pred, rapa	pred, rapa	noT	no	>8 weeks	low-dose
12	female	45	CSA, MMF	n/a	n/a	n/a	no	-	-
14	female	42	CSA, rapa, MMF	rapa, pred	rapa, pred	rapa, pred	skin	>15 weeks	initial high doses
15	male	66	rapa, MMF, pred	rapa, MMF, pred	rapa, MMF, pred	rapa, pred	no	>25 weeks	low-dose
16	female	34	CSA, MMF	CSA, MMF	CSA, MMF, pred	hydrocort	skin	~6 weeks	initial high doses
17	male	58	MMF, CSA, rapa	rapa, MMF	rapa	rapa	no	-	-
18	male	45	CSA, pred, budesonid	rapa, pred	rapa, pred	n/a	liver, IT	>14 weeks	initial high doses
22	male	48	rapa, MMF	rapa, MMF	rapa, MMF	noT	no	-	-
24	male	49	CSA, rapa	CSA, rapa	n/a	n/a	no	-	-
26	male	65	CSA, MMF	CSA, MMF	CSA	CSA	no	-	-

CSA = cyclosporine, rapa = rapamycin, hydrocort = hydrocortisone, pred = prednisolone, MMF = mycophenolate mofetil, CS = corticosteroid, IT = intestinal tract, low-dose (<1 mg/kg), high-dose (>1 mg/kg)

Untouched NK cells were cultured at a concentration of 1 x 10^6 cells/ml in the presence of 1000 U/ml IL-2 (Proleukin® S) overnight if not stated otherwise. Cell harvesting was performed with a cell scraper using pre-warmed HBSS buffer. After a centrifugation step, cells were resuspended at a cell concentration of 1 x 10^6 cell/ml in fresh cell medium.

2.2.2.4 Direct NK-DC co-cultivation

For experiments analyzing the direct cell-to-cell contact, either pre-stimulated NK cells or moDCs were co-cultured with the counterpart cell type. NK cells and moDCs were chosen from the same PBMC donor to avoid NK cell-mediated DC lysis.

NK cells were stimulated after overnight incubation in IL-2. MoDCs were stimulated on the fifth day after monocyte isolation. The stimulation concentrations were 5 µg/ml for the AI and 10 µg/ml for the AS cell wall fraction. The *A. fumigatus* lysate was used at a working concentration of 1 µg/ml (for NK cell stimulation) and 5 µg/ml (for stimulation of moDCs), respectively. As a positive control, NK cells were stimulated with 500 IU/ml IL-15 and moDCs were stimulated with 1 µg/ml lipopolysaccharide. After 24 h of stimulation, the stimulated cell type was co-cultured with the unstimulated counterpart cell type for 16 h. This incubation time was adopted from previous studies that analyzed NK-DC cross-talk [233].

Pre-stimulated NK cell cultures were washed two times to remove the stimulants from the supernatants and were adjusted to 2 x 10^6 cells/ml. Unstimulated moDCs were harvested on the fifth day after monocyte isolation, supernatants were removed, and cells were adjusted to a cell concentration of 2 x 10^6 cells/ml. Co-cultures were set by mixing 0.6 x 10^6 cells each to a final volume of 1.2 ml in a 12-well plate. Accordingly, pre-stimulated moDCs were harvested on the sixth day after monocyte isolation and co-cultured with NK cells pre-incubated in IL-2 overnight.

2.2.2.5 Transfer of moDC supernatants or cytokines on NK cells

To analyze the ability of moDC supernatants to activate NK cells, moDCs were stimulated with inactivated *A. fumigatus* germ tubes (MOI 1), AI fraction (5 µg/ml), the Dectin-1 ligand ‘zymosan depleted’ (100 µg/ml), the Dectin-1/TLR-2 ligand zymosan (10 µg/ml), or the TLR-2/TLR-6 ligand FSL-1 (100 ng/ml). Stimulation of Dectin-1 silenced moDCs was performed in a volume of 1 ml in 12-well plates at a cell concentration of 1 x 10^6 cells/ml. An incubation time of 9 h was chosen since moDCs displayed appropriate Dectin-1 silencing after this time. TLR-2 blocked moDCs were stimulated for 24 h since moDC activation by the positive control FSL-1 was not observed at earlier time points. Stimulation of moDCs after TLR-2 blocking was performed at a cell concentration of 1 x 10^6 cells/ml in a volume

of 0.4 ml in 24-well plates. The supernatants of stimulated moDCs were harvested by centrifugation and were transferred directly onto resting NK cells. NK cells were used after isolation from PBMCs without pre-stimulation with IL-2. For that, NK cells were adjusted to a cell concentration of 20 x 10^6 cells/ml, and 10 µl of NK cell suspension was dissolved in 190 µl moDC-derived supernatant and plated in 96-well plates for 16 h.

To analyze whether soluble factors can mediate NK cell activation, NK cells were stimulated in the presence of cytokines and chemokines for 16 h. Each cytokine or chemokine was used in a lower and higher concentration: IL-6 (10 ng/ml and 50 ng/ml), IL-10 (1 ng/ml and 5 ng/ml), IP-10 (4 ng/ml and 5 ng/ml) and IL-12 (5 ng/ml and 10 ng/ml). Additionally, NK cells were treated with a combination of all cytokines and chemokines, either with the lower or higher concentration. After 16 h, NK cell activation was measured by flow cytometry using an anti-CD69 antibody.

2.2.2.6 Culture of K-562 cells

The human lymphoblast cell line K-562 (ATCC® CCL-243™) was cultured in RPMI 1640 + 10 % FCS at a cell concentration of 1 x 10^6 cells/ml. Cells were cultured in T75-flasks and medium was exchanged every two to three days.

2.2.2.7 Cryopreservation and thawing of cells

For cryopreservation, cells were centrifuged for 10 min at 300 x g and resuspended in freezing medium (FCS + 8 % DMSO) at a maximal cell concentration of 5 x 10^7 cells/ml. Cryotubes were immediately placed in a cryogenic storage system (“Mister Frosty”) at - 80 °C for 24 h before cells were shifted into liquid nitrogen for long-term storage. For cell thawing, cryotubes were thawed in a water bath (37 °C), and thawed cells were transferred into 10 ml of pre-warmed cell culture medium (RPMI + 10 % FCS). After a centrifugation step, cells were resolved in cell culture medium to remove the remainings of the freezing medium. Thawed PBMCs were used for isolating NK cells, which were pre-stimulated with IL-2 overnight. K-562 cells were frozen in complete growth medium supplemented with 5 % DMSO.

2.2.3 Gene expression analysis

2.2.3.1 RNA isolation

Up to 1 x 10^6 NK cells and 0.5 x 10^6 moDCs cultured in 24- or 12- well plates were harvested for RNA isolation. Therefore, cells were detached with a cell scraper or a pipette

tip and transferred into a 1.5 ml reaction tube. An RNA stabilizing agent (400 µl) was added to the empty well to detach the remaining cells. Meanwhile, the collected cells in the 1.5 ml reaction tube were centrifuged at 500 x g for 5 min, and the RNA stabilizing agent was transferred onto the cell pellet. Samples were stored at -20 °C until RNA was isolated.

RNA isolation was performed using the RNeasy Mini Kit. On the day of RNA isolation, the samples were thawed and centrifuged for 10 min at 5,000 x g (4 °C). The cell pellet was resuspended in 350 µl RLT lysis buffer, and samples were mixed and supplemented with 350 µl of 70 % ethanol. The cell homogenates were applied onto an RNeasy Mini spin column and centrifuged at 8,000 x g for 30 sec (RT). All following centrifugation steps were performed at 8,000 x g for 30 sec. After washing the columns one time with 700 µl RW1 buffer and two times with 500 µl RPE buffer, columns were centrifuged dry at full speed (13,200 x g, 1 min). The RNA was eluted in 30 µl pre-warmed RNAsefree water (8,000 x g, 2 min) and a spectrophotometer was used to determine the RNA concentration. The 260/280 and 260/230 ratios were used to analyze the RNA quality (with values of 2.0 and 2.0-2.2 being the optimum).

2.2.3.2 cDNA synthesis

First-strand copy DNA (cDNA) was synthesized using 100-500 ng RNA in a volume of 10 µl (filled up with RNase free water). To that, 10 µl of the master mix, constituting of the following components, was pipetted:

Table 13: Mastermix for cDNA synthesis.

Reagent	Volume per sample (in µl)
5X Reaction buffer	4
Random hexamer primer	1
RNAse inhibitor	1
Reverse transcriptase	2

The reverse transcription protocol consisted of the following steps: 5 min at 25 °C, 60 min at 37 °C, and 5 min at 70 °C. CDNA was diluted (1:2 for 100 ng used RNA to 1:50 for 500 ng used RNA), and stored at -20 °C.

2.2.3.3 Real-time (RT) PCR

The used primers are listed in Table 7. Primer pairs were generated with the NCBI Pick Primer tool and designed in that way that they span an exon-exon junction. Additionally, primer pairs were separated by at least one intron on the corresponding genomic DNA (gDNA) to prevent and distinguish the unintended amplification of the gDNA. Primers were

diluted in nuclease-free water to a stock solution of 10 µM and stored at -20 °C. The real-time (RT) PCR was pipetted as shown in Table 14.

Table 14: RT-PCR master mix.

Reagent	Volume per sample
Forward primer [10 µg/ml]	1 µl
Reverse primer [10 µg/ml]	1 µl
Nuclease-free water	4 µl
SYBR® Green Mix	10 µl
Diluted cDNA	4 µl

Samples were pipetted in duplicates, and *ALAS1* was used as a housekeeping gene control. Fast thermal cycling was performed by initial polymerase activation and cDNA denaturation at 95 °C for 30 sec, followed by 40 cycles of denaturation at 95 °C for 3 sec and an annealing/extension phase at 60 °C for 30 sec. Lastly, a melting curve analysis was performed by thermal heating from 60 °C to 95 °C in 0.5 °C steps.

The quantified cDNA fragments were analyzed with gel electrophoresis for the right band size. Therefore, 0.5 g agarose was diluted in 50 ml 1X TAE buffer. The solution was heated until the complete agarose was dissolved before adding 4 µl of ethidium bromide. A 15-well gel comb was applied after pouring the liquid gel into a gel electrophoresis chamber. 1X TAE solution was poured into the chamber until the gel was completely covered. The DNA was mixed with 5X sample loading dye, and the samples were pipetted into the gel pockets. 7 µl of the DNA ladder (100 kb) was applied, and the gel electrophoresis was performed at 150 mA for 50 min. The right band size of the amplicons was checked with an AlphaImager™ Light Cabinet.

RT-PCR was analyzed with the StepOne™ Software. Therefore, the automated baseline tool was used, and the threshold for the fluorescence signal was set to 0.1. The Cycle Threshold mean (Ct mean) was calculated from the duplicates and the relative gene expression of moDCs or NK cells treated with siRNA targeting Dectin-1 or *A. fumigatus* germ tubes was calculated with the following equation:

$$\text{Relative gene expression} = \frac{2^{(Ct_{\text{mean control}} - Ct_{\text{mean treatment}})_{\text{target gene}}}}{2^{(Ct_{\text{mean control}} - Ct_{\text{mean treatment}})_{\text{ALAS}}}} \quad (2)$$

‘Control’ samples were either formerly treated moDCs with non-silencing control or unstimulated NK cells. ‘Treatment’ samples were either moDCs treated with siRNA targeting Dectin-1 or stimulated NK cells.

2.2.3.4 Dectin-1 silencing

MoDCs were harvested on the fourth day after monocyte isolation and were resuspended in RPMI 1640 (without phenol-red) to reach a concentration of 1 × 10^7 cells/ml. To 100 µl of moDC suspension, 6.6 µl of Dectin-1 siRNA [20 µM] or non-silencing control were added, before the solution was transferred into a 4-mm electroporation cuvette. The electroporation was performed using an electroporation pulse generator set to a rectangle pulse of 340 V for 10 ms. MoDCs were plated in cell culture medium with FCS and fresh cytokines in 12-well plates (BD Falcon) at a cell concentration of 1 ×10^6 cells/ml. After 24 h, moDCs were stimulated with the AI cell wall fraction, inactivated *A. fumigatus* germ tubes, depleted zymosan, and zymosan, as recently described [234]. Real-time (RT) PCR monitored the efficiency of Dectin-1 silencing. Therefore, RNA was isolated, cDNA was generated, and RT-PCR was performed as described above. Gene silencing of Dectin-1 was 86.38 % compared to the transfection control.

2.2.4 Protein analysis

2.2.4.1 Flow cytometry

Cell cultures were harvested with a cell scraper, and 1 x 10^5 – 5 x 10^5 cells were analyzed per FACS tube. Samples were washed with 2-3 ml of pre-cooled HBSS buffer before a centrifugation step was performed. All centrifugation steps concerning the preparation of flow cytometric probes were performed at 800 x g for 5 min. For analysis of surface proteins, 100 µl of pre-cooled HBSS buffer supplemented with 1 % FCS and 0.5 % EDTA were added. Antibodies or isotype controls were applied at the appropriate concentrations (Table 8), and FACS tubes were incubated in the dark at 4 °C for 20 min. Cells were washed with 2-3 ml of HBSS buffer, resuspended in a cell concentration of 1 x 10^5 cells in 100 µl, and analyzed by flow cytometry immediately. For intracellular stainings, cells were fixed after washing off the unbound surface antibodies using the BD Cytofix/Cytoperm™ protocol. For that, cells were resuspended in 0.5 ml of fixation reagent and incubated in the dark at 4 °C. After two washing steps with 2 ml of Perm/Wash™ buffer, intracellular antibody staining was performed in the dark (RT) for 30 min. Two additional washing steps with Perm/Wash™ buffer were performed, and cells were resuspended in 1 x 10^5 cells in 100 µl of Perm/Wash™ reagent.

During the process of moDC generation, cells lose the surface expression of CD14 and induce the expression of CD1a. The purity of moDCs was monitored by $CD14^-/CD1a^+$ gating [234]. NK cells were gated into CD3-/NKp46+ cells as recently described [235]. NK cell purity was consistently over 95 %. Unstained cells were used for adjusting the forward and

side scatter (FSC and SSC), and flow cytometric compensation was performed by staining cells with fluorescent antibodies against highly expressed surface markers. Isotype controls were used in each experiment. Flow cytometric analysis was performed on a FACSCalibur (BD), and data were analyzed by BD CellQuest™ Pro and FlowJo software.

NK cell binding to fungal hyphae was assessed by measuring the CD56 Mean Fluorescence Intensity (MFI) after fungal co-culture (NKAF) and in control cells (NK). CD56 binding to the fungus was calculated with the following equation:

$$\text{Relative CD56} = \frac{\text{CD56 MFI (NKAF)}}{\text{CD56 MFI (NK)}} \quad (3)$$

Similar to CD56 binding, fungal mediated actin polymerization was calculated by dividing the F-actin signal from NK cells co-cultured with the fungus (NKAF) through the F-actin MFI measured in control cells (NK):

$$\text{Relative F-actin} = \frac{\text{SiR-647 MFI (NKAF)}}{\text{SiR-647 MFI (NK)}} \quad (4)$$

2.2.4.2 Singleplex and multiplex immunoassays

All enzyme-linked-immunosorbent assays (ELISA) were performed as described by the manufacturers. For singleplex assays, either 96-well medium binding or half-area, high-binding plates were used. ELISAs with 96-well half-area plates were performed with one-fourth of the volume described by the manufacturer. The washing buffer consisted of PBS supplemented with 0.05 % Tween® 20 if not stated otherwise in the manufacturer's protocol. The colorimetric reaction was stopped with 0.5 M H_2SO_4, and the absorbance was measured with an ELISA reader. The multiplex immunoassays were kindly performed by Dr. Kerstin Hünniger (HKI, Jena). For that, a volume of 50-100 µl of cell culture supernatants was stored at -20 °C and sent on dry-ice to Jena. The assay was performed according to the manufacturer's instructions.

2.2.4.3 Immunoblotting

NK cells cultured alone or with *A. fumigatus* germ tubes were harvested after incubation for 6 h and transferred into a 1.5 ml reaction tube. After centrifugation at 500 g for 5 min, supernatants were removed and cell pellets were lysed on ice with 30 µl of PE buffer. Lysates were treated for 3x 10 sec with an ultrasonic processor (amplitude: 40 %, cycle: 1) and centrifuged at full speed (4 °C) for 10 min. Supernatants were removed to a fresh 1.5 ml reaction tube, and the protein concentration was determined using a spectrophotometer.

Cell lysates were mixed with 4X SDS loading buffer to a maximal volume of 30 µl and heated to 95 °C for 5 min. Protein samples (10-20 µg) were loaded on a gel (4-20 % Mini-PROTEAN® TGX™ Precast Protein Gels) together with 7 µl of the protein ladder (170-10 kDa). Gels were inserted into the gel-electrophoresis chamber filled with 1X TGS running buffer. A constant amperage (15 mA for one gel, 30 mA for two gels) was applied and increased to 30 or 50 mA after 20 min, respectively. After a total electrophoresis time of 50 min, gels were removed and incubated in pre-cooled (4 °C) blotting buffer, together with filter papers and blotting membranes (4.5 µm pore size, nitrocellulose), for 5-15 min.

Semi-dry blotting was performed at 75 mA for 2 h. As a control for successful protein transfer, gels were stained with 20 ml of SimplyBlue™ staining solution for 24 h. Membranes were stained with 20 ml Ponceau staining solution for 2-3 min and were cut accordingly to the expected band sizes for CD56 (120-220 kDa) and SDHA (70 kDa). Ponceau staining was washed away with ddH_2O for 2x 10 min. Membranes were blocked for 30 min on a laboratory seesaw; therefore, the blocking solution was chosen after the 1st antibody staining solution and was performed either with 5 % BSA or milk in TBST. Membranes were transferred into boxes containing 12 ml of the first-antibody solution and were put on a seesaw overnight at 4 °C. Membranes were incubated for 3x 10 min in boxes containing 20 ml TBST and were transferred into the secondary-antibody solution (1:10,000 in 5 % BSA or milk in TBST) for 2-3 h (RT).

After washing off the secondary-antibody solution in 20 ml TBST for 3x 10 min, membranes were transferred into a cassette for x-ray films. The remaining TBST on the membranes was removed carefully with a paper towel by placing the towel at the membrane's border. The membranes were incubated with a freshly prepared dilution of horseradish peroxidase (HRP) substrate solution (Clarity™ Western ECL Substrate) for 5 min. This solution contains a luminol-based chemiluminescent substrate that detects HRP conjugates, which are attached to the secondary antibody. The chemiluminescent detection was performed in a dark chamber. Therefore, three tanks containing development solution, VE-H_2O, and fixation solution were prepared. X-rays were laid on membranes for the luminescent transfer (1-10 min) and were developed and fixed by incubation of the x-ray in the respective tank. After that, x-rays were scanned and analyzed by Fiji software using the Gel Analysing Tool. Relative protein content was calculated with the housekeeping protein as a control. Therefore, the area of the bands was measured in pixel, and the area of the CD56 protein bands was divided by the area measured for the housekeeping protein band. The original x-ray films are shown in the supplementary information in our manuscript [235].

2.2.4.4 Receptor blocking

MoDCs were harvested on the fifth day after monocyte isolation and treated with 10 µg/ml TLR-2 blocking antibody or isotype control at 37 °C for 1 h. Therefore, moDCs were incubated in cell medium in a 1.5 ml reaction tube at a cell concentration of 2 × 10^6 cells/ml. After blocking, the antibody or isotype control was diluted to 5 µg/ml during moDC stimulation at a cell concentration of 1×10^6 cells/ml. As a control for successful TLR-2 blocking, moDCs were stained with a goat anti-mouse antibody and analyzed by flow cytometry.

The CD56 blocking antibody was derived by immunizing 5 week–old Balb/C mice with activated (CD56+) NK cells. NK cell clones (EC1 and SA260 for A76 and Z25 mAbs, respectively) or a polyclonal NK cell population (for AZ20 mAb) were used. After different cell fusions, the antibody was selected for the ability to induce lysis in redirected killing assays against target cells [236]. CD56 blocking was performed as recently described [235]. Therefore, NK cells were blocked in 1.5 ml reaction tubes containing 10 µg/ml GPR165 (IgG2a) monoclonal antibody or isotype control diluted in cell culture medium at a cell concentration of 4 x 10^6 cells/ml. Blocking was performed at 37 °C for 30 min, cells were diluted to 1 x10^6 cells/ml, and NK cells were cultured alone or with *A. fumigatus* germ tubes at 37 °C for 9 h. During the culture, the blocking antibody or isotype control was 4 fold diluted.

2.2.4.5 Microscopy

Scanning electron microscopy (SEM)

NK cells were seeded alone or with *A. fumigatus* germ tubes (MOI 0.5) on microscopic coverslips coated with poly-D-lysine. 3 h post-incubation, samples were washed with PBS and were fixed for 12–18 h at 4 °C in a solution of 2.5 % glutaraldehyde, 2.5 mM $MgCl_2$, 50 mM KCl, and 50 mM cacodylic acid, pH 7.2. Afterward, samples were washed with 50 mM cacodylic acid, pH 7.2 and then, dehydrated stepwise with acetone, critical point dried and metal coated with gold-palladium. Specimens were examined with a field emission scanning electron microscope using a detector for secondary electrons (SEI detector) at 5 kV and a magnification of ×10,000.

Confocal Laser Scanning Microscopy (CLSM)

8-well Lab-Tek® chambers were treated with 500 µl/well 0.5 M NaOH for 30 min, washed with 3x 500 µl/well of sterile water, and coated with 150 µl/well of poly-D-lysine solution (1:200 in sterile water). Poly-D-lysine was used for increasing the cell attachment to the well bottom in wells that later contained NK cells. NK cells were adjusted to 1 x 10^6/ml in 200 µl of cell medium with or without the presence of 0.1 x 10^6 *A. fumigatus* germ tubes.

Chambers were incubated at 37 °C for 6 h. The supernatant was removed and cells were fixed in 3 % formaldehyde (FA) in RPMI at 37 °C for 10 min or in 0.67 % FA for 30 min. All reagents and procedures after the fixation step were performed at RT under sterile conditions, direct light was avoided, and incubation in antibody solutions was performed in the dark. Samples were washed three times, blocked for 30 min with 5 % BSA in HBSS, and stained in 1:50 with anti-CD56 antibody solution for 1 h. After washing the specimens five times for 5 min each with HBSS, samples were fixed for 10 min. After three washing steps, samples were resuspended in 500 µl HBSS and analyzed the following day at the CLSM. The microscopic settings were adjusted as recently described [235]. CLSM images of the NK cell-*A. fumigatus* interaction were acquired with a LSM700 system (Carl Zeiss) with a plan-apochromat 63 ×/1.40 oil immersion objective.

Direct stochastic optical reconstruction microscopy (dSTORM)

Samples were prepared as described above. *D*STORM imaging of *A. fumigatus* incubated NK cells and control NK cells was performed in photoswitching buffer (100 mM mercaptoethylamine in PBS pH 7.4). 2D measurements were conducted on an inverted wide-field fluorescence microscope (IX-71; Olympus) as described previously[237-239]. For each measurement 15,000 images with an exposure time of 20 ms and irradiation intensity of ~7 kW/cm^2 were recorded using highly inclined and laminated optical sheet (HILO) illumination. For 3D *d*STORM measurements [240] an Axio Observer.Z1 (Carl Zeiss Microscopy) equipped with a water-immersion objective (LD C-Apochromat 63×/1.15 W Corr M27; Carl Zeiss Microscopy) was used. Fluorophores were excited with a 150 mW 640 nm laser (iBeam Smart 640-S; Toptica) which was spectrally cleaned (MaxDiode LD01-640/8; Semrock). Emission and excitation light was separated using a dichroic mirror (BrightLine Di01-R405/466/532/635-25 × 36; Semrock) and a bandpass filter (ZET405/488/532/642 m, Chroma) and the wavelength range of the emitted light was specified further with a single bandpass filter (E700/75 m; Chroma). Astigmatism of the point spread function (PSF) was introduced by a 250 mm achromatic cylindrical lens (Thorlabs). Fluorophores were detected by an EMCCD camera (iXon Ultra DU897U-CSO; Andor). At least 30,000 frames at a frame rate of 54 Hz were collected for each 3D measurement. The open source rapi*d*STORM [225], version 3.3.1 software was used to reconstruct *d*STORM images from the recorded 2D and 3D image stacks.

Structured Illumination Microscopy (SIM)

18 mm round glass objective slides were placed in a 12-well plate. Slides were treated with NaOH and poly-D-lysine, and NK cell-*A.fumigatus* co-cultures or NK cell cultures were performed as described above. Supernatants were removed, and samples were fixed as described above. Slides were transferred in a dark, humid staining chamber. Blocking and

staining were performed by adding a volume of 150 µl on the objective slides. The antibody staining solution was prepared as described above. Slides were washed five times with 200 µl of HBSS, and fixed with 3 % FA in RPMI for 10 min. The phalloidin staining solution (1:100 in HBSS) was applied for 24 h. After that, slides were washed five times with HBSS (5 min) and treated with a fixation solution for 10 min. The remaining fluid was removed, specimens were embedded with three droplets of ProLong Gold™ solution, transferred upside-down onto microscope slides, and dried for 24 h. Microscopic specimens were analyzed on a Zeiss Elyra S.1 SIM using the Plan-Apochromat 63x/1.4 Oil objective in combination with 642nm, 561nm, and 405nm laser lines. Z-stacks with slice spacings of 300 nm were taken, and emission signals were recorded with an sCMOS PCO Edge 5.5 and analyzed with the ZEN 2.3 SP1 software. For visualization, maximum intensity projections of reconstructed z-stacks were used. To quantify the actin signal of each NK cell, z-stacks were projected as summed slices. A constant circular area was moved over each NK cell, and the intensity was measured using Fiji [241].
Whole images, and not only parts, were adjusted regarding brightness and contrast.

2.2.5 Statistics

In Chapter 1 and 2, data are displayed as means and standard error of the mean (SEM). When two groups were compared, data were analyzed with two-tailed, paired t-test. When comparing multiple conditions, data were analyzed by one-way ANOVA with correction for multiple testing by FDR method of Benjamini and Hochberg. As the number of replicates per experiment increased in Chapter 3, D'Agostino-Pearson omnibus test was used to analyze data regarding their normal distribution. Normally distributed data were either analyzed with an unpaired t-test with Welch's correction or a paired t-test. Data that did not follow Gaussian's distribution were analyzed with a Mann-Whitney test. When more than two groups were analyzed (multiple comparisons), normally distributed data were tested by one-way ANOVA with correction for multiple testing by FDR correction. Data not following Gaussian's distribution were tested with a Kruskal-Wallis test with FDR correction (no data matching) or with a Friedman test with FDR correction (matched data). Data are displayed as means with and without standard deviation (SD) in case of normal distribution and medians with and without range when data were not following normal distribution. Statistical analysis was performed with GraphPad Prism 7. Statistical significance is indicated with asterisks as follows: * $p < 0.05$, ** $p < 0.01$, *** $p < 0.001$).

2.2.6 Funding

This study was supported by the Deutsche Forschungsgemeinschaft (DFG) within the Collaborative Research Center CRC124 FungiNet “Pathogenic fungi and their human host: Networks of interaction” (Hermann Einsele and Juergen Loeffler, project A2).

2.2.7 Ethics statement

The use of whole blood and LRS chamber specimens was approved by the Ethical Committee of the University Hospital of Wuerzburg (#34/15, #302/15). Data analysis was conducted anonymously.

3 Results

Chapter 1:

First insights in NK-DC cross-talk and the importance of soluble factors during infection with *A. fumigatus*

The following work was published in:

Frontiers in Cellular and Infection Microbiology, August 2018

Introduction

The saprophytic mold *A. fumigatus* causes infections in immunocompromised hosts, especially those suffering from hematological malignancies or undergoing alloSCT [242]. IA is the most severe form of the disease where inhaled *A. fumigatus* conidia germinate and grow into deeper lung tissues and become angio-invasive. After germination, fungal antigens are exposed and lead to substantial immunological responses mediated by immune cells of the innate and adaptive immune system [243, 244]. DCs are phagocytic cells that are key components of the innate immune system that function as antigen-presenting cells [245]. Phagocytosis of pathogens activates DCs upon they migrate into secondary lymphoid organs and present pathogenic antigens to T cells [246]. Therefore, DCs play an essential role by linking innate and adaptive immune responses. DCs interact with *A. fumigatus* through the internalization receptor Dectin-1 that binds to surface β-1,3-glucans and thereby initiates DC maturation [132]. Dectin-1 can synergize with TLR-2, which mediates enhanced cytokine production [134]. Signals derived from Dectin-1 and TRL-2 result in the activation of the nuclear factor κB signaling pathway [242]. Furthermore, TLR-9 recognizes *A. fumigatus* DNA, which induces the production of pro-inflammatory cytokines in mouse bone marrow-derived DCs and human pDCs [247].

NK cells contribute to the innate immune system and play an important role in tumor surveillance and lysis of target cells [248]. Besides the interaction with human cells, NK cells further participate in the control of several pathogens, including viruses and fungi [191, 249, 250]. NK cells have been shown to interact with *Cryptococcus neoformans*, *Candida albicans,* and *Mucorales spp.* [251]. Dependent on the underlying host immune status, NK cells exerted either a beneficial or a detrimental effect on the outcome of systemic *Candida* infection in murine infection models [252]. NK cells were shown to directly bind the fungal hyphae by the neural cell adhesion molecule (NCAM-1, CD56), which leads to the secretion of macrophage inflammatory protein (MIP)-1α, MIP-1β, and RANTES (regulated on activation, normal T cell expressed and secreted protein) [235].

Additionally, it is known that NK cell stimulation with germ tubes induces the secretion of perforin that mediates anti-fungal activity by so far unknown mechanisms [253]. DCs and NK cells interact in lymphoid organs and inflamed tissue [148-150]. NK-DC cross-talk can lead to activation of both cell types, and this reciprocal activation is induced by soluble and contact-mediated factors [148]. The direct cell contact leads to high doses of cytokines at the immunological synapse, e.g., synaptic IL-12 enhances NK cell activation and cytotoxicity [254]. However, the reciprocal interactions between DCs and NK cells in the presence of the fungus have not been studied before. Therefore, we firstly investigated *in vitro* NK-DC cross-talk in the presence of *A. fumigatus* by flow cytometry and cytokine profiling.

Results

Direct cell-to-cell contact was analyzed by the co-culture of previously stimulated cells with the unstimulated counterpart cell type. For stimulation of cells, alkali-insoluble (AI) and alkali-soluble (AS) mycelium cell wall fractions, as well as *A. fumigatus* (AF) lysate, were used. AI is rich in β-1,3 glucans, chitin, galactomannans, and galactosaminogalactans, whereas AS consists of α-1,3 glucans and galactomannans [228]. AF lysate is a whole cell lysate, and in contrast to the cell wall fractions also includes intracellular stimulants. All three stimulants induced a significant up-regulation of the DC maturation markers HLA-DR, CD80, CD86, CD40, and CCR7, with AF lysate showing the most prominent effect on moDC maturation (Fig. 11a-e). After the determination of moDC maturation, the supernatants containing the soluble stimulants were removed by medium exchange, and moDCs were co-cultured with autologous, resting NK cells for 16 h (Fig. 11f). Interestingly, NK cells upregulated the activation marker CD69 after co-culture with stimulated moDCs, whereas unstimulated moDCs did not induce NK cell activation (Fig. 11f).

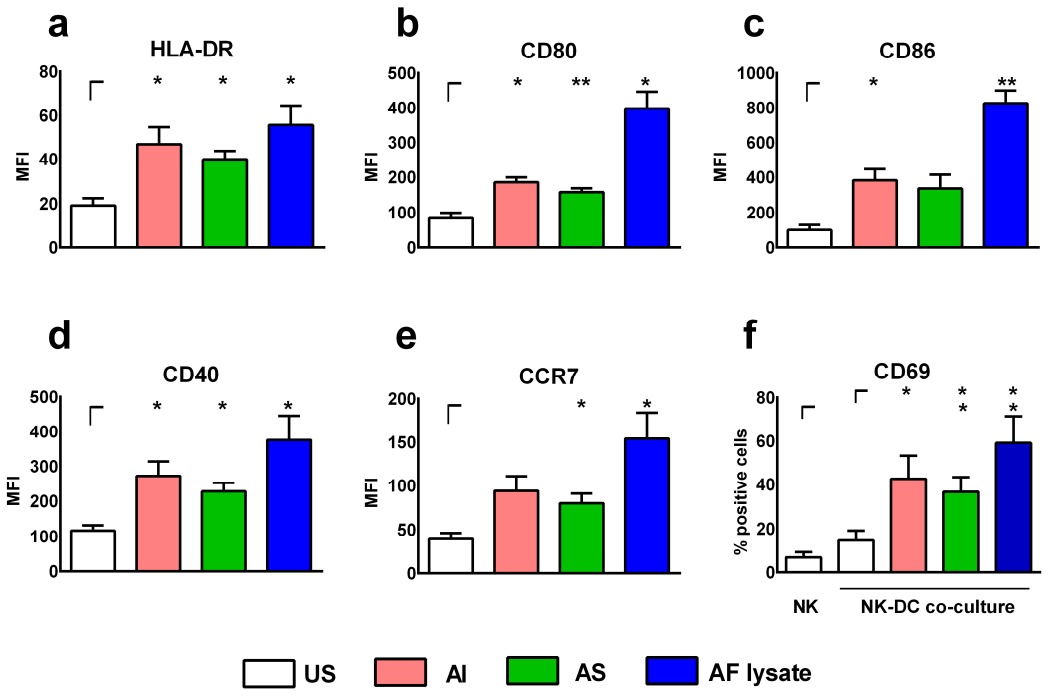

Figure 11: *A. fumigatus* stimulated moDCs can activate autologous, resting NK cells. MoDCs were either left untreated (US) or were stimulated with soluble (AS, 10 µg/ml) and insoluble (AI, 5 µg/ml) cell wall fractions or *A. fumigatus* lysate (AF lysate, 5 µg/ml) for 24 h. Flow cytometry was performed to measure the mean fluorescence intensity (MFI) of the maturation markers (a) HLA-DR, (b) CD80, (c) CD86, (d) CD40, and (e) CCR7. (f) NK cells were left untreated (NK) or co-cultured with previously AI, AS, AF lysate stimulated or unstimulated MoDCs (US). NK cell activation was measured by the percentage of CD69 expressing NK cells. Data are represented as mean + SEM of three independent experiments. A student's test was performed, and significant differences are marked by asterisks (* $p < 0.05$, ** $p < 0.01$).

Experiments were also performed vice versa by stimulating NK cells with AI, AS, and AF lysate for 24 h. NK cells increased their CD69 expression after stimulation with AF lysate (Fig. 12a) but showed no significant up-regulation after treatment with AI or AS, even when stimulated with concentrations up to 20 µg/ml (Fig. 12b).

To investigate whether activated NK cells can transfer stimulating signals to immature moDCs, NK cells were treated either with AF lysate or plain medium for 24 h (Fig. 12a). Supernatants were removed, and NK cells were resuspended in fresh medium before NK-DC co-cultures were set for 16 h. MoDCs displayed a significant up-regulation of the maturation markers CD80 and CD86 after co-cultivation with NK cells stimulated with the AF lysate but not after co-culture with unstimulated NK cells (Fig. 12c, d), indicating that only activated NK cells can induce moDC maturation. These experiments firstly showed that moDCs and NK cells interact during infection with *A. fumigatus*, resulting in cell maturation or activation.

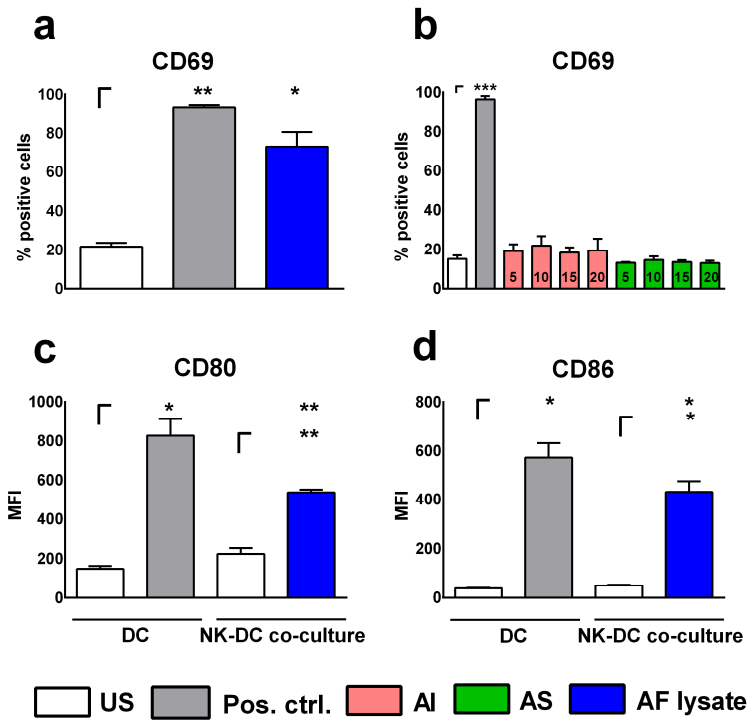

Figure 12: NK cell activation after stimulation with fungal components and NK-DC co-culture. NK cells were left untreated (NK US) or were stimulated with (a) the *A. fumigatus* lysate (NK AF lysate, 1 µg/ml), (b) alkali-insoluble (AI) and alkali-soluble (AS) cell wall fractions (5 – 20 µg/ml) or the positive control (Pos. ctrl, 500 U/ml IL-15) for 24 h. NK cell activation was quantified by the expression of CD69 positive NK cells. MoDCs were either left untreated (US) or were co-cultured with autologous, unstimulated (NK US) or pre-stimulated (NK AF lysate) NK cells for 16 h. As a positive control, MoDCs were stimulated with 1 µg/ml LPS (Pos. ctrl.). MoDC maturation was investigated by the measurement of the mean fluorescence intensity (MFI) of (c) CD80 and (d) CD86 costimulatory molecules. Data are represented as mean + SEM of three independent experiments. A student's t-test was performed and significant differences are marked by asterisks (* $p < 0.05$, ** $p < 0.01$, *** $p < 0.001$).

In summary, moDCs were stimulated by all three stimulants (Fig. 11a-e), while NK cells exhibited cell activation only after stimulation with AF lysate (Fig. 12a). However, NK cells were successfully stimulated by moDCs that were treated with stimulants that were not able to directly activate NK cells, implying that moDCs are relevant cells for NK cell activation during infection with *A. fumigatus*. Human NK cells express low amounts of Dectin-1 and TLR-2 on their surface [235]; therefore, stimulation with TLR-2 and Dectin-1 ligands induce moDC maturation (Fig. 13a, b) but no NK cell activation (Fig. 13c).

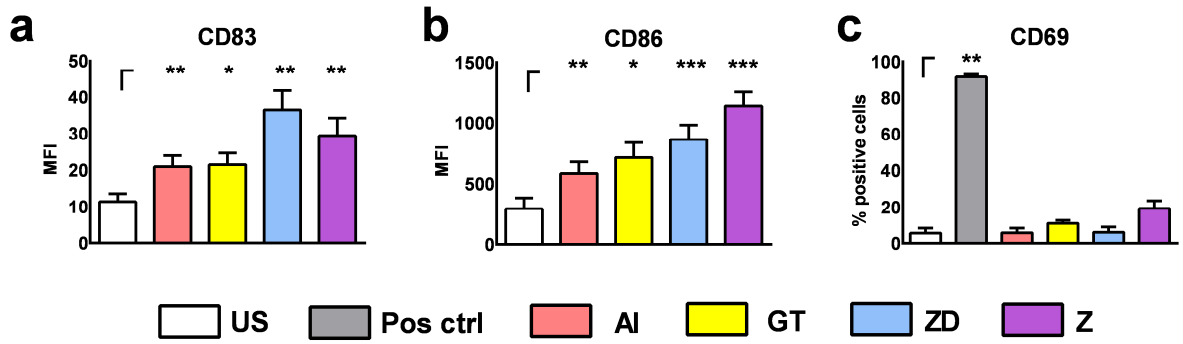

Figure 13: Stimulation of moDCs and NK cells with cell wall fraction, inactivated germ tubes, depleted zymosan, and zymosan. MoDCs were left untreated (DC US) or were stimulated with alkali-insoluble cell wall fraction (AI, 5 µg/ml), inactivated *A. fumigatus* germ tubes (GT, MOI 1), depleted zymosan (ZD, 100 µg/ml), or zymosan (Z, 10 µg/ml) for 9 h. MoDC maturation was analyzed by the measurement of the mean fluorescence intensity (MFI) of (A) CD83 and (B) CD86. Data are represented as mean + SEM of n = 6 independent experiments. (C) NK cells were left untreated (NK) or were stimulated with either the positive control (IL-15, 500 U/ml), AI (5 µg/ml), GT (MOI 1), ZD (100 µg/ml), or Z (10 µg/ml) for 16 h. NK cell activation was investigated by measuring the percentage of CD69 expression with flow cytometry. Data are represented as mean + SEM (C) n = 3 independent experiments. A student's t-test was performed and significant differences are marked by asterisks (* $p < 0.05$, ** $p < 0.01$, *** $p < 0.001$).

To investigate whether Dectin-1 or TLR-2 signaling in moDCs may be responsible for NK cell activation by the secretion of cytokines, we transferred supernatants from Dectin-1 and TLR-2 silenced or blocked moDC stimulations onto resting, autologous NK cells. For stimulation, we used different components containing ligands for Dectin-1 and TLR-2. Dectin-1 recognizes the highly abundant β-(1,3)-glucans in the cell wall of *A. fumigatus* [109], and TLR-2 binds to fungal conidia and hyphae [255].

Mock silenced moDCs, and Dectin-1 silenced moDCs were stimulated with AI, inactivated *A. fumigatus* germ tubes (GT), depleted zymosan (ZD) and zymosan (Z) for 9 h before moDC supernatants were transferred onto autologous, resting NK cells for 16 h. Gene silencing of Dectin-1 was 86.38 % compared to transfection control (Fig. 14a). Supernatants from unstimulated moDCs enhanced CD69 expression (mock: 19.37 %, siRNA: 16.27 %) compared to NK cells treated with blank medium (4.90 %, Fig. 14b). Mock silenced moDC supernatants of AI, GT, or ZD stimulations induced a moderate CD69 expression (41.26-

48.84 %, Fig. 14b), whereas supernatants derived from stimulation with Z boosted NK cell activation (90.76 %, Fig. 14b). Soluble factors of mock silenced moDCs induced higher CD69 expression (41.3 %) compared to Dectin-1 silenced moDCs (33.1 %) when stimulated with the Dectin-1 ligand ZD (Fig. 14b). Supernatants from moDCs stimulated with AI showed a trend towards decreased NK cell activation compared to mock silenced controls treated with AI (Fig. 14b). However, Dectin-1 silencing could not significantly reduce NK cell activation, concluding that there might be other moDC receptors besides Dectin-1 with more impact on NK cell activation.

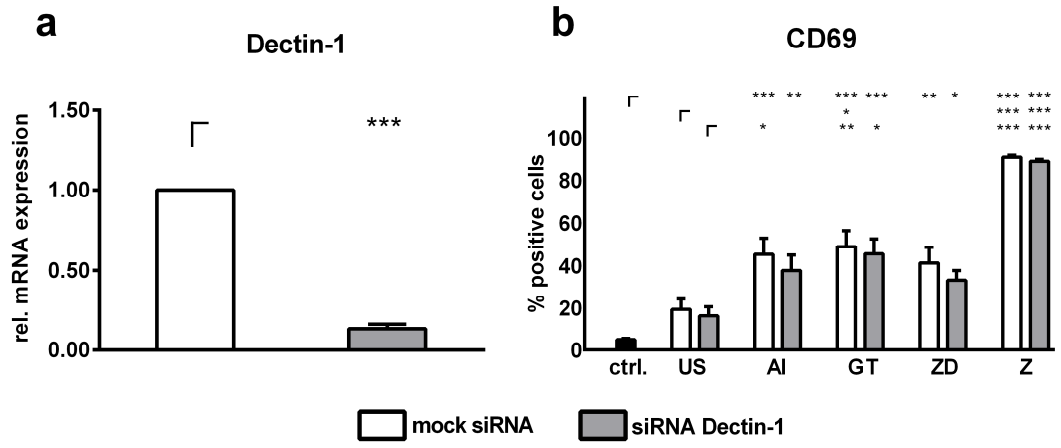

Figure 14: Soluble factors derived from Dectin-1 silenced and mock silenced moDCs activate autologous NK cells. (a) MoDCs were electroporated with Dectin-1 siRNA or mock siRNA and were cultured for 24 h at 37 °C. RNA was isolated from 1 x 10^6 cells and was converted to cDNA. RT-PCR was performed to quantify Dectin-1 downregulation on the mRNA level. Dectin-1 mRNA expression level of Dectin-1 silenced moDCs was calculated compared to mock control. (b) Dectin-1 silenced or mock silenced moDCs were stimulated with the alkali-insoluble cell wall fraction (AI, 5 µg/ml), inactivated *A. fumigatus* germ tubes (GT, MOI 1), depleted zymosan (ZD, 100 µg/ml), zymosan (Z, 10 µg/ml), or were left untreated (US) for 9 h. Soluble factors from moDC stimulation were transferred onto resting, autologous NK cells for 16 h. The expression of CD69 assessed NK cell activation. Data are represented as mean + SEM of n = 5 independent experiments. Statistical analyses were performed by (a) student's t-test or (b) ANOVA + Bonferroni correction and significant differences are marked by asterisks (* $p < 0.05$, ** $p < 0.01$, *** $p < 0.001$).

Thus, we next tested whether TLR-2 signaling in moDCs is important for moDC-mediated NK cell activation. Therefore, moDCs were incubated with a TLR-2 blocking antibody (bAb) or isotype control for 1 h before cells were stimulated with AI, GT, ZD, and Z for 24 h. FSL, a synthetic diacylated lipoprotein derived from *Mycoplasma salivarium* [256], is recognized by TLR-2/TLR-6 heterodimers [257] and was used as a positive control as suggested by the manufacturer. As a control for successful TLR-2 blocking, bAb and control-treated moDCs were stained after 24 h with a goat anti-mouse secondary antibody (Fig. 15a, b). MoDC maturation was measured by flow cytometry using an anti-CD80 antibody (Fig. 15c). The TLR-2/-6 ligand FSL induced a significant up-regulation of CD80 on moDCs treated with the isotype control but not with the TLR-2 bAb, confirming successful TLR-2

blocking (Fig. 15c). However, TLR-2 blocking had no influence on CD80 up-regulation on moDCs stimulated with AI, GT, ZD and Z compared to unstimulated controls (Fig. 15c).

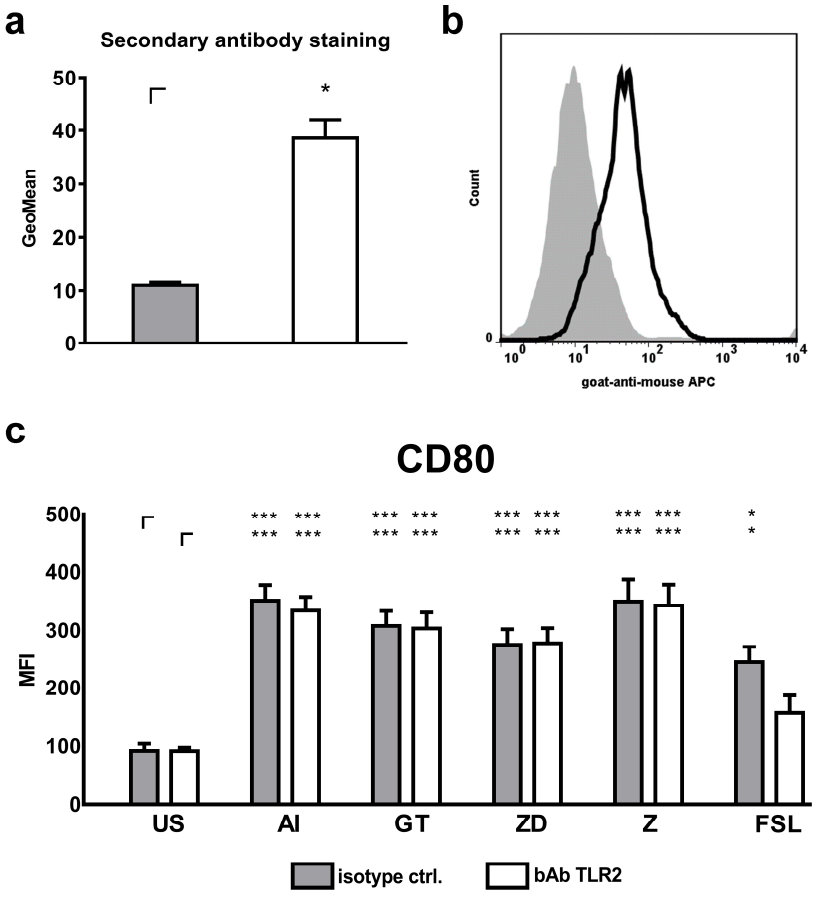

Figure 15: TLR-2 blocking and moDC stimulation. MoDCs were treated with TLR-2 blocking antibody (10 µg/ml) or isotype control at a cell concentration of 2 x 10^6 cells/ml for 1 h at 37 °C. (a) TLR-2 blocking was monitored by staining the blocking antibody with a secondary goat anti-mouse antibody. (b) Fluorescence histogram of the secondary antibody staining of one out of 3 independent experiments is shown. MoDCs were diluted to 1 x 10^6 cells/ml with medium and stimulated with the alkali-insoluble cell wall fraction (AI, 5 µg/ml), inactivated *A. fumigatus* germ tubes (GT, MOI 1), depleted zymosan (ZD, 100 µg/ml), zymosan (Z, 10 µg/ml), FSL (100 ng/ml) or were left untreated (US) for 24 h. (A) MoDCs treated with TLR-2 blocking antibody or isotype control were stained with goat anti-mouse secondary antibody. Geo Mean of fluorescence was analyzed from n = 3 independent experiments. A student's t-test was performed and significant differences are marked with an asterisk (* $p < 0.05$ (c) CD80 mean fluorescence intensity (MFI). Data are represented as mean + SEM of n = 5 independent experiments. ANOVA + Bonferroni correction was performed and significant differences are marked by asterisks (* $p < 0.05$, *** $p < 0.001$).

FSL-treated moDCs induced a decreased CD69 up-regulation on NK cells when TLR-2 was blocked compared to isotype-treated moDCs (Fig. 16a). Notably, NK cells were not activated by FSL in direct stimulations (Fig. 16b). TLR-2 blocking had no influence on NK cell activation when NK cells were incubated in Z stimulated DC supernatants (Fig. 16a). Taken together, neither Dectin-1 nor TLR-2 inhibition could prevent moDC-mediated NK

cell activation when we used cell wall fractions (AI) or whole fungal structures (GT) for stimulation. In contrast, NK cell activation was specific for the used moDC stimulus, since stimulation with Z yielded in the highest NK cell activation (Fig. 14b, 6a).

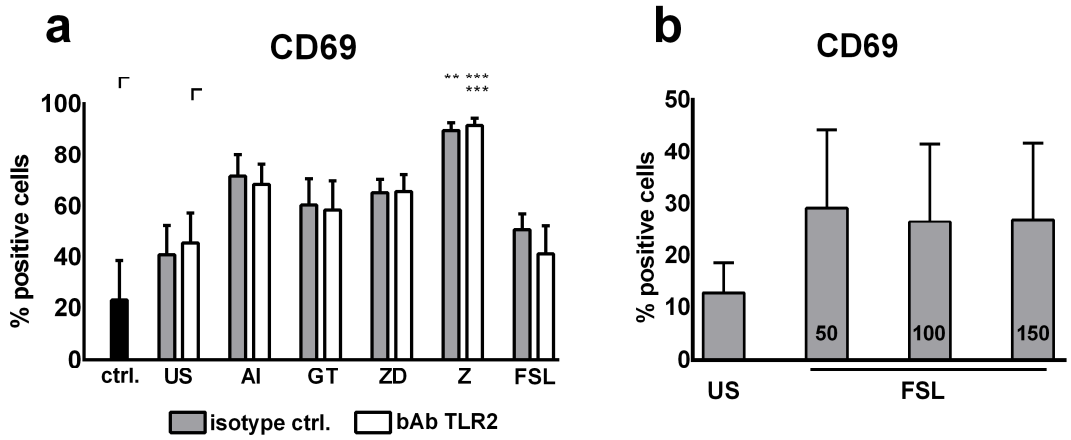

Figure 16: Soluble factors derived from TLR-2 blocked moDCs activate autologous NK cells. MoDCs treated with TLR-2 blocking antibody (10 µg/ml) or isotype control were stimulated with the alkali-insoluble cell wall fraction (AI, 5 µg/ml), inactivated *A. fumigatus* germ tubes (GT, MOI 1), depleted zymosan (ZD, 100 µg/ml), zymosan (Z, 10 µg/ml), FSL (100 ng/ml) or were left untreated (US) for 24 h. Soluble factors from moDC stimulation were transferred onto resting, autologous NK cells for 16 h. (a) NK cell activation was assessed by the expression of CD69. Untreated NK cells were used as a control (ctrl.). (b) NK cells were stimulated with FSL ligand (50 ng/ml, 100 ng/ml or 150 ng/ml) for 16 h. Data are represented as mean + SEM of (a) n = 4, (b) = 3 independent experiments. Statistical analyses were performed by (a) ANOVA + Bonferroni correction or (b) a student's t-test and significant differences are marked by asterisks (* $p < 0.05$, ** $p < 0.01$, *** $p < 0.001$).

To analyze which soluble factors are secreted after stimulation with Z, several cytokines and chemokines which play a role in general immune reactions (IFN-γ, IL-6, IL-8, IL-10, IL-1α, IL-1β, MIP-3α, TNF-α) or are specifically important for NK cell activation (IL-2, IL-12p70, IL-15, IL-18, IP-10) were analyzed by multiplex immunoassay (Fig. 17a-h). Secretion of IFN-γ, IL-2, IL-15, IL-18, and IL-1α was weak or not detectable after stimulation of moDCs with the different stimuli (data not shown). In contrast, high levels of IL-1β, IL-8, TNF-α, and MIP-3α were detected after all stimulations (IL-1β: 96.42-232.77 pg/ml; IL-8: 2.95-3.97 ng/ml; TNF-α: 5.5-28.03 ng/ml; MIP-3α: 1.29-4.24 ng/ml, Fig 17a-d). IL-6 and IL-10 were highly secreted after all stimulations but showed the highest secretion after treatment with Z (Fig. 7e, h). Furthermore, stimulation with Z boosted the secretion of IL-12p70 and Interferon-γ-inducible protein (IP)-10 (Fig. 17f, g). These results showed that the stimulating properties of Z are beneficial for cytokine secretion and NK cell activation.

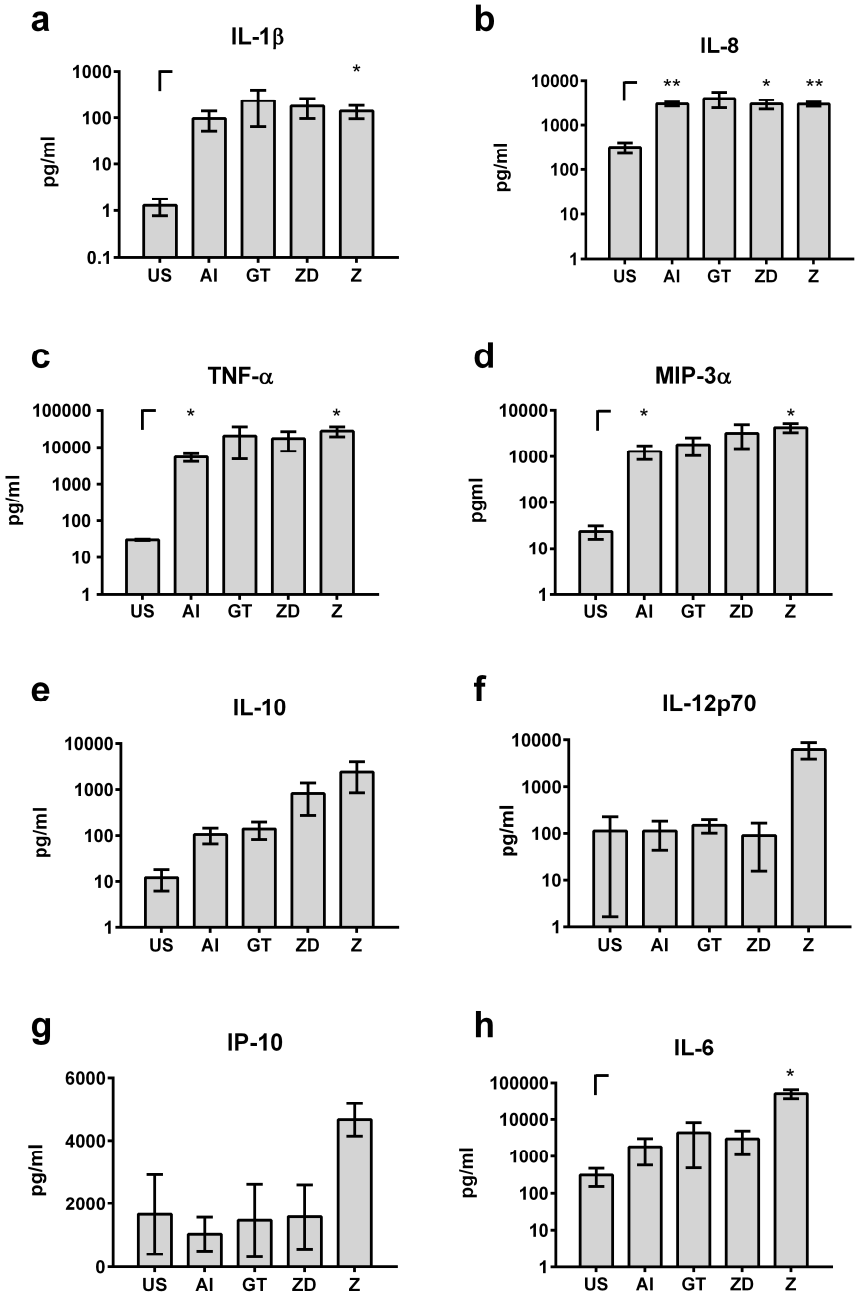

Figure 17: Cytokines and chemokines in moDC supernatants. MoDCs were stimulated with the alkali-insoluble cell wall fraction (AI, 5 µg/ml), inactivated *A. fumigatus* germ tubes (GT, MOI 1), depleted zymosan (ZD, 100 µg/ml), zymosan (Z, 10 µg/ml), or were left untreated (US) for 9 h. IL-1β (a), IL-8 (b), TNF-α (c), MIP-3α (d), IL-10 (e), IL-12p70 (f), IP-10 (g), and IL-6 (h) cytokine levels were analyzed by multiplex immunoassay. Data are represented as mean +/- SEM of n = 3 independent experiments. A student's t-test was performed to compare treated samples (AI, GT, ZD, Z) with un-stimulated (US) samples. Significant differences are marked by asterisks (* $p < 0.05$, ** $p < 0.01$).

To test whether the measured cytokines and chemokines after moDC stimulation are sufficient to induce CD69 expression by NK cells, we thawed PBMCs, isolated NK cells, and stimulated those with cytokines and chemokines (Fig. 18). We specifically focused on cytokines and chemokines showing the highest concentrations after stimulation with Z (Fig. 17e-h), since Z stimulated moDC supernatants induced the highest NK cell activation (Fig.

14b, 16a) and therefore were the most prominent candidates containing important cytokines and chemokines in NK-DC cross-talk. Thus, NK cells were stimulated with a lower and a higher concentration of IL-6, IL-12, IP-10 and IL-10 within the measured range of secreted cytokines and chemokines after moDC stimulation with Z (Fig. 17e-h).

However, only IL-15 could induce such a high CD69 expression on NK cells measured with Z stimulated moDC supernatants before (Fig 18). In consequence, the cytokines and chemokines tested alone or in combination were not responsible for CD69 expression.

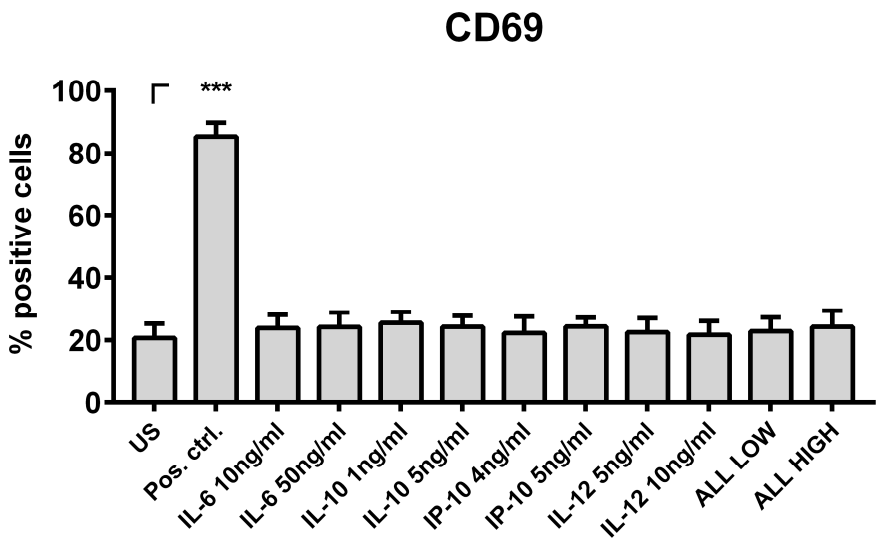

Figure 18: NK cell stimulation with cytokines and chemokines. NK cells were isolated from thawed PBMCs and were stimulated with IL-6 (10 ng/ml and 50 ng/ml), IL-10 (1 ng/ml and 5 ng/ml), IP-10 (4 ng/ml and 5 ng/ml), IL-12 (5 ng/ml and 10 ng/ml) or the combination of all cytokines and chemokines in low or high concentration, respectively. After 16 h, NK cell activation was analyzed by flow cytometry. Data are represented as mean + SEM of n = 3 independent experiments. A student's t-test was performed to compare treated samples with unstimulated (US) samples. Significant differences are marked by asterisks (*** $p < 0.001$).

Discussion

Stimulation with antigen-pulsed donor DCs can enhance the proliferation status of PBMCs derived from stem cell recipients [258] and induces a protective Th1 response [143]. Also, NK cell counts and reconstitution time inversely correlate with a higher risk of developing mold infections after stem cell transplantation showing that NK cells might have a protective effect against *A. fumigatus* [199]. NK-DC cross-talk may be beneficial against pathogens in several ways. Firstly, it has been shown that TLR-activated DCs can induce IFN-γ secretion by NK cells [145], which is essential for the stimulation of further cell types such as alveolar macrophages to phagocytose fungal spores [147, 198]. Secondly, NK cell killing of pathogens or pathogen-infected cells may be enhanced by DCs. For example, CXCL10 secretion after infection of DCs with *Mycobacterium tuberculosis* enhanced NK cell migration to sites of infection where they killed pathogen-infected cells [259].

To investigate if and how DCs modulate the NK cell immune response against *A. fumigatus*, we investigated the immune cell cross-talk after stimulation with inactivated *A. fumigatus* germ tubes and other ligands. The primary focus was put on the fungal receptors Dectin-1 and TLR-2, which are known to be expressed on moDCs but hardly on NK cells. We initially analyzed whether NK cells and moDCs can transfer activation signals during cell-to-cell contact. Indeed, both cell types showed activation or maturation after stimulation with *A. fumigatus* lysate and, therefore, can transfer stimulating signals to autologous, resting, or immature cells, showing that these immune cells can communicate during *A. fumigatus* infections. Interestingly, moDCs recognized cell wall fractions of *A. fumigatus* that contain the Dectin-1 specific ligand β-(1,3)-glucan and could activate NK cells even when the stimulus did not directly activate those. Since NK cells rarely express Dectin-1 or TLR-2 on their surface [235], these experiments supported our hypothesis that DCs have a substantial role in NK cell activation, which may also play a role *in vivo* during infection with *A. fumigatus*.

TLR-2, TLR-4, Dectin-1 and Dectin-2 are important fungal recognition receptors on DCs [123, 260, 261]. While *A. fumigatus* conidia and hyphae modulate TLR-2 and TLR-4 signaling [260], galactomannan is specifically bound by Dectin-2 [262], and β-(1,3)-glucans are recognized by Dectin-1 [109]. To analyze the impact of moDC-mediated Dectin-1 signaling on NK cells, we silenced Dectin-1 and stimulated moDCs with ligands for Dectin-1. The polysaccharide β-(1,3)-glucan is a component of the fungal cell wall and therefore represented in cell wall fractions, inactivated germ tubes, and yeast-derived cell wall preparations of zymosan. Hot alkali treatment of zymosan results in the removal of TLR-2 stimulating agents and, therefore, depleted zymosan is exclusively stimulating Dectin-1. However, Dectin-1 silenced moDCs stimulated with ZD were still able to up-regulate CD69 expression

on NK cells, assuming that only a few amounts of unsilenced receptors are sufficient for moDC maturation. We noticed no significant difference in the induction of NK cell activation between stimulated moDCs treated with Dectin-1 or mock siRNA, concluding that Dectin-1 has no important impact on moDC-mediated NK cell activation.

Next, we analyzed the influence of TLR-2 on moDC-mediated NK cell activation. FSL was used as a positive control recommended by the manufacturer. FSL is no exclusive TLR-2 ligand and, additionally, stimulates TLR-6. There was decreased moDC maturation after FSL stimulation when TLR-2 was blocked; however, other stimulants showed no differences in inducing moDC maturation and NK cell activation after TLR-2 blocking. Thus, we conclude that neither Dectin-1 nor TLR-2 are essential for moDC-mediated NK cell activation, or that other functional receptors are able to compensate for the function of these receptors. Redundancy of fungal receptor function was also hypothesized by Chai *et al.* after they observed that Dectin-1 polymorphism resulted in less secretion of TNF-α and IL-6 from PBMCs but had no influence on cytokine secretion in monocyte-derived macrophages. Concludingly, they hypothesized that other receptors could compensate for lost Dectin-1 signaling [263]. It has been shown that Dectin-1 and TLR-2 can synergize to mediate macrophage activation by mycobacteria [264]. Thus, future experiments are required to analyze the effects of simultaneous blocking of Dectin-1 and TLR-2 on NK cell activation.

DCs secreted intermediate to high amounts of IL-1β, TNF-α, and MIP-3α, which are cytokines secreted after activation of Dectin-1 [261, 265]. High NK cell activation was mediated after transferring supernatants of Z-stimulated moDCs. We detected specific Z-induced cytokines that might be responsible for NK cell activation, namely IL-12p70, IL-6, IL-10, and IP-10. While IL-6 and IL-10 are general pro- and anti-inflammatory cytokines [266], IL-12p70 and IP-10 were described to induce NK cell activation and to be partially dependent on TLR-2 signaling [267-269]. Therefore, we tested whether physiological concentrations of IL-6, IL-10, IL-12, or IP-10 can induce CD69 expression, as seen with supernatants of Z-stimulated moDCs. Even when used in combination, IL-6, IL-12, IL-10, or IP-10 were not able to induce CD69 expression on NK cells. In conclusion, other soluble factors induce NK cell activation after moDC stimulation with TLR-2/Dectin-1 ligands.

In summary, this is the first study that gives insight into NK-DC cross-talk during infection with *A. fumigatus in vitro*. Future studies are required to deeper characterize NK-DC cross-talk regarding the importance of cellular and soluble factors.

Chapter 2:

CD56 is a pathogen recognition receptor on human NK cells

The following work was published in:

Nature Scientific Reports, July 2017

Introduction

IA is a devastating disease caused by *A. fumigatus*, which affects immunocompromised patients suffering from hematological malignancies or undergoing alloSCT [270]. The mortality rate of HSCT patients diagnosed with IA ranges from 60-90 % [271], and the prognosis for long-term survival is extremely poor [272]. Recently, it was shown that alloSCT patients with probable/proven IA had a delayed reconstitution of natural killer (NK) cells for more than a year post-alloSCT [199]. Besides, patients with severe IA were found to have a lower NK cell count compared to patients with well-controlled IA, suggesting that NK cells play a critical role in immunity to IA.

NK cells comprise 5-15 % of the PBMCs in healthy individuals and belong to the innate immune system [273]. Upon activation, NK cells release immune-regulatory cytokines to stimulate other immune cells and display cytotoxicity directed against tumor or virus-infected cells by granule release [273]. NK cells are defined as CD56 positive and CD3 negative cells and can be distinguished into $CD3^{-}CD56^{dim}CD16^{+}$ and $CD3^{-}CD56^{bright}CD16^{-}$ cells. While $CD56^{dim}$ cells are more cytotoxic, $CD56^{bright}$ cells produce high levels of cytokines such as IFNγ and TNFα [176]. The function of NK cells is induced by the interplay of inhibitory and activating receptors [274], leading to cytotoxicity directed against tumors and virus-infected cells. Besides the recognition of these cells, NK cells also recognize other infectious pathogens, become activated, and as a response induce either lysis of these pathogens or trigger activation of other immune cells by cytokine release [191, 275, 276]. Consequently, an important function of NK cells in response to several fungal pathogens, including *A. fumigatus*, *C. albicans*, *C. neoformans,* and *Mucorales spp.* has been demonstrated [191, 249, 250, 253, 277-279].

Previous studies demonstrated that NK cells are activated by direct interaction with *A. fumigatus* germ tubes and hyphae [253, 277]. Upon activation, NK cells release cytotoxic granules containing granzyme and perforin, which damage *A. fumigatus* hyphae [253]. Direct contact with *A. fumigatus* germ tubes induces IFNγ release of NK cells, which interferes with fungal metabolic activity and growth [277]. Furthermore, studies in a neutropenic IA mouse model demonstrated that NK cell recruitment is essential for the clearance of the fungal infection and that IFNγ release by NK cells is critical for the immune defense during IA [147, 197, 198]. Although NK cells have been shown to play a crucial role in host-pathogen interaction during *A. fumigatus* infection, the underlying mechanism and the NK cell recognition receptors have not been identified to date.

Results

To identify possible PRRs on NK cells, the expression of several NK cell activating receptors and of the *A. fumigatus* PRRs TLR-2, TLR-4, and Dectin-1 [261, 280, 281] were analyzed in the presence of *A. fumigatus* after different incubation times using flow cytometry. Importantly, no difference in the expression of the mentioned receptors was noticed (Fig. 19). Even so, NKp30 has been described as a PRR for fungal pathogens [191, 192]; no significant changes were detected in the presence of *A. fumigatus* (Fig. 19).

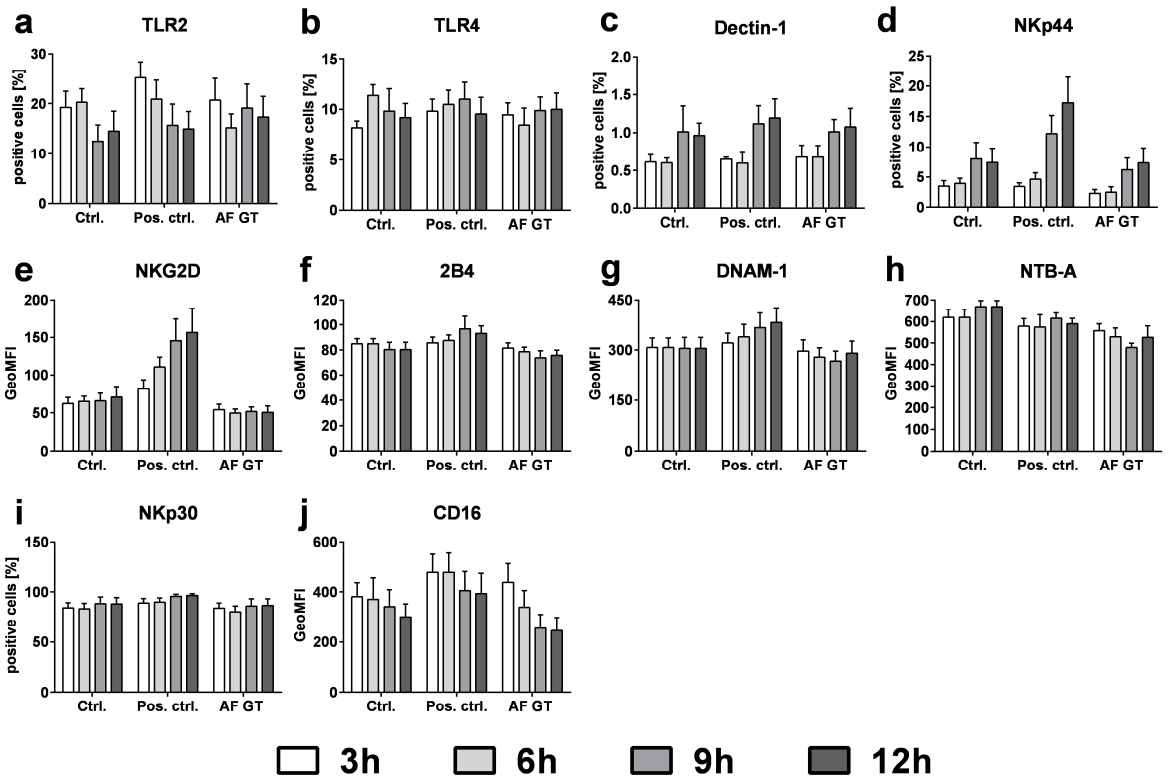

Figure 19: Expression of PRRs and NK cell activating receptors is not altered by the presence of *A. fumigatus*. Primary NK cells were pre-treated overnight with IL-2 (1000 U/ml). NK cells were treated with 500 U/ml IL-15 and IL-2 (Pos. ctrl.), with A. fumigatus germ tubes (AF GT) at MOI 0.5 or left untreated (Ctrl.) for 3 h, 6 h, 9 h, and 12 h. Flow cytometry was performed to analyze a) TLR-2, b) TLR-4, c) Dectin-1, d) NKp44, e) NKG2D, f) 2B4, g) DNAM-1, h) NTB-A, i) NKp30 and j) CD16 cell surface expression. NK cells were defined as $NKp46^{+}CD3^{-}$. For TLR-2, TLR-4, Dectin-1, NKp30, and NKp44 percent positive cells are shown whereas for NKG2D, 2B4, DNAM-1, CD16 and NTB-A the geometric mean fluorescence is visualized. Data are represented as mean + SEM of a) n = 5, b) n = 6, c) n = 4, d) n = 4, e) n= 4, f) n = 3, g) n = 3, h) n = 3, i) n = 5 and j) n = 5 independent experiments.

CD56 used in combination with CD3 is a well-known characterization marker to distinguish NK cells from other immune cells such as T-cells or monocytes [282, 283]. Surprisingly, we detected a prominent reduction of CD56 fluorescence positivity of NK cells after co-cultivation with *A. fumigatus* germ tubes compared to control NK cells (Fig. 20a). Additionally, NK cells were observed to upregulate the CD69 receptor (Fig. 20b) upon fungal

contact, indicating NK cell activation [284]. Interestingly, the reduction of CD56 fluorescence positivity of NK cells started as early as 2 h post-incubation (Fig. 20c). To evaluate whether this effect was dependent on the fungal MOI, we investigated the decrease of CD56 fluorescence positivity of NK cells at different MOIs 6 h after co-cultivation. A significant decrease of CD56 fluorescence positivity of NK cells (71.9 %) was observed at an MOI of 0.1 compared to control NK cells (97 %) (Fig. 20d).

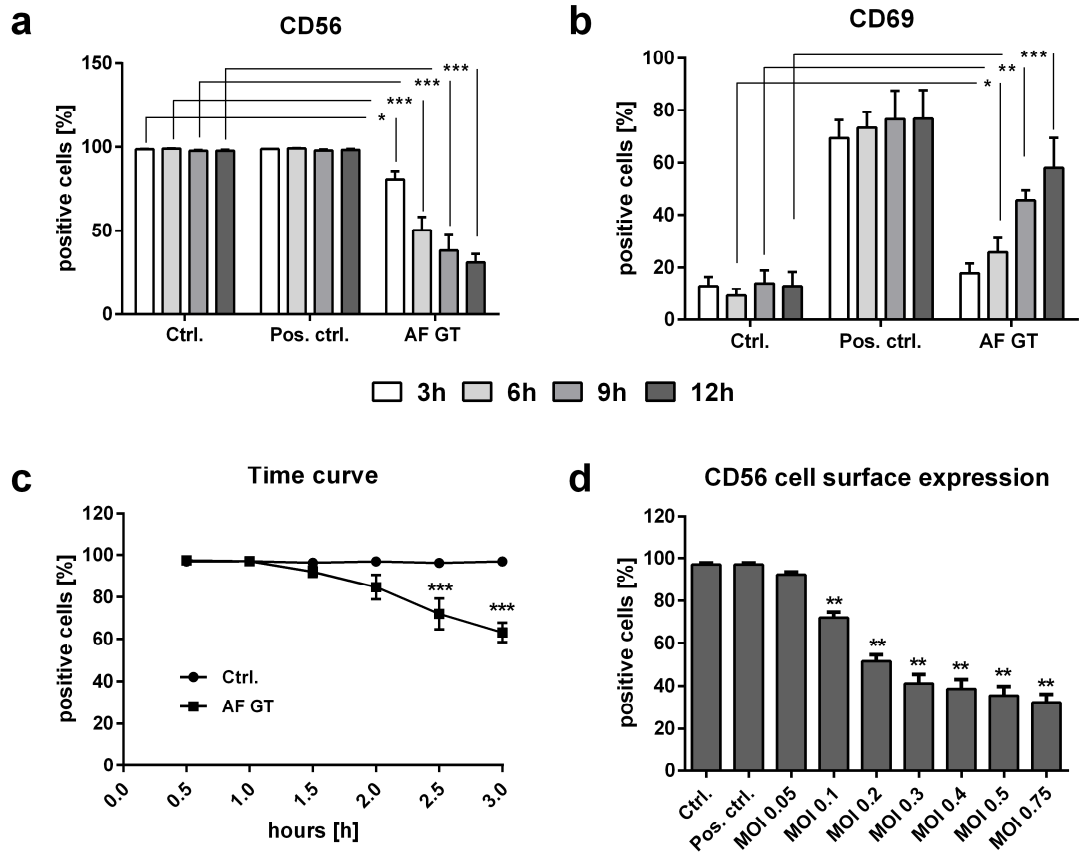

Figure 20: Reduction in CD56 positivity after fungal contact. NK cells were treated with 500 U/ml IL-15 and IL-2 (Pos. Ctrl.), with *A. fumigatus* germ tubes (AF GT, MOI 0.5) or left untreated (Ctrl.) for different periods of time. Flow cytometry was performed to analyze (a) CD56 expression (n = 4), (b) CD69 expression (n = 5), (c) time-dependent down-regulation of CD56 (n = 5) and (d) CD56 expression after treatment with different MOIs of *A. fumigatus* germ tubes (AF GT, n = 3). NK cells were incubated for 3, 6, 9 and 12 h to determine (a) CD56 and (b) CD69 expression. To determine the time-dependent down-regulation of CD56 NK cells were incubated for 0.5, 1, 1.5, 2, 2.5 and 3 h (c). To assess the effect of different fungal MOIs, NK cells were incubated for 6 h (d). NK cells were defined as $NKp46^{+}CD3^{-}$. Data are represented as mean + SEM. Significant differences were are marked by asterisks (* $p < 0.05$, ** $p < 0.01$, *** $p < 0.001$).

A potential mechanism that could provoke down-regulation of protein expression on the cell surface is apoptosis. Mycotoxins produced by *A. fumigatus* are not only able to inhibit DNA and RNA synthesis in affected cells, but can also induce apoptosis by cell membrane alterations [285]. To investigate whether the reduction of CD56 fluorescence positivity of NK cells was caused by the induction of apoptosis, NK cells were stained with Annexin V

to identify apoptotic NK cells. NK cells confronted with *A. fumigatus* germ tubes for 9 h showed a reduction of CD56 fluorescence positivity (Fig. 21a), while only a few NK cells were both, CD56 negative and Annexin V positive. However, the CD56 negative NK cells were mostly negative for Annexin V (54.6 %), indicating that apoptosis is not induced in these cells (Fig. 21a).

To better understand the mechanism of CD56 reduction, we determined CD56 gene expression in NK cells confronted with *A. fumigatus* germ tubes for different incubation times. In the control experiments, the expression of CD56 mRNA was time-dependently increased after treatment with IL-15 and IL-2 (Fig. 21b), whereas the expression of CD56 mRNA in NK cells co-cultivated with *A. fumigatus* was not altered (Fig. 21b). These results indicated that gene expression was not differentially regulated by exposure to *A. fumigatus* and that a different mechanism is responsible for the reduction of CD56 positive NK cells. To study potential CD56 shedding upon contact of NK cells with *A. fumigatus*, cell culture supernatants were collected from co-cultures after 3, 6, 9, and 12 h and the supernatants were tested for CD56 by ELISA. The level of CD56 in the supernatant was observed to be equal or below the smallest standard for all samples and no significant changes in CD56 levels were detected at any of the incubation times of the co-culture experiments (Fig. 21c). Thus, CD56 shedding from the cell surface during NK cell – *A. fumigatus* interaction could be excluded as a possible mechanism.

To investigate whether CD56 was internalized upon contact with *A. fumigatus*, NK cells were co-cultured with *A. fumigatus* germ tubes for 6 h before CD56 was surface- and intracellularly-labeled. CD56 on the cell surface of NK cells cultured with germ tubes was significantly reduced compared to control NK cells, while the intracellular CD56 signal did not change (Fig. 21d). Even when only the intracellular signal was measured by former trypsinization of surface receptors, CD56 levels did not change (Fig. 21d). The protein concentration of CD56 was evaluated to investigate whether CD56 protein was degraded or protein synthesis was inhibited in NK cells exposed to *A. fumigatus* potentially due to the release of mycotoxins [285]. Cells were harvested after co-culture with *A. fumigatus* for 4 h, and protein lysates were subsequently prepared for western blot analysis. The signal of the CD56 protein in *A. fumigatus* treated NK cells was comparable with the ones of control cells (Fig. 21e). Since we detected a decrease in CD56 fluorescence positivity of NK cells in flow cytometry but not by western blotting, we concluded that this effect might be the consequence of fewer antigen-antibody interactions due to sterical problems.

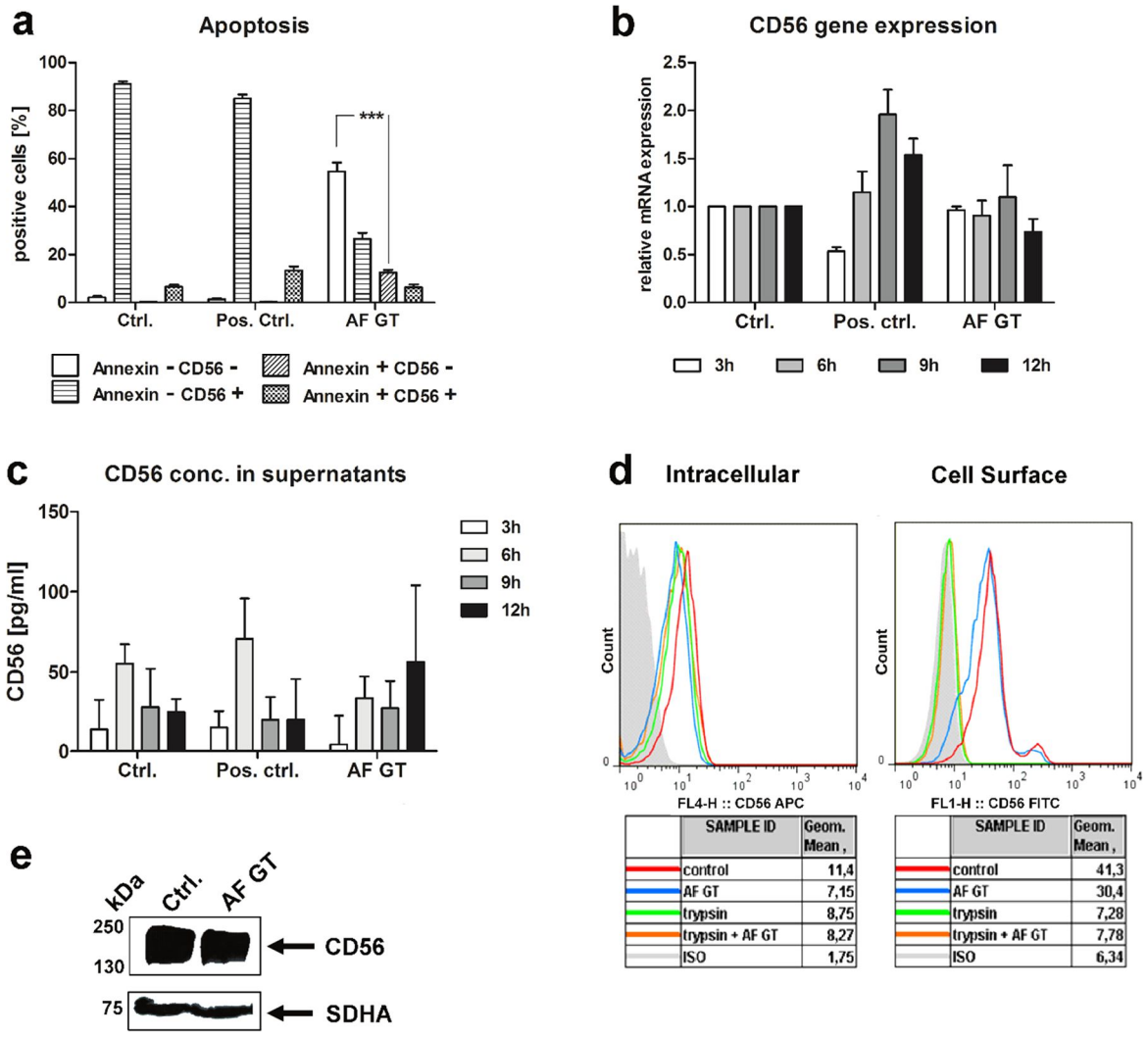

Figure 21: CD56 reduction is not induced by apoptosis, deregulation of protein, and gene expression. NK cells were either treated with 500 U/ml IL-15 and IL-2 (Pos. ctrl.), with *A. fumigatus* germ tubes (AF GT, MOI 0.5) or left untreated (Ctrl.). (a) Induction of apoptosis was determined 9 h after co-cultivation, and (b) mRNA/transcript expression after different incubation times was quantified by real-time RT-qPCR. (c) CD56 withdrawal was analyzed by ELISA. (d) Intracellular and membranous CD56 expression was analyzed by flow cytometry 6 h after co-cultivation. To detect only intracellular CD56 signal, NK cells were treated with trypsin before intracellular staining. (e) Protein concentrations were visualized by western blot analyses 4 h after co-cultivation. Blots were cropped and image processing was performed by Adobe Photoshop software. Representative data of five independent experiments. Data of (a–d) are represented as mean + SEM for n = 3. Significant differences are marked by asterisks (** $p < 0.01$).

NK cells were shown to release IFNγ and perforin upon direct contact with *A. fumigatus* [253, 277]. Thus we investigated the role of direct contact on the reduction of CD56 fluorescence positivity of NK cells. Co-cultures were prepared, separating NK cells and *A. fumigatus* germ tubes with transwell permeable membranes. The membranes were small enough to prohibit the contact of cells and *A. fumigatus* but large enough for molecules such as cytokines or mycotoxins to diffuse into the lower compartment. Expression of CD56 and CD69 on the surface of NK cells was determined after a 6 h cultivation. As a positive control,

IL-15 and IL-2 were added to the transmembrane system to activate NK cells (Fig. 22a). Separation of *A. fumigatus* germ tubes and NK cells by the transwell membrane did not induce NK cell activation, nor was CD56 fluorescence positivity of NK cells reduced (Fig. 22a). These results demonstrate that the reduction of CD56 fluorescence positivity of NK cells was not mediated via a fungal-derived soluble factor but was depended on direct contact with *A. fumigatus.*

To determine whether the decrease of CD56 fluorescence positivity of NK cells was regulated by the interaction with live germ tubes, NK cells were co-cultivated with inactivated *A. fumigatus* germ tubes, inactivated *C. albicans,* and live *A. fumigatus* germ tubes. NK cells exhibit cytotoxicity against tumor cells and become activated upon contact with these cells [286]; therefore, NK cells cultivated in the presence of the cancer cell line K562 served as a positive control. Cells were incubated for 12 h with different targets. Then, CD56 and CD69 fluorescence positive cells were determined. K562 cells induced significant activation of NK cells that was comparable to the activation of NK cells treated with IL-15 and IL-2 but showed no decrease of CD56 (Fig. 22b). Inactivated *C. albicans* and *A. fumigatus* did not induce the reduction of CD56 fluorescence positivity nor the activation of NK cells (Fig. 22b). Live *A. fumigatus* germ tubes activated NK cells and significantly reduced the number of CD56 fluorescence positive NK cells (Fig. 22b), suggesting that the decrease of CD56 fluorescence positivity of NK cells was only induced by live *A. fumigatus*.

From these experiments, we hypothesized that CD56 interacts as a recognition receptor for *A. fumigatus.* A further potential mechanism hypothesized for the reduction of CD56 fluorescence positivity of NK cells upon contact with *A. fumigatus* germ tubes is that CD56 acts as an interaction receptor for *A. fumigatus.*

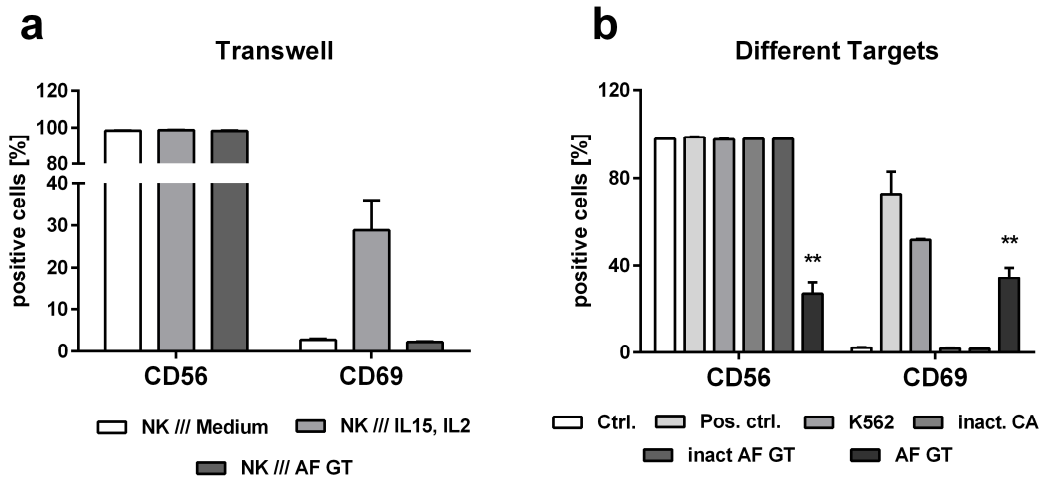

Figure 22: Reduction of CD56 is a result of the direct fungal contact. (a) NK cells were separated from fungal germ tubes (AF GT, MOI 0.5), medium supplemented with 500 U/ml IL-15 and IL-2 (Pos. ctrl) or medium (Ctrl.) by a transwell membrane (n = 3). (b) NK cells were cultured alone (Ctrl.), with 500 U/ml IL-15 and IL-2 (Pos. ctrl.), with K562 at an effector to target ratio of 5:1 (K562), with inactivated *C. albicans* (inact. CA, MOI 0.5) and with live and inactivated *A. fumigatus* germ tubes (AF GT, inact. AF GT, MOI 0.5, n = 6). Data are represented as mean + SEM. Significant differences are marked by asterisks (** $p < 0.01$).

SEM, CLSM, and *d*STORM microscopy were used to determine whether or not human NK cells interact directly with *A. fumigatus* hyphae and if CD56 is re-located during this interaction. NK cells were cultured alone or in the presence of *A. fumigatus* germ tubes for 3 h, and SEM pictures were taken from NK cell-*A. fumigatus* co-cultures. NK cells were observed interacting directly with *A. fumigatus,* and the interaction site was mostly at the hyphal part of the fungus (Fig. 23). We observed a close interaction of NK cells with *A. fumigatus* suggesting that NK cells recognize the fungus via specific receptors.

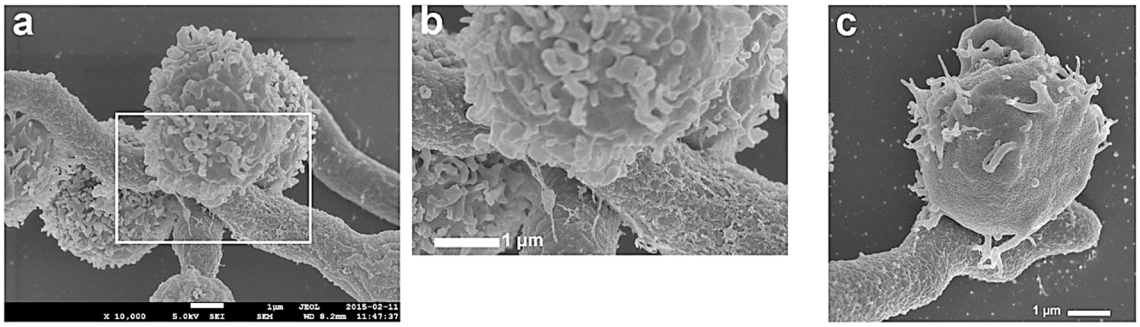

Figure 23: Direct contact with *A. fumigatus* hyphae. NK cells-*A. fumigatus* 3 h co-culture specimens were inspected with a field emission SEM using a detector for secondary electrons at 5 kV and a magnification of ×10,000. Representative result of two independent experiments performed in duplicates. Picture (b) is a zoom-in of (a), illustrating the interaction site of NK cells with *A. fumigatus* hyphae. Scale bar for (a–c): 1 µm.

To further confirm this observation and the possibility that CD56 is a recognition receptor we performed CLSM and super-resolution *d*STORM microscopy. After the cultivation of NK cells in the presence of *A. fumigatus* for different incubation times, CD56 localization was determined. Indeed, NK cells incubated with *A. fumigatus* revealed a strong CD56 signal at the contact site, whereas other parts of the plasma membrane exhibited only a weak signal (Fig. 24b, d, f). In contrast, the CD56 fluorescence signal in control cells was homogenously distributed on the plasma membrane (Fig. 24a, c). 3D-*d*STORM analysis revealed a concentration of CD56 fluorescence at the interaction site and in lanes surrounding the interaction site (Fig. 24e, f).

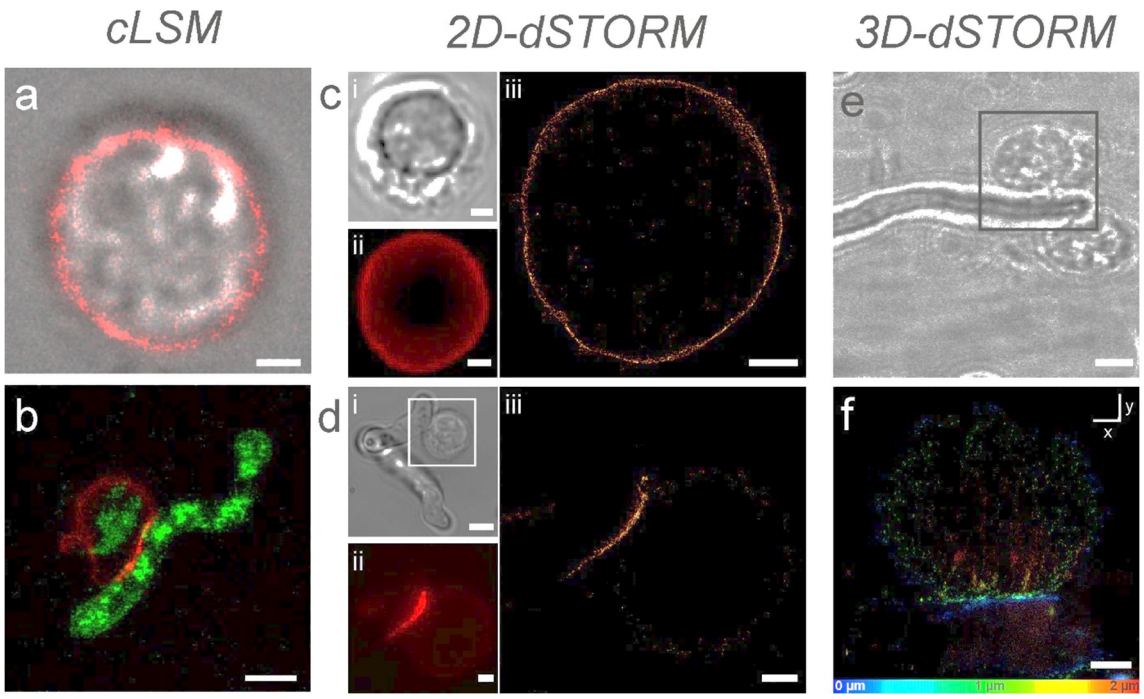

Figure 24: CD56 re-organization to the interaction site. NK cells and NK cells-*A. fumigatus* co-cultures were visualized with (a,b) CLSM, (c,d) 2D *d*STORM, and (e,f) 3D *d*STORM after staining with anti-CD56. NK cells were either left untreated (a,c) or incubated with *A. fumigatus* germ tubes (MOI 0.5) for 3 h (b,d–f). (b) Autofluorescence was recorded to visualize NK cell-*A. fumigatus* interaction. Transmitted light pictures (ci, di), (e), widefield fluorescence images (cii, dii), and *d*STORM images (ciii, diii) of the interaction site were compared. In (f) the x-y projection of a reconstructed 3D dSTORM image is given, which is color-coded in z. (e) The transmitted light picture is a zoom out of (f) illustrating two NK cells that interact with *A. fumigatus*. Scale bars: 1.5 µm (c, dii,iii), 2 µm (b,f), 3 µm (a,e), 4 µm (di), and 5 µm (b). 3D stack showing interaction site of NK cell *and A. fumigatus* (e,f). NK cells were incubated for 3 h with *A. fumigatus*, after that stained with anti-CD56-Alexa Fluor 647, and visualized in 3D.

We further observed that CD56 relocalization occurs in a time-dependent manner (Fig. 25a). At 3 h and 6 h after initiation of co-culture, CD56 signal is observed at the fungal interface and still ubiquitously distributed in the remaining NK cell membrane, which is not interacting with the fungus. At 9 h and 12 h, the CD56 signal is detected at the fungal interface but not in the remaining NK cell membrane anymore (Fig. 25a).

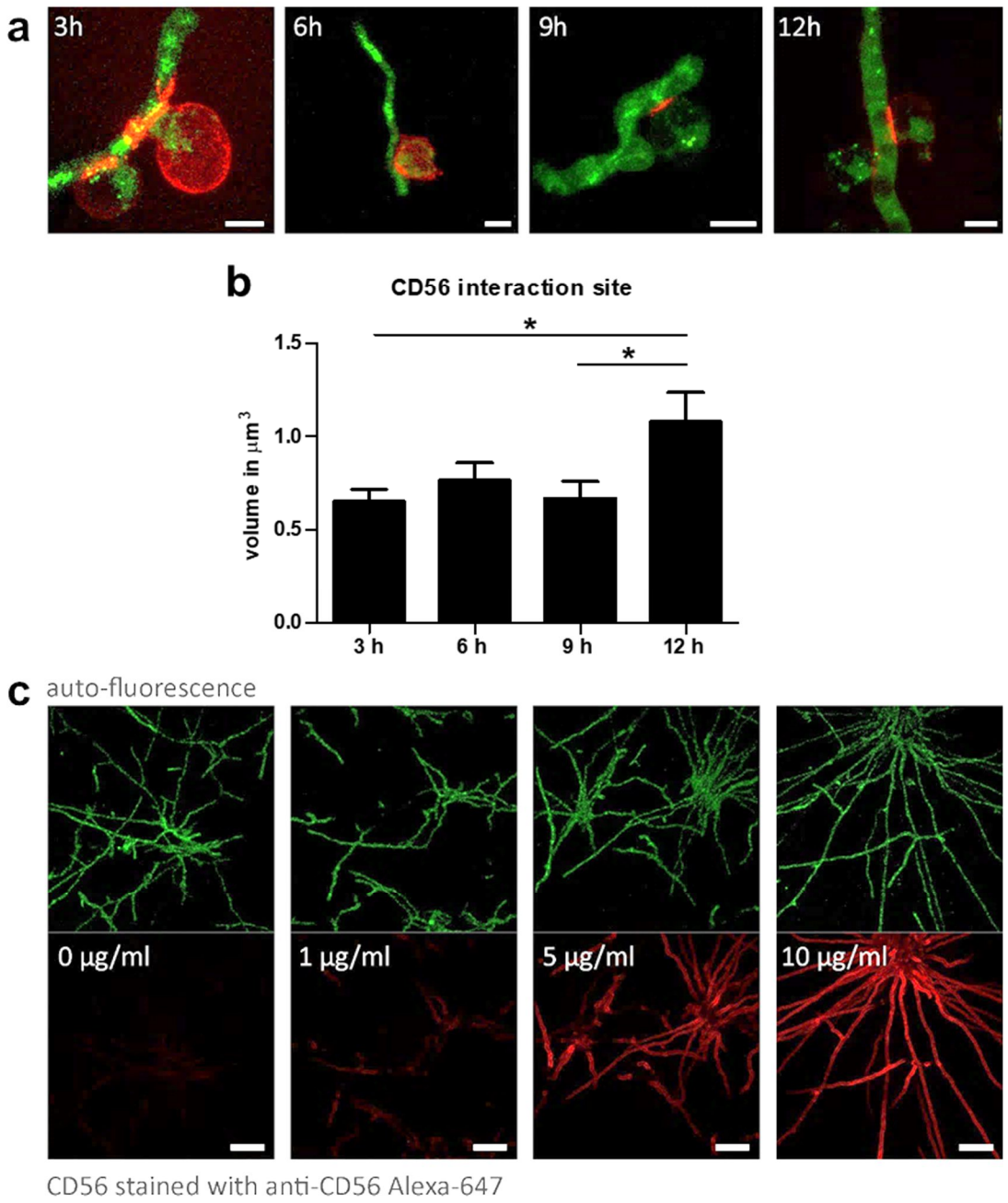

Figure 25: Time course of the NK cell-*A. fumigatus* interaction and direct binding of CD56 to the fungus. (a) NK cells were cultured with *A. fumigatus germ tubes* (MOI 0.5) for 3, 6, 9, and 12 h. CLSM pictures were taken from these co-cultures. (b) A total number of 154 interaction sites per time point (3, 6, 9, and 12 h) were analyzed from one donor by CLSM. We performed image analysis using Fiji software with the 3D object counter plugin to evaluate the volume in μm^3 of relocated CD56 at the fungal interaction site. Significant differences are indicated by an asterisk (*p <0.05) and were analyzed by one-way ANOVA. (c) Fungal hyphae were incubated for 6 h with 0, 1, 5, and 10 µg/ml soluble CD56 and afterward stained with anti-CD56 antibody. Alexa 647-labeled anti-CD56 antibody was used to visualize the distribution of CD56, while germ tubes were detected by their autofluorescence. Scale bars represent 5 µm (a) and 30 µm (b).

To proof that the interaction site is increasing time-dependently, we measured the length and amount of CD56 stained interaction sites after 3, 6, 9, and 12 h of co-culture, respectively. Indeed, the highest counts and the greatest lengths of interaction sites were

detectable after 12 h of co-cultivation (Fig. 25b), confirming that CD56 is re-localized to the fungal interface in a time-dependent manner. To elucidate whether CD56 is directly interacting with the fungus or if CD56 accumulation at the fungal interface is mediated by indirect mechanisms, we co-cultured live *A. fumigatus* germ tubes with different concentrations of soluble CD56 protein for 6 h and afterward stained the samples with a fluorescent anti-CD56 antibody (Fig. 25c). As a control, *A. fumigatus* germ tubes were cultured alone and were stained with fluorescent anti-CD56 antibody to exclude the possibility of unspecific antibody binding to the fungus (Fig 25c). In contrast to the negative control, incubation of *A. fumigatus* with soluble CD56 resulted in the staining of fungal structures after incubation with an anti-CD56 antibody (Fig. 25c). These experiments showed that CD56 is time-dependently relocalized to the fungal interface and directly binds the fungus.

It is well known that NK cells encounter the cytoskeleton when they recognize and lyse target cells [287]. While the actin cytoskeleton plays a role in the early recognition of target cells and enables receptor reorganization [287], cell lysis occurs to later time points and is mediated by the transport of lytic granules to the target interface via microtubules [287]. To investigate whether the actin or the microtubule cytoskeleton plays a role in the re-organization of CD56, we treated NK cells with either actin or microtubules inhibiting agents and then co-cultured NK cells with *A. fumigatus* germ tubes for 0, 3, 6, and 9 h, respectively. Cytochalasin D is preventing actin polymerization and elongation by binding to existing actin filaments [288], whereas colchicine binds to soluble tubulin dimers and thereby inhibits microtubule polymerization [289] and the transport of granules to the membrane [290]. NK cells treated with cytochalasin D compared to control NK cells did not show any differences in the CD56 fluorescence positivity of NK cells (Fig. 26a). However, when NK cells were challenged with the fungus we detected significantly less CD56 reduction of fluorescence positivity in cytochalasin D treated samples compared to controls, concluding that relocalization of CD56 is inhibited (Fig. 26a). In contrast, treatment with colchicine did not change the reduction of CD56 positivity in NK – *A. fumigatus* co-cultures compared to co-cultures without microtubule inhibition (Fig. 26b). In consequence, inhibition of actin polymerization but not inhibition of the microtubules impaired CD56 relocalization to the fungal interaction site concluding that CD56 plays a role in the early fungal recognition. To further functionally analyze the role of CD56, we blocked CD56 on the NK cell surface using an anti-CD56 blocking antibody before co-cultivation of NK cells with *A. fumigatus* germ tubes for 9 h (Fig. 26c). The blocked CD56 receptor was still recognized by the flow cytometric antibody directed against CD56 since NK cells treated with the blocking antibody displayed the same percentage of CD56 positivity as unblocked NK cells (Fig 26c). In the presence of the fungus, CD56 blocking restored the number of CD56 fluorescence positive NK cells to 55 %

after fungal co-culture compared to 20 % when CD56 was not blocked (Fig. 26c). Interestingly, treatment with CD56 blocking antibody significantly decreased the fungal-induced activation of NK cells (13.3 %) compared to NK cells on which CD56 was not blocked (18.5 %) (Fig. 26c).

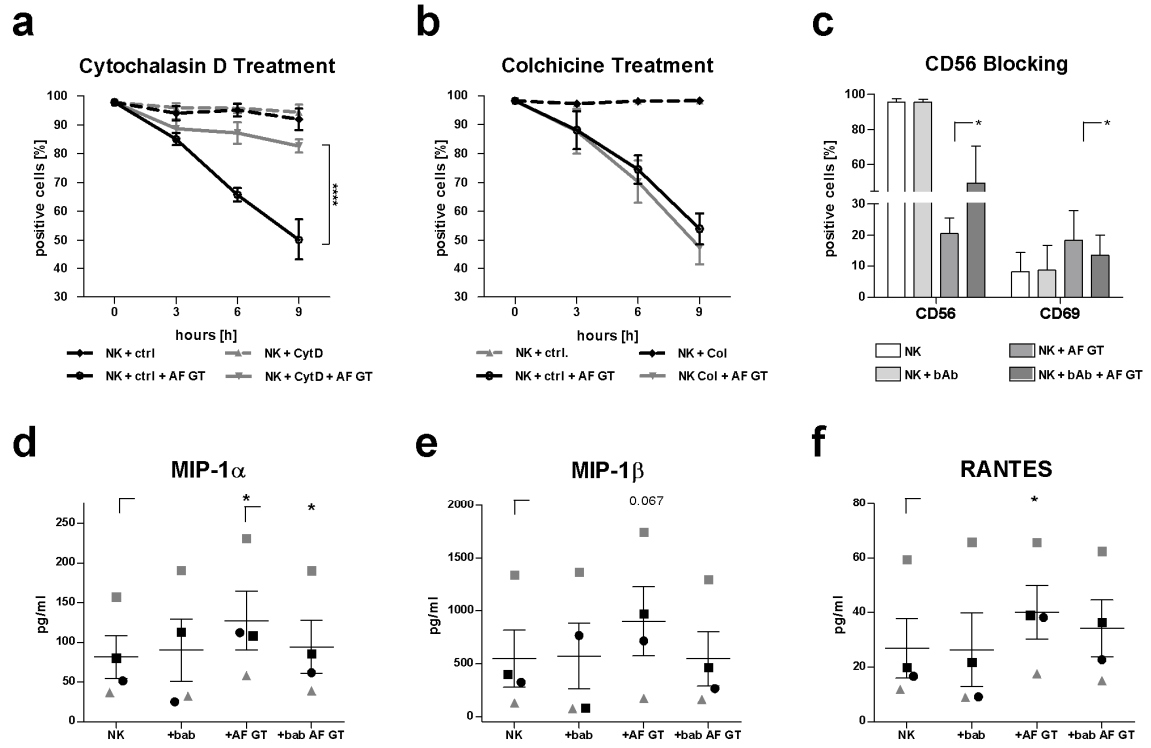

Figure 26: CD56 mediated fungal recognition is dependent on actin, and CD56 blocking inhibits NK cell function. NK cells were incubated with (a) cytochalasin D (Cyt. D, n = 4), (b) colchicine (Col., n = 3), and (c) CD56 blocking antibody (bAb, n = 4) before co-cultivation with the fungus (AF GT). The percentage of CD56 positive cells was determined after incubation with the fungus for 0, 3, 6, and 9 h. A paired student's t-test was performed to compare NK + ctrl + AF GT against NK + CytD + AF GT or NK + Col + AF GT (a,b). Control samples were cultured in the presence of the corresponding control solution. The percentage of CD56 and CD69 positive cells was assessed after a co-cultivation time of 9 h. CD56 and CD69 expression were analyzed using flow cytometry. NK cells were defined as $NKp46^{+}CD3^{-}$. Supernatants derived from CD56 blocking experiments were analyzed by ProcartaPlex™ multiplex immunoassays (n = 4, d–f). The concentration of (d) MIP-1α, (e) MIP-1β, and (f) RANTES detectable in supernatants is displayed in pg/ml. A paired student's t-test was performed to compare (c) NK + AF GT against NK + bAb + AF GT and (d–f) NK against + AF GT and + AF GT against + bAb AF GT. Data are represented as mean +/- SEM. Significant differences are indicated by an asterisk (* $p < 0.05$).

To further characterize the effects on CD56 blocking in the NK cell response to the fungus, culture supernatants from CD56 blocked and unblocked NK cells were analyzed by multiplex immunoassay (Fig. 26d-f). Challenging unblocked NK cells with *A. fumigatus* provoked a significant induction in the secretion of MIP-1α and RANTES while MIP-1β showed a tendency ($p = 0.067$) to be higher secreted after fungal stimulation (Fig. 26d-f). This fungal mediated cytokine secretion was reduced when CD56 was blocked on the NK cell surface

compared to the unblocked NK cells in the presence of the fungus. We detected no significant differences between CD56 blocked NK cells with and without fungal stimulation (Fig. 26d-f). Indeed, we further observed a significant reduction for MIP-1α secretion in CD56 blocked NK cells challenged with the fungus compared to unblocked NK cells in the presence of the fungus (Fig. 26d). These blocking experiments verified the functional role of CD56, confirming that CD56 is a recognition receptor for *A. fumigatus*. To investigate whether CD56 fluorescence positivity of NK cells was also reduced in the presence of other *Aspergillus* species, pre-stimulated NK cells were cultured with *A. niger*, *A. clavatus*, *A. flavus,* and *A. fumigatus* germ tubes for 6 h. The expression of CD56 and CD69 was then determined using flow cytometry. All *Aspergillus* species tested induced a reduction of CD56 (Fig. 27a). However, NK cells confronted with *A. fumigatus* germ tubes displayed a significantly higher decrease of CD56 fluorescence positivity of NK cells compared to *A. niger*, *A. flavus,* and *A. clavatus* (Fig. 27a).

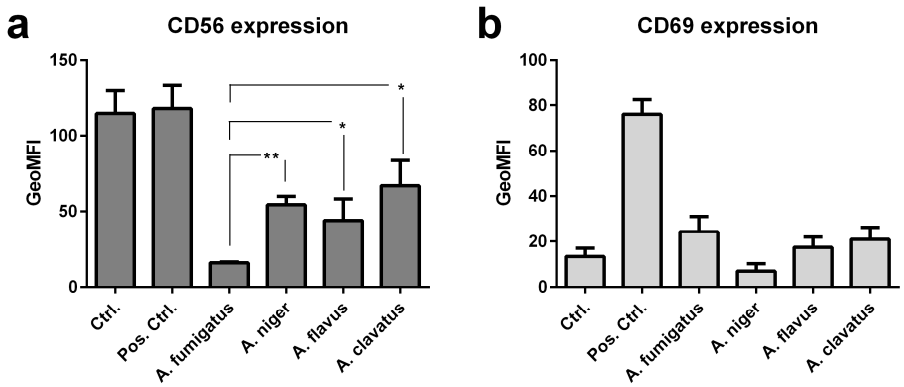

Figure 27: The reduction of CD56 is not as stringent for other *Aspergillus* species as it is for *A. fumigatus*. Primary NK cells were pre-treated overnight with IL-2 (1000 U/ml). Pre-treated NK cells were cultured in the presence of germ tubes of *A. fumigatus*, *A. niger*, *A. flavus* or *A. clavatus* at MOI 0.5, or were left untreated (Ctrl.) for 6 h. NK cells treated with 500 U/ml IL-15 and IL-2 served as the control for NK cell activation (Pos. ctrl.). The expression of (a) CD56 and (b) CD69 was analyzed using flow cytometry. NK cells were defined as $NKp46^{+}CD3^{-}$. Data are represented as mean of the geometric mean fluorescence intensity (GeoMFI) + SEM of n = 4 independent experiments. Significant differences between AF GT treated NK cells and NK cells treated with the other *Aspergilli* are indicated by asterisks (* $p < 0.05$; ** $p < 0.01$).

NK cells co-cultivated with *A. fumigatus*, *A. flavus,* and *A. clavatus* displayed an increase in the CD69 expression indicating NK cell activation, whereas NK cells treated with *A. niger* showed a decrease in CD69 expression compared to control NK cells (Fig. 27b). These results suggest that *Aspergillus* species express a specific molecule on their surface recognized by CD56 on NK cells.

Discussion

This study is the first to visualize the direct interaction of NK cells and *A. fumigatus* and to show that CD56 has a functional role during fungal recognition. NK cells can recognize fungal pathogens and induce their lysis [191, 249, 275, 276]. Besides their antifungal activity towards *C. albicans*, *C. neoformans*, *Paracoccidioides brasiliensis* [291], and *Coccidioides immitis* [292], it was shown that NK cells recognize *A. fumigatus* and display antifungal activity directed against the hyphae [277, 293]. However, the mechanism of this interaction is still poorly understood.

Previous studies demonstrated that NK cells form direct conjugates with *C. neoformans* [292, 294] and that NKp30 and NKp46 act as fungal PRRs [191, 192]. These publications and our previous studies [277] suggested that the interaction of NK cells and *A. fumigatus* is mediated by a PRR. Unexpectedly, neither experimentally tested NK cell activating receptors nor the known fungal recognizing receptor NKp30 were modulated upon co-culture with *A. fumigatus*. Surprisingly, we observed a striking decrease of CD56 fluorescence positivity on the NK cell surface upon exposure to the fungus. By quantifying the NCAM/CD56 protein concentration in the supernatant of NK cell-*A. fumigatus* co-cultures, we could exclude that NCAM/CD56 was neither shed from the cell surface nor was the secreted isoform of NCAM/CD56 expressed. Mycotoxins have an impact on the mRNA and protein expression of host cells, but our analyses clearly showed that the secreted mycotoxins have no influence on the expression level of CD56 on transcriptome and protein level of NK cells.

On neuronal cells, NCAM/CD56 can be endocytosed and is then mostly recycled to the cell surface, whereas a minority of the endocytosed NCAM/CD56 is degraded [295]. Analyses showed that NCAM/CD56 was not internalized upon contact with *A. fumigatus.* Thus, we speculated about a potential binding of CD56 to the fungus that is masking the molecule as it was seen as well for NKp30 in the studies of Li *et al.* [191]. Indeed, we were able to show a direct interaction of NK cells with live *A. fumigatus* by SEM, CLSM, and super-resolution *d*STORM microscopy, which showed that NCAM/CD56 distribution on the NK cell surface markedly changed after fungal contact. Besides, NCAM/CD56 re-location was observed until the complete CD56 signal was detected at the fungal interaction site and the lengths and amounts of the interaction site increased over time.

Furthermore, we could exclude that CD56 is shed from the NK cell surface and bound to *A. fumigatus* by CLSM microscopy. In NK cell-*A. fumigatus* co-cultures we were not able to detect any CD56 outside of the interaction site with NK cells. NCAM/CD56 positive NK

cells were also decreased in the presence of other *Aspergillus* species but less when compared to *A. fumigatus* suggesting that *A. fumigatus* is expressing a CD56 ligand with a higher abundance.

Two isoforms (140 kD and 180 kD) of NCAM show transmembrane binding and have intracellular domains while the 120 kD isoform has a glycosyl-phosphatidylinositol membrane anchor but no intracellular domains [296]. While the three isoforms have different C-termini, the N-terminal extracellular domains are identical in all three isoforms [297]. Therefore, we used the 120 kD isoform to test whether CD56 is directly interacting with *A. fumigatus*. By microscopy, we showed that soluble CD56 directly binds in a concentration-dependent manner to growing *A. fumigatus* structures, confirming our previous observations and hypothesis.

Blocking of CD56 did not only reduce fungal mediated NK cell activation but further inhibited the amount of secreted cytokines. Chemokines like MIP-1α, MIP-1β, and RANTES are secreted by human blood NK cells [298, 299]. MIP-1α, MIP-1β, and RANTES modulate the migratory behavior of leukocytes, and their importance in cryptococcal infections was highlighted by the study from Huffnagle and McNeil [300]. Huffnagle and McNeil showed that depletion of either MIP-1α or the common MIP-1α, MIP-1β, and RANTES receptor CCR5 conferred to a higher fungal burden and inhibited leukocyte recruitment in the central nervous system of knockout mice [300]. The role of the CCR5 ligands MIP-1α, MIP-1β, and RANTES were also highlighted in another study that reported an abolished NK cell accumulation at sites of infection in $CCR5^{-/-}$mice [301]. A decreased detection of MIP-1α, MIP-1β, and RANTES in supernatants derived from samples in which NK cells were blocked with CD56 and challenged with the fungus compared to control co-cultures suggests a crucial role for these chemokines in the immune response directed against the fungus.

Based on these results and the previous publications, we conclude that CD56 is involved in the secretion of MIP-1α, MIP-1β, and RANTES to recruit further leukocytes such as NK cells, monocytes, and neutrophils to sites of *A. fumigatus* infections. Recently, Mace *et al.* demonstrated that CD56 is accumulated at the developmental synapse to stromal cells and that CD56 is co-localized with F-actin [215]. By showing that CD56 re-localization is dependent on the actin cytoskeleton, we could confirm the findings of Mace *et al.* [215]. A recent study published by Voigt *et al.* demonstrated a decrease of NCAM/CD56 expression in the presence of live *C. albicans* [279]. In addition, it was shown that the surface protein gp63 of *Leishmania* further reduces CD56 fluorescence positivity, indicating that NCAM/CD56 plays a functional role in the recognition of eukaryotic and prokaryotic pathogens expressing a specific molecule on their cell surface. These publications further strengthen our hypothesis that NCAM/CD56 is a fungal PRR [193].

The functional role of NCAM/CD56 expressed by NK cells referring to NK cell cytotoxicity against tumor cells has been controversially discussed. On the one hand, it was observed that NCAM/CD56 had no impact on the lysis of target cells [302, 303], whereas, on the other hand, other groups demonstrated that the cytotoxicity of NK cells interacting with NCAM-expressing target cells is enhanced by NCAM/CD56 [304, 305]. These reports suggested a functional role of NCAM/CD56 in the recognition of target cells and the induction of cytotoxicity. These observations and our findings suggest that NCAM/CD56 is a PRR and plays a functional role in NK cell cytotoxicity. Our study provides novel insights into the interaction of NK cells and *A. fumigatus* as well as in NK cell biology.

Chapter 3:

Reconstituting NK cells after alloSCT reveal impaired recognition of *A. fumigatus* mediated by corticosteroids

Introduction

Following alloSCT, patients are characterized by a period of profound T and B cell deficiency until the completion of immune system reconstitution, which can take up to two years [62]. During this critical period of cell deficiency, in which a patient is more susceptible to bacterial, viral, and fungal infections, cellular components of innate immunity are of major importance as they represent the first line of immune defense. Phagocytes, such as monocytes and dendritic cells, communicate with the adaptive immune system, thereby modulating inflammatory responses. Cytokines, chemokines, and chemokine receptors play essential roles in immunity against opportunistic pathogens and may determine the type of effector response.

NK cell development starts in the bone marrow and secondary lymphoid organs until NK cells reach a defined stage, enter the bloodstream, and seed into peripheral organs [306]. Interestingly, NK cells are not restricted after migration but can circulate from organ to blood and *vice versa*, as shown in the study by Marquardt *et al.* [307]. NK cells constitute approximately 10 % of lymphocytes in blood [308] and can be subdivided into $CD56^{dim}$ and $CD56^{bright}$ cells [161]. While $CD56^{bright}$ NK cells do not express the Fc receptor CD16 and are potent cytokine producers, CD16 is highly expressed on $CD56^{dim}$ NK cells, and this subset can efficiently lyse target cells [161]. There is strong evidence for a gradual differentiation from $CD56^{bright}$ cells into $CD56^{dim}$ NK cells [164, 165, 309]. Under healthy conditions, the equilibrium between $CD56^{bright}$ and $CD56^{dim}$ NK cells is on the side of $CD56^{dim}$ NK cells, which represent ~90 % of blood NK cells [308]. In recipients of an allograft, the percentage of $CD56^{bright}$ NK cells in the peripheral blood increases to 40-50 %, while $CD56^{dim}$ NK cells are underrepresented [166].

NK cells are essential during fungal infections, which has been shown in mouse models as well as in clinical studies. Morrison *et al.* showed in a neutropenic mouse model that CCL2 depletion inhibited pulmonary NK cell migration and favored the development of IA [197]. In a later study, NK cell-derived IFN-γ was shown to be essential to control fungal infections in neutropenic mice, and depletion of NK cells or IFN-γ resulted in a higher fungal burden [147, 198]. Confirming the importance of NK cells in humans, Stuehler *et al.* monitored recipients of an allograft over 12 months and found a clear correlation between reduced NK cell counts and delayed NK cell reconstitution with a higher risk of developing IA in patients receiving alloSCT [199]. These studies highlighted the role of NK cells during fungal infections in immunocompromised hosts and were influential for this study.

Results

To monitor NK cell counts and subsets in healthy donors and patients after successful treatment of AML (acute myeloid leukemia), ALL (acute lymphatic leukemia) or multiple myeloma (MM) by alloSCT, we analyzed blood at 60, 90, and 120 days after alloSCT and in healthy controls. In line with previous studies [310], total NK cell counts were similar within 60-120 days after transplantation compared to healthy controls (Fig. 28a). Patients after alloSCT experience a period of immune deficiency in which T cells are underrepresented [62]; thus, the percentage of other cell types in PBMCs increases. When the percentage of NK cells (Fig. 28b) measured in PBMCs was plotted against the percentage of T cells after alloSCT (Fig. 28c), a negative correlation was observed ($p < 0.0001$), confirming that the higher percentage of NK cells in PBMCs was associated with T cell deficiency (Fig. 28d).

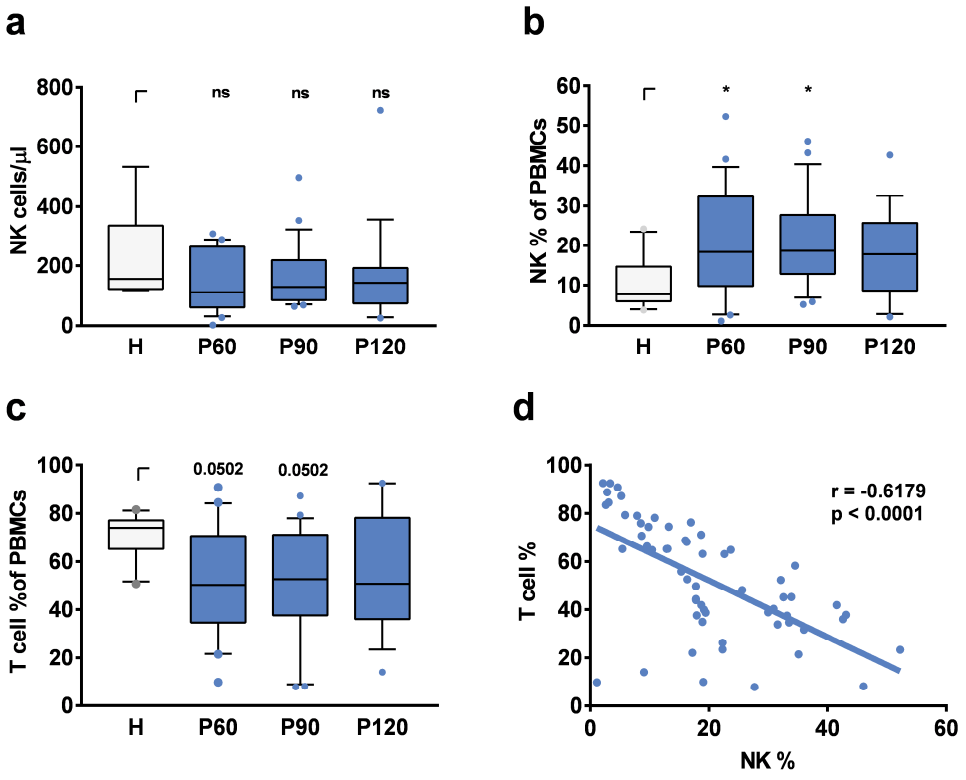

Figure 28: NK and T cell composition in patients after alloSCT and healthy controls. (a) Total NK cell counts per µl, (b) NK cell percentages in PBMCs and (c) T cell percentages in PBMCs were measured in the peripheral blood from healthy individuals (H) or patients 60, 90, or 120 days post-alloSCT (P60, P90, P120). Statistics were analyzed by (a) Kruskal-Wallis test with FDR correction (Benjamini and Hochberg), (b, c) one-way ANOVA with FDR correction (Benjamini and Hochberg, * $q < 0.05$, $F_B[3, 70] = 2.248$, $F_c[3, 70] = 1.964$). Data were acquired from (a-c) n = 10 (H), n = 22 (P_60), n = 23 (P_90) and n = 19 (P_120) independent experiments. (d) NK/ T cell ratios were calculated by Pearson correlation. Data were obtained from n = 60 different experiments including time points ranging from 60-120 days post-alloSCT patients (n = 26).

NK cells obtained from healthy donors or after alloSCT were analyzed for the expression of specific surface markers (Fig. 29). Therefore, NK cells were stained with anti-CD56

and anti-CD16 antibodies and gated into $CD56^{bright}CD16^{-}$, $CD56^{bright}CD16^{+}$, and $CD56^{dim}CD16^{++}$ subsets (Fig. 29a). NK cells derived after alloSCT significantly displayed lower amounts of $CD56^{dim}CD16^{++}$ cells, whereas the proportion of $CD56^{bright}CD16^{+}$ and $CD56^{bright}CD16^{-}$ cells was higher (Fig. 29b). There were no significant differences detectable when we analyzed the CD56 and CD16 MFI within each subset between healthy donors and recipients of an allograft, concluding that the phenotypic expression of CD56 and CD16 within subsets remains unchanged after alloSCT (Fig. 29c, d). These experiments showed that NK cell recovery after alloSCT is a fast process; however, NK cell subset distribution does not recover by 180 days post-alloSCT.

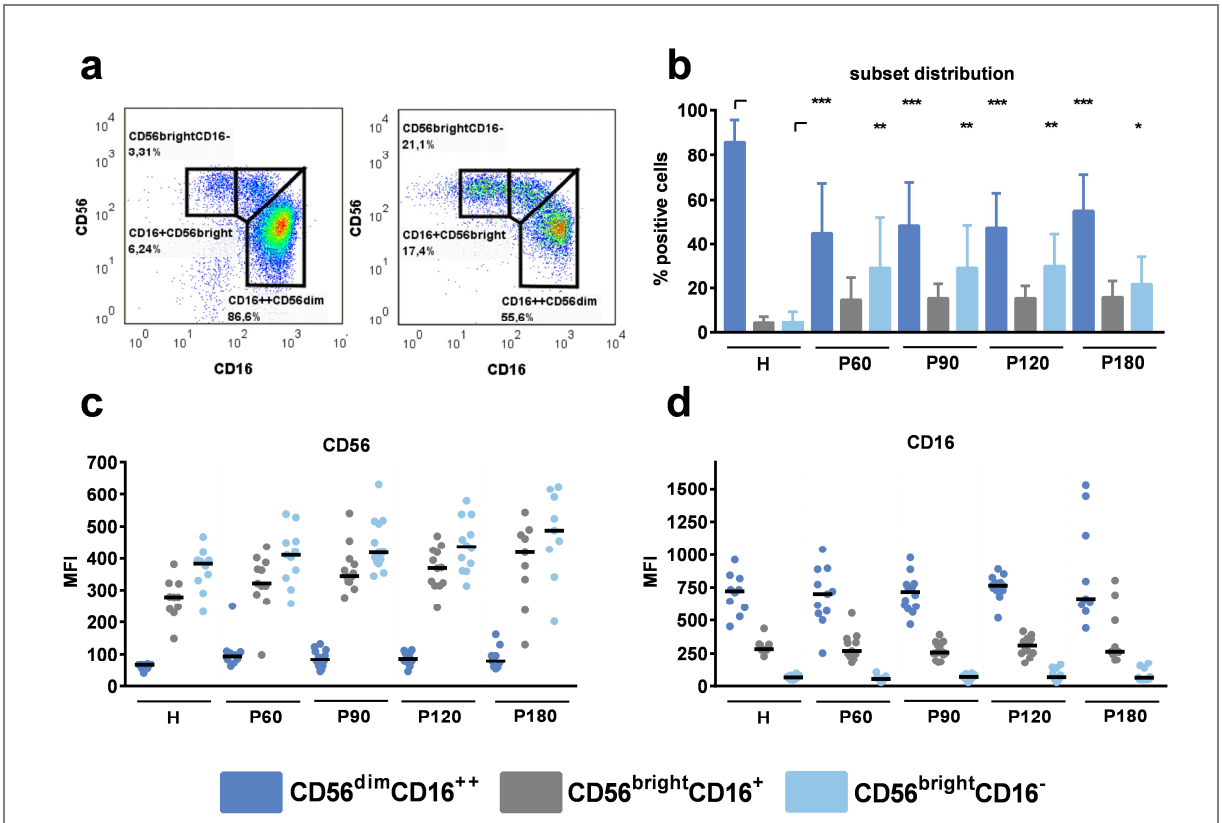

Figure 29: NK cell subsets in reconstituting NK cells. NK cells were pre-stimulated with 1000 U/ml IL-2 overnight. (a) Representative gating strategies for healthy individuals (left) and recipients of an allograft (right). (b) NK cell subsets were compared between healthy individuals and recipients of an allograft. Data are displayed as mean + SD. (c) CD56 MFI and (d) CD16 MFI within NK cell subset were analyzed by flow cytometry. Data were acquired from n = 10 (H); n = 11 (P60); n = 14 (P90); n = 12 (P120); n = 9 (P180) different experiments. Medians are displayed. Statistical analysis was performed by (b) one-way ANOVA ($CD16^{++}CD56^{dim}$ and $CD16^{+}CD56^{bright}$, F[14, 156] = 25.87) and Kruskal-Wallis test ($CD16^{-}CD56^{bright}$). Corrections for multiple testing were performed by the FDR method of Benjamini and Hochberg. Statistical significances are marked by asterisks (* $p < 0.05$, ** $p < 0.01$, *** $p < 0.001$).

CD56 is a PRR on human NK cells, and stimulation with *A. fumigatus* germ tubes causes relocalization of the normal homogenously distributed CD56 from the NK cell surface to the fungal interface, resulting in a reduced detection of CD56 by flow cytometry. Furthermore, CD56 binding to the fungus induces the secretion of the chemokines MIP-1α, MIP-1β, and RANTES, which initiates the recruitment of further immune cells [235]. Since we observed an increased expression of CD56 on peripheral blood NK cells obtained after alloSCT, we next analyzed whether transplantation influences the binding of NK cells to the fungus. Therefore, we co-cultured NK cells from alloSCT recipients or healthy individuals with *A. fumigatus* germ tubes for 6 h before analyzing the cells by flow cytometry. To distinguish between $CD16^-$ and $CD16^+$ NK cells, which show a higher and a lower expression of CD56, we gated NK cells into $CD16^+$ and $CD16^-$ cells and analyzed CD56 expression within each population by flow cytometry. Relative CD56 values were calculated through dividing CD56 expression after fungal co-culture by CD56 expression before fungal co-culture (Equation 3 in the chapter *2.2.4.1 Flow Cytometry*, *Methods*). Thus, low relative CD56 values indicated a strong binding of CD56 (Fig. 30).

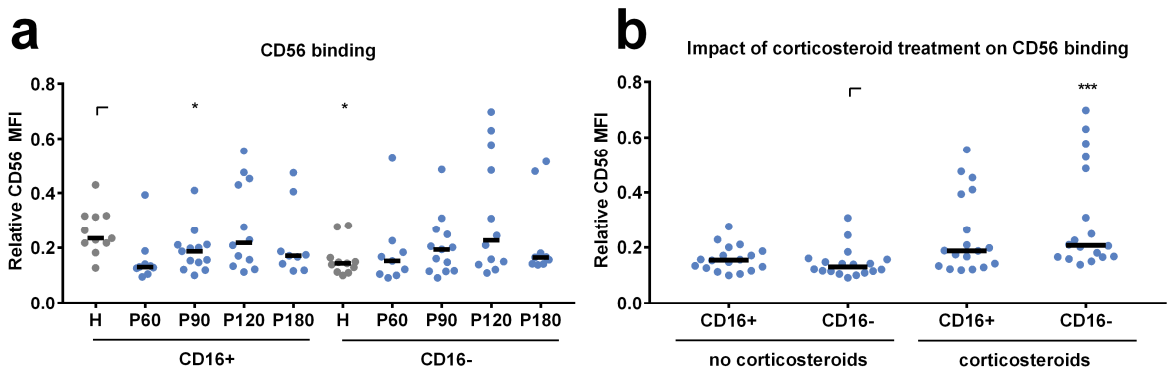

Figure 30: Corticosteroid treatment inhibits CD56 binding to the fungus. NK cells were pre-stimulated with 1000 U/ml IL-2 overnight before NK cells were co-cultured with *A. fumigatus* germ tubes (AF, MOI 0.5) or plain medium at 37 °C for 6 h. NK cells were gated into NKp46+/CD16+ or NKp46+/CD16- cells. CD56 mean fluorescence intensity (MFI) was evaluated by flow cytometry with and without fungal co-culture. Relative CD56 expression was calculated for alloSCT NK cells (P) and healthy controls (H). Values for relative CD56 expression were grouped regarding (a) the time after alloSCT and (b) corticosteroid treatment. Data were acquired from (a) n = 11 (H); n = 9 (P60), n = 13 (P90); n = 12 (P120); n = 9 (P180) and (b) n = 18 experiments. Medians are displayed. Significant differences were calculated by the Kruskal-Wallis test with correction for multiple testing by the FDR method of Benjamini and Hochberg and are marked by asterisks (* $p < 0.05$; *** $p < 0.001$).

Independent of the total amount of CD56 molecules on the cell surface, healthy $CD16^-$ NK cells displayed lower relative CD56 values compared to healthy $CD16^+$ NK cells, indicating better fungal binding by $CD16^-$ cells (Fig. 30a). In contrast, there was no detectable difference between $CD16^+$ and $CD16^-$ cells in alloSCT patients (Fig. 30a). The binding capacity of NK cells obtained after alloSCT did not change over time; however, we detected outliers leading to high standard deviations in each group (Fig. 30a).

Thus, we next analyzed whether additional factors contributed to the detected outliers and high standard deviation. Corticosteroids have anti-inflammatory and immunosuppressive effects and are administered to prevent graft rejection after alloSCT [311]. Additionally, several cell functions, e.g., cytotoxicity, cell metabolism, and cytokine production, are suppressed by glucocorticoid treatment [312-314]. Indeed, corticosteroid treatment during the blood collection time points negatively affected CD56 binding to the fungus (Fig. 30b, Table 12 on page 36), confirming an adverse effect of corticosteroids on NK cell function.

Our previous studies demonstrate that CD56 relocalization to the fungal interface is dependent on actin [235]. Since NK cells obtained from patients treated with corticosteroids after alloSCT showed reduced CD56 relocalization (Fig. 30), we hypothesized that this might be due to cytoskeletal defects. Thus, we first analyzed whether fungal stimulation induces actin polymerization by co-culturing NK cells obtained from healthy controls or after alloSCT with *A. fumigatus* germ tubes for 6 h. Co-cultures were fixed and stained with fluorescently labeled phalloidin. SIM was used to visualize actin dynamics in NK cells with sub-diffraction spatial resolution [315]. Indeed, the presence of *A. fumigatus* germ tubes induced actin polymerization measured by higher fluorescent staining of the F-actin binding probe phalloidin in NK cells from healthy individuals (Fig. 31a). In particular, the fluorescence of phalloidin increased at cell surface areas where the NK cell membrane interacted with the fungal hyphae (marked by arrow), concluding that actin polymerization is induced by fungal hyphae (Fig. 31a). Indeed, quantitative analysis with Fiji software revealed that the fluorescence signal of F-actin increased in all three tested healthy donors after fungal co-culture (Fig. 31b).

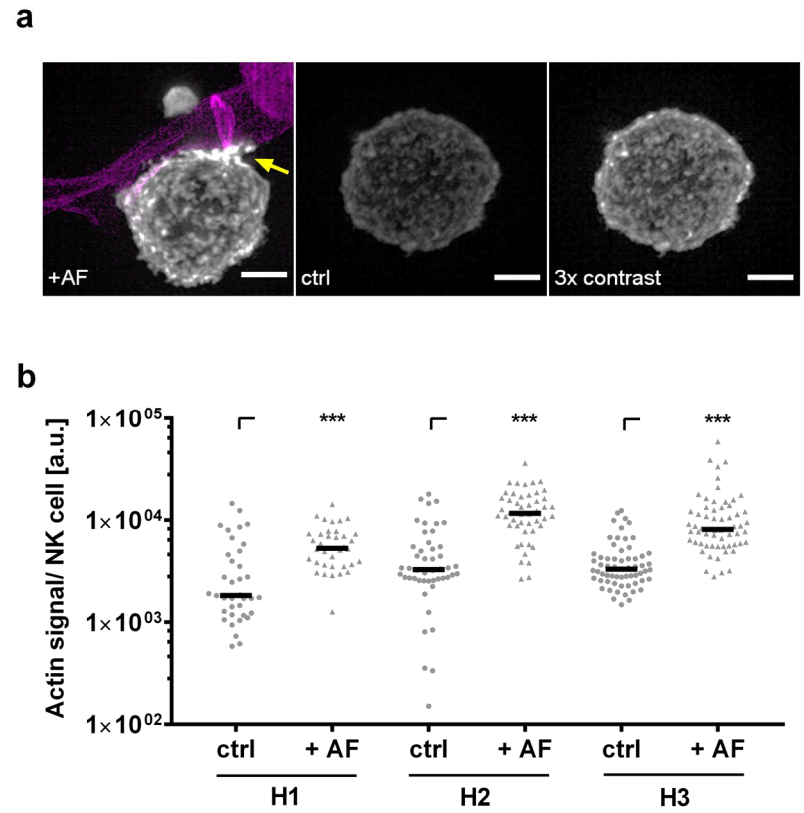

Figure 31: *A. fumigatus* stimulates F-Actin in NK cells. NK cells were pre-stimulated with 1000 U/ml IL-2 overnight. NK cells were co-cultured with (AF, MOI 0.5) or without (ctrl) *A fumigatus* germ tubes for 6 h. Cultures were fixed, and F-actin was stained with phalloidin staining solution for 24 h. Calcofluor was used to visualize the fungal cell wall. (a) Fluorescence intensities were compared between NK cells treated with *A. fumigatus* germ tubes (AF, left) or control cells (ctrl, middle). To better visualize the distribution of F-actin on control cells, we displayed the fluorescence signal of phalloidin with three times higher contrast (right). Increases in F-actin levels by fungal treatment are marked by an arrow. Fungal hyphae are displayed in magenta. Representative data from n = 3 different experiments are shown. (b) Quantification of the actin signal per NK cell derived from n = 37 (H1), n = 48 (H2), and n = 62 (H3) SIM z-stacks. Data are displayed in medians and arbitrary units. Statistics were calculated by Wilcoxon test to compare the control samples and the fungal treated samples within each donor. Significant differences are displayed by asterisks (*** $p < 0.001$).

Next, we analyzed the actin cytoskeleton with live-cell staining using flow cytometry. NK cells obtained from healthy individuals or patients 60, 90, 120, or 180 days post alloSCT were incubated with *A. fumigatus* germ tubes for 6 h, co-cultures were harvested, and cells were incubated in 1 µM SiR 647 F-actin binding peptides (Fig. 32). The induction of actin was calculated by dividing the actin signal after fungal co-culture by the actin signal before fungal co-culture (Fig. 32). To analyze the dependency of CD56 binding on the actin induction, we plotted relative CD56 values obtained from NK cells after alloSCT against the individual fungal mediated actin induction (Fig. 32a). Relative CD56 values negatively correlated with the induction of actin ($p = 0.0054$, two-tailed Spearman correlation), indicating that CD56 relocalization is dependent on fungal mediated actin polymerization (Fig. 32a).

In contrast to CD56 binding, fungal mediated actin polymerization was dependent on the time point of blood collection after alloSCT. Interestingly, NK cells collected at early time points after alloSCT showed a weaker fungal mediated actin polymerization (mean at day 60: 1.69) in comparison to later time points (mean at day 180: 3.69) or healthy controls (mean: 3.26, Fig. 32b). We hypothesized that these effects might be due to different actin polymerization within NK cell subsets. Therefore, we analyzed fungal mediated actin polymerization in $CD16^+$ and $CD16^-$ NK cells. $CD16^+$ and $CD16^-$ NK cells showed no differences in actin polymerization after *A. fumigatus* co-culture (Fig. 32c), concluding that the reduced actin polymerization after alloSCT is related to alternative mechanisms, e.g., NK cell development.

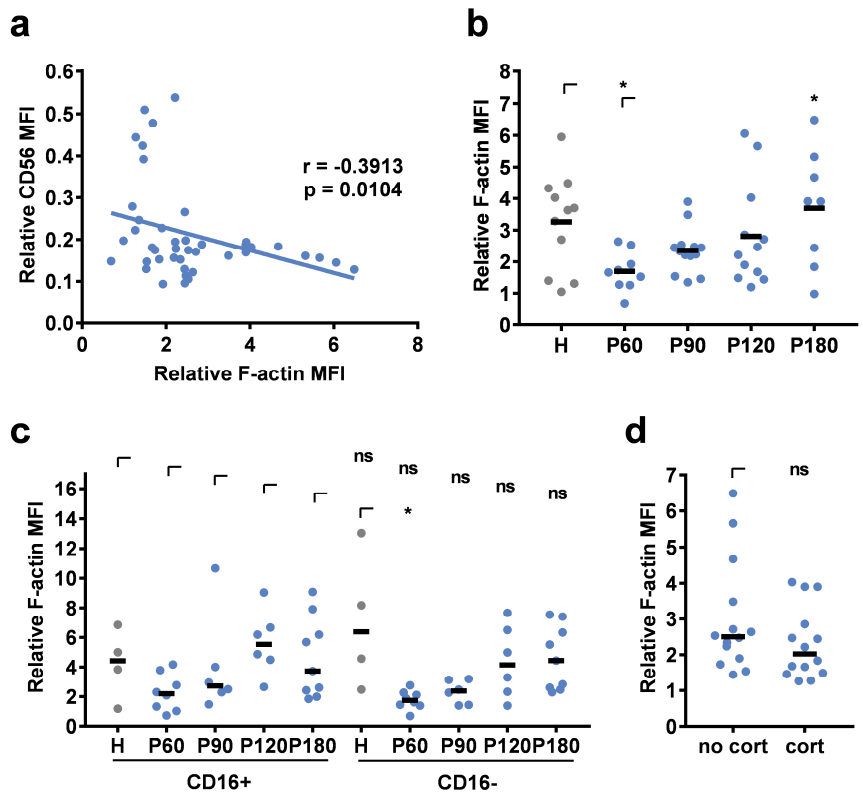

Figure 32: Actin induction following fungal stimulation recovers within 6 months after alloSCT. NK cells were isolated from patients 60, 90, 120, and 180 days after alloSCT (P) or healthy controls (H). For analysis, NK cells were pre-stimulated with 1000 U/ml IL-2 overnight and afterward co-cultured with *A. fumigatus* germ tubes (MOI 0.5) or alone for 6 h. NK cells were treated with the F-Actin binding probe Sir647 for 50 min before cells were analyzed by flow cytometry. Relative actin induction was calculated by the division of Sir647 MFI after fungal co-culture with Sir647 MFI of control cells. Data were acquired from (a) n = 44, (b) n = 11 (H); n = 9 (P60), n = 13 (P90); n = 12 (P120); n = 8 (P180) and (c) n = 4 (H); n = 8 (P60); n = 6 (P90); n = 6 (P120); n = 9 (P180) different experiments. Data are displayed as (b) means and (c,d) medians.Significant differences were calculated by (a) two-tailed Spearman correlation, (b) One-way ANOVA with FDR correction ($F[4, 48] = 3.112$), (c) Kruskal-Wallis test with FDR correction to compare within NK cell subsets, Wilcoxon test to compare between NK cell subsets, and (d) unpaired t-test with Welch's correction. Statistical significance is marked by an asterisk ($* p < 0.05$).

Since CD56 binding to the fungus was dependent on fungal mediated actin polymerization (Fig. 32a) and CD56 binding was negatively affected by corticosteroid treatment (Fig. 30b), we next analyzed whether actin polymerization changed during corticosteroid treatment. Therefore, we grouped patients into corticosteroid receiving and non-corticosteroid receiving cohorts and only included samples matching the time after alloSCT and further drug treatment. However, fungal mediated actin induction was not affected in alloSCT NK cells during corticosteroid treatment (Fig. 32d), concluding that the actin cytoskeleton is not the primary target of corticosteroids investigated in this study.

NK cells secrete MIP-1α, MIP-1β, and RANTES after direct co-culture with *A. fumigatus* germ tubes, and blocking of CD56 inhibits the secretion of those chemokines leading to the conclusion that CD56 is triggering soluble responses to *A. fumigatus* hyphae [235]. MIP-1α, MIP-1β, and RANTES are secreted explicitly by $CD16^{+}CD56^{dim}$ NK cells, which are underrepresented early after alloSCT (Fig. 29b) [316]. To analyze $CD16^{+}CD56^{dim}$ NK cells, we separated $CD16^{+}$ from $CD16^{-}$ cells by CD16 positive magnetic isolation (Figure 33a). $CD16^{+}$ cells derived 90 days after alloSCT secreted significantly lower amounts of MIP-1α and showed a reduced secretion of MIP-1β and RANTES after fungal stimulation compared to healthy controls, indicating functional deficiencies of this subset (Fig. 33b-d).

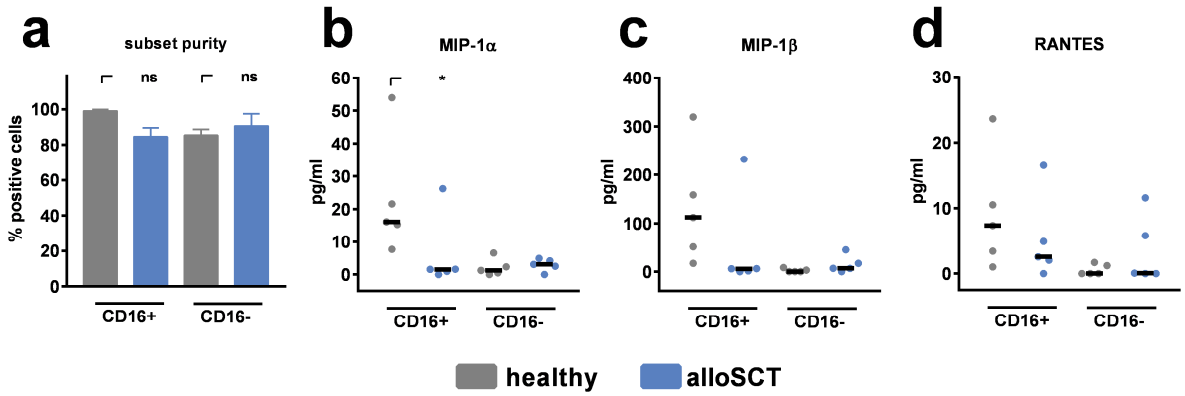

Figure 33: Chemokine secretion is inhibited in CD16+ cells after alloSCT. NK cells were obtained from healthy individuals or 90 days after alloSCT and were pre-stimulated with 1000 U/ml IL-2 overnight. (a) NK cell subsets were isolated with CD16 magnetic bead positive isolation, and subset purity was analyzed by flow cytometry. NK cell subsets were co-cultured with *A. fumigatus* germ tubes (AF, MOI 0.5) or plain medium for 6 h at 37 °C. Supernatants were collected, and chemokine levels of (b) MIP-1α, (c) MIP-1β, and (d) RANTES were analyzed. Data are displayed as (a) medians + range, (b-d) medians and were acquired from n = 5 different experiments. Significant differences were calculated by the Kruskal-Wallis test with correction for multiple testing by the FDR method of Benjamini and Hochberg and marked by an asterisk (* $p < 0.05$).

To investigate the impact of corticosteroids on cytokine and chemokine secretion, we analyzed the supernatants of NK cell-*A. fumigatus* co-cultures from healthy individuals or alloSCT patients with and without corticosteroid treatment. CXCL8 is an important, pro-

inflammatory chemokine for PMN recruitment and showed inhibited secretion during corticoid therapy. However, measured chemokine levels were below the stimulatory concentration [317] (Fig. 34a). IL-1α was shown to induce the NF-κB pathway and to be mandatory for leukocyte recruitment during *A. fumigatus* infections. Demonstrated by a murine infection model with *A. fumigatus*, the concentration of pulmonary IL-1α increased after fungal challenge and reached 1000 pg/ml after 48 h [318, 319]. After 6 h of NK cell-*A. fumigatus* co-culture, the concentration of secreted IL-1α was 24 pg/ml for healthy individuals, while lower concentrations were observed for patients after alloSCT that additionally were reduced after corticosteroid treatment (< 7 pg/ml) (Fig. 34b).

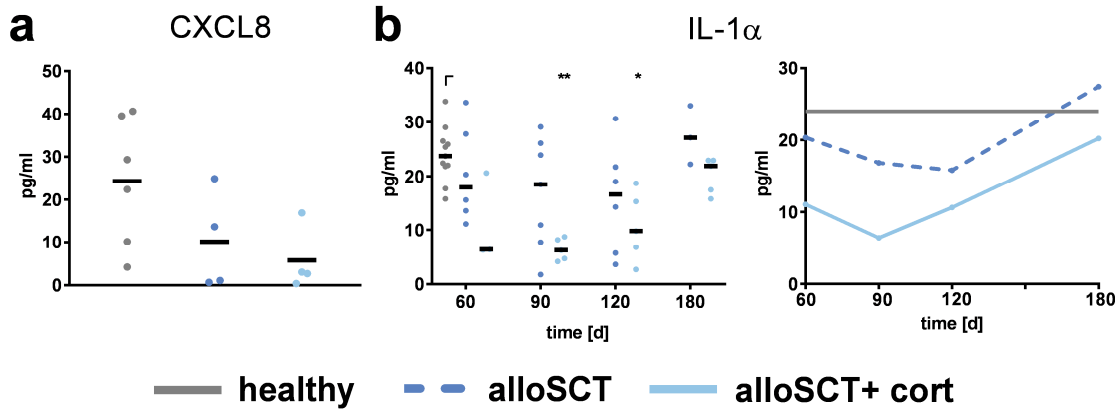

Figure 34: IL-1α and CXCL8 secretion after NK cell-*A. fumigatus* co-cultures. NK cells were collected (a) 90 or 120 days after alloSCT or (b) 60, 90, 120, and 180 days after alloSCT or from healthy controls and were incubated with 1000 U/ml IL-2 overnight before the medium was exchanged and NK cells were cultured alone or with *A. fumigatus* germ tubes for 6 h. Supernatants were collected, and (a) CXCL8 and (b) IL-1α were determined by multiplex immunoassay. Data were acquired from (a) n = 6 (healthy); n = 4 (alloSCT); n = 4 (alloSCT+cort) and (b) n = 11 (H), n = 6 (alloSCT 60), n = 7 (alloSCT 90), n = 6 (alloSCT 120), n = 3 (alloSCT 180), n = 3 (cort 60), n = 5 (cort 90), n = 120 (cort 120), n = 5 (cort 180) experiments. Data are displayed as (a) medians and (b) means. Statistical analysis was performed by (a) one-way ANOVA with FDR correction and (b) Kruskal-Wallis test with FDR correction. Significant differences are marked by asterisks (* $p < 0.05$, ** $p < 0.01$).

NK cells were shown to damage fungal hyphae by the secretion of perforin [253]. Thus, we analyzed if the release of those cytotoxic molecules is reduced in reconstituting NK cells (Figure 35). The fungal-mediated secretion of perforin was comparable between NK cells derived from healthy individuals or recipients of an allograft with or without corticosteroid therapy, concluding that corticosteroids had no impact on perforin secretion in NK cells (Figure 35). To analyze if other soluble factors induce fungal damage, we performed an XTT assay with supernatants of former NK cell-*A.fumigatus* co-cultures and NK cell single cultures. Therefore, *A. fumigatus* hyphae were grown overnight in RPMI medium before medium was exchanged with NK cell-*A. fumigatus* or NK cell supernatants. After 6 h, supernatants were replaced by XTT reagent and the fungal metabolism was measured with

an absorbance reader after 30 min. The fungal damage was calculated as explained before (*2.2.1.5 Metabolic analysis, Methods*) and was comparable to other studies [293]. Similar to the secretion of perforin, corticosteroids did not influence the NK cell-mediated fungal damage (Figure 35).

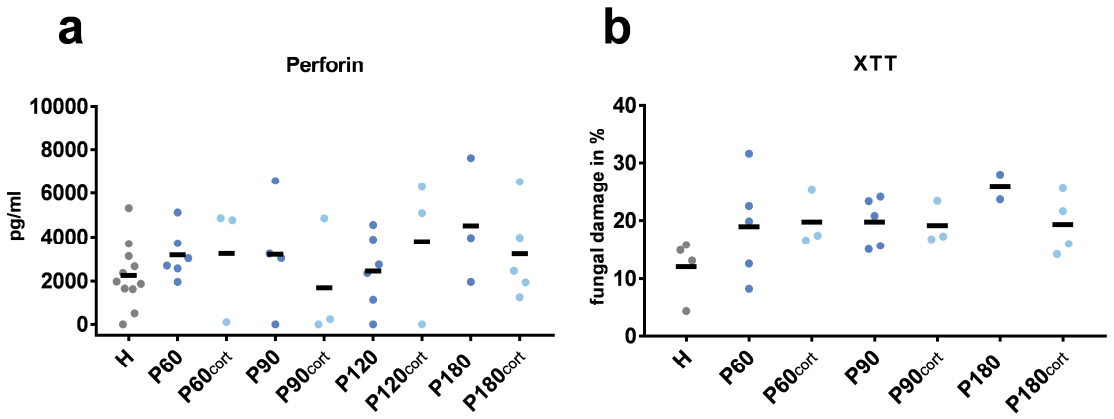

Figure 35: Perforin and XTT analysis of NK-*A. fumigatus* supernatants. (a) NK cells were pre-stimulated with 1000 U/ml IL-2 overnight. NK cells obtained after alloSCT (P), after alloSCT and corticosteroid treatment (P_{cort}) or from healthy controls (H) were co-cultured with *A. fumigatus* germ tubes (AF, MOI 0.5) or plain medium for 6 h at 37 °C. The concentration of perforin in supernatants was analyzed by multiplex immunoassay. Data were acquired from n = 11 (H), n = 6 (P60), n = 3 ($P60_{cort}$), n = 4 (P90), n = 3 ($P90_{cort}$), n = 6 (P120), n = 3 ($P120_{cort}$), n = 3 (P180), n = 5 ($P180_{cort}$) experiments. (b) $0.5x10^5$ *A. fumigatus* conidia/well were plated in 96 well plates and grown for 15 h at 37°C. Supernatants from NK single cultures or NK-*A. fumigatus* co-cultures were added onto grown *A. fumigatus* biofilms. Plates were incubated for 6 h at 37°C before supernatants were removed, wells were washed with PBS, and XTT reagent was added for 30 min at 37°C. Fungal metabolism was calculated compared to controls. Data were acquired from n = 4 (H), n = 5 (P60), n = 3 ($P60_{cort}$), n = 5 (P90), n = 3 ($P90_{cort}$), n = 2 (P180), n = 4 ($P180_{cort}$) experiments. Statistical analysis was performed by Kruskal-Wallis test with FDR correction.

In contrast, the secretion of the CD56 mediated chemokines MIP-1α, MIP-1β, and RANTES was reduced early after alloSCT but normalized to healthy levels on day 180 (Fig. 36). Interestingly, corticosteroid treatment further reduced the secretion of MIP-1α, MIP-1β, and RANTES by NK cells. This defect was significant for 120 days post-alloSCT (Fig. 36).

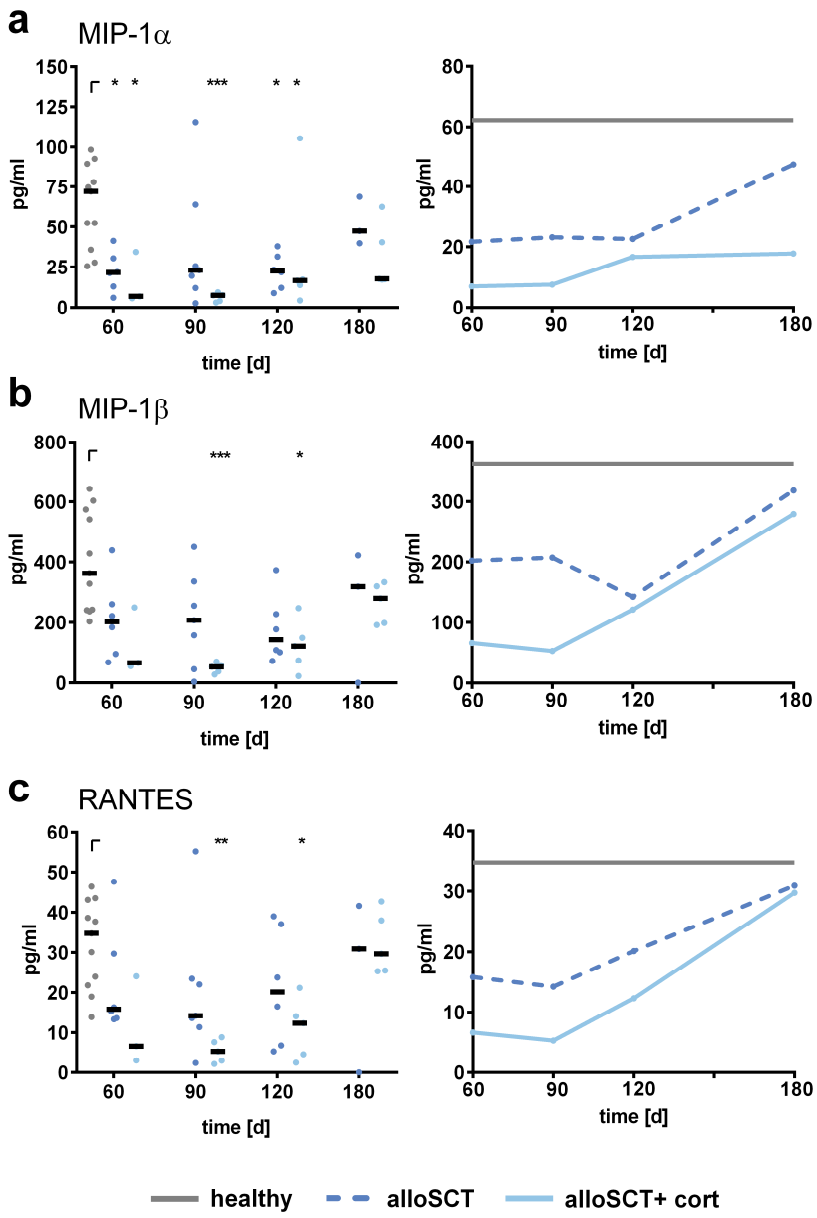

Figure 36: Chemokine secretion by alloSCT NK cells and healthy controls. NK cells were pre-stimulated with 1000 U/ml IL-2 overnight. NK cells obtained after alloSCT with and without corticosteroid treatment (alloSCT + cort) or from healthy controls (H) were co-cultured with *A. fumigatus* germ tubes (AF, MOI 0.5) or plain medium at 37 °C for 6 h. Supernatants were collected, and chemokine levels of (a) MIP-1α, (b) MIP-1β, and (c) RANTES were analyzed. Data were acquired from n = 11 (H), n = 6 (alloSCT 60), n = 7 (alloSCT 90), n = 6 (alloSCT 120), n = 3 (alloSCT 180), n = 3 (cort 60), n = 5 (cort 90), n = 120 (cort 120), and n = 5 (cort 180) experiments. Data are displayed as medians. Significant differences were calculated by Kruskal-Wallis test with correction for multiple testing by the FDR method of Benjamini and Hochberg. Statistical significances are marked by asterisks (* $p < 0.05$, ** $p < 0.01$, *** $p < 0.001$).

Since we observed defects in CD56 binding and chemokine secretion of NK cells obtained from patients after corticosteroid treatment, we next analyzed the effects of corticosteroids on healthy NK cells *ex vivo*. Therefore, we stimulated NK cells for 40 h with physiological levels of prednisolone that are present in patients during an acute phase treatment.

Corticosteroids were shown to decrease the expression of surface NK cell activation receptors [320]. Indeed, we observed a down-regulation of NKp46 and CD69 after stimulating healthy NK cells with prednisolone *ex vivo* (Figure 37a, b). In compliance to the negligible effects of corticosteroids on fungal-mediated actin polymerization and perforin secretion after alloSCT, prednisolone had no impact on the F-actin content and perforin release in healthy NK cells (Figure 37c, d).

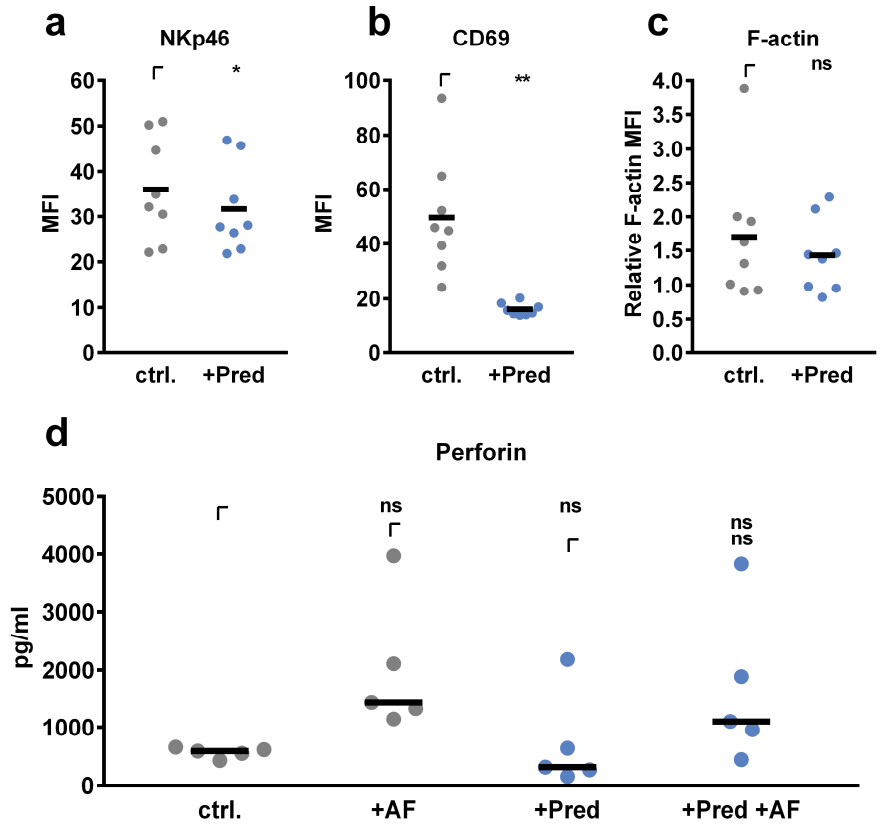

Figure 37: Prednisolone treatment of healthy NK cells decreases the expression of the activation markers NKp46 and CD69 but has no impact on fungal mediated perforin secretion. NK cells were treated with 25 µg/ml prednisolone in the presence of 1000 U/ml IL-2 for 40 h. The medium was exchanged, and NK cells were either cultured alone or with *A. fumigatus* germ tubes (MOI 0.5) for 6 h. Cells were analyzed regarding the surface expression of (a) NKp46 and (b) CD69 using flow cytometry. (c) F-actin was stained using Sir647 fluorescent probes. Supernatants were analyzed with (d) perforin ELISA. Data were acquired from (a-c) n = 8, (d) n = 5 different experiments. Data are displayed as (a-c) means and (d) medians. Statistical analyses were performed by (a-c) paired t-test and (d) Friedman test with FDR correction for multiple testing (Benjamini and Hochberg). Significant differences are marked by asterisks (* $p < 0.05$, ** $p < 0.01$).

Prednisolone had no effect on either NK cell viability nor on the cell amount measured by a cell viability analyzer (Fig. 38a). After treatment, the medium was exchanged, and NK cells were co-cultured with *A. fumigatus* germ tubes for 6 h. Prednisolone induced the down-regulation of CD56 MFI on the NK cell's surface, which made relative CD56 binding an unreliable readout for analyzing prednisolone treatment *ex vivo* (Fig. 38b).

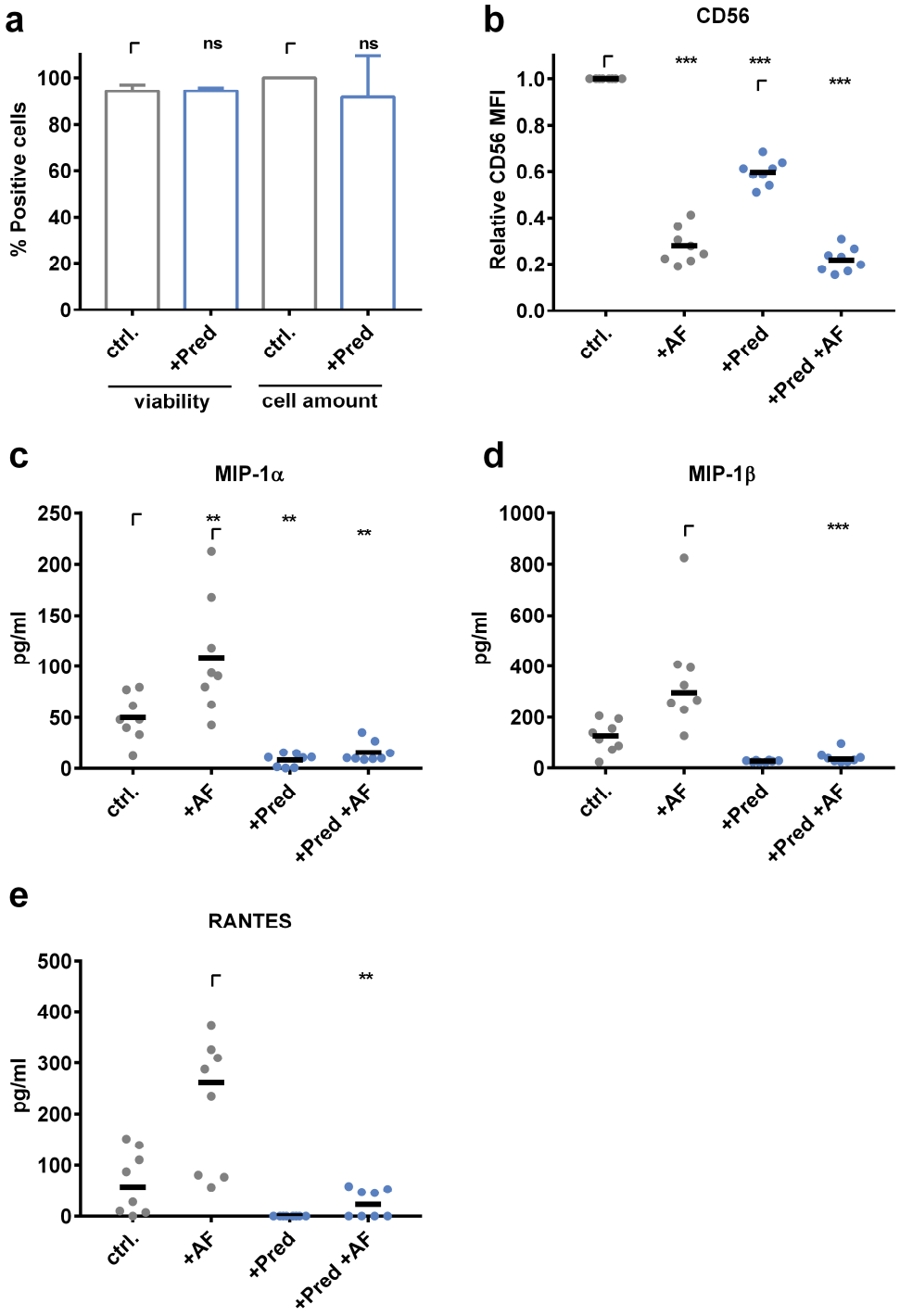

Figure 38: Prednisolone treatment of healthy NK cells reduces CD56 mediated chemokine secretion of MIP-1α, MIP-1β, and RANTES. NK cells were cultured with 1000 U/ml IL-2 in the presence of 25 µg/ml prednisolone for 40 h. (a) NK cell viability and cell counts were monitored by trypan blue staining using a cell viability analyzer (Beckman Coulter Vicell XR). NK cell-*A. fumigatus* (MOI 0.5) co-cultures were set for 6 h. (b) CD56 mean fluorescence intensity (MFI) was analyzed by flow cytometry. The secretion of (c) MIP-1α and (d) MIP-1β and (e) RANTES was analyzed by multiplex immunoassay. Data were acquired from (a) n = 5, (b-e) n = 8 different experiments. Data are displayed as (a) means + SD, (b,c) means, and (d,e) medians. Statistics were calculated by (a) paired t-test, (b, c) one-way ANOVA with FDR correction (F_B[1.452, 10.16] = 445.2, F_C[1.198, 8.385] = 21.46) and (d, e) Friedman test with FDR correction. Statistical significances are marked by asterisks (** $p < 0.01$, *** $p < 0.001$).

Notably, the down-regulation of CD56 MFI was not observed in corticosteroid treated NK cells obtained after alloSCT (Fig. 39). Since we could not use CD56 binding as a readout for prednisolone treatment *ex vivo*, we concentrated on the chemokines MIP-1α, MIP-1β, and RANTES, which were previously shown to be directly linked to CD56 mediated fungal binding [235]. Interestingly, prednisolone treatment abrogated the ability to secrete those chemokines in fungal stimulated NK cells (Fig. 38c-e).

From these experiments, we concluded that corticosteroids have detrimental effects on the fungal binding and secretion of cytokines and chemokines, while the fungal-mediated actin polymerization and perforin release were not influenced by corticosteroids.

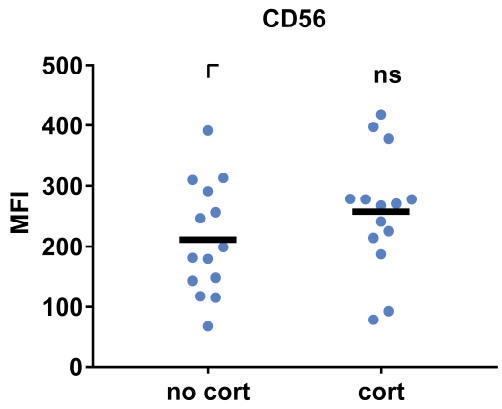

Figure 39: CD56 MFI is not altered on NK cells obtained from corticosteroid recipients. NK cells derived after alloSCT were incubated with 1000 U/ml IL-2 overnight before the medium was exchanged, and NK cells were cultured for 6 h in RPMI + FCS. The surface expression of CD56 was determined by flow cytometry. Mean fluorescence intensities (MFI) of CD56 was determined in NK cells obtained from patients with (cort) or without corticosteroid (no cort) treatment. Samples were matched regarding time after alloSCT and further drug treatment. Data were acquired from n = 14 experiments. Data are displayed as medians. Statistical analysis was performed by unpaired t-test with Welch's correction.

Discussion

Patients after alloSCT are at an increased risk of IA due to a long-term state of T/B cell deficiency [62]. Besides, a lack of innate immune cells such as neutrophils further negatively impacts on the outcome of IA [321]. Stuehler *et al.* correlated NK cell counts and NK cell reconstitution with a higher risk of developing IA, which underlined the role of NK cells in the defense against *A. fumigatus* [199]. NK cells are not activated by the exposure to *A. fumigatus* conidia, nor do they phagocytose other *A. fumigatus* morphologies [253]. Following contact with *A. fumigatus*, NK cells release perforin, which was shown to directly inhibit fungal metabolism [253]. To analyze the antifungal activity of NK cells, we co-cultured NK cells with *A. fumigatus* germ tubes, transferred the supernatants of co-cultures to *A. fumigatus* hyphae and measured the fungal metabolism after 6 h. Indeed, supernatants of former co-cultures contained elevated levels of perforin and inhibited the fungal metabolism, which was comparable in supernatants derived from NK cells after alloSCT and healthy controls.

By comparing CD56 and CD16 expression levels on NK cells obtained after alloSCT and healthy controls, we confirmed the presence of more immature $CD16^{-}CD56^{bright}$ NK cells in the peripheral blood of allograft recipients which persisted in most of the patients until 180 days post-transplant. The interaction of NK cells with *A. fumigatus* is mediated by the neuronal cell adhesion molecule (NCAM-1, CD56), which binds to interacting hyphae in an actin and time-dependent manner. Blocking of CD56 reduced the secretion of MIP-1α, MIP-1β, and RANTES after fungal stimulation [235]. CD56 relocalization is accompanied by decreased detection of CD56 on NK cells, which could be explained either by fungal shielding of CD56 molecules and therefore reduced flow cytometric antibody binding and/ or transfer of CD56 molecules from the NK cell to the surface of *A. fumigatus* germ tubes. Therefore, strong binding to the fungus results in lower CD56 percent positivity on NK cells [235].

CD56 binding was enhanced on the $CD56^{bright}$ compared to the $CD56^{dim}$ subset in healthy individuals, which might be because $CD56^{bright}$ cells also display a slightly higher fungal mediated actin polymerization. We detected no significant differences in fungal binding between NK cells derived from healthy individuals or alloSCT patients independent from the time point of blood draw; however, CD56 binding after alloSCT was distributed inhomogeneously and showed outliers. We further considered the possibility that different drug treatments might influence NK cell binding to fungal pathogens. Indeed, CD56 binding was inhibited when blood samples were collected from patients during corticosteroid therapy that is mainly applied to treat acute or chronic-graft-versus-host disease (GvHD). Interestingly, patients developing acute or chronic GvHD after alloSCT have also an increased risk

for IA, especially when receiving corticosteroids [322]. Therefore, we next focused on the impact of corticosteroid treatment on NK cell function.

Former studies report that CD56 relocalization to the fungal interface is abolished after disruption of actin dynamics by cytochalasin D, concluding actin-dependent CD56 relocalization [235]. We supported these findings by showing that a higher fungal mediated actin induction correlated with higher CD56 relocalization. We further demonstrated that the overall potential for fungal mediated actin polymerization was reduced in NK cells obtained after alloSCT. Interestingly, this was a time-dependent effect and actin defects recovered within 180 days post-alloSCT at which time actin induction was similar to healthy controls.

Until now, it has not been clear why NK cells obtained early after alloSCT show a lower potential for actin polymerization. Actin polymerization is crucial for NK cell differentiation, activation, and cytotoxicity [158, 323, 324]. Interestingly, the recent work from Lee and Mace has revealed that NK cell motility increases with cell maturation, concluding that the actin cytoskeleton may fully develop over time [158]. Since actin dynamics are crucial for several cellular processes, this may impact further functions in NK cells and other cell types post-alloSCT that have to be investigated in future studies. However, corticosteroids had no impact on fungal mediated actin polymerization in alloSCT patients or NK cells from healthy donors treated *ex vivo* with prednisolone, concluding that corticosteroids may specifically inhibit the CD56 signaling pathway downstream of actin rearrangements.

We analyzed CD56 downstream signaling and, interestingly, corticosteroid treatment inhibited the secretion of MIP-1α, MIP-1β, and RANTES in NK cells obtained at day 60-120 post-alloSCT. After 180 days, chemokine levels from corticosteroid treated NK cells normalized to that of healthy control levels which may be due to tapering of corticosteroid treatment over time, as corticosteroids are primarily used to treat GvHD after alloSCT [311, 325]. Therefore, low-level doses of corticosteroids to later time points may only marginally impact chemokine secretion. Corticosteroid treatment *ex vivo* inhibits NK cell-mediated tumor cell lysis, IFN-γ secretion, and the downregulation of NK cell activation receptors [320]. The primary corticosteroid agent for treatment of a GvHD is prednisolone, thus we tested the effect of prednisolone on NK cells from healthy individuals *ex vivo*. We observed a downregulation of NK cell surface markers; however, fungal mediated perforin secretion was not affected. Until now, the mechanisms of NK cell-mediated cytotoxicity towards fungal pathogens are not evident and might include mechanisms different from the ones relevant for tumor cell lysis. This would explain the persistence of fungal mediated perforin secretion when compared to reduced cytotoxicity towards tumor cells after corticosteroid treatment [320]. Furthermore, NK cells derived from patients after alloSCT receiving corticosteroid therapy showed no differences in the fungal mediated perforin secretion.

Glucocorticoids intracellularly bind to glucocorticoid receptors which are then transported into the nucleus. GR can either bind to glucocorticoid response elements (GREs), and function as transcriptional inducers or repressors, or interact with other transcription factors, thereby influencing their target gene expression [73-76]. In particular, glucocorticoids can inhibit NF-κB target gene expression by increasing the export rate of the activated p65 (RelA) NF-κB subunit from the nucleus to the cytoplasm [76]. MIP-1α, MIP-1β, and RANTES are NF-κB target genes, and their biological function is to recruit leukocytes to sites of inflammation and the initiation of a protective Th1 response [326-330].

IL-1α is essential for the recruitment of neutrophils to sites of *A. fumigatus* infections [331]. In particular, IL-1α signaling was shown to induce the secretion of several other chemokines, including MIP-1α, and MIP-1β [319]. We could show that IL-1α secretion was inhibited during corticosteroid therapy. This and the fact that NK cells during corticosteroid therapy also secreted lower amounts of the chemokines MIP-1α, MIP-1β, and RANTES indicates that NK cells from patients receiving corticosteroid therapy might have functional defects in their capacity to recruit further immune cells, e.g., neutrophils, to sites of inflammation.

We demonstrated that CD56 binding and secretion of chemokines involved in the CD56 signaling pathway is impaired after corticosteroid treatment, suggesting that CD56 may activate NF-κB signaling after fungal binding. Since it was previously shown that NK cells have a protective effect on the outcome of IA [199], our data demonstrated that corticosteroid treatment might favor the development of IA also by suppressing NK cell function in addition to effects on other immune cells.

4 Discussion

4.1 Classical PRRs on NK cells and moDCs

Anti-fungal immune cell functions are initiated by the recognition of PAMPs on the pathogen's surface. Depending on the receptor repertoire on the immune cell, PAMPs may activate different cell signaling pathways. DCs express a wide range of fungal specific PRRs, e.g., TLR-2, Dectin-1, MR, and DC-SIGN (see *1.2.2 Dendritic cells, Introduction*), and, consequently, recognize and interact with all kinds of *A. fumigatus* morphologies. In contrast, *A. fumigatus* conidia, which are surrounded by an immunological inert rodlet layer, are not recognized by NK cells [253, 332]. Instead, NK cells are activated by *A. fumigatus* germ tubes and hyphae, to which they form tight contacts to the extracellular parts. Since NK cells do not phagocytose fungal morphologies, only extracellular PRRs are able to mediate fungal stimulated NK cell activation and were investigated in this study.

Therefore, it was analyzed to which extent NK cells express known fungal PRRs on their surface. The surface expression of the chitin receptor TLR-2 ranged on NK cells from 1-27 %. Chitin is a cell wall component of fungal conidia and germ tubes, and previous studies reported the internalization of TLR-2 from the cell surface after phagocytosis of *A. fumigatus* conidia [255]. However, NK cells did not interact with *A. fumigatus* conidia [253] and showed no changes in the TLR-2 protein expression on their surface when co-cultured with *A. fumigatus* germ tubes. Furthermore, stimulation of NK cells with the TLR-2/Dectin-1 ligand zymosan did not induce NK cell activation, leading to the conclusion that TLR-2 is not responsible for fungal mediated NK cell activation.

Similar to TLR-2, TLR-4 expression did not change on the NK cell's surface after stimulation with live *A. fumigatus* germ tubes and remained below 15 %. Former studies showed that the polysaccharide galactomannan suppresses TLR-4 signaling and thereby favors the evasion of host immune responses [37]. Therefore, a possible role for TLR-4 in inducing NK cell activation and fungal recognition was excluded.

Several C-type lectin receptors, e.g., Dectin-1, NKp30, or MelLec, were described to be important fungal PRRs [23, 109, 191]; thus, their expression was analyzed in more detail. NK cells rarely expressed Dectin-1 on their surface (<2 %). In contrast, NKp30, which is also recognizing β-(1,3)-glucan [196], was highly expressed on NK cells (83-88 %). However, NKp30 expression did not change after challenging NK cells with *A. fumigatus* germ tubes. Also, NK cells were neither stimulated by the Dectin-1 ligand 'zymosan depleted', which is produced by hot-alkali treatment of zymosan, nor by β-(1,3)-glucan- containing cell

wall fractions of *A. fumigatus* hyphae, concluding that Dectin-1 and NKp30 are not involved in fungal recognition.

The activating receptor NKp46 recognizes protein structures on *C. glabrata* [192]. One recent study showed that NKp46 is down-regulated on NK cells after co-culture with *A. fumigatus*, the authors concluded that NKp46 is binding to a fungal ligand [333]. The Epa proteins bound by NKp46 are *Candida* specific. Hence, they can not be responsible for NKp46 down-regulation on NK cells interacting with *A. fumigatus* [333-335]. Besides fungal binding, down-regulation of surface receptors might be induced by fungal mediated apoptosis [336]. Indeed, our study showed that the down-regulation of NKp46 after fungal co-culture was directly associated with the emergence of apoptotic cells, as indicated by Annexin V/NKp46+ co-staining (data not shown). Thus, NKp46 was used as a marker for NK cell vitality and was not further considered as a fungal recognition receptor.

Besides NKp46, NKG2D was also down-regulated in the same study by Santiago *et al.* after co-culture with *A. fumigatus* germ tubes [333]. Similar to NKp46, the authors hypothesized that the down-regulation of NKG2D might be induced by binding to a fungal ligand [333]. In contrast, we did not observe any down-regulation of NKG2D following fungal co-culture in our study. Varying results between the study by Santiago *et al.* and ours (see *Chapter 3*) might occur from different incubation times and NK cell gating strategies in flow cytometry. Santiago *et al.* used overnight incubations for NK cell-*A. fumigatus* co-cultures, whereas we used a maximal co-incubation time of 12 hours.

After 12 hours, the number of viable NK cells that could be used for flow cytometry dramatically decreased. It has been shown that NK cell exhaustion leads to the down-regulation of activating surface receptors [337]. In particular, NKG2D was shown to be down-regulated on NK cells during chronic viral infections [338]. Thus, the differences in NKG2D surface detection in the study from Santiago *et al.* and ours might be explained by NK cell exhaustion due to the longer co-incubation times with *A. fumigatus* germ tubes in their study [333].

The other NK cell receptors (NTB-A, NKp44, 2B4, and DNAM-1) that we tested showed no differential protein expression upon fungal co-culture and were therefore not considered as fungal interaction partners. The incubation with cell wall fractions, depleted zymosan, inactivated germ tubes, or zymosan did not activate NK cells. One possible explanation is the low expression of classical surface receptors for *A. fumigatus* on NK cells, which does not allow them to recognize major polysaccharides on the fungal cell wall.

In contrast, moDCs express a wide range of fungal specific PRRs, and, consequently, are stimulated by inactivated germ tubes, TLR-2 and Dectin-1 ligands, and polysaccharide-containing cell wall fractions. These ligands induced the up-regulation of the moDC co-

stimulatory receptors CD80, CD86, CD83, and CD40, which are routinely used for assessing moDC maturation since they bind to naïve T cells and can induce T cell differentiation into pro- or anti-inflammatory cells [339-341]. Additionally, up-regulation of the C-C chemokine receptor type 7 (CCR7) and the MHC class ll receptor, HLA-DR, was observed. These markers are essential for antigen presentation and homing to secondary lymphoid tissues [342, 343]. The up-regulation of co-stimulatory molecules, homing receptors, and molecules for antigen presentation proved the capacity of the used ligands and cell wall fractions to induce DC maturation.

4.2 NK-DC cross-talk

4.2.1 Contact-dependent cell activation

NK-DC cross-talk plays an important role in infections with various pathogens, e.g., viruses, bacteria, and parasites [344-346]. Thus, the goal was to assess whether moDCs and NK cells can activate each other in the context of fungal infections. It was important to use autologous cells since NK cells can recognize and lyse allogeneic cells if HLA-C allotypes do not match [347]. Furthermore, high NK:DC ratios were shown to induce NK cell-mediated DC lysis, which is why our study used an NK:DC ration of 1:1 [348].

Due to the broader receptor repertoire, moDCs recognized more stimulants and subsequently induced NK cell activation measured by CD69 expression when those were not able to recognize the stimulus. NK cells were not activated after stimulation with polysaccharide- containing stimulants, even when the cell wall fractions were used in fourfold higher concentrations as used for moDC stimulation, concluding the absence of the respective receptors on NK cells.

In contrast, the whole-cell lysate from *A. fumigatus* was able to stimulate NK cells. According to the manufacturer, this lysate contains not only polysaccharide structures but also intracellular and extracellular proteins. NK cells were activated by stimulation with the *A. fumigatus* lysate and transferred activation signals onto autologous, immature moDCs, confirming that both cell types can activate the counterpart, immature or resting cell type.

4.2.2 NK cell activation by soluble factors

At sites of inflammation and pathogenic growth, monocytes may acquire an inflammatory phenotype and develop into inflammatory DCs, which can secrete pro-inflammatory cytokines and chemokines and thereby initiate a protective Th1 response [127]. Those inflammatory DCs share a high content of enriched expressed genes with *in vitro* generated moDCs [128].

To investigate whether *in vitro* generated moDCs can induce NK cell activation by secreted factors, moDCs were stimulated with *A. fumigatus* morphologies, cell wall fractions, or ligands of PRRs recognizing *A. fumigatus.* Notably, NK cells were not activated by the ligands used for moDC stimulation. Therefore, the moDC supernatants could only induce NK cell activation if moDCs secreted soluble factors that activated NK cells.

TLR-2 activation leads to the recruitment of the myeloid differentiation primary response protein 88 (MyD88), the induction of the NF-κB signaling pathway [349], and gene expression of the pro-inflammatory cytokines and chemokines IL12B, TNF-α, IL-8, IL-6, IL-1β, and CCL3 [107]. Furthermore, TLR-2 can collaborate with Dectin-1 and thereby potentiate Dectin-1 mediated ROS production and the secretion of IL-12 and TNF-α [350]. Inhibition of the β-(1,3)-glucan receptor Dectin-1 was shown to reduce lung inflammation while increasing the fungal burden in *A. fumigatus* infected mice [261]. Following ligand binding, Dectin-1 is phosphorylated by Src kinases. Canonical and non-canonical NF-κB signaling, MAPK signaling, and NFAT activation were shown to be induced by Dectin-1 stimulation [135-140]. The soluble response includes the secretion of TNF, CXCL2, IL-23, IL-6, IL-10, and IL-2 [350-353].

The alkali-insoluble cell wall fraction contains β-glucans, chitin, galactomannan, and galactosaminogalactan [228]. Galactomannan and galactosaminogalactan were shown to have anti-inflammatory effects on immune cell function [37, 354]. Furthermore, the TLR-2 stimulatory capacity of chitin is abolished through de-acetylation by hot-alkali treatment [107, 355]. Therefore, it is likely that the moDC-stimulating ligands in the cell wall fraction are mainly β-glucans, which was confirmed by the similar cytokine profile secreted by depleted zymosan and cell wall fraction- stimulated moDCs.

Inactivation of *A. fumigatus* germ tubes with ethanol preserves the recognition of polysaccharides by immune cells. The main sugars in the cell wall of *A. fumigatus* are galactosaminogalactan (GAG), galactomannan, β-glucans, α-glucans, and chitin [33]. Shielded by the upper polysaccharide layers, chitin is localized adjacent to the fungal cell membrane. Thus, the limited accessibility of chitin on inactivated germ tubes may hinder TLR-2 mediated recognition and cytokine secretion compared to the stimulation with the pure ligands (zymosan). The limited detection of chitin on inactivated germ tubes and in cell wall fractions would explain the similar cytokine profile when moDCs were stimulated with depleted zymosan, inactivated germ tubes, and cell wall fractions.

In contrast, moDC stimulation with zymosan specifically increased the secretion of IL-12p70, IL-6, IL-10, and IP-10, which resulted in the highest NK cell activation. While IL-6 and IL-10 are general pro- and anti-inflammatory cytokines [266], IL-12p70 and IP-10 have been described as inducers of NK cell activation and are at least partially dependent on TLR2 signaling [267, 269, 356]. However, stimulation with those cytokines, even when used in combination, could not induce NK cell activation, concluding that additional soluble factors derived from moDCs are essential for NK cell activation.

It was hypothesized that either Dectin-1 or TLR-2 blocking abrogates zymosan mediated NK cell activation. However, Dectin-1 silencing had no significant impact on mediating

NK cell activation since CD69 expression on NK cells was up-regulated by Dectin-1 silenced moDCs stimulated with depleted zymosan. These findings led to the conclusion that only a few amounts of unsilenced receptors are sufficient for DC maturation and NK cell activation. The blocking of TLR-2 signaling via antibody treatment inhibited the up-regulation of the co-stimulatory molecule CD80 when moDCs were stimulated with TLR-2/TLR-6 ligands. Since there was no pure TLR-2 ligand commercially available, the TLR-2/TLR-6 stimulating ligand FSL-1 was used as a positive control. Blocking of TLR-2 did not influence NK cell activation, even when moDCs were stimulated with the Dectin-1/TLR-2 ligand zymosan. Therefore, it was concluded that similar to Dectin-1, very few receptors of TLR-2 are sufficient to secrete cytokines that induce NK cell activation, or that other functional receptors can compensate TLR-2 receptor functions.

Receptor redundancy was discussed before by showing that a polymorphism in Dectin-1 resulted in less secretion of TNF-α and IL-6 by PBMCs but had no influence on cytokine secretion in monocyte-derived macrophages, concluding that other receptors can compensate the lost Dectin-1 signaling [263]. Since Dectin-1 can synergize with TLR-2, future studies may include the simultaneous blocking and silencing of TLR-2 and Dectin-1 to analyze whether the receptor synergism is important for cytokine secretion that stimulates NK cells.

4.3 CD56 as a PRR on human NK cells

4.3.1 CD56 binding to the fungus

The C-type lectin receptor CD69 is up-regulated on NK cells shortly after induction of different NK cell activation pathways [357, 358]. Therefore, we used CD69 expression to determine the NK cell activation status in our study. The expression of CD69 increased time-dependently after setting NK cell-*A. fumigatus* co-cultures and showed the highest induction after 12 hours. Meanwhile, the detection of CD56 decreased when NK cells were analyzed by flow cytometry. Interestingly, blocking of CD56 before fungal co-culture inhibited NK cell activation, concluding that fungal recognition by CD56 is directly involved in mediating NK cell activation.

The binding to the fungus was associated with a decreased detection of CD56 surface molecules. It is known that relocalization of receptors to fungus- containing phagolysosomes reduces their surface expression [255], thus, we analyzed whether CD56 was internalized. We used two different anti-CD56 antibody clones to distinguish extra- and intracellular CD56. We first performed an extracellular protein staining with one antibody clone, followed by fixation and internal protein staining with another antibody clone. Additionally, we used trypsin to cut off all extracellular CD56 molecules before NK cells were fixed and stained intracellularly. All stainings showed no internal fluorescent signal for CD56, concluding that CD56 was not internalized. In contrast, Santiago *et al.* reported that around 60 % of CD56 is internalized after co-culture with *A. fumigatus*. In that study, one monoclonal antibody was used to stain extra- and intracellular CD56 molecules. The fixation of cells after the surface staining might have led to a higher accessibility of extracellular CD56 proteins that were not bound by antibodies during the first staining. Thus, the increased CD56 signal after fixation might have been derived from extracellular origin and not, as concluded, from the cytoplasm.

A. fumigatus secretes serine proteases that contribute to respiratory tract inflammation [359]. To analyze whether fungal proteases degraded CD56, the protein content of CD56 was analyzed by western blotting. The total protein amount of CD56 was not reduced after fungal co-culture, confirming that fungal proteases did not degrade CD56.

The secretion of CD56 into the supernatant was reported before [360]; therefore, we performed an enzyme-linked immunosorbent assay to check if CD56 was released into the supernatant. The concentration of secreted CD56 did not change after fungal co-culture, leading to the conclusion that CD56 remains at the surface after binding. Thus, alternative

mechanisms besides secretion, internalization, or degradation are responsible for the reduced CD56 detection on the cell surface.

The shielding of CD56 by a fungal interaction partner might explain its reduced detection by flow cytometry. Since this was observed with three different antibody clones that recognized different antigens on CD56, a large area of the CD56 protein might be shielded by fungal structures. Similarly, the antibody-mediated detection of concentrated CD56 protein at the fungal interface could be inhibited compared to homogeneously distributed CD56 on cells cultured alone, resulting in a decreased detection of the fluorescent signal.

Furthermore, a strong interaction with the fungus may lead to remaining CD56 protein on the fungal surface after harvesting NK cell-*A. fumigatus* co-cultures. This hypothesis can be supported by the observations we made during microscopic analysis. Before and after staining of NK cell-*A. fumigatus* co-cultures with antibodies directed against CD56, extensive washing steps were performed with up to five washes per well. The applied shear-forces may lead to the detachment of some NK cells from the fungus, and, indeed, some CD56-dense patches were observed on *A. fumigatus* hyphae without the presence of NK cells. These CD56-dense patches were only observed on fungal hyphae that were co-cultured with NK cells and further had a similar length and structure as NK cell-*A. fumigatus* interaction sites. Therefore, it is likely that these patches reflect former interaction sites and that the respective NK cell interacting with the fungus was washed away in later washing steps. Similar shear-forces may apply when preparing the co-cultures for flow cytometry, and, therefore, membranous structures reflecting former interaction sites might stay on the fungal surface after detaching co-cultures from the well bottom or during washing steps.

In conclusion, it is likely that CD56 is either shielded by the fungus or other CD56 molecules or remains at the fungal interaction site after harvesting NK cells from former co-cultures, which leads to a decreased detection of CD56 when analyzed by flow cytometry.

4.3.2 CD56 mediates actin rearrangements

Mace *et al.* demonstrated in an *ex vivo* CD34+ cell culture on stromal cells that CD56 has a role in actin rearrangements and NK cell development. Interestingly, migration of CD34+ cells correlated with the occurrence of CD56 expression at the cell surface, and CD56 interactions with stromal cells were essential for NK cell maturation since blocking of CD56 favored the accumulation of immature CD34+ cells. From these experiments, the authors concluded that CD56-mediated NK cell migration is essential for NK cell maturation [215].

It is known that actin plays a role in target cell lysis, as the initiation of cytotoxicity is mediated by the relocalization of activating receptors to the immunological synapse. While this process was shown to be actin-dependent, the latter reorganization of cytotoxic granules to the target cell interface was dependent on microtubules [287].

Thus, CD56-mediated actin polymerization may represent the initial NK cell response towards the fungus. Pre-treatment of healthy NK cells with the actin polymerization inhibitor cytochalasin D resulted in inhibited CD56 relocalization to the fungal interface. In contrast, inhibition of the microtubule cytoskeleton by colchicine did not influence CD56 relocalization, concluding that CD56 is reorganized to the interaction site as an early event in target cell recognition mediated by actin. Indeed, the amount of relocalized CD56 molecules directly correlated with the induction of actin polymerization in NK cells obtained from recipients of an allograft after fungal stimulation.

In neuronal cells, the proposed model of CD56 signaling involves a phosphorylation cascade leading to neurite outgrowth [361]. After CD56 relocalization to lipid rafts, the intracellular p21- activated kinase (Pak1) is dephosphorylated and forms a complex with the Pak-interacting exchange factor (PIX) and the cell division control protein 42 homolog (cdc42). This complex formation induces the autophosphorylation and activation of Pak1, which in turn, phosphorylates the LIM kinase (LIMK). LIMK phosphorylates cofilin at Ser3 and thereby reduces its actin-depolymerizing activity. Consequently, actin is polymerized, which promotes growth cone motility and generation of traction forces required for neurite outgrowth [361]. Future studies may investigate whether the CD56 downstream kinases in neurons are also present in NK cells, and, whether their phosphorylation status is influenced by stimulation with *A. fumigatus*.

4.3.3 The fungal interaction partner of CD56

Fungal inactivation by different treatments, e.g., ethanol, formaldehyde, or heat, influences the stability of proteins. In contrast, those treatments hardly influence the polysaccharide structure, as Dectin-1 and TLR-2 are still able to recognize their fungal ligands after pre-treatment of fungi with heat or ethanol [41, 362].

Treatment of proteins with ethanol or heat disrupts the hydrogen bonds and thus leads to the destruction of the proteins to the primary amino acid sequence, while fixation with formaldehyde destructs the proteins to the secondary structure [363-365]. Incubation of *A. fumigatus* germ tubes in ethanol or at high temperatures abrogated fungal mediated NK cell activation and CD56 binding when NK cells were analyzed by flow cytometry (data not shown). Similarly, NK cells did not attach to *A. fumigatus* hyphae and showed no CD56 relocalization when hyphae were fixed for microscopic analyses before NK cells were

added. Consequently, NK cell recognition and CD56 binding are either dependent on live fungus or an intact protein structure at the fungal surface.

While the polysaccharide-containing cell wall fractions did not stimulate NK cell binding or activation, the whole-cell lysate was able to induce NK cell activation, but not CD56 binding. In contrast to the cell wall fractions, the whole-cell lysate further contains intracellular antigens that are not accessible for NK cells when they are incubated with whole fungal morphologies. Therefore, other receptors besides CD56 might be involved in mediating NK cell activation when fungal lysates are used.

Additional experiments that were performed in the lab but are not part of this thesis lead to the hypothesis that the interaction partner of CD56 might have carbohydrate portions. Sodium periodate ($NaIO_4$) reacts with vicinal diols in ring structures of polysaccharides, leading to the break of the ring structure [366]. By the oxidation of the carbohydrate portion of glycoproteins, periodate induces the release of formaldehyde as a byproduct of this reaction [367]. Mild treatment of *A. fumigatus* hyphae with the oxidating reagent did not affect the fungal viability but diminished CD56 binding and secretion of MIP-1α. Since sugars are important PAMPs, the interaction partner of CD56 likely contains protein as well as carbohydrate structures. Interestingly, there is evidence in the literature showing that reduced detection of CD56 in flow cytometry is observed after co-incubation of NK cells with the glycoprotein gp63 from *Leishmania major*, leading to the hypothesis that CD56 might bind to glycoproteins [193].

4.4 Analysis of NK cell function after alloSCT

4.4.1 NK cell reconstitution and phenotypic analysis

Phagocytotic cells of the innate immune system are mandatory for fungal clearance. Inhaled *A. fumigatus* conidia are killed by alveolar macrophages, which are mainly resident lung cells derived from very early developmental events, or, to a lesser extent, differentiate from circulating bone-marrow-derived adult monocytes [368, 369]. During the onset of pulmonary lung infections, PMNs are recruited from the blood within hours and clear fungal pathogens by ROS production [370, 371]. The process of fungal mediated ROS production in PMNs is impaired early after alloSCT but recovers 90 days post-alloSCT [199].

Additionally, neutropenic or monocytopenic patients may display reduced or absent cell counts and therefore are prone to develop IA [321, 372]. In that phase, other immune cells are necessary for the recruitment of leukocytes and clearance of the fungus. In particular, NK cells were shown to have a protective effect against *Aspergillus* infections by secreting IFN-γ that stimulates macrophages to phagocytose fungal morphologies in neutropenic mice [147]. Furthermore, it is known that patients after alloSCT have an increased risk of developing IA in case of lower NK cell counts or delayed NK cell reconstitution, concluding that NK cells have anti-fungal functions after stem cell transplantation [199].

The individual immune cell reconstitution after alloSCT was shown to range from 14 days to 2 years [59]. PMNs belong to the first cell types that reconstitute after stem cell transplantation; monocytes and NK cell counts were shown to be fully reconstituted 30 days post-alloSCT, and T and B cell compartment reconstitution can take up to two years [59, 199, 373]. In this study, we analyzed the NK cell reconstitution and characterized the phenotype of reconstituting NK cells by measuring the surface expression of CD56 and CD16. It is generally accepted that $CD56^{bright}$ NK cells represent the more immature subset since they have longer telomeres and can differentiate into $CD56^{dim}$ NK cells *in vitro* and *in vivo* [164, 165].

While NK cell counts 60 days post-alloSCT were comparable to the counts of healthy individuals, NK cell phenotypes were shifted towards the immature $CD56^{bright}CD16^{neg}$ and intermediate $CD56^{bright}CD16^{pos}$ subset. This abnormal subset distribution persisted for over 180 days post-alloSCT. To analyze whether there are differences within healthy and reconstituting NK cell subsets, surface expression of CD56 and CD16 was analyzed on the three NK cell subsets. The fluorescence signals derived from CD56 and CD16 stainings did not differ within $CD56^{bright}CD16^{neg}$, $CD56^{bright}CD16^{pos}$, and $CD56^{dim}CD16^{pos}$ NK cells, showing that the amount of CD56 and CD16 molecules within subsets is comparable. In conclusion,

NK cell maturation is a long-lasting process, and reconstituting NK cells may reflect functional differences compared to fully matured NK cells in healthy individuals.

4.4.2 The influence of corticosteroids on NK cell function

Corticosteroid therapy is used for the treatment of GvHD [71, 72]. In our study, 59 % of the patients received either long-term low-dose or short-term high-dose corticosteroid treatment. The occurrence of GvHD (35 %) was treated with corticosteroids for up to 15 weeks with initial high doses (>1 mg/kg) that rapidly were tapered over time. Corticosteroid therapy without the incidence of GvHD (24 %) was applied in cases of adrenal insufficiency that was treated with Hydrocortison®, a corticosteroid with a lower duration of action compared to prednisolone. Patients further received low-dose corticosteroids when the blood concentrations for other immunosuppressive agents (e.g., cyclosporine) were below the aimed concentration level for a short time.

Fungal binding was analyzed by co-culturing NK cells derived from alloSCT patients or healthy donors with *A. fumigatus* germ tubes. The binding of reconstituting NK cells was very inhomogeneous, characterized by outliers that showed diminished CD56 binding. Interestingly, when reconstituting NK cells were grouped regarding corticosteroid administration, NK cells in groups of corticosteroid-treated patients displayed reduced fungal binding. Previous CD56 blocking experiments showed that the secretion of MIP-1α, MIP-1β, and RANTES was dependent on CD56-binding to the fungus. Since corticosteroid therapy did not only reduce CD56 binding but furthermore inhibited the secretion of those chemokines, we concluded that MIP-1α, MIP-1β, and RANTES are regulated downstream of CD56 signaling.

Since $CD56^{dim}$ NK cells are the major subset to secrete chemokines before target cell lysis [316], we analyzed whether the reduced abundance of $CD56^{dim}$ NK cells after alloSCT was responsible for the decreased chemokine secretion. Therefore, we performed CD16 positive cell isolation from NK cells to separate $CD56^{bright}CD16^{neg}$ and $CD56^{dim}CD16^{pos}$ cells in alloSCT patients and healthy individuals. While $CD56^{bright}CD16^{neg}$ cells hardly secreted MIP-1α, MIP-1β, and RANTES, $CD56^{dim}CD16^{pos}$ NK cells showed fungal-induced chemokine secretion. Notably, NK cells derived from recipients of an allograft secreted lower amounts of chemokines compared to healthy individuals, concluding functional defects in reconstituting $CD56^{dim}$ NK cells. Thus, the reduced abundance of mature $CD56^{dim}$ NK cells, functional defects, and corticosteroid therapy negatively influenced the secretion of MIP-1α, MIP-1β, and RANTES during fungal co-culture.

To verify that the reduced fungal binding and chemokine secretion was caused by corticosteroid therapy, healthy NK cells were treated *ex vivo* with corticosteroids. Therefore, the commonly administered corticosteroid prednisolone was applied comparable to *in vivo* concentrations. Notably, the duration of corticosteroid incubation greatly varied between patients and NK cells from healthy individuals. While patients received corticosteroids over weeks, healthy NK cells were stimulated for 40 hours only. A longer cultivation of NK cells was not possible due to the reduced life-span of primary NK cells when cultured *ex vivo*. Additionally, we decided not to expand primary NK cells *ex vivo* since this alters the expression of surface receptors and modulates cell functions [374].

It was shown in literature that corticosteroids down-regulate NK cell activation receptors by unknown mechanisms [320]. Indeed, the natural killer activating receptor NKp46 and the marker for NK cell activation, CD69, were down-regulated on NK cells after prednisolone treatment *ex vivo*. CD56 expression was not affected on NK cells derived from patients receiving corticosteroids but on healthy NK cells treated with prednisolone *ex vivo*. CD56 down-regulation might have occurred due to similar mechanisms that are responsible for the down-regulation of NKp46 and CD69, and made the measurement of CD56 binding not feasible for healthy NK cells treated with prednisolone *ex vivo*.

As mentioned before, CD56 is relocalized to the fungal interaction site by actin-dependent mechanisms. Thus, the impact of corticosteroids on the actin cytoskeleton was investigated by live NK cell staining with the cell-permeable probe Sir647, which is structurally derived from high affinity F-actin binding toxins [375, 376]. The probe efficiently stained F-actin without affecting NK cell viability. Actin polymerization was induced in NK cells upon fungal stimulation, and the increase in F-actin positively correlated with CD56 binding to the fungus. Fungal-mediated actin polymerization was not affected by corticosteroids that were administered to alloSCT patients during therapy or healthy NK cells *ex vivo*. Hence, corticosteroids may inhibit the CD56 signaling independent from actin.

Fungal-mediated actin polymerization was time-dependently regulated after alloSCT. While NK cells obtained early after alloSCT (60 days) showed a decreased fungal-mediated actin polymerization, NK cells collected after 180 days displayed normal fungal-mediated F-actin induction. The actin cytoskeleton is crucial for NK cell differentiation, activation, and cytotoxicity [158, 323, 324]. Lee and Mace extensively studied the role of actin dynamics during NK cell maturation and demonstrated that cell motility and maturation were tightly linked to each other, concluding that the actin cytoskeleton is important for NK cell differentiation [158]. This finding might explain why NK cells obtained early after alloSCT display a reduced fungal-mediated actin induction compared to more matured NK cells collected 180 days post-alloSCT. Since actin dynamics are crucial for several cellular processes in all

types of cells, it might be interesting to analyze the fungal-mediated actin polymerization in other cell types after alloSCT.

Infections of NK cells with *A. fumigatus* trigger the release of perforin *in vitro*, which is sufficient to inhibit the fungal metabolism measured by XTT [293]. It was shown that corticosteroids inhibit NK cell cytotoxicity towards tumor cells [320, 377]; thus, we analyzed fungal-mediated perforin secretion during corticosteroid therapy. However, corticosteroids had no influence on the secretion of perforin in NK cells derived from corticosteroid-treated patients or healthy donors. Additionally, corticosteroid therapy did not alter the ability of NK cells to inhibit fungal metabolism, indicating that there might be different cytotoxic mechanisms towards tumors and fungi.

In contrast, treatment of healthy NK cells *ex vivo* with prednisolone abrogated the secretion of MIP-1α, MIP-1β, and RANTES following fungal stimulation. These data confirmed the observations made with NK cells derived from corticosteroid-treated patients that showed inhibited secretion of those chemokines. Hence, corticosteroids were probably responsible for the decreased chemokine secretion in recipients of an allograft.

IL-1α is a cytokine that was previously shown to be protective against *Aspergillus* infections as IL-1α signaling is critical for leukocyte recruitment in pulmonary fungal infections [319]. Interestingly, IL-1α secretion was reduced after fungal stimulation when i) NK cells from donors of an allograft received corticosteroid therapy or ii) CD56 was blocked in healthy NK cells (data not shown). Thus, the secretion of IL-1α, in combination with MIP-1α, MIP-1β, and RANTES, might be induced by CD56 signaling.

The cell-permeable glucocorticoids bind to respective receptors in the cytoplasm. After ligand binding to the receptor, receptor complexes are translocated into the nucleus where they bind to glucocorticoid response elements and thereby function as transcriptional inducers or repressors. Additionally, glucocorticoid receptor complexes can further interact with other transcription factors and influence their target gene expression [73-76]. In particular, glucocorticoids can inhibit NF-κB target gene expression by increasing the export rate of the activated p65 (RelA) NF-κB subunit from the nucleus to the cytoplasm [76]. NF-κB signaling induces the transcription of MIP-1α, MIP-1β, and RANTES, which is important for the recruitment of leukocytes and initiation of a protective Th1 response [326-330]. Since CD56 binding and specific chemokine secretion was impaired after corticosteroid therapy, CD56 may be involved in NF-κB activation. Hence, the protective effect of NK cells against *A. fumigatus* infections shown in other studies might be due to the activation of NF-κB signaling.

4.5 Conclusions

In this study, we analyzed the interaction of different immune cells with the pathogenic fungus *A. fumigatus*. While DCs express a large panel of PRRs, including the ones known to bind fungal structures, NK cells are innate immune cells that do not express typical PRRs. Therefore, we analyzed the ability of fungus-activated moDCs to induce NK cell activation. MoDCs could induce NK cell activation after stimulation with fungal morphologies or important PRR ligands when these stimuli did not directly activate NK cells. Thus, DCs exhibited NK cell supporting function, which highlights the importance of immune cell cross-talk during pathogenic infections (Figure 40).

Moreover, we identified the neuronal cell adhesion molecule (NCAM-1, CD56) as the PRR for *A. fumigatus* on NK cells. This non-classical PRR recognized fungal structures displayed on hyphae but not on conidia. Fungal recognition required live fungus since CD56 did not bind to inactivated *A. fumigatus* germ tubes. The relocalization of CD56 to the fungal interaction site was shown to induce the secretion of MIP-1α, MIP-1β, and RANTES. Furthermore, the fungal PAMP recognized by CD56 was not *A. fumigatus*-specific since the PRR also bound to other *Aspergillus spp.* However, the PAMP must have the highest expression on *A. fumigatus*, as this species induced the greatest CD56 relocalization on NK cells (Figure 40).

In this study, we analyzed the functional differences between reconstituting NK cells in allograft recipients and healthy individuals. Besides the presence of more immature $CD56^{bright}CD16^{-}$ NK cells in the peripheral blood of alloSCT patients, reconstituting NK cells showed an inhibited CD56 mediated fungal binding. This binding was significantly reduced when patients received corticosteroid therapy. Furthermore, NK cells obtained from patients during corticosteroid treatment showed an inhibited secretion of MIP-1α, MIP-1β, and RANTES, which were identified to be secreted after CD56 binding. Additionally, e*x vivo* treatment of healthy NK cells with corticosteroids revealed inhibited secretion of those chemokines. Thus, corticosteroids were identified to have detrimental effects on NK cell function during infection with *A. fumigatus* (Figure 40).

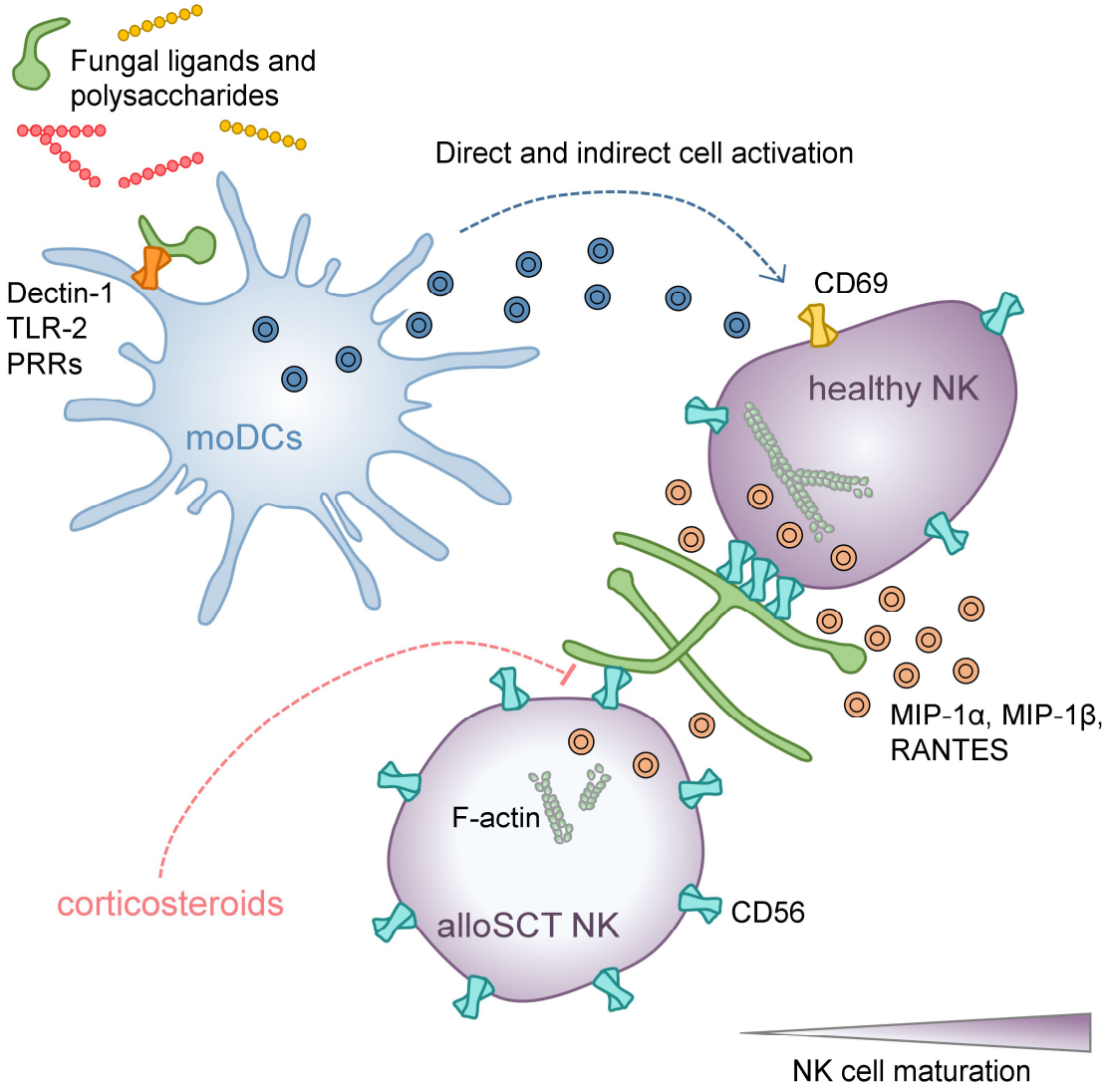

Figure 40: Conclusions of the study. MoDCs recognize more fungal ligands and polysaccharides compared to NK cells that do not express high amounts of the respective PRRs, e.g., Dectin-1 and TLR-2. Subsequently, moDCs secrete pro- and anti-inflammatory cytokines and chemokines, like IL-1β, IL-6, IL-8, IL-10, IL-12p70, IP-10, MIP-3α, and TNF-α. Soluble factors from moDCs are able to activate autologous NK cells measured by CD69 expression. Therefore, moDCs display supporting function in NK cell activation. The PRR CD56 recognizes hyphal structures on the surface of *A. fumigatus* hyphae. Blocking of CD56 inhibits the secretion of the chemokines MIP-1α, MIP-1β, and RANTES, which are important for leukocyte recruitment in inflamed tissue. After alloSCT, NK cell subsets are shifted towards the $CD56^{bright}$ phenotype. Corticosteroid therapy inhibits fungal recognition and chemokine secretion by CD56. Furthermore, actin polymerization following fungal stimulation is inhibited early after alloSCT but recovers until day 180 post-alloSCT. Thus, fungal responses are inhibited after alloSCT.

4.6 Future perspectives

The interaction of innate and adaptive immunity is essential to control and clear invading fungal pathogens. Still, little is known about NK-DC interactions during *A. fumigatus* pathogenicity. Interestingly, it was demonstrated that DCs could enhance surface expression of CD56 on NK cells in direct NK-DC co-cultures, resulting in the up-regulation of NK cell-mediated cytotoxicity [378, 379]. Thus, future studies may investigate whether DCs can enhance fungal recognition of NK cells by inducing the up-regulation of CD56.

CD56 is used as a characterization marker to discriminate NK cell subsets in the peripheral blood. Only recently, several studies claim that CD56 might induce NK cell cytotoxicity [216, 217, 380]. However, the mechanism of CD56 mediated lysis of target cells stays elusive until now. Thus, the role of CD56 in NK cell-mediated fungal cytotoxicity might be investigated in future studies. It would be interesting to analyze CD56-knockout NK cells regarding their ability to secrete perforin after fungal challenge. Furthermore, NK cell cytotoxicity was shown to be mediated by polysialic acid (PSA) residues loaded on the Ig5 domain of CD56 [219]; therefore, future studies might focus on the influence of PSA on fungal damage measured with an XTT assay.

Until now, it remains elusive what the fungal interaction partner for CD56 could be. CD56 is a glycoprotein that can interact with components of the extracellular matrix (EM), e.g., heparin or collagen [210, 211]. The EM of *A. fumigatus* contains sugars and proteins [381, 382]. Additionally, collagen-like genes with a possible extracellular location were identified in different *Aspergillus* species, including *A. fumigatus,* that suggest the presence of collagen-like proteins on the fungal surface [383]. Therefore, future studies might clarify whether the EM of *A. fumigatus* is involved in NK cell recognition. CD56 forms homophilic interactions by the interaction of the Ig domains in an antiparallel fashion on *trans* localized CD56 molecules [209]. Therefore, another possibility to find an interaction partner would be to search for CD56 similar motifs on the fungal cell surface by bioinformatic tools. Additionally, a possible interaction partner might be identified by protein pull-down. To achieve this, tagged CD56 protein containing only the extracellular domain might be incubated with *A. fumigatus* whole-cell homogenates, followed by analysis of the protein complex with mass spectrometry.

These experiments would help to characterize the role of CD56 on NK cells, and, by doing this, would give new insights into NK cell-fungal interactions and general NK cell biology.

References

1. Schmidt, A. and D.I. Schmidt, *J.B. Georg W. Fresenius and the description of the species Aspergillus fumigatus in 1863.* Contrib Microbiol, 1999. 2: p. 1-4.
2. Fresenius, G., *Beiträge zur Mykologie.* Frankfurt am Main, Brönner 1863: p. 81-82.
3. von Klopotek, A.A.v.L., *Über das Vorkommen und Verhalten von Schimmelpilzen bei der Kompostierung Städtischer Abfallstoffe.* Kluwer Academic Publishers, 1962. 28(1): p. 141-160.
4. Mullins, J., R. Harvey, and A. Seaton, *Sources and incidence of airborne Aspergillus fumigatus (Fres).* Clin Allergy, 1976. 6(3): p. 209-17.
5. O'Gorman, C.M., H. Fuller, and P.S. Dyer, *Discovery of a sexual cycle in the opportunistic fungal pathogen Aspergillus fumigatus.* Nature, 2009. 457(7228): p. 471-4.
6. Aimanianda, V., et al., *Surface hydrophobin prevents immune recognition of airborne fungal spores.* Nature, 2009. 460: p. 1117.
7. Shibuya, K., et al., *Histopathology of experimental invasive pulmonary aspergillosis in rats: pathological comparison of pulmonary lesions induced by specific virulent factor deficient mutants.* Microb Pathog, 1999. 27(3): p. 123-31.
8. Latge, J.P., *The pathobiology of Aspergillus fumigatus.* Trends Microbiol, 2001. 9(8): p. 382-9.
9. Thau, N., et al., *rodletless mutants of Aspergillus fumigatus.* Infect Immun, 1994. 62(10): p. 4380-8.
10. Valsecchi, I., et al., *Role of Hydrophobins in Aspergillus fumigatus.* Journal of fungi (Basel, Switzerland), 2017. 4(1): p. 2.
11. Thau, N., et al., *rodletless mutants of Aspergillus fumigatus.* Infection and immunity, 1994. 62(10): p. 4380-4388.
12. Beauvais, A., et al., *Deletion of the alpha-(1,3)-glucan synthase genes induces a restructuring of the conidial cell wall responsible for the avirulence of Aspergillus fumigatus.* PLoS Pathog, 2013. 9(11): p. e1003716.
13. Latge, J.P., *Tasting the fungal cell wall.* Cell Microbiol, 2010. 12(7): p. 863-72.
14. Latge, J.P., et al., *Specific molecular features in the organization and biosynthesis of the cell wall of Aspergillus fumigatus.* Med Mycol, 2005. 43 Suppl 1: p. S15-22.
15. Heinekamp, T., et al., *Aspergillus fumigatus melanins: interference with the host endocytosis pathway and impact on virulence.* Frontiers in microbiology, 2013. 3: p. 440-440.
16. Thywißen, A., et al., *Conidial Dihydroxynaphthalene Melanin of the Human Pathogenic Fungus Aspergillus fumigatus Interferes with the Host Endocytosis Pathway.* Frontiers in Microbiology, 2011. 2(96).
17. Chai, L.Y., et al., *Aspergillus fumigatus conidial melanin modulates host cytokine response.* Immunobiology, 2010. 215(11): p. 915-20.
18. Taubitz, A., et al., *Role of Respiration in the Germination Process of the Pathogenic Mold Aspergillus fumigatus.* Current Microbiology, 2007. 54(5): p. 354.
19. Gauthier, T., et al., *Trypacidin, a spore-borne toxin from Aspergillus fumigatus, is cytotoxic to lung cells.* PloS one, 2012. 7(2): p. e29906-e29906.

20. Konig, S., et al., *Gliotoxin from Aspergillus fumigatus Abrogates Leukotriene B4 Formation through Inhibition of Leukotriene A4 Hydrolase.* Cell Chem Biol, 2019. 26(4): p. 524-534.e5.
21. Sun, W.K., et al., *Dectin-1 is inducible and plays a crucial role in Aspergillus-induced innate immune responses in human bronchial epithelial cells.* Eur J Clin Microbiol Infect Dis, 2012. 31(10): p. 2755-64.
22. Droemann, D., et al., *Toll-like receptor 2 is expressed by alveolar epithelial cells type II and macrophages in the human lung.* Histochem Cell Biol, 2003. 119(2): p. 103-8.
23. Stappers, M.H.T., et al., *Recognition of DHN-melanin by a C-type lectin receptor is required for immunity to Aspergillus.* Nature, 2018. 555(7696): p. 382-386.
24. Madan, T., et al., *Binding of pulmonary surfactant proteins A and D to Aspergillus fumigatus conidia enhances phagocytosis and killing by human neutrophils and alveolar macrophages.* Infect Immun, 1997. 65(8): p. 3171-9.
25. Braem, S.G., et al., *Effective Neutrophil Phagocytosis of Aspergillus fumigatus Is Mediated by Classical Pathway Complement Activation.* J Innate Immun, 2015. 7(4): p. 364-74.
26. Chazalet, V., et al., *Molecular typing of environmental and patient isolates of Aspergillus fumigatus from various hospital settings.* Journal of clinical microbiology, 1998. 36(6): p. 1494-1500.
27. Hospenthal, D.R., K.J. Kwon-Chung, and J.E. Bennett, *Concentrations of airborne Aspergillus compared to the incidence of invasive aspergillosis: lack of correlation.* Med Mycol, 1998. 36(3): p. 165-8.
28. Latge, J.P., A. Beauvais, and G. Chamilos, *The Cell Wall of the Human Fungal Pathogen Aspergillus fumigatus: Biosynthesis, Organization, Immune Response, and Virulence.* Annu Rev Microbiol, 2017. 71: p. 99-116.
29. van de Veerdonk, F.L., et al., *Aspergillus fumigatus morphology and dynamic host interactions.* Nat Rev Microbiol, 2017. 15(11): p. 661-674.
30. Beauvais, A., et al., *Aspergillus cell wall and biofilm.* Mycopathologia, 2014. 178(5-6): p. 371-7.
31. Latge, J.P. and A. Beauvais, *Functional duality of the cell wall.* Curr Opin Microbiol, 2014. 20: p. 111-7.
32. Fontaine, T., et al., *Molecular organization of the alkali-insoluble fraction of Aspergillus fumigatus cell wall.* J Biol Chem, 2000. 275(36): p. 27594-607.
33. Gow, N.A.R., J.P. Latge, and C.A. Munro, *The Fungal Cell Wall: Structure, Biosynthesis, and Function.* Microbiol Spectr, 2017. 5(3).
34. Ram, A.F., et al., *The cell wall stress response in Aspergillus niger involves increased expression of the glutamine : fructose-6-phosphate amidotransferase-encoding gene (gfaA) and increased deposition of chitin in the cell wall.* Microbiology, 2004. 150(Pt 10): p. 3315-26.
35. Briard, B., et al., *Galactosaminogalactan of Aspergillus fumigatus, a bioactive fungal polymer.* Mycologia, 2016. 108(3): p. 572-80.
36. Robinet, P., et al., *A polysaccharide virulence factor of a human fungal pathogen induces neutrophil apoptosis via NK cells.* J Immunol, 2014. 192(11): p. 5332-42.
37. Chai, L.Y., et al., *Aspergillus fumigatus cell wall components differentially modulate host TLR2 and TLR4 responses.* Microbes Infect, 2011. 13(2): p. 151-9.

38. Steger, M., et al., *beta-1,3-glucan-lacking Aspergillus fumigatus mediates an efficient antifungal immune response by activating complement and dendritic cells.* Virulence, 2018: p. 1-13.
39. Wang, M., et al., *Mannan-binding lectin directly interacts with Toll-like receptor 4 and suppresses lipopolysaccharide-induced inflammatory cytokine secretion from THP-1 cells.* Cell Mol Immunol, 2011. 8(3): p. 265-75.
40. Gersuk, G.M., et al., *Dectin-1 and TLRs permit macrophages to distinguish between different Aspergillus fumigatus cellular states.* J Immunol, 2006. 176(6): p. 3717-24.
41. Hellmann, A.-M., et al., *Human and Murine Innate Immune Cell Populations Display Common and Distinct Response Patterns during Their In Vitro Interaction with the Pathogenic Mold Aspergillus fumigatus.* Frontiers in Immunology, 2017. 8: p. 1716.
42. Parkinson, D.R., *Interleukin-2 in cancer therapy.* Semin Oncol, 1988. 15(6 Suppl 6): p. 10-26.
43. Weidmann, E., et al., *Lactate dehydrogenase-release assay: A reliable, nonradioactive technique for analysis of cytotoxic lymphocyte-mediated lytic activity against blasts from acute myelocytic leukemia.* Annals of Hematology, 1995. 70(3): p. 153-158.
44. Kamai, Y., et al., *Interactions of Aspergillus fumigatus with vascular endothelial cells.* Med Mycol, 2006. 44 Suppl 1: p. S115-7.
45. Park, S.J. and B. Mehrad, *Innate immunity to Aspergillus species.* Clin Microbiol Rev, 2009. 22(4): p. 535-51.
46. Laufer, P., et al., *Allergic bronchopulmonary aspergillosis in cystic fibrosis.* Journal of Allergy and Clinical Immunology, 1984. 73(1, Part 1): p. 44-48.
47. Greenberger, P.A. and R. Patterson, *Allergic bronchopulmonary aspergillosis and the evaluation of the patient with asthma.* J Allergy Clin Immunol, 1988. 81(4): p. 646-50.
48. Patterson, R., M. Rosenberg, and M. Roberts, *Evidence that Aspergillus fumigatus growing in the airway of man can be a potent stimulus of specific and nonspecific IgE formation.* Am J Med, 1977. 63(2): p. 257-62.
49. Cenci, E., et al., *Th1 and Th2 cytokines in mice with invasive aspergillosis.* Infect Immun, 1997. 65(2): p. 564-70.
50. Patil, S. and R. Patil, *"Fleeting pulmonary infiltrates in allergic bronchopulmonary aspergillosis" Misdiagnosed as tuberculosis.* Int J Mycobacteriol, 2018. 7(2): p. 186-190.
51. Chabi, M.L., et al., *Pulmonary aspergillosis.* Diagnostic and Interventional Imaging, 2015. 96(5): p. 435-442.
52. Denning, D.W., *Therapeutic outcome in invasive aspergillosis.* Clin Infect Dis, 1996. 23(3): p. 608-15.
53. Marr, K.A., et al., *Epidemiology and outcome of mould infections in hematopoietic stem cell transplant recipients.* Clin Infect Dis, 2002. 34(7): p. 909-17.
54. Abdel Hameed, A.A., I.H. Yasser, and I.M. Khoder, *Indoor air quality during renovation actions: a case study.* J Environ Monit, 2004. 6(9): p. 740-4.
55. Mahieu, L.M., et al., *A prospective study on factors influencing aspergillus spore load in the air during renovation works in a neonatal intensive care unit.* J Hosp Infect, 2000. 45(3): p. 191-7.
56. Pini, G., et al., *Invasive pulmonary aspergillosis in neutropenic patients and the influence of hospital renovation.* Mycoses, 2008. 51(2): p. 117-22.

57. Schmitt, H.J., et al., *Aspergillus species from hospital air and from patients.* Mycoses, 1990. 33(11-12): p. 539-41.
58. Hahn, T., et al., *Efficacy of high-efficiency particulate air filtration in preventing aspergillosis in immunocompromised patients with hematologic malignancies.* Infect Control Hosp Epidemiol, 2002. 23(9): p. 525-31.
59. Ogonek, J., et al., *Immune Reconstitution after Allogeneic Hematopoietic Stem Cell Transplantation.* Frontiers in immunology, 2016. 7: p. 507-507.
60. Moore, D.C., *Drug-Induced Neutropenia: A Focus on Rituximab-Induced Late-Onset Neutropenia.* P & T : a peer-reviewed journal for formulary management, 2016. 41(12): p. 765-768.
61. Gerson, S.L., et al., *Prolonged granulocytopenia: the major risk factor for invasive pulmonary aspergillosis in patients with acute leukemia.* Ann Intern Med, 1984. 100(3): p. 345-51.
62. Corre, E., et al., *Long-term immune deficiency after allogeneic stem cell transplantation: B-cell deficiency is associated with late infections.* Haematologica, 2010. 95(6): p. 1025-9.
63. Fukuda, T., et al., *Risks and outcomes of invasive fungal infections in recipients of allogeneic hematopoietic stem cell transplants after nonmyeloablative conditioning.* Blood, 2003. 102(3): p. 827-833.
64. Montserrat Rovira, J.M., Enric Carreras, *The EBMT Handbook - Haematopoietic Stem Cell Transplantation.* ESH European School of Haematology, 2012. Chapter 12 - Infections after HSCT.
65. Gratwohl, A., et al., *Cause of death after allogeneic haematopoietic stem cell transplantation (HSCT) in early leukaemias: an EBMT analysis of lethal infectious complications and changes over calendar time.* Bone Marrow Transplant, 2005. 36(9): p. 757-69.
66. Anasetti, C., et al., *Effect of HLA incompatibility on graft-versus-host disease, relapse, and survival after marrow transplantation for patients with leukemia or lymphoma.* Hum Immunol, 1990. 29(2): p. 79-91.
67. Martin, P.J., et al., *A retrospective analysis of therapy for acute graft-versus-host disease: initial treatment.* Blood, 1990. 76(8): p. 1464-72.
68. Reikvam, H., et al., *Patients with Treatment-Requiring Chronic Graft versus Host Disease after Allogeneic Stem Cell Transplantation Have Altered Metabolic Profiles due to the Disease and Immunosuppressive Therapy: Potential Implication for Biomarkers.* Frontiers in Immunology, 2018. 8(1979).
69. Nassiri, N., et al., *Ocular graft versus host disease following allogeneic stem cell transplantation: a review of current knowledge and recommendations.* J Ophthalmic Vis Res, 2013. 8(4): p. 351-8.
70. Pasquini, M., et al., *2013 report from the Center for International Blood and Marrow Transplant Research (CIBMTR): current uses and outcomes of hematopoietic cell transplants for blood and bone marrow disorders.* Clin Transpl, 2013: p. 187-97.
71. Hockenbery, D.M., et al., *A randomized, placebo-controlled trial of oral beclomethasone dipropionate as a prednisone-sparing therapy for gastrointestinal graft-versus-host disease.* Blood, 2007. 109(10): p. 4557-63.
72. Martin, P.J., et al., *First- and second-line systemic treatment of acute graft-versus-host disease: recommendations of the American Society of Blood and Marrow Transplantation.* Biology of blood and marrow transplantation : journal of the American Society for Blood and Marrow Transplantation, 2012. 18(8): p. 1150-1163.

73. Jantzen, H.M., et al., *Cooperativity of glucocorticoid response elements located far upstream of the tyrosine aminotransferase gene.* Cell, 1987. 49(1): p. 29-38.
74. Beato, M., *Gene regulation by steroid hormones.* Cell, 1989. 56(3): p. 335-44.
75. Beato, M., M. Truss, and S. Chavez, *Control of transcription by steroid hormones.* Ann N Y Acad Sci, 1996. 784: p. 93-123.
76. Nelson, G., et al., *NF-kappaB signalling is inhibited by glucocorticoid receptor and STAT6 via distinct mechanisms.* J Cell Sci, 2003. 116(Pt 12): p. 2495-503.
77. Hong, H. and B.C. Jang, *Prednisone inhibits the IL-1beta-induced expression of COX-2 in HEI-OC1 murine auditory cells through the inhibition of ERK-1/2, JNK-1 and AP-1 activity.* Int J Mol Med, 2014. 34(6): p. 1640-6.
78. Masera, R.G., et al., *Natural killer cell activity in the peripheral blood of patients with Cushing's syndrome.* Eur J Endocrinol, 1999. 140(4): p. 299-306.
79. Fauci, A.S., *Mechanisms of corticosteroid action on lymphocyte subpopulations. II. Differential effects of in vivo hydrocortisone, prednisone and dexamethasone on in vitro expression of lymphocyte function.* Clin Exp Immunol, 1976. 24(1): p. 54-62.
80. Goulding, N.J., et al., *Novel pathways for glucocorticoid effects on neutrophils in chronic inflammation.* Inflamm Res, 1998. 47 Suppl 3: p. S158-65.
81. Rinehart, J.J., et al., *Effects of corticosteroids on human monocyte function.* The Journal of clinical investigation, 1974. 54(6): p. 1337-1343.
82. Schaffner, A. and T. Schaffner, *Glucocorticoid-induced impairment of macrophage antimicrobial activity: mechanisms and dependence on the state of activation.* Rev Infect Dis, 1987. 9 Suppl 5: p. S620-9.
83. Roilides, E., et al., *Prevention of corticosteroid-induced suppression of human polymorphonuclear leukocyte-induced damage of Aspergillus fumigatus hyphae by granulocyte colony-stimulating factor and gamma interferon.* Infect Immun, 1993. 61(11): p. 4870-7.
84. Badiee, P., *Evaluation of human body fluids for the diagnosis of fungal infections.* BioMed research international, 2013. 2013: p. 698325-698325.
85. Bretagne, S., et al., *Serum Aspergillus galactomannan antigen testing by sandwich ELISA: practical use in neutropenic patients.* J Infect, 1997. 35(1): p. 7-15.
86. White, P.L., et al., *Clinical Performance of Aspergillus PCR for Testing Serum and Plasma: a Study by the European Aspergillus PCR Initiative.* Journal of clinical microbiology, 2015. 53(9): p. 2832-2837.
87. del Rocío Reyes-Montes, M., et al., *Molecular Diagnosis of Invasive Aspergillosis*, in *Molecular Medicine*, D.S.N.a.D.H. Amri, Editor. 2018, IntechOpen.
88. Springer, J., et al., *Comparison of Performance Characteristics of Aspergillus PCR in Testing a Range of Blood-Based Samples in Accordance with International Methodological Recommendations.* Journal of clinical microbiology, 2016. 54(3): p. 705-711.
89. Ullmann, A.J., et al., *Diagnosis and management of Aspergillus diseases: executive summary of the 2017 ESCMID-ECMM-ERS guideline.* Clin Microbiol Infect, 2018. 24 Suppl 1: p. e1-e38.

90. Karageorgopoulos, D.E., et al., *beta-D-glucan assay for the diagnosis of invasive fungal infections: a meta-analysis.* Clin Infect Dis, 2011. 52(6): p. 750-70.
91. Marr, K.A., et al., *Antifungal therapy decreases sensitivity of the Aspergillus galactomannan enzyme immunoassay.* Clin Infect Dis, 2005. 40(12): p. 1762-9.
92. Thornton, C.R., *Development of an immunochromatographic lateral-flow device for rapid serodiagnosis of invasive aspergillosis.* Clinical and vaccine immunology : CVI, 2008. 15(7): p. 1095-1105.
93. Koczula, K.M. and A. Gallotta, *Lateral flow assays.* Essays in biochemistry, 2016. 60(1): p. 111-120.
94. Wagner, K., et al., *Molecular detection of fungal pathogens in clinical specimens by 18S rDNA high-throughput screening in comparison to ITS PCR and culture.* Sci Rep, 2018. 8(1): p. 6964.
95. Donnelly, J.P., et al., *Revision and Update of the Consensus Definitions of Invasive Fungal Disease From the European Organization for Research and Treatment of Cancer and the Mycoses Study Group Education and Research Consortium.* Clinical Infectious Diseases, 2019.
96. De Pauw, B., et al., *Revised definitions of invasive fungal disease from the European Organization for Research and Treatment of Cancer/Invasive Fungal Infections Cooperative Group and the National Institute of Allergy and Infectious Diseases Mycoses Study Group (EORTC/MSG) Consensus Group.* Clinical infectious diseases : an official publication of the Infectious Diseases Society of America, 2008. 46(12): p. 1813-1821.
97. Mohr, J., et al., *Current options in antifungal pharmacotherapy.* Pharmacotherapy, 2008. 28(5): p. 614-45.
98. Groll, A.H., et al., *Clinical pharmacology of antifungal compounds.* Infect Dis Clin North Am, 2003. 17(1): p. 159-91, ix.
99. Kelly, S.L., A. Arnoldi, and D.E. Kelly, *Molecular genetic analysis of azole antifungal mode of action.* Biochem Soc Trans, 1993. 21(4): p. 1034-8.
100. Lass-Flörl, C., *Triazole Antifungal Agents in Invasive Fungal Infections.* Drugs, 2011. 71(18): p. 2405-2419.
101. Sagatova, A.A., et al., *Triazole resistance mediated by mutations of a conserved active site tyrosine in fungal lanosterol 14alpha-demethylase.* Sci Rep, 2016. 6: p. 26213.
102. Bustamante, B., et al., *Azole resistance among clinical isolates of Aspergillus fumigatus in Lima-Peru.* Medical Mycology, 2019.
103. Verweij, P.E., et al., *[Azole resistance in Aspergillus fumigatus in the Netherlands--increase due to environmental fungicides?].* Ned Tijdschr Geneeskd, 2012. 156(25): p. A4458.
104. Sun, W.K., et al., *Dectin-1 is inducible and plays a crucial role in Aspergillus-induced innate immune responses in human bronchial epithelial cells.* European Journal of Clinical Microbiology & Infectious Diseases, 2012. 31(10): p. 2755-2764.
105. Biology, L.I.f.N.P.R.a.I. *Virulence of Aspergillus fumigatus and Host-Pathogen Interactions* 2019 [cited 2019 17.10.19]; Interaction of A. fumigatus with the human innate immune system]. Available from: https://www.leibniz-hki.de/en/virulence-of-aspergillus-fumigatus.html.
106. Feinberg, H., et al., *Mechanism of pathogen recognition by human dectin-2.* J Biol Chem, 2017. 292(32): p. 13402-13414.

107. Fuchs, K., et al., *The fungal ligand chitin directly binds and signals inflammation dependent on oligomer size and TLR2.* bioRxiv, 2018: p. 270405.
108. Kasperkovitz, P.V., M.L. Cardenas, and J.M. Vyas, *TLR9 is actively recruited to Aspergillus fumigatus phagosomes and requires the N-terminal proteolytic cleavage domain for proper intracellular trafficking.* J Immunol, 2010. 185(12): p. 7614-22.
109. Brown, G.D., et al., *Dectin-1 Is A Major -Glucan Receptor On Macrophages.* Journal of Experimental Medicine, 2002. 196(3): p. 407-412.
110. Taylor, P.R., et al., *The beta-glucan receptor, dectin-1, is predominantly expressed on the surface of cells of the monocyte/macrophage and neutrophil lineages.* J Immunol, 2002. 169(7): p. 3876-82.
111. Herre, J., et al., *The role of Dectin-1 in antifungal immunity.* Crit Rev Immunol, 2004. 24(3): p. 193-203.
112. Han, X., et al., *beta-1,3-Glucan-induced host phospholipase D activation is involved in Aspergillus fumigatus internalization into type II human pneumocyte A549 cells.* PLoS One, 2011. 6(7): p. e21468.
113. Thieblemont, N., et al., *CR1 (CD35) and CR3 (CD11b/CD18) mediate infection of human monocytes and monocytic cell lines with complement-opsonized HIV independently of CD4.* Clin Exp Immunol, 1993. 92(1): p. 106-13.
114. Thornton, B.P., et al., *Analysis of the sugar specificity and molecular location of the beta-glucan-binding lectin site of complement receptor type 3 (CD11b/CD18).* J Immunol, 1996. 156(3): p. 1235-46.
115. Philippe, B., et al., *Killing of Aspergillus fumigatus by Alveolar Macrophages Is Mediated by Reactive Oxidant Intermediates.* Infection and Immunity, 2003. 71(6): p. 3034-3042.
116. Henriet, S., et al., *Invasive fungal infections in patients with chronic granulomatous disease.* Adv Exp Med Biol, 2013. 764: p. 27-55.
117. McCormick, A., et al., *NETs formed by human neutrophils inhibit growth of the pathogenic mold Aspergillus fumigatus.* Microbes Infect, 2010. 12(12-13): p. 928-36.
118. Brinkmann, V., et al., *Neutrophil extracellular traps kill bacteria.* Science, 2004. 303(5663): p. 1532-5.
119. Fogg, D.K., et al., *A Clonogenic Bone Marrow Progenitor Specific for Macrophages and Dendritic Cells.* Science, 2006. 311(5757): p. 83-87.
120. Steinman, R.M. and Z.A. Cohn, *Identification of a novel cell type in peripheral lymphoid organs of mice. I. Morphology, quantitation, tissue distribution.* J Exp Med, 1973. 137(5): p. 1142-62.
121. Guilliams, M., et al., *Dendritic cells, monocytes and macrophages: a unified nomenclature based on ontogeny.* Nature reviews. Immunology, 2014. 14(8): p. 571-578.
122. Perussia, B., V. Fanning, and G. Trinchieri, *A leukocyte subset bearing HLA-DR antigens is responsible for in vitro alpha interferon production in response to viruses.* Nat Immun Cell Growth Regul, 1985. 4(3): p. 120-37.
123. Loures, F.V., et al. *Recognition of Aspergillus fumigatus hyphae by human plasmacytoid dendritic cells is mediated by dectin-2 and results in formation of extracellular traps*. PLoS Pathog, 2015. 11, e1004643 DOI: 10.1371/journal.ppat.1004643.

124. Lother, J., et al., *Human dendritic cell subsets display distinct interactions with the pathogenic mould Aspergillus fumigatus.* Int J Med Microbiol, 2014. 304(8): p. 1160-8.
125. Ueda, Y., et al., *Frequencies of dendritic cells (myeloid DC and plasmacytoid DC) and their ratio reduced in pregnant women: comparison with umbilical cord blood and normal healthy adults.* Hum Immunol, 2003. 64(12): p. 1144-51.
126. Colic, M., et al., *Differentiation of human dendritic cells from monocytes in vitro using granulocyte-macrophage colony stimulating factor and low concentration of interleukin-4.* Vojnosanit Pregl, 2003. 60(5): p. 531-8.
127. Leon, B., M. Lopez-Bravo, and C. Ardavin, *Monocyte-derived dendritic cells formed at the infection site control the induction of protective T helper 1 responses against Leishmania.* Immunity, 2007. 26(4): p. 519-31.
128. Sander, J., et al., *Cellular Differentiation of Human Monocytes Is Regulated by Time-Dependent Interleukin-4 Signaling and the Transcriptional Regulator NCOR2.* Immunity, 2017. 47(6): p. 1051-1066.e12.
129. Serrano-Gomez, D., J.A. Leal, and A.L. Corbi, *DC-SIGN mediates the binding of Aspergillus fumigatus and keratinophylic fungi by human dendritic cells.* Immunobiology, 2005. 210(2-4): p. 175-83.
130. Skrzypek, F., et al., *Dectin-1 is required for human dendritic cells to initiate immune response to Candida albicans through Syk activation.* Microbes and infection / Institut Pasteur, 2009. 11: p. 661-70.
131. Chieppa, M., et al., *Cross-linking of the mannose receptor on monocyte-derived dendritic cells activates an anti-inflammatory immunosuppressive program.* J Immunol, 2003. 171(9): p. 4552-60.
132. Mezger, M., et al., *Proinflammatory Response of Immature Human Dendritic Cells is Mediated by Dectin-1 after Exposure to Aspergillus fumigatus Germ Tubes.* The Journal of Infectious Diseases, 2008. 197(6): p. 924-931.
133. Kaisar, M.M.M., et al., *Dectin-1/2-induced autocrine PGE2 signaling licenses dendritic cells to prime Th2 responses.* PLoS biology, 2018. 16(4): p. e2005504-e2005504.
134. Ferwerda, G., et al., *Dectin-1 synergizes with TLR2 and TLR4 for cytokine production in human primary monocytes and macrophages.* Cell Microbiol, 2008. 10(10): p. 2058-66.
135. Gringhuis, S.I., et al., *Dectin-1 directs T helper cell differentiation by controlling noncanonical NF-κB activation through Raf-1 and Syk.* Nature Immunology, 2009. 10(2): p. 203-213.
136. Gross, O., et al., *Card9 controls a non-TLR signalling pathway for innate anti-fungal immunity.* Nature, 2006. 442(7103): p. 651-6.
137. Hara, H., et al., *The adaptor protein CARD9 is essential for the activation of myeloid cells through ITAM-associated and Toll-like receptors.* Nat Immunol, 2007. 8(6): p. 619-29.
138. Marakalala, M.J., A.M. Kerrigan, and G.D. Brown, *Dectin-1: a role in antifungal defense and consequences of genetic polymorphisms in humans.* Mammalian genome : official journal of the International Mammalian Genome Society, 2011. 22(1-2): p. 55-65.
139. Goodridge, H.S., R.M. Simmons, and D.M. Underhill, *Dectin-1 stimulation by Candida albicans yeast or zymosan triggers NFAT activation in macrophages and dendritic cells.* J Immunol, 2007. 178(5): p. 3107-15.

140. Slack, E.C., et al., *Syk-dependent ERK activation regulates IL-2 and IL-10 production by DC stimulated with zymosan.* Eur J Immunol, 2007. 37(6): p. 1600-12.
141. LeibundGut-Landmann, S., et al., *Syk- and CARD9-dependent coupling of innate immunity to the induction of T helper cells that produce interleukin 17.* Nat Immunol, 2007. 8(6): p. 630-8.
142. Ramirez-Ortiz, Z.G. and T.K. Means, *The role of dendritic cells in the innate recognition of pathogenic fungi (A. fumigatus, C. neoformans and C. albicans).* Virulence, 2012. 3(7): p. 635-46.
143. Bozza, S., et al., *A dendritic cell vaccine against invasive aspergillosis in allogeneic hematopoietic transplantation.* Blood, 2003. 102(10): p. 3807-14.
144. Chijioke, O. and C. Munz, *Dendritic cell derived cytokines in human natural killer cell differentiation and activation.* Front Immunol, 2013. 4: p. 365.
145. Kamath, A.T., C.E. Sheasby, and D.F. Tough, *Dendritic cells and NK cells stimulate bystander T cell activation in response to TLR agonists through secretion of IFN-alpha beta and IFN-gamma.* J Immunol, 2005. 174(2): p. 767-76.
146. Park, S.J., M.D. Burdick, and B. Mehrad, *Neutrophils mediate maturation and efflux of lung dendritic cells in response to Aspergillus fumigatus germ tubes.* Infect Immun, 2012. 80(5): p. 1759-65.
147. Park, S.J., et al., *Early NK cell-derived interferon-gamma is essential to host defense in neutropenic invasive aspergillosis.* Journal of immunology (Baltimore, Md. : 1950), 2009. 182(7): p. 4306-4312.
148. Cooper, M., *NK cell and DC interactions.* Trends in Immunology, 2004. 25(1): p. 47-52.
149. Vitale, M., et al., *NK-dependent DC maturation is mediated by TNFalpha and IFNgamma released upon engagement of the NKp30 triggering receptor.* Blood, 2005. 106(2): p. 566-71.
150. Fernandez, N.C., et al., *Dendritic cells directly trigger NK cell functions: cross-talk relevant in innate anti-tumor immune responses in vivo.* Nat Med, 1999. 5(4): p. 405-11.
151. Jinushi, M., et al., *Critical role of MHC class I-related chain A and B expression on IFN-alpha-stimulated dendritic cells in NK cell activation: impairment in chronic hepatitis C virus infection.* J Immunol, 2003. 170(3): p. 1249-56.
152. Pallandre, J.R., et al., *Dendritic cell and natural killer cell cross-talk: a pivotal role of CX3CL1 in NK cytoskeleton organization and activation.* Blood, 2008. 112(12): p. 4420-4.
153. Borg, C., et al., *NK cell activation by dendritic cells (DCs) requires the formation of a synapse leading to IL-12 polarization in DCs.* Blood, 2004. 104(10): p. 3267-75.
154. Pende, D., et al., *Expression of the DNAM-1 ligands, Nectin-2 (CD112) and poliovirus receptor (CD155), on dendritic cells: relevance for natural killer-dendritic cell interaction.* Blood, 2006. 107(5): p. 2030-6.
155. Joao Calmeiro, M.C., Celia Gomes, Amilcar Falcao, Maria Teresa Cruz and Bruno Miguel Neves, *Highlighting the Role of DC-NK Cell Interplay in Immunbiology ad Immunotherapy*. 2018: IntechOpen.
156. Luetke-Eversloh, M., M. Killig, and C. Romagnani, *Signatures of human NK cell development and terminal differentiation.* Front Immunol, 2013. 4: p. 499.
157. Freud, A.G., et al., *The Broad Spectrum of Human Natural Killer Cell Diversity.* Immunity, 2017. 47(5): p. 820-833.

158. Lee, B.J. and E.M. Mace, *Acquisition of cell migration defines NK cell differentiation from hematopoietic stem cell precursors.* Molecular biology of the cell, 2017. 28(25): p. 3573-3581.
159. Lanier, L.L., et al., *Subpopulations of human natural killer cells defined by expression of the Leu-7 (HNK-1) and Leu-11 (NK-15) antigens.* J Immunol, 1983. 131(4): p. 1789-96.
160. Lanier, L.L., et al., *The relationship of CD16 (Leu-11) and Leu-19 (NKH-1) antigen expression on human peripheral blood NK cells and cytotoxic T lymphocytes.* J Immunol, 1986. 136(12): p. 4480-6.
161. Caligiuri, M.A., *Human natural killer cells.* Blood Journal, 2008.
162. Cooper, M.A., et al., *Human natural killer cells: a unique innate immunoregulatory role for the CD56(bright) subset.* Blood, 2001. 97(10): p. 3146-51.
163. Walzer, T., et al., *Natural killer cells: from CD3(-)NKp46(+) to post-genomics meta-analyses.* Curr Opin Immunol, 2007. 19(3): p. 365-72.
164. Romagnani, C., et al., *CD56brightCD16- killer Ig-like receptor- NK cells display longer telomeres and acquire features of CD56dim NK cells upon activation.* J Immunol, 2007. 178(8): p. 4947-55.
165. Chan, A., et al., *CD56bright human NK cells differentiate into CD56dim cells: role of contact with peripheral fibroblasts.* J Immunol, 2007. 179(1): p. 89-94.
166. Dulphy, N., et al., *An Unusual CD56brightCD16low NK Cell Subset Dominates the Early Posttransplant Period following HLA-Matched Hematopoietic Stem Cell Transplantation.* The Journal of Immunology, 2008. 181(3): p. 2227-2237.
167. Brandt, C.S., et al., *The B7 family member B7-H6 is a tumor cell ligand for the activating natural killer cell receptor NKp30 in humans.* J Exp Med, 2009. 206(7): p. 1495-503.
168. Baychelier, F., et al., *Identification of a cellular ligand for the natural cytotoxicity receptor NKp44.* Blood, 2013. 122(17): p. 2935-42.
169. Rosental, B., et al., *Proliferating cell nuclear antigen is a novel inhibitory ligand for the natural cytotoxicity receptor NKp44.* J Immunol, 2011. 187(11): p. 5693-702.
170. Martinet, L. and M.J. Smyth, *Balancing natural killer cell activation through paired receptors.* Nat Rev Immunol, 2015. 15(4): p. 243-54.
171. Karre, K., et al., *Selective rejection of H-2-deficient lymphoma variants suggests alternative immune defence strategy.* Nature, 1986. 319(6055): p. 675-8.
172. Long, E.O., et al., *Controlling natural killer cell responses: integration of signals for activation and inhibition.* Annu Rev Immunol, 2013. 31: p. 227-58.
173. Moretta, A., et al., *Receptors for HLA class-I molecules in human natural killer cells.* Annu Rev Immunol, 1996. 14: p. 619-48.
174. Moretta, L., et al., *Surface NK receptors and their ligands on tumor cells.* Semin Immunol, 2006. 18(3): p. 151-8.
175. Bennett, E.M., et al., *Cutting edge: adenovirus E19 has two mechanisms for affecting class I MHC expression.* J Immunol, 1999. 162(9): p. 5049-52.
176. Cooper, M.A., T.A. Fehniger, and M.A. Caligiuri, *The biology of human natural killer-cell subsets.* Trends in Immunology, 2001. 22(11): p. 633-640.
177. Mace, E.M., et al., *Cell biological steps and checkpoints in accessing NK cell cytotoxicity.* Immunol Cell Biol, 2014. 92(3): p. 245-55.
178. Law, R.H., et al., *The structural basis for membrane binding and pore formation by lymphocyte perforin.* Nature, 2010. 468(7322): p. 447-51.

179. Cohnen, A., et al., *Surface CD107a/LAMP-1 protects natural killer cells from degranulation-associated damage.* Blood, 2013. 122(8): p. 1411-8.
180. Lopez, J.A., et al., *Perforin forms transient pores on the target cell plasma membrane to facilitate rapid access of granzymes during killer cell attack.* Blood, 2013. 121(14): p. 2659-68.
181. Andrade, F., et al., *Granzyme B directly and efficiently cleaves several downstream caspase substrates: implications for CTL-induced apoptosis.* Immunity, 1998. 8(4): p. 451-60.
182. Sutton, V.R., et al., *Initiation of apoptosis by granzyme B requires direct cleavage of bid, but not direct granzyme B-mediated caspase activation.* The Journal of experimental medicine, 2000. 192(10): p. 1403-1414.
183. Metkar, S.S., et al., *Granzyme B activates procaspase-3 which signals a mitochondrial amplification loop for maximal apoptosis.* The Journal of cell biology, 2003. 160(6): p. 875-885.
184. Prager, I., et al., *NK cells switch from granzyme B to death receptor–mediated cytotoxicity during serial killing.* 2019. 216(9): p. 2113-2127.
185. Zamai, L., et al., *Natural killer (NK) cell-mediated cytotoxicity: differential use of TRAIL and Fas ligand by immature and mature primary human NK cells.* J Exp Med, 1998. 188(12): p. 2375-80.
186. Strasser, A., P.J. Jost, and S. Nagata, *The many roles of FAS receptor signaling in the immune system.* Immunity, 2009. 30(2): p. 180-92.
187. Zhu, Y., B. Huang, and J. Shi, *Fas ligand and lytic granule differentially control cytotoxic dynamics of natural killer cell against cancer target.* Oncotarget, 2016. 7(30): p. 47163-47172.
188. Wang, J., et al., *Caspase-10 is an initiator caspase in death receptor signaling.* Proceedings of the National Academy of Sciences of the United States of America, 2001. 98(24): p. 13884-13888.
189. McIlwain, D.R., T. Berger, and T.W. Mak, *Caspase functions in cell death and disease.* Cold Spring Harb Perspect Biol, 2013. 5(4): p. a008656.
190. Sprick, M.R., et al., *Caspase-10 is recruited to and activated at the native TRAIL and CD95 death-inducing signalling complexes in a FADD-dependent manner but can not functionally substitute caspase-8.* The EMBO journal, 2002. 21(17): p. 4520-4530.
191. Li, Shu S., et al., *The NK Receptor NKp30 Mediates Direct Fungal Recognition and Killing and Is Diminished in NK Cells from HIV-Infected Patients.* Cell Host & Microbe, 2013. 14(4): p. 387-397.
192. Vitenshtein, A., et al., *NK Cell Recognition of Candida glabrata through Binding of NKp46 and NCR1 to Fungal Ligands Epa1, Epa6, and Epa7.* Cell Host Microbe, 2016. 20(4): p. 527-534.
193. Lieke, T., et al., *Leishmania surface protein gp63 binds directly to human natural killer cells and inhibits proliferation.* Clin Exp Immunol, 2008. 153(2): p. 221-30.
194. Iversen, A.-C., et al., *Human NK Cells Inhibit Cytomegalovirus Replication through a Noncytolytic Mechanism Involving Lymphotoxin-Dependent Induction of IFN-β.* The Journal of Immunology, 2005. 175(11): p. 7568-7574.
195. Le-Barillec, K., et al., *Roles for T and NK Cells in the Innate Immune Response to Shigella flexneri.* The Journal of Immunology, 2005. 175(3): p. 1735-1740.
196. Li, S.S., et al., *Identification of the fungal ligand triggering cytotoxic PRR-mediated NK cell killing of Cryptococcus and Candida.* Nature Communications, 2018. 9(1): p. 751.

197. Morrison, B.E., et al., *Chemokine-mediated recruitment of NK cells is a critical host defense mechanism in invasive aspergillosis.* Journal of Clinical Investigation, 2003. 112(12): p. 1862-1870.
198. Park, S.J., et al., *Early NK cell-derived IFN-{gamma} is essential to host defense in neutropenic invasive aspergillosis.* J Immunol, 2009. 182(7): p. 4306-12.
199. Stuehler, C., et al., *Immune Reconstitution After Allogeneic Hematopoietic Stem Cell Transplantation and Association With Occurrence and Outcome of Invasive Aspergillosis.* J Infect Dis, 2015. 212(6): p. 959-67.
200. Ditlevsen, D.K., et al., *NCAM-induced intracellular signaling revisited.* J Neurosci Res, 2008. 86(4): p. 727-43.
201. Cunningham, B.A., et al., *Neural cell adhesion molecule: structure, immunoglobulin-like domains, cell surface modulation, and alternative RNA splicing.* Science, 1987. 236(4803): p. 799-806.
202. Murray, B.A., et al., *Isolation of cDNA clones for the chicken neural cell adhesion molecule (N-CAM).* Proceedings of the National Academy of Sciences of the United States of America, 1984. 81(17): p. 5584-5588.
203. Owens, G.C., G.M. Edelman, and B.A. Cunningham, *Organization of the neural cell adhesion molecule (N-CAM) gene: alternative exon usage as the basis for different membrane-associated domains.* Proceedings of the National Academy of Sciences of the United States of America, 1987. 84(1): p. 294-298.
204. Nguyen, C., et al., *Localization of the human NCAM gene to band q23 of chromosome 11: the third gene coding for a cell interaction molecule mapped to the distal portion of the long arm of chromosome 11.* The Journal of Cell Biology, 1986. 102(3): p. 711-715.
205. Murray, B.A., et al., *Cell surface modulation of the neural cell adhesion molecule resulting from alternative mRNA splicing in a tissue-specific developmental sequence.* J Cell Biol, 1986. 103(4): p. 1431-9.
206. Hemperly, J.J., et al., *Sequence of a cDNA clone encoding the polysialic acid-rich and cytoplasmic domains of the neural cell adhesion molecule N-CAM.* Proc Natl Acad Sci U S A, 1986. 83(9): p. 3037-41.
207. Walmod, P.S., et al., *Zippers make signals: NCAM-mediated molecular interactions and signal transduction.* Neurochem Res, 2004. 29(11): p. 2015-35.
208. Chothia, C. and E.Y. Jones, *The molecular structure of cell adhesion molecules.* Annu Rev Biochem, 1997. 66: p. 823-62.
209. Soroka, V., et al., *Structure and interactions of NCAM Ig1-2-3 suggest a novel zipper mechanism for homophilic adhesion.* Structure, 2003. 11(10): p. 1291-301.
210. Probstmeier, R., et al., *Interactions of the neural cell adhesion molecule and the myelin-associated glycoprotein with collagen type I: involvement in fibrillogenesis.* J Cell Biol, 1992. 116(4): p. 1063-70.
211. Herndon, M.E., C.S. Stipp, and A.D. Lander, *Interactions of neural glycosaminoglycans and proteoglycans with protein ligands: assessment of selectivity, heterogeneity and the participation of core proteins in binding.* Glycobiology, 1999. 9(2): p. 143-55.
212. Kelly-Rogers, J., et al., *Activation-induced expression of CD56 by T cells is associated with a reprogramming of cytolytic activity and cytokine secretion profile in vitro.* Hum Immunol, 2006. 67(11): p. 863-73.

213. Roothans, D., et al., *CD56 marks human dendritic cell subsets with cytotoxic potential.* Oncoimmunology, 2013. 2(2): p. e23037.
214. Van Acker, H.H., et al., *CD56 Homodimerization and Participation in Anti-Tumor Immune Effector Cell Functioning: A Role for Interleukin-15.* Cancers (Basel), 2019. 11(7).
215. Mace, E.M., et al., *Human NK cell development requires CD56-mediated motility and formation of the developmental synapse.* Nature Communications, 2016. 7: p. 12171.
216. Taouk, G., et al., *CD56 expression in breast cancer induces sensitivity to natural killer-mediated cytotoxicity by enhancing the formation of cytotoxic immunological synapse.* Sci Rep, 2019. 9(1): p. 8756.
217. Valgardsdottir, R., et al., *Direct involvement of CD56 in cytokine-induced killer-mediated lysis of CD56+ hematopoietic target cells.* Exp Hematol, 2014. 42(12): p. 1013-21.e1.
218. Reiners, K.S., et al., *Soluble ligands for NK cell receptors promote evasion of chronic lymphocytic leukemia cells from NK cell anti-tumor activity.* Blood, 2013. 121(18): p. 3658-3665.
219. Nelson, R.W., P.A. Bates, and U. Rutishauser, *Protein determinants for specific polysialylation of the neural cell adhesion molecule.* J Biol Chem, 1995. 270(29): p. 17171-9.
220. Drake, P.M., et al., *Polysialic acid, a glycan with highly restricted expression, is found on human and murine leukocytes and modulates immune responses.* Journal of immunology (Baltimore, Md. : 1950), 2008. 181(10): p. 6850-6858.
221. Angata, K., M. Suzuki, and M. Fukuda, *Differential and cooperative polysialylation of the neural cell adhesion molecule by two polysialyltransferases, PST and STX.* J Biol Chem, 1998. 273(43): p. 28524-32.
222. Moebius, J.M., et al., *Impact of polysialylated CD56 on natural killer cell cytotoxicity.* BMC Immunology, 2007. 8(1): p. 13.
223. Mouyna, I., et al., *A 1,3-beta-glucanosyltransferase isolated from the cell wall of Aspergillus fumigatus is a homologue of the yeast Bgl2p.* Microbiology, 1998. 144 (Pt 11): p. 3171-80.
224. Beauvais, A., et al., *Two alpha(1-3) glucan synthases with different functions in Aspergillus fumigatus.* Appl Environ Microbiol, 2005. 71(3): p. 1531-8.
225. Wolter, S., et al., *rapidSTORM: accurate, fast open-source software for localization microscopy.* Nature Methods, 2012. 9: p. 1040.
226. Leonhardt, I., et al., *The fungal quorum-sensing molecule farnesol activates innate immune cells but suppresses cellular adaptive immunity.* mBio, 2015. 6(2): p. e00143-e00143.
227. da Silva Ferreira, M.E., et al., *The akuB(KU80) mutant deficient for nonhomologous end joining is a powerful tool for analyzing pathogenicity in Aspergillus fumigatus.* Eukaryot Cell, 2006. 5(1): p. 207-11.
228. Henry, C., J.P. Latge, and A. Beauvais, *alpha1,3 glucans are dispensable in Aspergillus fumigatus.* Eukaryot Cell, 2012. 11(1): p. 26-9.
229. Vanderheiden, G.J., A.C. Fairchild, and G.R. Jago, *Construction of a laboratory press for use with the French pressure cell.* Applied microbiology, 1970. 19(5): p. 875-877.
230. Berridge, M.V., P.M. Herst, and A.S. Tan, *Tetrazolium dyes as tools in cell biology: new insights into their cellular reduction.* Biotechnol Annu Rev, 2005. 11: p. 127-52.

231. Paull, K.D., et al., *The synthesis of XTT: A new tetrazolium reagent that is bioreducible to a water-soluble formazan.* Journal of Heterocyclic Chemistry, 1988. 25(3): p. 911-914.
232. Meshulam, T., et al., *A Simplified New Assay for Assessment of Fungal Cell Damage with the Tetrazolium Dye, (2,3)-bis-(2-Methoxy-4-Nitro-5-Sulphenyl)-(2H)-Tetrazolium-5-Carboxanilide (XTT).* The Journal of Infectious Diseases, 1995. 172(4): p. 1153-1156.
233. Krebs, D.L., et al., *Lyn-Dependent Signaling Regulates the Innate Immune Response by Controlling Dendritic Cell Activation of NK Cells.* The Journal of Immunology, 2012. 188(10): p. 5094-5105.
234. Weiss, E., et al., *First Insights in NK—DC Cross-Talk and the Importance of Soluble Factors During Infection With Aspergillus fumigatus.* Front Cell Infect Microbiol, 2018. 8.
235. Ziegler, S., et al. *CD56 Is a Pathogen Recognition Receptor on Human Natural Killer Cells*. Scientific Reports, 2017. 7, DOI: 10.1038/s41598-017-06238-4.
236. Pende, D., et al., *Identification and molecular characterization of NKp30, a novel triggering receptor involved in natural cytotoxicity mediated by human natural killer cells.* The Journal of experimental medicine, 1999. 190(10): p. 1505-1516.
237. van de Linde, S., et al., *Direct stochastic optical reconstruction microscopy with standard fluorescent probes.* Nature Protocols, 2011. 6: p. 991.
238. Burgert, A., et al., *Artifacts in single-molecule localization microscopy.* Histochem Cell Biol, 2015. 144(2): p. 123-31.
239. Letschert, S., et al., *Super-resolution imaging of plasma membrane glycans.* Angew Chem Int Ed Engl, 2014. 53(41): p. 10921-4.
240. Proppert, S., et al., *Cubic B-spline calibration for 3D super-resolution measurements using astigmatic imaging.* Opt Express, 2014. 22(9): p. 10304-16.
241. Schindelin, J., et al., *Fiji: an open-source platform for biological-image analysis.* Nat Methods, 2012. 9(7): p. 676-82.
242. Brahm H. Segal, M.D., *Aspergillosis.* The New England Journal of Medicine, 2009. 360: p. 1870-84.
243. Morton, C.O., et al., *Direct interaction studies between Aspergillus fumigatus and human immune cells; what have we learned about pathogenicity and host immunity?* Front Microbiol, 2012. 3: p. 413.
244. Jolink, H., et al., *Characterization of the T-cell-mediated immune response against the Aspergillus fumigatus proteins Crf1 and catalase 1 in healthy individuals.* J Infect Dis, 2013. 208(5): p. 847-56.
245. Banchereau, S., *Dendritic cellls and the control of immunity.* Nature, 1998. 392: p. 245-252.
246. Randolph, G.J., V. Angeli, and M.A. Swartz, *Dendritic-cell trafficking to lymph nodes through lymphatic vessels.* Nat Rev Immunol, 2005. 5(8): p. 617-28.
247. Ramirez-Ortiz, Z.G., et al., *Toll-like receptor 9-dependent immune activation by unmethylated CpG motifs in Aspergillus fumigatus DNA.* Infect Immun, 2008. 76(5): p. 2123-9.
248. Waldhauer, I. and A. Steinle, *NK cells and cancer immunosurveillance.* Oncogene, 2008. 27(45): p. 5932-43.
249. Mavoungou, E., et al., *A Duffy binding-like domain is involved in the NKp30-mediated recognition of Plasmodium falciparum-parasitized erythrocytes by natural killer cells.* J Infect Dis, 2007. 195(10): p. 1521-31.

250. Schmidt, S., et al., *Rhizopus oryzae hyphae are damaged by human natural killer (NK) cells, but suppress NK cell mediated immunity.* Immunobiology, 2013. 218(7): p. 939-44.
251. Schmidt, S., L. Tramsen, and T. Lehrnbecher *Natural Killer Cells in Antifungal Immunity*. Frontiers in Immunology, 2017. 8, 1623 DOI: 10.3389/fimmu.2017.01623.
252. Quintin, J., et al., *Differential role of NK cells against Candida albicans infection in immunocompetent or immunocompromised mice.* Eur J Immunol, 2014. 44(8): p. 2405-14.
253. Schmidt, S., et al. *Human natural killer cells exhibit direct activity against Aspergillus fumigatus hyphae, but not against resting conidia*. J Infect Dis, 2011. 203, 430-5 DOI: 10.1093/infdis/jiq062.
254. Zhang, C., et al., *Interleukin-12 improves cytotoxicity of natural killer cells via upregulated expression of NKG2D.* Hum Immunol, 2008. 69(8): p. 490-500.
255. Chai, L.Y., et al., *Modulation of Toll-like receptor 2 (TLR2) and TLR4 responses by Aspergillus fumigatus.* Infect Immun, 2009. 77(5): p. 2184-92.
256. Shibata, K., et al., *The N-terminal lipopeptide of a 44-kDa membrane-bound lipoprotein of Mycoplasma salivarium is responsible for the expression of intercellular adhesion molecule-1 on the cell surface of normal human gingival fibroblasts.* J Immunol, 2000. 165(11): p. 6538-44.
257. Okusawa, T., et al., *Relationship between structures and biological activities of mycoplasmal diacylated lipopeptides and their recognition by toll-like receptors 2 and 6.* Infect Immun, 2004. 72(3): p. 1657-65.
258. Grazziutti, M., et al., *Dendritic cell-mediated stimulation of the in vitro lymphocyte response to Aspergillus.* Bone Marrow Transplant, 2001. 27(6): p. 647-52.
259. Lande, R., et al., *IFN-alpha beta released by Mycobacterium tuberculosis-infected human dendritic cells induces the expression of CXCL10: selective recruitment of NK and activated T cells.* J Immunol, 2003. 170(3): p. 1174-82.
260. Netea, M.G., et al., *Aspergillus fumigatus evades immune recognition during germination through loss of toll-like receptor-4-mediated signal transduction.* J Infect Dis, 2003. 188(2): p. 320-6.
261. Steele, C., et al., *The beta-glucan receptor dectin-1 recognizes specific morphologies of Aspergillus fumigatus.* PLoS Pathog, 2005. 1(4): p. e42.
262. Reedy, J.L., Wuethrich, M. A., Latge, J. P. & Vyas, J. M. , *Dectin-2 is a receptor for galactomannan. .*
The Aspergillus Website http:/www.aspergillus.org.uk/content/dectin-2-receptor-galactomannan, 2016.
263. Chai, L.Y.A., et al., *The Y238X Stop Codon Polymorphism in the Human β-Glucan Receptor Dectin-1 and Susceptibility to Invasive Aspergillosis.* The Journal of Infectious Diseases, 2011. 203(5): p. 736-743.
264. Yadav, M. and J.S. Schorey, *The β-glucan receptor dectin-1 functions together with TLR2 to mediate macrophage activation by mycobacteria.* Blood, 2006. 108(9): p. 3168-3175.
265. Kock, G., et al., *Regulation of dectin-1-mediated dendritic cell activation by peroxisome proliferator-activated receptor-gamma ligand troglitazone.* Blood, 2011. 117(13): p. 3569-74.
266. Turner, M.D., et al., *Cytokines and chemokines: At the crossroads of cell signalling and inflammatory disease.* Biochimica et Biophysica Acta (BBA) - Molecular Cell Research, 2014. 1843(11): p. 2563-2582.

267. Roberts, L.M., et al. *TLR2 Signaling is Required for the Innate, but Not Adaptive Response to LVS clpB*. Front Immunol, 2014. 5, 426 DOI: 10.3389/fimmu.2014.00426.
268. Christof Lehmann, M.Z.a.L.U., *Activation of natural killer cells with interleukin 2 (IL-2) and IL-12 increases perforin binding and subsequent lysis of tumour cells.* British Journal of Haematology, 2001. 114: p. 660-665.
269. Liu, F., et al., *IP-10 and fractalkine induce cytotoxic phenotype of murine NK cells.* Science bulletin, 2016. 2016 v.61: p. pp. 202-211.
270. Segal, B.H., *Aspergillosis.* N Engl J Med, 2009. 360(18): p. 1870-84.
271. Singh, N. and D.L. Paterson, *Aspergillus Infections in Transplant Recipients.* Clin Microbiol Rev, 2005. 18(1): p. 44-69.
272. Salmeron, G., et al., *Persistent poor long-term prognosis of allogeneic hematopoietic stem cell transplant recipients surviving invasive aspergillosis.* Haematologica, 2012. 97(9): p. 1357-63.
273. Robertson, M.J. and J. Ritz, *Biology and clinical relevance of human natural killer cells.* Blood, 1990. 76(12): p. 2421-38.
274. Lanier, L.L., *Up on the tightrope: natural killer cell activation and inhibition.* Nat Immunol, 2008. 9(5): p. 495-502.
275. Lieke, T., et al., *NK cells contribute to the control of Trypanosoma cruzi infection by killing free parasites by perforin-independent mechanisms.* Infect Immun, 2004. 72(12): p. 6817-25.
276. Small, C.L., et al., *NK cells play a critical protective role in host defense against acute extracellular Staphylococcus aureus bacterial infection in the lung.* J Immunol, 2008. 180(8): p. 5558-68.
277. Bouzani, M., et al., *Human NK cells display important antifungal activity against Aspergillus fumigatus, which is directly mediated by IFN-gamma release.* J Immunol, 2011. 187(3): p. 1369-76.
278. Schmidt, S., et al., *Natural killer cell-mediated damage of clinical isolates of mucormycetes.* Mycoses, 2016. 59(1): p. 34-8.
279. Jessica Voigt, K.H., Maria Bouzani, Ilse D. Jacobsen, Dagmar Barz, Bernhard Hube, Jürgen Löffler and Oliver Kurzai, *Human Natural Killer Cells Acting as Phagocytes Against Candida albicans and Mounting an Inflammatory Response That Modulates Neutrophil Antifungal Activity.* The Journal of Infectious Disease 2014. 616-26.
280. Braedel, S., et al., *Aspergillus fumigatus antigens activate innate immune cells via toll-like receptors 2 and 4.* Br J Haematol, 2004. 125(3): p. 392-9.
281. Meier, A., et al., *Toll-like receptor (TLR) 2 and TLR4 are essential for Aspergillus-induced activation of murine macrophages.* Cell Microbiol, 2003. 5(8): p. 561-70.
282. Lanier, L.L., et al., *Identity of Leu-19 (CD56) leukocyte differentiation antigen and neural cell adhesion molecule.* J Exp Med, 1989. 169(6): p. 2233-8.
283. Ritz, J., et al., *Characterization of functional surface structures on human natural killer cells.* Adv Immunol, 1988. 42: p. 181-211.
284. Francisco Borrego, J.P.a.R.S., *Regulation of CD69 expression on human natural killer cells: differential involvement of protein kinase C and protein tyrosine kinases.* Eur. J. Immunol., 1993.
285. Abad, A., et al., *What makes Aspergillus fumigatus a successful pathogen? Genes and molecules involved in invasive aspergillosis.* Rev Iberoam Micol, 2010. 27(4): p. 155-82.
286. Lozzio, B.B.L.a.C.B., *Properties and usefulness of the original K-562 human myelogenous leukemia cell line.* Leukemia Research, 1979. 3: p. 363-370.

287. Orange, J.S., *Formation and function of the lytic NK-cell immunological synapse.* Nat Rev Immunol. , 2008.
288. Mortensen, K. and L.I. Larsson, *Effects of cytochalasin D on the actin cytoskeleton: association of neoformed actin aggregates with proteins involved in signaling and endocytosis.* Cell Mol Life Sci, 2003. 60(5): p. 1007-12.
289. Margolis, R.L. and L. Wilson, *Addition of colchicine--tubulin complex to microtubule ends: the mechanism of substoichiometric colchicine poisoning.* Proc Natl Acad Sci U S A, 1977. 74(8): p. 3466-70.
290. Orange, J.S., et al., *The mature activating natural killer cell immunologic synapse is formed in distinct stages.* Proc Natl Acad Sci U S A, 2003. 100(24): p. 14151-6.
291. Jimenez, B.E. and J.W. Murphy, *In vitro effects of natural killer cells against Paracoccidioides brasiliensis yeast phase.* Infect Immun, 1984. 46(2): p. 552-8.
292. Petkus, A.F. and L.L. Baum, *Natural killer cell inhibition of young spherules and endospores of Coccidioides immitis.* J Immunol, 1987. 139(9): p. 3107-11.
293. Schmidt, S., et al., *Human natural killer cells exhibit direct activity against Aspergillus fumigatus hyphae, but not against resting conidia.* The Journal of infectious diseases, 2011. 203(3): p. 430-435.
294. Levitz, S.M., M.P. Dupont, and E.H. Smail, *Direct activity of human T lymphocytes and natural killer cells against Cryptococcus neoformans.* Infect Immun, 1994. 62(1): p. 194-202.
295. Diestel, S., et al., *NCAM is ubiquitylated, endocytosed and recycled in neurons.* J Cell Sci, 2007. 120(Pt 22): p. 4035-49.
296. Nybroe, O. and E. Bock, *Structure and function of the neural cell adhesion molecules NCAM and L1.* Adv Exp Med Biol, 1990. 265: p. 185-96.
297. Leshchyns'ka, I. and V. Sytnyk, *Intracellular transport and cell surface delivery of the neural cell adhesion molecule (NCAM).* Bioarchitecture, 2015. 5(3-4): p. 54-60.
298. Marta Nieto, F.N., Juan José Perez-Villar, Miguel Angel del Pozo, Roberto González-Amaro, Mario Mellado, José M. R. Frade, Carlos Marínez-A, Miguel López-Botet and Francisco Sánchez-Madrid, *Roles of Chemokines and Receptor Polarization in NK-Target Cell Interactions.* The Journal of Immunology, 1998. 161: p. 3330-3339.
299. Todd A. Fehniger, G.H., Haixin Yu, Michael I. Para, Zale P. Bernstein, William A. O'Brien and Michael A. Caligiuri, *Natural Killer Cells from HIV-1+ Patients Produce C-C Chemokines and Inhibit HIV-1 Infection.* The Journal of Immunology, 1998. 161: p. 6433-6438.
300. McNeil, G.B.H.a.L.K., *Dissemination of C. neoformans to the central nervous system: role of chemokines, Th1 immunity and leukocyte recruitment* Journal of NeuroVirology, 1999. 5.
301. Bonfa, G., et al., *CCR5 controls immune and metabolic functions during Toxoplasma gondii infection.* PLoS One, 2014. 9(8): p. e104736.
302. Lanier, L.L., et al., *Molecular and functional analysis of human natural killer cell-associated neural cell adhesion molecule (N-CAM/CD56).* J Immunol, 1991. 146(12): p. 4421-6.
303. Pandolfi, F., et al., *Expression of cell adhesion molecules in human melanoma cell lines and their role in cytotoxicity mediated by tumor-infiltrating lymphocytes.* Cancer, 1992. 69(5): p. 1165-73.

304. Nitta, T., et al., *Involvement of CD56 (NKH-1/Leu-19 antigen) as an adhesion molecule in natural killer-target cell interaction.* J Exp Med, 1989. 170(5): p. 1757-61.
305. Takasaki, S., et al., *CD56 directly interacts in the process of NCAM-positive target cell-killing by NK cells.* Cell Biol Int, 2000. 24(2): p. 101-8.
306. Bjorkstrom, N.K., H.G. Ljunggren, and J. Michaelsson, *Emerging insights into natural killer cells in human peripheral tissues.* Nat Rev Immunol, 2016. 16(5): p. 310-20.
307. Marquardt, N., et al., *Human lung natural killer cells are predominantly comprised of highly differentiated hypofunctional CD69-CD56dim cells.* J Allergy Clin Immunol, 2017. 139(4): p. 1321-1330 e4.
308. Campbell, K.S. and J. Hasegawa, *Natural killer cell biology: an update and future directions.* J Allergy Clin Immunol, 2013. 132(3): p. 536-44.
309. Moretta, L., *Dissecting CD56dim human NK cells.* Blood, 2010. 116(19): p. 3689-91.
310. Ullah, M.A., G.R. Hill, and S.-K. Tey, *Functional Reconstitution of Natural Killer Cells in Allogeneic Hematopoietic Stem Cell Transplantation.* Frontiers in Immunology, 2016. 7: p. 144.
311. Quellmann, S., et al., *Corticosteroids for preventing graft-versus-host disease after allogeneic myeloablative stem cell transplantation.* Cochrane Database Syst Rev, 2008(3): p. Cd004885.
312. Thum, M.Y., et al., *Prednisolone suppresses NK cell cytotoxicity in vitro in women with a history of infertility and elevated NK cell cytotoxicity.* Am J Reprod Immunol, 2008. 59(3): p. 259-65.
313. Scheinman, R.I., et al., *Characterization of mechanisms involved in transrepression of NF-kappa B by activated glucocorticoid receptors.* Mol Cell Biol, 1995. 15(2): p. 943-53.
314. Elftman, M.D., et al., *Corticosterone impairs dendritic cell maturation and function.* Immunology, 2007. 122(2): p. 279-90.
315. Gustafsson, M.G., *Surpassing the lateral resolution limit by a factor of two using structured illumination microscopy.* J Microsc, 2000. 198(Pt 2): p. 82-7.
316. Fauriat, C., et al., *Regulation of human NK-cell cytokine and chemokine production by target cell recognition.* Blood, 2010. 115(11): p. 2167-76.
317. Das, S.T., et al., *Monomeric and dimeric CXCL8 are both essential for in vivo neutrophil recruitment.* PloS one, 2010. 5(7): p. e11754-e11754.
318. Wolf, J.S., et al., *IL (interleukin)-1alpha promotes nuclear factor-kappaB and AP-1-induced IL-8 expression, cell survival, and proliferation in head and neck squamous cell carcinomas.* Clin Cancer Res, 2001. 7(6): p. 1812-20.
319. Caffrey, A.K., et al., *IL-1alpha signaling is critical for leukocyte recruitment after pulmonary Aspergillus fumigatus challenge.* PLoS Pathog, 2015. 11(1): p. e1004625.
320. Ohira, M., et al., *Impact of Steroids on Natural Killer Cells Against Cytotoxicity and Hepatitis C Virus Replication.* Transplant Proc, 2017. 49(5): p. 1160-1164.
321. Muhlemann, K., et al., *Risk factors for invasive aspergillosis in neutropenic patients with hematologic malignancies.* Leukemia, 2005. 19(4): p. 545-50.
322. Labbe, A.C., et al., *High incidence of invasive aspergillosis associated with intestinal graft-versus-host disease following nonmyeloablative transplantation.* Biol Blood Marrow Transplant, 2007. 13(10): p. 1192-200.

323. Carisey, A.F., et al., *Nanoscale Dynamism of Actin Enables Secretory Function in Cytolytic Cells.* Curr Biol, 2018. 28(4): p. 489-502.e9.
324. Watzl, C. and E.O. Long, *Natural killer cell inhibitory receptors block actin cytoskeleton-dependent recruitment of 2B4 (CD244) to lipid rafts.* The Journal of experimental medicine, 2003. 197(1): p. 77-85.
325. Bacigalupo, A., et al., *Steroid treatment of acute graft-versus-host disease grade I: a randomized trial.* Haematologica, 2017. 102(12): p. 2125-2133.
326. Moriuchi, H., M. Moriuchi, and A.S. Fauci, *Nuclear factor-kappa B potently up-regulates the promoter activity of RANTES, a chemokine that blocks HIV infection.* J Immunol, 1997. 158(7): p. 3483-91.
327. Grove, M. and M. Plumb, *C/EBP, NF-kappa B, and c-Ets family members and transcriptional regulation of the cell-specific and inducible macrophage inflammatory protein 1 alpha immediate-early gene.* Mol Cell Biol, 1993. 13(9): p. 5276-89.
328. Widmer, U., et al., *Genomic cloning and promoter analysis of macrophage inflammatory protein (MIP)-2, MIP-1 alpha, and MIP-1 beta, members of the chemokine superfamily of proinflammatory cytokines.* J Immunol, 1993. 150(11): p. 4996-5012.
329. Schrum, S., et al., *Synthesis of the CC-chemokines MIP-1alpha, MIP-1beta, and RANTES is associated with a type 1 immune response.* J Immunol, 1996. 157(8): p. 3598-604.
330. Huang, C. and S.M. Levitz, *Stimulation of macrophage inflammatory protein-1alpha, macrophage inflammatory protein-1beta, and RANTES by Candida albicans and Cryptococcus neoformans in peripheral blood mononuclear cells from persons with and without human immunodeficiency virus infection.* J Infect Dis, 2000. 181(2): p. 791-4.
331. Caffrey-Carr, A.K., et al., *Interleukin 1α Is Critical for Resistance against Highly Virulent Aspergillus fumigatus Isolates.* Infection and immunity, 2017. 85(12): p. e00661-17.
332. Aimanianda, V., et al., *Surface hydrophobin prevents immune recognition of airborne fungal spores.* Nature, 2009. 460(7259): p. 1117-21.
333. Santiago, V., et al., *Human NK Cells Develop an Exhaustion Phenotype During Polar Degranulation at the Aspergillus fumigatus Hyphal Synapse.* Frontiers in Immunology, 2018. 9(2344).
334. Gabaldón, T. and L. Carreté, *The birth of a deadly yeast: tracing the evolutionary emergence of virulence traits in Candida glabrata.* FEMS Yeast Research, 2015. 16(2).
335. Gabaldón, T., et al., *Comparative genomics of emerging pathogens in the Candida glabrata clade.* BMC Genomics, 2013. 14(1): p. 623.
336. Daly, P., et al., *Culture filtrates of Aspergillus fumigatus induce different modes of cell death in human cancer cell lines.* Mycopathologia, 1999. 146(2): p. 67-74.
337. Bi, J. and Z. Tian, *NK Cell Exhaustion.* Frontiers in immunology, 2017. 8: p. 760-760.
338. Sun, C., et al., *TGF-beta1 down-regulation of NKG2D/DAP10 and 2B4/SAP expression on human NK cells contributes to HBV persistence.* PLoS Pathog, 2012. 8(3): p. e1002594.
339. Linsley, P.S., et al., *Human B7-1 (CD80) and B7-2 (CD86) bind with similar avidities but distinct kinetics to CD28 and CTLA-4 receptors.* Immunity, 1994. 1(9): p. 793-801.

340. Grewal, I.S., J. Xu, and R.A. Flavell, *Impairment of antigen-specific T-cell priming in mice lacking CD40 ligand.* Nature, 1995. 378(6557): p. 617-20.
341. Aerts-Toegaert, C., et al., *CD83 expression on dendritic cells and T cells: correlation with effective immune responses.* Eur J Immunol, 2007. 37(3): p. 686-95.
342. Seth, S., et al., *CCR7 essentially contributes to the homing of plasmacytoid dendritic cells to lymph nodes under steady-state as well as inflammatory conditions.* J Immunol, 2011. 186(6): p. 3364-72.
343. Pinet, V., et al., *Antigen presentation mediated by recycling of surface HLA-DR molecules.* Nature, 1995. 375(6532): p. 603-6.
344. Swiecki, M., et al., *Plasmacytoid dendritic cell ablation impacts early interferon responses and antiviral NK and CD8(+) T cell accrual.* Immunity, 2010. 33(6): p. 955-66.
345. Guan, H., et al., *NK cells enhance dendritic cell response against parasite antigens via NKG2D pathway.* J Immunol, 2007. 179(1): p. 590-6.
346. Franca Gerosa, B.B.-G., Carla Nisii, Viviana Marchesini, Giuseppe Carra and Giorgio Trinchieri, *Reciprocal Activating Interaction between Natural Killer Cells and Dendritic Cells.* J. Exp. Med., 2002.
347. Ichise, H., et al., *NK Cell Alloreactivity against KIR-Ligand-Mismatched HLA-Haploidentical Tissue Derived from HLA Haplotype-Homozygous iPSCs.* Stem Cell Reports, 2017. 9(3): p. 853-867.
348. Diego Piccioli, S.S., Emiliano Melandri and Nicholas M. Valiante, *Contact-dependent Stimulation and Inhibition of Dendritic Cells by Natural Killer Cells.* J. Exp. Med., 2002.
349. Akira, S., M. Yamamoto, and K. Takeda, *Role of adapters in Toll-like receptor signalling.* Biochem Soc Trans, 2003. 31(Pt 3): p. 637-42.
350. Gantner, B.N., et al., *Collaborative induction of inflammatory responses by dectin-1 and Toll-like receptor 2.* J Exp Med, 2003. 197(9): p. 1107-17.
351. Brown, G.D., et al., *Dectin-1 mediates the biological effects of beta-glucans.* J Exp Med, 2003. 197(9): p. 1119-24.
352. Rogers, N.C., et al., *Syk-dependent cytokine induction by Dectin-1 reveals a novel pattern recognition pathway for C type lectins.* Immunity, 2005. 22(4): p. 507-17.
353. Kataoka, K., et al., *Activation of macrophages by linear (1right-arrow3)-beta-D-glucans. Impliations for the recognition of fungi by innate immunity.* J Biol Chem, 2002. 277(39): p. 36825-31.
354. Gresnigt, M.S., et al., *A polysaccharide virulence factor from Aspergillus fumigatus elicits anti-inflammatory effects through induction of Interleukin-1 receptor antagonist.* PLoS Pathog, 2014. 10(3): p. e1003936.
355. No, H.K., et al., *Effective deacetylation of chitin under conditions of 15 psi/121 degrees C.* J Agric Food Chem, 2000. 48(6): p. 2625-7.
356. Lehmann, C., M. Zeis, and L. Uharek, *Activation of natural killer cells with interleukin 2 (IL-2) and IL-12 increases perforin binding and subsequent lysis of tumour cells.* Br J Haematol, 2001. 114(3): p. 660-5.
357. F. Borrego, M.J.R., J. Ritz, J. Pena and R. Solana, *CD69 is a stimulatory receptor for natural killer cell and its cytotoxic effect is blockedd by CD94 inhibitory receptor.* Immunology 1999.
358. Marden, C.M., et al., *CD69 Is Required for Activated NK Cell-Mediated Killing of Resistant Targets.* Blood, 2005. 106(11): p. 3322-3322.

359. Namvar, S., et al., *Aspergillus fumigatus proteases, Asp f 5 and Asp f 13, are essential for airway inflammation and remodelling in a murine inhalation model.* Clin Exp Allergy, 2015. 45(5): p. 982-993.
360. Hinkle, C.L., et al., *Metalloprotease-induced ectodomain shedding of neural cell adhesion molecule (NCAM).* J Neurobiol, 2006. 66(12): p. 1378-95.
361. Li, S., et al., *The neural cell adhesion molecule (NCAM) associates with and signals through p21-activated kinase 1 (Pak1).* J Neurosci, 2013. 33(2): p. 790-803.
362. Murciano, C., et al., *Both viable and killed Candida albicans cells induce in vitro production of TNF-alpha and IFN-gamma in murine cells through a TLR2-dependent signalling.* Eur Cytokine Netw, 2007. 18(1): p. 38-43.
363. Booth, N., *The denaturation of proteins: Denaturation in the presence of alcohol.* The Biochemical journal, 1930. 24(6): p. 1699-1705.
364. Mallamace, F., et al., *Energy landscape in protein folding and unfolding.* Proceedings of the National Academy of Sciences, 2016. 113(12): p. 3159-3163.
365. Mason, J.T. and T.J. O'Leary, *Effects of formaldehyde fixation on protein secondary structure: a calorimetric and infrared spectroscopic investigation.* J Histochem Cytochem, 1991. 39(2): p. 225-9.
366. Kristiansen, K.A., A. Potthast, and B.E. Christensen, *Periodate oxidation of polysaccharides for modification of chemical and physical properties.* Carbohydr Res, 2010. 345(10): p. 1264-71.
367. Spiro, R.G., *PERIODATE OXIDATION OF THE GLYCOPROTEIN FETUIN.* J Biol Chem, 1964. 239: p. 567-73.
368. Landsman, L. and S. Jung, *Lung macrophages serve as obligatory intermediate between blood monocytes and alveolar macrophages.* J Immunol, 2007. 179(6): p. 3488-94.
369. Tan, S.Y. and M.A. Krasnow, *Developmental origin of lung macrophage diversity.* Development, 2016. 143(8): p. 1318-27.
370. Mircescu, M.M., et al., *Essential role for neutrophils but not alveolar macrophages at early time points following Aspergillus fumigatus infection.* The Journal of infectious diseases, 2009. 200(4): p. 647-656.
371. Shevchenko, M.A., et al., *Aspergillus fumigatus Infection-Induced Neutrophil Recruitment and Location in the Conducting Airway of Immunocompetent, Neutropenic, and Immunosuppressed Mice.* J Immunol Res, 2018. 2018: p. 5379085.
372. Parody, R., et al., *Predicting survival in adults with invasive aspergillosis during therapy for hematological malignancies or after hematopoietic stem cell transplantation: Single-center analysis and validation of the Seattle, French, and Strasbourg prognostic indexes.* Am J Hematol, 2009. 84(9): p. 571-8.
373. Retiere, C., et al., *Impact on early outcomes and immune reconstitution of high-dose post-transplant cyclophosphamide vs anti-thymocyte globulin after reduced intensity conditioning peripheral blood stem cell allogeneic transplantation.* Oncotarget, 2018. 9(14): p. 11451-11464.
374. Wagner, J., et al., *A Two-Phase Expansion Protocol Combining Interleukin (IL)-15 and IL-21 Improves Natural Killer Cell Proliferation and Cytotoxicity against Rhabdomyosarcoma.* Frontiers in immunology, 2017. 8: p. 676-676.
375. D'Este, E., et al., *STED nanoscopy reveals the ubiquity of subcortical cytoskeleton periodicity in living neurons.* Cell Rep, 2015. 10(8): p. 1246-51.

376. Bubb, M.R., et al., *Jasplakinolide, a cytotoxic natural product, induces actin polymerization and competitively inhibits the binding of phalloidin to F-actin.* J Biol Chem, 1994. 269(21): p. 14869-71.
377. Holbrook, N.J., W.I. Cox, and H.C. Horner, *Direct suppression of natural killer activity in human peripheral blood leukocyte cultures by glucocorticoids and its modulation by interferon.* Cancer Res, 1983. 43(9): p. 4019-25.
378. Anguille, S., et al., *Interleukin-15 Dendritic Cells Harness NK Cell Cytotoxic Effector Function in a Contact- and IL-15-Dependent Manner.* PLoS One, 2015. 10(5): p. e0123340.
379. Bontkes, H.J., et al., *Tumor associated antigen and interleukin-12 mRNA transfected dendritic cells enhance effector function of natural killer cells and antigen specific T-cells.* Clin Immunol, 2008. 127(3): p. 375-84.
380. Van Acker, H.H., et al., *CD56 in the Immune System: More Than a Marker for Cytotoxicity?* Frontiers in immunology, 2017. 8: p. 892-892.
381. Mitchell, K.F., R. Zarnowski, and D.R. Andes, *Fungal Super Glue: The Biofilm Matrix and Its Composition, Assembly, and Functions.* PLoS pathogens, 2016. 12(9): p. e1005828-e1005828.
382. Reichhardt, C., et al., *Analysis of the Aspergillus fumigatus Biofilm Extracellular Matrix by Solid-State Nuclear Magnetic Resonance Spectroscopy.* Eukaryotic cell, 2015. 14(11): p. 1064-1072.
383. Tuntevski, K., et al., *Aspergillus collagen-like genes (acl): identification, sequence polymorphism, and assessment for PCR-based pathogen detection.* Applied and environmental microbiology, 2013. 79(24): p. 7882-7895.
384. Hefter, M., et al., *Human primary myeloid dendritic cells interact with the opportunistic fungal pathogen Aspergillus fumigatus via the C-type lectin receptor Dectin-1.* Medical Mycology, 2016. 55(5): p. 573-578.
385. Voltersen, V., et al., *Proteome Analysis Reveals the Conidial Surface Protein CcpA Essential for Virulence of the Pathogenic Fungus Aspergillus fumigatus.* MBio, 2018. 9(5).
386. Srivastava, M., et al., *Aspergillus fumigatus Challenged by Human Dendritic Cells: Metabolic and Regulatory Pathway Responses Testify a Tight Battle.* Frontiers in Cellular and Infection Microbiology, 2019. 9(168).

Appendix

List of Tables

List of Figures

Abbreviations

ABPA	Allergic bronchopulmonary aspergillosis
AI	Alkali-insoluble
alloSCT	Allogeneic stem cell transplantation
APC	Allophycocyanin
AS	Alkali-soluble
ATCC	American type culture collection
CD	Cluster of differentiation
CLSM	Confocal laser scanning microscopy
dSTORM	Direct stochastical reconstruction microscopy
FA	Formaldehyde
F-actin	Filamentous actin
FCS	Fetal calf serum
FITC	Fluorescein isothiocyanate
GT	Germ tubes
GvHD	Graft-versus-host disease
HLA	Human leukocyte antigen
IA	Invasive aspergillosis
IL	Interleukin
IS	Immunological synapse
LPS	Lipopolysaccharide
MHC	Major histocompatibility complex
MIP	Macrophage inflammatory protein
moDC	Monocyte-derived dendritic cell
MOI	Multiplicity of infection
NK	Natural killer
OD	Optical density
PAMP	Pathogen-associated molecular pattern
PBMCs	Peripheral blood mononuclear cells
pDC	Plasmacytoid dendritic cells
PE	Phycoerythrin
PerCP	Peridinin-chlorophyll-protein
PMN	Polymorphonuclear leukocyte
PRR	Pathogen recognition receptor
RANTES	Regulated upon activation, normal T cell expressed and secreted
ROS	Reactive oxygen species
RT	Room temperature
SD	Standard deviation
SEM	Scanning electron microscopy
SEM	Standard error of the mean
SIM	Structured illumination microscopy
TLR	Toll-like-receptor
Z	Zymosan
ZD	Depleted zymosan

List of Publications

Data from this study are published as:

- **"CD56 is a pathogen recognition receptor on human natural killer cells."** [235]
  Sabrina Ziegler*, Esther Weiss*, Anna-Lena Schmitt, Jan Schlegel, Anne Burgert, Ulrich Terpitz, Markus Sauer, Lorenzo Moretta, Simona Sivori, Ines Leonhardt, Oliver Kurzai, Hermann Einsele, and Juergen Loeffler. *Scienctific Reports*, 2017
  *These authors contributed equally to the manuscript

- **"First insights in NK-DC cross-talk and the importance of soluble factors during infection with *Aspergillus fumigatus"*** [234]
  Esther Weiss, Sabrina Ziegler, Mirjam Fliesser, Anna-Lena Schmitt, Kerstin Hünniger, Oliver Kurzai, Charles-Oliver Morton, Hermann Einsele, and Juergen Loeffler. *Front Cell Infect Microbiol*, 2018

Data from this study will be published as:

- **"Reconstituting NK cells after allogeneic stem cell transplantation reveal impaired recognition of *Aspergillus fumigatus* mediated by corticosteroids"**
  Esther Weiss, Jan Schlegel, Ulrich Terpitz, Michael Weber, Joerg Linde, Anna-Lena Schmitt, Kerstin Hünniger, Lothar Marischen, Florian Gamon, Joachim Bauer, Claudia Löffler, Oliver Kurzai, Charles Oliver Morton, Markus Sauer, Hermann Einsele, and Juergen Loeffler.

During the time course of this PhD thesis, I was involved in several related projects (apart from this study) that resulted in the following publications:

- **"Human primary myeloid dendritic cells interact with the opportunistic fungal pathogen *Aspergillus fumigatus* via the C-type lectin receptor Dectin-1"** [384]
  Maike Hefter, Jasmin Lother, Esther Weiss, Anna-Lena Schmitt, Mirjam Fliesser, Hermann Einsele, and Juergen Loeffler. *Medical Mycology*, 2017

- **"Proteome analysis reveals the conidial surface protein CcpA essential for virulence of the pathogenic fungus *Aspergillus fumigatus*."** [385]
  Vera Voltersen*, Matthew Blango*, Sahra Herrmann, Franziska Schmidt, Thorsten Heinekamp, Maria Strassburger, Thomas Krüger, Petra Bacher, Jasmin Lother, Esther Weiss, Kerstin Hünniger, Hong Liu, Peter Hortschansky, Alexander Scheffold, Jürgen Löffler, Sven Krappmann, Sandor Nietzsche, Oliver Kurzai, Hermann Einsele, Olaf Kniemeyer, Scott Filler, Utz Reichard, Axel Brakhage. *MBio,* 2018
  *These authors contributed equally to the manuscript

- ***"Aspergillus fumigatus* challenged by human dendritic cells: metabolic and regulatory pathway responses testify a tight battle"** [386]
  Mugdha Srivastava, Elena Bencurova, Shishir K. Gupta, Esther Weiss, Juergen Loeffler, and Thomas Dandekar. *Front. Cell. Infect. Microbiol.*, 2019

Statement of individual author contributions

Statement of individual author contributions to figures/tables/chapters included in the manuscripts

Publication #1:

Sabrina Ziegler*****, Esther Weiss*****, Anna-Lena Schmitt, Jan Schlegel, Anne Burgert, Ulrich Terpitz, Markus Sauer, Lorenzo Moretta, Simona Sivori, Ines Leonhardt, Oliver Kurzai, Hermann Einsele & Juergen Loeffler: "CD56 is a pathogen recognition receptor on human natural killer cells" *Scientific Reports,* volume 7, Article number: 6138 (2017) ***equal contribution**

Figure	**Author Initials,** Responsibility decreasing from left to right				
1	SZ	EW	JL, AS	HE	SS, LM, IL, OK,
2	SZ	EW	JL, AS	HE	SS, LM, IL, OK,
3	SZ	EW	JL, AS	HE	SS, LM, IL, OK,
4	SZ	EW	JL, AS	HE	SS, LM, IL, OK,
5	EW	JS, SZ, AB	UT, MS, JL	AS, HE	SS, LM, IL, OK
6	EW	JS, SZ, AB	UT, MS, JL	AS, HE	SS, LM, IL, OK
7	EW	SZ, AS, KH	JL, OK	HE	JS, AB, UT, MS,
8	SZ	EW	JL, AS	HE	SS, LM, IL, OK,
Suppl. Fig 1	SZ	EW	JL, AS	HE	SS, LM, IL, OK,
Suppl. Fig 2	SZ	EW	JL, AS	HE	SS, LM, IL, OK,
Suppl. Fig 3	EW	AS, SZ	JL	HE	SS, LM, IL, OK,
Suppl. Fig 4	EW	AS, SZ	JL	HE	SS, LM, IL, OK,
Suppl. Fig 5	EW	JS, AB, AS, SZ	JL	HE	SS, LM, IL, OK,
Suppl. Fig 6	EW	AS, JS, SZ	JL	HE	SS, LM, IL, OK,
Suppl. Video 1	JS	EW	JL, AB, AS, SZ	HE	SS, LM, IL, OK,

Publication #2:

Esther Weiss , Sabrina Ziegler, Mirjam Fliesser, Anna-Lena Schmitt, Kerstin Hünniger, Oliver Kurzai, Charles Oliver Morton, Hermann Einsele and Juergen Loeffler: "First insights in NK-DC crosstalk and the importance of soluble factors during infection with *Aspergillus fumigatus*". Frontiers in Cellular and Infection Microbiology 2018; 8. 10.3389/fcimb.2018.0028

Figure	**Author Initials,** Responsibility decreasing from left to right				
1	EW	AS, SZ, MJ	JL	HE	KH, OK, CM
2	EW	AS, SZ, MJ	JL	HE	KH, OK, CM
3	EW	AS, SZ, MJ	JL	HE	KH, OK, CM
4	EW	AS, SZ, MJ	JL	HE	KH, OK, CM
5	EW	AS, SZ, MJ	JL	HE	KH, OK, CM
6	EW	AS, SZ, MJ	JL	HE	KH, OK, CM
7	EW	AS, SZ, MJ	JL	HE	KH, OK, CM
8	EW	KH	AS, SZ, MJ, JL	HE	OK, CM
9	EW	AS, SZ, MJ	JL	HE	KH, OK, CM
Sup Fig 1	EW	AS, SZ, MJ	JL	HE	KH, OK, CM
Sup Fig 2	EW	AS, SZ, MJ	JL	HE	KH, OK, CM

Manuscript #3:

Esther Weiss *****, Jan Schlegel *****, Ulrich Terpitz, Michael Weber, Joerg Linde, Anna-Lena Schmitt, Kerstin Hünniger, Lothar Marischen, Joachim Bauer, Claudia Löffler, Oliver Kurzai, Charles Oliver Morton, Markus Sauer, Hermann Einsele[#], and Juergen Loeffler[#]. „Reconstituting NK cells after allogeneic stem cell transplantation reveal impaired recognition of *Aspergillus fumigatus* mediated by corticosteroids". ***shared first authorship, [#]shared last authorship**

Figure	**Author Initials,** Responsibility decreasing from left to right				
1	EW	JS, UT	HE, JL	MW, JLi, AS, KH, LM	JB, CL, OK, CM, MS
2	EW	JS, UT	HE, JL	MW, JLi, AS, KH, LM	JB, CL, OK, CM, MS
3	EW	JS, UT	HE, JL	MW, JLi, AS, KH, LM	JB, CL, OK, CM, MS
4	JS	EW, UT	HE, JL	MW, JLi, AS, KH, LM	JB, CL, OK, CM, MS
5	EW	JS, UT	HE, JL	MW, JLi, AS, KH, LM	JB, CL, OK, CM, MS
6	EW, JSc	JS, UT	HE, JL	MW, JLi, AS, KH, LM	JB, CL, OK, CM, MS
7	EW	JS, UT	HE, JL	MW, JLi, AS, KH, LM	JB, CL, OK, CM, MS
8	EW	JS, UT	HE, JL	MW, JLi, AS, KH, LM	JB, CL, OK, CM, MS
Sup Fig 1	EW	JS, UT	HE, JL	MW, JLi, AS, KH, LM	JB, CL, OK, CM, MS
Sup Fig 2	EW	JS, UT	HE, JL	MW, JLi, AS, KH, LM	JB, CL, OK, CM, MS
Sup Table 1	EW	JS, UT	HE, JL	MW, JLi, AS, KH, LM	JB, CL, OK, CM, MS

I also confirm my primary supervisor's acceptance.

_____

Doctoral Researcher's Name Date Place Signature

Statement of individual author contributions and of legal second publication rights

Publication #1:

Sabrina Ziegler*****, Esther Weiss*****, Anna-Lena Schmitt, Jan Schlegel, Anne Burgert, Ulrich Terpitz, Markus Sauer, Lorenzo Moretta, Simona Sivori, Ines Leonhardt, Oliver Kurzai, Hermann Einsele & Juergen Loeffler: "CD56 is a pathogen recognition receptor on human natural killer cells" *Scientific Reports,* volume 7, article number: 6138 (2017), DOI: 10.1038/s41598-017-06238-4 ***equal contribution**

Participated in	**Author Initials,** Responsibility decreasing from left to right				
Study Design Methods Development	SZ, EW, HE, JL	JS, AB, UT, MS	AS	SS, IL	OK, LM
Data Collection	SZ, EW	JS, AB, AS	IL	SS	OK, LM, JL, HE, UT, MS
Data Analysis and Interpretation	SZ, EW	JS, AB	MS, JL, HE, UT	IL, OK, AS	SS, LM
Manuscript Writing	SZ, EW	JS, AB	JL, MS, UT, HE	IL, OK	SS, LM, AS

Publication #2:

Esther Weiss, Sabrina Ziegler, Mirjam Fliesser, Anna-Lena Schmitt, Kerstin Hünniger, Oliver Kurzai, Charles Oliver Morton, Hermann Einsele and Juergen Loeffler: "First insights in NK-DC crosstalk and the importance of soluble factors during infection with *Aspergillus fumigatus*", *Front. Cell. Infect. Microbiol*., volume 8, artice number: 288 (2018), DOI: 10.3389/fcimb.2018.00288

Participated in	**Author Initials,** Responsibility decreasing from left to right				
Study Design	EW, SZ	MF, JL	HE	AS, KH	OK, CM
Data Collection	EW	AS, KH	SZ	MF	OK, CM, JL, HE
Data Analysis and Interpretation	EW	SZ, MF, JL	AS, KH	HE	OK, CM
Manuscript Writing	EW	SZ, MF, JL	KH	OK, CM, HE	AS

Manuscript #3:

Esther Weiss *****, Jan Schlegel *****, Ulrich Terpitz, Michael Weber, Joerg Linde, Anna-Lena Schmitt, Kerstin Hünniger, Lothar Marischen, Joachim Bauer, Claudia Löffler, Oliver Kurzai, Charles Oliver Morton, Markus Sauer, Hermann Einsele[#], and Juergen Loeffler[#]. „Reconstituting NK cells after allogeneic stem cell transplantation reveal impaired recognition of Aspergillus fumigatus mediated by corticosteroids". ***shared first authorship, [#]shared last authorship**

Participated in	**Author Initials,** Responsibility decreasing from left to right				
Study Design Methods Development	EW, JS, JL, HE, AS	UT	MS, LM	JB, CL	KH, MW, JLi, OK, CM
Data Collection	EW, JS	AS	LM, KH	CL, JB	JL, JLi, MW, OK, CM, UT, MS, HE
Data Analysis and Interpretation	EW, JS	MW	LM, UT	JL, MS, HE	AS, KH, CM, OK, JLi, CL, JB
Manuscript Writing	EW	JS, JL	CM, HE, KH, UT, LM	MS	AS, JB, CL, MW, JLi, OK

The doctoral researcher confirms that she/he has obtained permission from both the publishers and the co-authors for legal second publication.

The doctoral researcher and the primary supervisor confirm the correctness of the above mentioned assessment.

_____

Doctoral Researcher's Name Date Place Signature

_____

Primary Supervisor's Name Date Place Signature

Affidavit / Eidesstattliche Erklärung

I hereby confirm that my thesis entitled “Host-pathogen interactions of natural killer cells and *Aspergillus fumigatus*: relevance of immune cell cross-talk and fungal recognition receptors” is the result of my own work. I did not receive any help or support from commercial consultants. All sources and / or materials applied are listed and specified in the thesis.
Furthermore, I confirm that this thesis has not yet been submitted as part of another examination process neither in identical nor in similar form.

…….....

Place, Date, Signature

Hiermit erkläre ich an Eides statt, die Dissertation „Wirt-Pathogen Interaktionen von natürlichen Killerzellen und *Aspergillus fumigatus*: Revelanz von Immunzellinteraktionen und fungalen Erkennungsrezeptoren“ eigenständig, d.h. insbesondere selbständig und ohne Hilfe eines kommerziellen Promotionsberaters, angefertigt und keine anderen als die von mir angegebenen Quellen und Hilfsmittel verwendet zu haben.
Ich erkläre außerdem, dass die Dissertation weder in gleicher noch in ähnlicher Form bereits in einem anderen Prüfungsverfahren vorgelegen hat.

…….....

Ort, Datum, Unterschrift